



University
of Glasgow

Mordi, Ify Raphael (2015) The clinical utility of cardiovascular magnetic resonance. MD thesis.

<http://theses.gla.ac.uk/6200/>

Copyright and moral rights for this thesis are retained by the author

A copy can be downloaded for personal non-commercial research or study, without prior permission or charge

This thesis cannot be reproduced or quoted extensively from without first obtaining permission in writing from the Author

The content must not be changed in any way or sold commercially in any format or medium without the formal permission of the Author

When referring to this work, full bibliographic details including the author, title, awarding institution and date of the thesis must be given.

The Clinical Utility of Cardiovascular Magnetic Resonance

Dr. Ify Raphael Mordi
MBCHB, MRCP (UK)

**Submitted in fulfilment of the requirements of the Degree of
Doctor of Medicine (MD)**

Institute of Cardiovascular and Medical Sciences
College of Medical, Veterinary and Life Sciences
University of Glasgow
March 2015

Abstract

The use of cardiovascular magnetic resonance (CMR), particularly in the cardiovascular research setting, has grown exponentially in the past 20 years. While CMR is increasingly used in clinically, it has yet to be incorporated into routine clinical practice and guidelines in the majority of conditions. One of the main reasons for this is the relative paucity of evidence for its diagnostic and prognostic utility and cost-effectiveness compared to more established non-invasive imaging techniques such as echocardiography and nuclear imaging. For CMR to become part of routine clinical care, more evidence of its utility is required.

The overall aim of this thesis was to demonstrate the clinical utility of CMR by using it to examine 5 clinical questions that pose a relevant dilemma to physicians in a cohort of patients referred for clinically indicated CMR studies.

CMR has two major advantages over transthoracic echocardiography, the most commonly used technique in our centre (and in most worldwide). Firstly, it is the gold standard for assessment of left ventricular volumes and function, and secondly, it has the ability to characterise the myocardium using specific imaging sequences and intravenous gadolinium contrast (known as late gadolinium enhancement – LGE). The first study in this thesis explored the potential benefit of a CMR protocol using these benefits to predict prognosis in an unselected cohort of patients. In this study I found that the assessment of myocardial function using ejection fraction and deformation imaging (strain) and assessment of the presence of fibrosis using LGE had incremental prognostic significance in addition to clinical predictors of outcome in all patients, including in those with ejection fractions greater than 35% (commonly thought to be patients at lower risk of adverse events).

During scanning of this cohort of patients, it became apparent that CMR imaging of myocardial scar in patients with a history of prior myocardial infarction (MI) had the ability to identify fat within the infarcted territory, known as lipomatous metaplasia, which had been recognised pathologically but is not identified by echocardiography. The tissue characterisation ability of CMR has for the first time allowed this to be identified non-invasively ante-mortem. Pathological studies had suggested that lipomatous metaplasia was associated with adverse remodeling, while recent animal studies had suggested that the presence of myocardial fat within infarcts was pro-arrhythmogenic. In this study I showed that the presence of lipomatous metaplasia was indeed independently associated with

mortality and ventricular arrhythmias, suggesting that it perhaps provides an arrhythmogenic substrate.

The next study explored the use of LGE in addition to established clinical markers in patients undergoing implantable cardioverter-defibrillator (ICD) implantation for ischaemic or dilated cardiomyopathy. These patients met the current clinical criteria for ICD implantation and also had testing of NT-proBNP, a marker of cardiac strain that is associated with adverse prognosis. The patients all underwent pre-implantation CMR. I found that the presence of LGE and a high NT-proBNP was associated with a higher risk of death and ICD activation, perhaps hinting at a role for CMR in providing further risk stratification in this group of patients.

Following on from this, I looked at the diagnostic capabilities of CMR. Characterisation of patients with mildly impaired left ventricular systolic function is important as early identification of cardiomyopathy can potentially allow early institution of life-saving therapies. Mild left ventricular impairment can however also be associated with the normal myocardial adaptations to exercise, known as athlete's heart. This poses a diagnostic dilemma, which may not be easily solved using current imaging techniques. I found that the use of a further CMR parameter to characterise tissue, T1 mapping, was able to discriminate between patients with early DCM and exercisers with normal physiological myocardial adaptation, perhaps providing a solution to this diagnostic challenge.

The final study explored the utility of dobutamine stress CMR (DSCMR) to diagnose significant coronary artery disease (CAD) in patients with left bundle branch block (LBBB) and clinically suspected CAD. CAD is the most common cause of LBBB, yet LBBB causes myocardial abnormalities that can make it difficult to diagnose CAD non-invasively, leading many patients to be referred for invasive coronary angiography (ICA) to confirm the diagnosis. Despite this, a substantial proportion of the patients with LBBB will not have significant CAD, meaning that ICA would be unnecessary. This study compared DSCMR with dobutamine stress echocardiography, with ICA as the gold standard. I found that DSCMR was significantly more accurate in diagnosis than dobutamine stress echocardiography, perhaps providing a technique that could be used as a gatekeeper to ICA.

This thesis shows that CMR can provide important diagnostic and prognostic information in a variety of cardiac conditions and can potentially help guide clinical decision-making.

Larger studies should be performed to confirm these findings, allowing for determination of cost-effectiveness and incorporation of CMR into routine clinical management.

Acknowledgements

I would like to thank my principal supervisor, Dr. Niko Tzemos for his advice, guidance and unwavering support throughout my period of research, and for giving me the opportunity to do this. I would also like to thank Professor Colin Berry and Dr. David Carrick for their help during this period of research.

I am very grateful to the radiology and nursing staff of the Golden Jubilee National Hospital, who were extremely helpful and accommodating in allowing me to perform the studies in this thesis.

I will be forever grateful of the support and advice provided by my family, who have guided me through this process and provided me with the inspiration and motivation to succeed; hopefully I have and will continue to make them proud.

Finally, I am most grateful and indebted to my wonderful wife, Natalie, who has supported me throughout. She has been my rock and motivation, and I dedicate this to her with my love.

Declaration

I declare that, except where reference is made to the contribution of others, this thesis is a result of my own work, written entirely by myself and has not been submitted for any other degree at the University of Glasgow or any other institution.

Ify Mordi

March 2015

List of Related Publications and Presentations

Publications

I Mordi, T Stanton, D Carrick, J McClure, K Oldroyd, C Berry, N Tzemos. Comprehensive Dobutamine Stress CMR Versus Echocardiography in LBBB and Suspected Coronary Artery Disease. *JACC Cardiovasc Imaging*. 2014 May;7(5):490-8.

I Mordi, PS Jhund, D Carrick, J Payne, RS Gardner, C Berry, N Tzemos. Late Gadolinium Enhancement and NT-proBNP for prediction of death and ventricular arrhythmia in patients with implantable cardioverter defibrillators. *JACC Cardiovasc Imaging*. 2014 Jun;7(6):561-9.

I Mordi, A Radjenovic, T Stanton, RS Gardner, A McPhaden, D Carrick, C Berry, N Tzemos. Prevalence and Prognostic Significance of Lipomatous Metaplasia in Patients with Prior Myocardial Infarction. *JACC Cardiovasc Imaging*. 2014 Nov 12.

I Mordi, N Tzemos. Non-invasive assessment of coronary artery disease in patients with left bundle branch block. *Int J Cardiol*. 2015 Jan 29;184C:47-55.

Presentations

I Mordi, J McClure, D Carrick, K Oldroyd, C Berry, N Tzemos. Utility of Comprehensive Dobutamine Stress MRI in the Diagnosis of Coronary Artery Disease in Patients with Left-Bundle Branch Block.

- European Society of Cardiology Congress 2012 (*oral*)
- Scottish Cardiac Society Autumn Meeting 2012 (*oral - awarded best abstract*)

I Mordi, PS Jhund, D Carrick, J Payne, RS Gardner, C Berry, N Tzemos. Late Gadolinium Enhancement and NT-proBNP for prediction of death and ventricular arrhythmia in patients with implantable cardioverter defibrillators.

- Royal Medical-Chirurgical Society 2013 (*oral*)
- British Society of Cardiovascular Magnetic Resonance 2013 (*poster*)

Abbreviations

(A)MI	(acute) myocardial infarction
¹ H	hydrogen nucleus (proton)
AF	atrial fibrillation
AUC	area under (the) curve
CAD	coronary artery disease
CI	confidence interval
CMR	cardiovascular magnetic resonance
CT (CA)	computed tomography (coronary angiography)
CVD	cardiovascular disease
Cx	circumflex artery
DCM	dilated non-ischaemic cardiomyopathy
DSCMR	dobutamine stress cardiovascular magnetic resonance
DSE	dobutamine stress echocardiography
ECG	electrocardiogram
ECV	extracellular volume
ECV	extracellular volume
EGE	early gadolinium enhancement
eGFR	estimated glomerular filtration rate
ETT	exercise tolerance test
FFR	fractional flow reserve
FLASH	fast low-angle shot
FOV	field of view
GCS	global circumferential strain
GLS	global longitudinal strain
HASTE	Half-Fourier Acquisition Single-Shot Turbo Spin-Echo
HCM	hypertrophic cardiomyopathy
HR	hazard ratio
I.M.	Ify Mordi
ICA	invasive coronary angiography
ICD	implantable cardioverter-defibrillator
ICM	ischaemic cardiomyopathy
IHD	ischaemic heart disease
LAD	left anterior descending artery
LBBB	left bundle branch block

LGE	late gadolinium enhancement
LM	lipomatous metaplasia
LVEF	left ventricular ejection fraction
MHz	megahertz
MI	myocardial infarction
MOLLI	Modified Look-Locker Inversion-recovery
MRI	magnetic resonance imaging
ms	milliseconds
N.T.	Niko Tzemos
NPV	negative predictive value
NSTEMI	non-ST elevation myocardial infarction
NT-proBNP	n-terminal pro-B type natriuretic peptide
PET	positron emission tomography
PPV	positive predictive value
PSIR	phase-sensitive inversion-recovery
RCA	right coronary artery
ROC	receiver-operator characteristic
RWMA	regional wall motion abnormality
SD	standard deviation(s)
SPAMM	spatial modulation of magnetisation
SPECT	single photon emission computed tomography
SSFP	steady state free precession
STEMI	ST elevation myocardial infarction
STIR	short-tau inversion-recovery
T	Tesla
TE	echo time
TI	inversion time
TOE	transoesophageal echocardiogram
TR	repetition time
TTE	transthoracic echocardiogram
UK	United Kingdom
WHO	World Health Organization

Contents

Abstract	2
Acknowledgements	5
Declaration	6
List of Related Publications and Presentations	7
Abbreviations	8
List of Figures	16
List of Tables	18
Chapter 1. Introduction	19
1.1. Preamble	20
1.2. Cardiovascular Disease – Definition and Epidemiology	20
1.3. Investigation of Cardiac Disease	23
1.3.1. Overview	23
1.3.2. Invasive Cardiac Investigations	24
1.3.3. Electrocardiography	25
1.3.4. Echocardiography	26
1.3.5. Nuclear Imaging	28
1.3.6. Multislice CT Coronary Angiography (CTCA)	29
1.4. Cardiovascular Magnetic Resonance (CMR)	30
1.4.1. Background	30
1.4.2. Generation of the MR Image	31
1.4.3. T1, T2 and T2* Imaging	34
1.5. The Clinical Utility of CMR – Current Knowledge	35
1.5.1. Acute Myocardial Infarction	36
1.5.2. Chronic Ischaemic Cardiomyopathy	38
1.5.3. Stable Angina	40
1.5.4. Dilated Non-Ischaemic Cardiomyopathy	41
1.5.5. Myocarditis	42
1.5.6. Hypertrophic Cardiomyopathy	43
1.5.7. Miscellaneous Conditions	44
1.6. Summary and Thesis Aims	45

Chapter 2. General Methods	47
2.1. Preamble	48
2.2. General Information	48
2.3. Standard CMR Protocol	48
2.3.1. Half-Fourier Acquisition Single-Shot Turbo Spin-Echo (HASTE)	49
2.3.2. Steady-State Free Precession “Cine” Imaging	50
2.3.3. T1-Weighted Imaging (“T1 Mapping”)	50
2.3.4. T2-Weighted Imaging	51
2.3.5. Tagging – Spatial Modulation of Magnetisation (SPAMM)	51
2.3.6. Early and Late Gadolinium Enhancement	52
2.4. CMR Image Analysis	52
2.4.1. Assessment of Left Ventricular Mass and Function	52
2.4.2. Assessment of T1- and T2-Weighted Imaging	53
2.4.3. Assessment of CMR Tagging	55
2.4.4. Assessment of Early and Late Gadolinium Enhancement	56
2.5. Statistical Analysis	57
2.6. Ethical Approval	58
Chapter 3. The Combined Incremental Prognostic Value of Left Ventricular Ejection Fraction, Late Gadolinium Enhancement and Global Circumferential Strain Assessed by Cardiovascular Magnetic Resonance	59
3.1. Introduction	60
3.2. Methods	61
3.2.1. Patient Selection	61
3.2.2. CMR Protocol	61
3.2.3. Follow-up	61
3.2.4. Statistical Methods	62
3.3. Results	63
3.3.1. Baseline Characteristics	63
3.3.2. Primary Outcome Analysis	66
3.3.3. Incremental Prognostic Value of CMR Parameters	67
3.3.4. Sub-analysis: Patients Without Severely Impaired LV Function	72
3.3.5. Reproducibility of GCS Measurements Using Tagging	75
3.4. Discussion	75

3.4.1. Study Findings	75
3.4.2. Clinical Context	76
3.4.3. The Additional Value of Global Circumferential Strain	77
3.4.4. Feasibility of CMR Tagging	78
3.4.5. Limitations	78
3.5. Conclusions	79

Chapter 4. Prevalence and Prognostic Significance of Lipomatous Metaplasia in Patients with Prior Myocardial Infarction 80

4.1. Introduction	81
4.2. Methods	82
4.2.1. Patient Selection	82
4.2.2. CMR Protocol	83
4.2.3. Clinical Follow-Up	84
4.2.4. Statistical Methods	85
4.3. Results	86
4.3.1. Baseline Characteristics	86
4.3.2. Comparison With CT	86
4.3.3. Incidence and Functional Impact of LM	89
4.3.4. Prediction of Adverse Cardiovascular Outcome	91
4.4. Discussion	95
4.4.1. Study Findings	95
4.4.2. Clinical Context	96
4.4.3. Lipomatous Metaplasia – A Novel Target for Therapeutic Intervention?	96
4.4.4. CMR in Lipomatous Metaplasia	97
4.4.5. Limitations	98
4.5. Conclusions	99

Chapter 5. Late Gadolinium Enhancement and NT-proBNP Identify a Population at Low Risk of Death or Arrhythmic Events in Patients With Primary Prevention Implantable Cardioverter Defibrillators 100

5.1. Introduction	101
5.2. Methods	103

5.2.1. Patient Selection	103
5.2.2. CMR Protocol	103
5.2.3. NT-proBNP Sampling	104
5.2.4. Defibrillator Implantation	104
5.2.5. Clinical Follow-Up	104
5.2.6. Statistical Methods	105
5.3. Results	106
5.3.1. Baseline Characteristics	106
5.3.2. Primary Outcome	108
5.4. Discussion	114
5.4.1. Study Findings	114
5.4.2. Clinical Context	115
5.4.3. LGE as a Marker of Adverse Outcome	115
5.4.4. NT-proBNP as a Marker of Adverse Outcome	116
5.4.5. The Combined Prognostic Value of LGE and NT-proBNP	117
5.4.6. Limitations	118
5.5. Conclusions	118

Chapter 6. Can Advanced CMR Parameters Help To Differentiate Between Early Dilated Non-Ischaemic Cardiomyopathy and Physiological Myocardial Adaptation To Exercise?..... 120

6.1. Introduction	121
6.2. Methods	123
6.2.1. Patient Selection	123
6.2.2. CMR Protocol	123
6.2.3. Statistical Methods	124
6.3. Results	125
6.3.1. Correlations Between Tissue Characteristics and Left Ventricular Function	125
6.3.2. Comparison between Exercisers, DCM Patients and Controls	125
6.4. Discussion	131
6.4.1. Study Findings	131
6.4.2. Clinical Context	131
6.4.3. T1 and T2 Mapping in DCM	132
6.4.4. Global Circumferential and Longitudinal Strain	133

6.4.5. What Is The Clinical Importance Of These Findings?	134
6.4.6. Limitations	135
6.5. Conclusions	135

Chapter 7. Comprehensive Dobutamine Stress MRI versus Dobutamine Stress Echocardiography in the Assessment of Patients with Left Bundle Branch Block and Suspected Coronary Artery Disease 136

7.1. Preamble	137
7.2. Introduction	137
7.2.1. The Clinical and Functional Impact of LBBB	138
7.2.2. Exercise ECG Stress Testing	140
7.2.3. Nuclear Imaging	140
7.2.4. Stress Echocardiography	143
7.2.5. Cardiac Computed Tomography	147
7.2.6. Cardiovascular Magnetic Resonance	148
7.3. Review Summary	149
7.4. Study Introduction	153
7.5. Methods	154
7.5.1. Patient Selection	154
7.5.2. Dobutamine Stress Echocardiography	155
7.5.3. Dobutamine Stress CMR	156
7.5.4. Invasive Coronary Angiography	158
7.5.5. Statistical Methods	159
7.6. Results	159
7.6.1. Baseline Characteristics	159
7.6.2. DSE and DSCMR Compared to ICA	161
7.7. Discussion	166
7.7.1. Study Findings	166
7.7.2. Clinical Context	167
7.7.3. DSCMR Cine Imaging vs. DSE	167
7.7.4. The Incremental Value of Perfusion and LGE	169
7.7.5. Limitations	170
7.8. Conclusions	171

Chapter 8. Discussion 172

8.1. Summary of Thesis Findings	173
8.2. Clinical Implications of the Thesis	173
8.3. Limitations of the Thesis	175
8.4. Future Directions	176
8.5. Conclusions	177
Appendix 1: Ethical Approval	178
Appendix 2: Protocol Submitted to Ethics Committee	182
References	187

List of Figures

Figure 1-1.	Cardiac Investigations	23
Figure 1-2.	Invasive Coronary Angiography	25
Figure 1-3.	A Normal 12-lead ECG	26
Figure 1-4.	The Simpson's Biplane Method for Assessment of LVEF	28
Figure 1-5.	Development of the Net Magnetisation	31
Figure 1-6.	Generation of the MRI signal using various magnetisations	32
Figure 1-7.	Parameters for T1 and T2-weighted Imaging	35
Figure 1-8.	Likelihood of Functional Recovery of Infarcted Myocardium Based on LGE	39
Figure 1-9.	Typical Patterns of LGE	43
Figure 2-1.	Standard CMR protocol	48
Figure 2-2.	An example of HASTE imaging	50
Figure 2-3.	Manual planimetry to obtain left ventricular mass and function using SSFP cine imaging	53
Figure 2-4.	T2, native T1 and post-contrast T1 maps in a normal patient	54
Figure 2-5.	CMR tagging for assessment of circumferential strain in a healthy control	55
Figure 2-6.	Quantification of late gadolinium enhancement imaging	57
Figure 3-1.	Correlation between LVEF and GCS	65
Figure 3-2.	Correlation between LVEF and LGE Percentage	65
Figure 3-3.	Correlation between GCS and LGE Percentage	66
Figure 3-4.	Incremental Value of CMR Parameters for Prediction of the Primary Outcome Shown by Improvement in Chi-Square	69
Figure 3-5.	Kaplan-Meier Curve For Survival Based on the Optimal LVEF Cut-Off	70
Figure 3-6.	Kaplan-Meier Curve For Survival Based on the Presence of LGE	71
Figure 3-7.	Kaplan-Meier Curve For Survival Based on the Optimal GCS Cut-Off	72
Figure 3-8.	Kaplan-Meier Curve For Survival Based on the Presence of LGE in Patients with LVEF $\geq 35\%$	73
Figure 3-9.	Kaplan-Meier Curve For Survival Based on the Optimal GCS Cut-Off in Patients with LVEF $\geq 35\%$	74
Figure 3-10.	Kaplan-Meier Curve For Survival Based on LVEF, GCS and LGE	75
Figure 4-1.	Summary of the CMR Examination Sequence	83
Figure 4-2.	Derivation of the Study Cohort	85
Figure 4-3.	Correlation Between CMR and CT for Identification of LM	87

Figure 4-4.	CMR Imaging of LM Using The Study Protocol	88
Figure 4-5.	CMR Imaging of Microvascular Obstruction Using The Study Protocol ..	88
Figure 4-6.	Kaplan-Meier Survival Curves by LM status for Prediction of the Primary Outcome	93
Figure 4-7.	Kaplan-Meier Survival Curves by LM status for Prediction of Ventricular Arrhythmia	95
Figure 5-1.	Summary of the Current ESC Heart Failure Guidelines (2012)	101
Figure 5-2.	Typical LGE Patterns	103
Figure 5-3.	Kaplan-Meier curves of the association between the combination of LGE and NT-proBNP for prediction of the primary outcome	113
Figure 5-4.	Kaplan-Meier curves of the association between the combination of LGE and NT-proBNP for prediction of appropriate ICD activation alone	114
Figure 6-1.	The Grey Area Between Athlete's Heart and DCM	122
Figure 6-2.	Typical Patterns using T1 Mapping and Tagging in a Healthy Control and a Patient with Severe DCM	128
Figure 6-3.	Comparison of Native T1 Times	129
Figure 6-4.	Comparison of ECV	130
Figure 6-5.	Receiver-operator Characteristic for Differentiation of Exercisers and DCM Patients	131
Figure 7-1.	The typical electrocardiographic pattern of left bundle branch block	139
Figure 7-2.	Dobutamine Stress Echocardiography in LBBB	144
Figure 7-3.	Computed Tomography in LBBB	147
Figure 7-4.	Study Summary	154
Figure 7-5.	DSE Protocol	156
Figure 7-6.	DSCMR Protocol	156
Figure 7-7.	An example of a patient correctly identified with CAD using DSCMR ..	163
Figure 7-8.	An example of a patient with a septal wall motion abnormality typical of LBBB correctly identified with CAD using DSCMR	164
Figure 7-9.	An example of a false positive septal wall motion abnormality for CAD using DSCMR cine imaging only but correctly identified as not having significant CAD using the comprehensive DSCMR examination	165
Figure 7-10.	The ischaemic cascade and the consequences for diagnostic accuracy of non-invasive imaging techniques	168

List of Tables

Table 1-1.	WHO ICD-10 Classification of Cardiovascular Disease (IX – Disorders of the Circulatory System)	22
Table 3-1.	Baseline Clinical Characteristics	63
Table 3-2.	Reasons for Referral for CMR Assessment	64
Table 3-3.	Baseline CMR Characteristics	64
Table 3-4.	Clinical Predictors of the Primary Outcome	67
Table 3-5.	Multivariable analysis Including CMR Parameters	68
Table 4-1.	Baseline Clinical Characteristics	89
Table 4-2.	Baseline CMR Characteristics	90
Table 4-3.	Univariable Predictors of the Primary Outcome	92
Table 4-4.	Multivariable Predictors of the Primary Outcome	94
Table 5-1.	Baseline clinical and CMR characteristics of the cohort stratified by aetiology	107
Table 5-2.	Clinical and CMR characteristics stratified according to occurrence of the primary outcome	109
Table 5-3.	Hazard ratio and 95% confidence interval for the association between clinical and CMR characteristics and death or ICD activation	110
Table 5-4.	Multivariable analysis for the prediction of death or appropriate ICD activation	111
Table 5-5.	Hazard ratio and 95% confidence interval for the association between optimal discriminatory level of late gadolinium enhancement and NT-proBNP and death or ICD activation	112
Table 5-6.	The New York Heart Association (NYHA) Classification for HF Symptoms	115
Table 6-1.	Baseline clinical and CMR characteristics	126
Table 7-1.	Summary of Advantages and Disadvantages of Non-Invasive Techniques For Investigation of CAD in LBBB	150
Table 7-2.	Baseline characteristics of the cohort	160
Table 7-3.	Haemodynamic data for DSCMR	161
Table 7-4.	Per-patient diagnostic performance of DSE and DSCMR	162
Table 7-5.	Percentage of patients correctly identified per vessel by echocardiography and CMR	166

1. Introduction

1.1. Preamble

Cardiovascular disease (CVD) is a major health burden in the modern era. Increasingly, non-invasive imaging techniques are being used to provide diagnostic and prognostic information that can be used clinically to impact patient management. Cardiovascular magnetic resonance imaging (CMR) is still a relatively new method of non-invasive cardiac investigation, but its value is being increasingly recognised. Nevertheless, it does lack some of the levels of evidence that other, more established, methods such as echocardiography and nuclear imaging have. In this chapter, I shall provide some background to investigation of CVD, before providing more details about CMR. Finally, I shall review the current evidence regarding the clinical use of CMR. In the following chapters, I aim to use CMR to answer important clinical questions that underline the clinical utility of CMR.

1.2. Cardiovascular Disease - Definition and Epidemiology

Cardiovascular disease is a term that covers all disease relating to the heart and vascular system and is a major cause of morbidity and mortality throughout the world. Recognised as a cause of disease throughout history, including by Leonardo da Vinci and William Osler, it has been noted even in the mummified bodies of Egyptian pharaohs (Allam et al., 2009). The commonest CVD conditions are coronary artery disease (CAD) and stroke. In 2010, almost 180,000 people in the UK died of CVD, and over 80,000 died of CAD – the biggest single cause of death in the UK (Townsend N, 2012). Despite an improvement in the CVD mortality in the UK, death rates still remain high compared to other Western European countries. In Scotland, the age-standardised death rate from CVD in 2010 was 126.7/100,000 for males and 68/100,000 for females.

The commonest causes of CVD morbidity include ischaemic heart disease (IHD) – encompassing myocardial infarction (MI – 2009 Scottish incidence 255/100,000 in males, 113/100,000 in females) and angina (48.6/100,000 in males, 37.7/100,000 in females) - and heart failure (HF – 2011 incidence 49/100,000 in males, 29.6/100,000 in females).

CVD encompasses a wide range of conditions, and classification into different types can be done in numerous ways, for example, classifying CVD as congenital or acquired, or ischaemic and non-ischaemic. Perhaps the most structured but broad method is that

Chapter 1: Introduction

proposed by the World Health Organization (WHO) in their International Statistical Classification of Diseases and Related Health Problems 10th Revision (ICD-10) which essentially divides CVD into 9 categories (table 1.1) (Organization, 2010).

Table 1-1. WHO ICD-10 Classification of Cardiovascular Disease (IX – Disorders of the Circulatory System)

Code	Group	Example sub-categories
I00-I09	Rheumatic diseases	Acute rheumatic fever Chronic rheumatic heart disease
I10-I15	Hypertensive heart disease	Essential hypertension Secondary hypertension Hypertensive heart disease
I20-I25	Ischaemic heart disease	Angina pectoris Unstable angina Acute MI Ischaemic cardiomyopathy
I26-I28	Pulmonary vascular disease	Pulmonary embolism Pulmonary hypertension
I30-I52	Other cardiac disease	Pericardial disease Endocarditis Valvular heart disease (non-rheumatic) Myocarditis Cardiomyopathies Heart failure Arrhythmias
I60-I69	Cerebrovascular disease	Cerebral haemorrhage Cerebral infarction
I70-I79	Arterial/capillary disease	Atherosclerosis Aortic aneurysm Peripheral vascular disease
I80-I89	Venous disease	Deep vein thrombosis
I95-I99	Other	Hypotension

Many of these conditions are encountered by and dealt with by cardiologists. Notably, congenital heart conditions are classified separately (with other congenital diseases), perhaps reflecting their specialist nature.

CVD accounts for a large proportion of all hospital activity. In 2009-2010, over 90,000 admissions to hospital in Scotland were due to heart disease specifically (Scotland, 2012) and total spending on cardiology services was £146 million, a 50% real-terms increase since 2002.

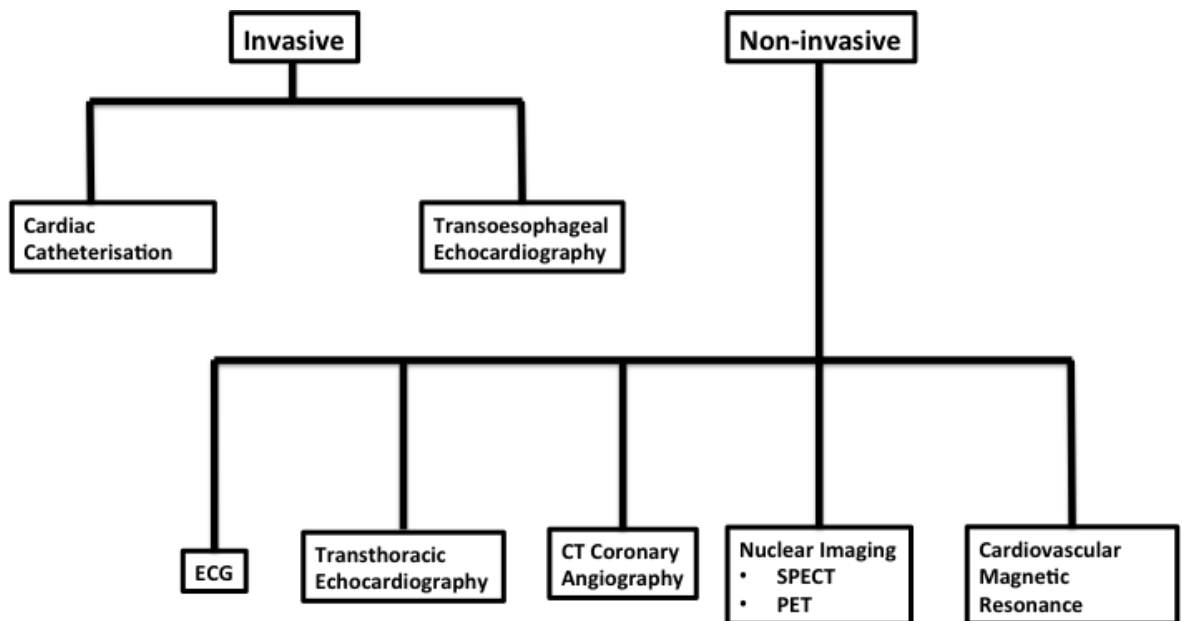
Given the burden in mortality and morbidity, as well as the cost of CVD, timely diagnosis and intervention is paramount.

1.3. Investigation of Cardiac Disease

1.3.1. Overview

Following the initial evaluation of the patient by taking a detailed history (identifying the patient's current issues, risk factors etc.) and examination, the next step is usually directed to investigations in order to arrive at a diagnosis and formulate an appropriate management plan. Cardiac investigations can be divided into 2 categories – invasive and non-invasive (figure 1-1).

Figure 1-1. Cardiac Investigations



In 1992 Fryback and Thornbury described the hierarchical model of diagnostic efficacy which defines six levels of evidence to underscore the use of diagnostic techniques as follows (Fryback and Thornbury, 1991):

1. *Technical efficacy*: These studies are commonly case reports or small case series that describe the methodology of the technique and seek to refine it.
2. *Diagnostic accuracy efficacy*: These studies seek to determine the diagnostic accuracy of the technique, for example sensitivity and specificity.
3. *Diagnostic thinking efficacy*: Studies in this category aim to help the referring clinician decide in which patient population the technique might have most benefit, for example whether to use the test in a low or high-risk population.
4. *Therapeutic efficacy*: These studies simply ask the question: does doing the test change patient management? Levels 2-4 can be combined as clinical efficacy measures.
5. *Patient outcome efficacy*: Do the benefits to the patient of the procedure outweigh the risks? Measures can include quality of life and cost.
6. *Societal efficacy*: Do the benefits of the procedure outweigh the costs to society?

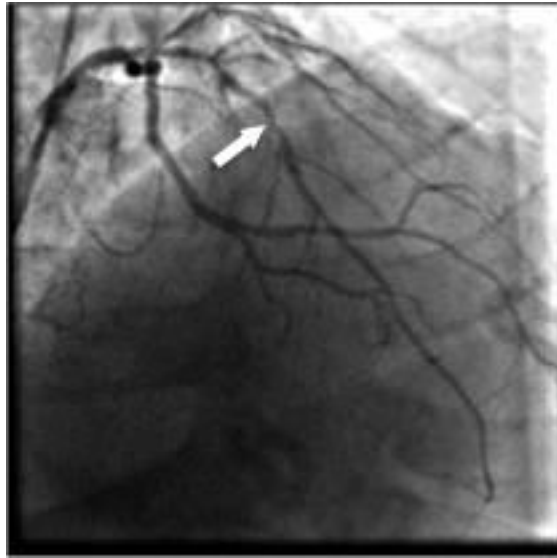
All of the investigations listed in figure 1-1 have large amounts of evidence to support their use, although (as one would expect), the older techniques such as cardiac catheterisation, echocardiography and SPECT have the most evidence behind them and numerous studies at levels 5 and 6, while newer techniques such as CT, CMR and PET remain at levels 2-4.

1.3.2. Invasive Cardiac Investigations

The commonest invasive cardiac investigation is cardiac catheterisation. Over 15,000 procedures are carried out each year in Scotland (Scotland, 2012). Cardiac catheterisation was first developed by Forssmann in 1929 who cannulated his antecubital fossa, guided a catheter up to his right atrium by fluoroscopy and took an X-ray to confirm the procedure. Following refinements to the procedure over the next decade, Forssmann was awarded the Nobel Prize for Physiology and Medicine in 1958 (along with Andre Cournand and Dickinson Richards) (Heiss, 1992). Cardiac catheterisation is actually two different procedures – left heart catheterisation, commonly carried out to assess the coronary arteries by angiography, and right heart catheterisation, which is usually conducted to assess cardiopulmonary haemodynamics in the setting of valvular heart disease, pulmonary vascular disease or congenital heart disease. Both techniques are carried out using local anaesthetic before cannulation of the required vessel – for left heart catheterisation this an artery (radial or femoral artery) while for right heart catheterisation the venous system is used (usually via the femoral vein). Catheters are then passed up to the heart using

fluoroscopic guidance. In left heart catheterisation the coronary arteries are selectively cannulated and contrast injected to identify the presence of significant CAD. Balloons and stents can then be introduced during the procedure (known as angioplasty) in order to fix flow-limiting stenoses.

Figure 1-2. Invasive Coronary Angiography



Invasive coronary angiogram showing a flow-limiting stenosis in the left anterior descending artery (arrow).

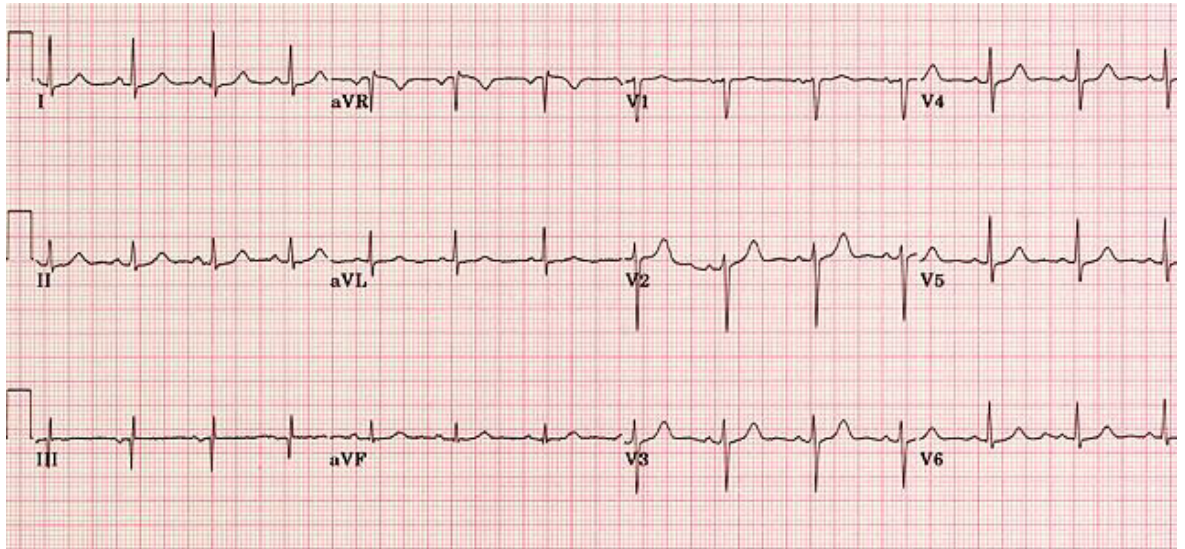
A large amount of level 6 evidence exists to support the use of invasive coronary angiography (ICA) and it is now a standard recommendation in numerous guidelines including in the setting of ST elevation myocardial infarction (Steg et al., 2012), non-ST elevation myocardial infarction (Hamm et al., 2011) and stable angina (Montalescot et al., 2013) amongst others. Adjunctive diagnostic tools can be added to ICA including pressure wire assessments (e.g. fractional flow reserve - FFR) to assess the significance of coronary stenoses (De Bruyne et al., 2012) and intracoronary imaging such as intravascular ultrasound (Parise et al., 2011) and optical coherence tomography (Bezerra et al., 2013).

1.3.3. Electrocardiography (ECG)

The ECG is the most basic and widely available non-invasive cardiac investigation. Waller recorded the first ECG in 1887, consisting of only 2 leads (Hurst, 1998), and it has been refined over the last century to become the standard 12-lead reading that is in widespread clinical use today. Various parameters and abnormalities have diagnostic and prognostic

value, and the ECG is an essential first part of the evaluation of any cardiac patient (De Bacquer et al., 1998a, De Bacquer et al., 1998b) (figure 1-3).

Figure 1-3. A Normal 12-lead ECG



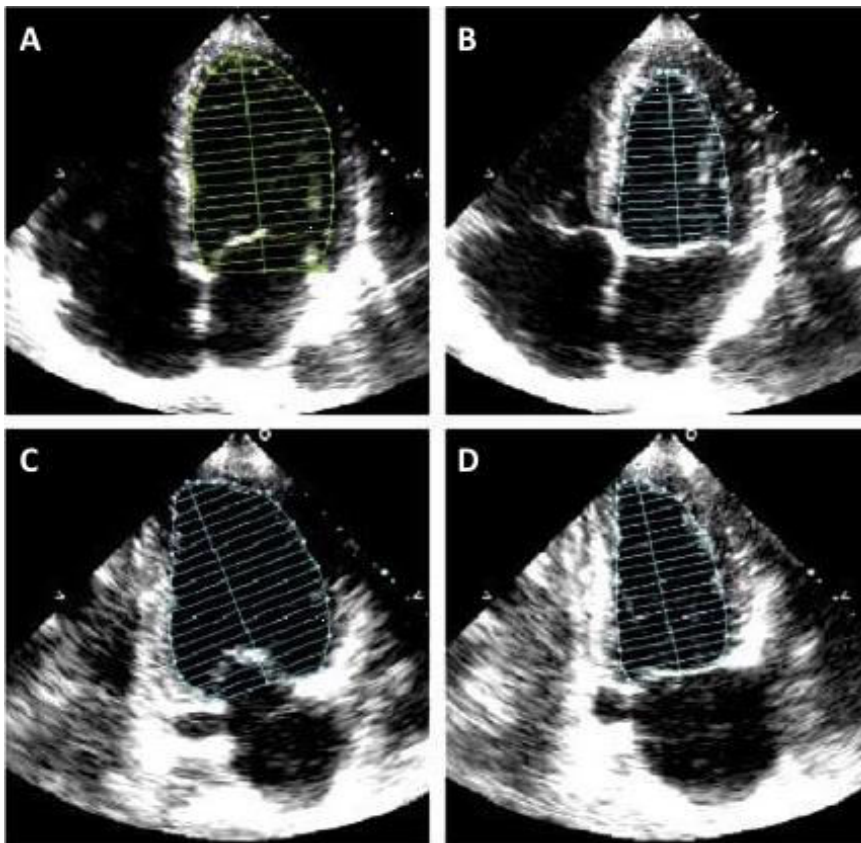
The ECG can be taken during exercise (exercise tolerance test – ETT). Changes during exercise can be predictive of the presence of ischaemia caused by significant coronary stenoses (Ashley et al., 2000), however its diagnostic accuracy is reduced in women and patients with resting ECG abnormalities which can make it difficult to know the significance of any exercise-induced changes (Montalescot et al., 2013), thus leading to the requirement of other investigations.

1.3.4. Echocardiography

The echocardiogram (echo) is a non-invasive test that uses ultrasound to image the heart. Either a transthoracic echo (TTE) or transoesophageal echo (TOE) can be performed, although only the TTE is non-invasive. It is cheap, portable and widely available and hence it is often the first investigation performed after the ECG. Using various views of the heart, cardiac chamber dimensions, volumes and function can be measured and valvular heart disease can be quantified (for which echo assessment is the gold-standard (Vahanian et al., 2012)). Left ventricular ejection fraction assessment by two-dimensional echocardiography has been shown to be an extremely powerful predictor of adverse outcome in several groups of patients, including post-MI (Sutton et al., 1994) and in idiopathic dilated cardiomyopathy (DCM) (Likoff et al., 1987).

Nevertheless, measurement of ejection fraction using two-dimensional TTE does have limitations. Firstly, it is not always possible to obtain adequate views of the heart due to patient body habitus or the positioning of the heart behind the ribs. Secondly, the measurement technique itself is limited as it relies on an approximation of the true shape of the heart. The standard technique used for assessment of left ventricular ejection fraction (LVEF) is known as Simpson's biplane. This uses the apical four-chamber and two-chamber views of the heart to measure end-systolic and end-diastolic volumes to estimate the ejection fraction (figure 1-4). This method is subject to limitations such as the difficulty in tracing the endocardial borders of the heart, and in patients with arrhythmias such as atrial fibrillation. Simpson's biplane technique is subject to a standard deviation of around 8.5% compared to the true ejection fraction (Otterstad et al., 1997), which can make a large difference to the management of patients, for example in patients with severe left ventricular systolic dysfunction (LVSD) in whom there are strict criteria, based on LVEF, for implantation of potentially life-saving therapies such as implantable cardioverter-defibrillators (ICDs) (McMurray et al., 2012).

Figure 1-4. The Simpson's Biplane Method for Assessment of LVEF



Assessment of LVEF using Simpson's Biplane. The endocardial borders are traced in both end-systole and end-diastole in both 4-chamber (A, B) and 2-chamber views (C, D).

Several techniques for improving the accuracy and reproducibility of LVEF measurement using echocardiography have been developed including 3-dimensional echocardiography (Jenkins et al., 2004), use of contrast (Olszewski et al., 2007) and deformation imaging (Marwick, 2006). Nevertheless, these techniques require more specialist expertise, are not as widely available as standard two-dimensional echo, and are still subject to some of the same image quality issues as basic TTE (Thomas et al., 2009).

1.3.5. Nuclear Imaging

Nuclear imaging (in cardiology) is most commonly used for myocardial perfusion imaging for the assessment of suspected angina, performed using single photon emission tomography (SPECT). A radioactive tracer is administered which is taken up by myocardium. Under stress (which can be induced by exercise or pharmacologically) any areas of myocardium subtended by ischaemic coronary arteries have reduced blood flow in comparison to myocardium supplied by healthy coronary arteries and hence a perfusion

defect is seen. One disadvantage of this technique is that (dependent on the tracer) the patient may have to return several days later for rest imaging due to the half-life of the tracer. SPECT has extremely good diagnostic accuracy for diagnosis of significant CAD (Elhendy et al., 2002) as well as being of excellent prognostic value (Hachamovitch et al., 1998). SPECT can also be used to measure LVEF with good accuracy (Tadamura et al., 1999). SPECT is limited however by its use of radiation, and its less widespread availability in the UK.

1.3.6. Multislice CT Coronary Angiography (CTCA)

Computed tomographic (CT) techniques have recently been optimised to allow coronary angiography assessment, which remains its main application in cardiology. CT has excellent spatial resolution allowing for good anatomical definition, although the 64-slice CT scanners in routine clinical use are not quite as good as ICA as yet (Piers et al., 2008). CT allows for non-invasive visualisation of epicardial coronary artery stenoses using contrast. CTCA has excellent diagnostic accuracy for identification of coronary stenoses (Budoff et al., 2008, Miller et al., 2008, Meijboom et al., 2008), and potentially may have an impact on clinical decision-making by reducing the number of unnecessary invasive angiograms, saving money and reducing the risk to patients of an invasive procedure (Chow et al., 2009).

CTCA does have some limitations however. The use of ionising radiation potentially increases the future risk of cancer, especially in younger women (due to breast tissue) (Einstein et al., 2007). This might limit its use in serial assessment of the cardiovascular system. Furthermore, the diagnostic accuracy of CTCA decreases with increasing levels of calcium within the coronary vasculature. While evaluation of the amount of calcium within the coronaries (the calcium score) is a predictor of adverse cardiovascular outcome in itself (Hou et al., 2012, Xie et al., 2013), increased levels of calcium make it difficult to ascertain the severity and significance of any CAD. For this reason CTCA is only currently recommended in patients with a low pre-test probability for CAD, essentially as a “rule-out” test (Montalescot et al., 2013, Skinner et al., 2010). The addition of perfusion imaging (Ko et al., 2012a) or CT-FFR assessment (Norgaard et al., 2014) might in future widen the population in whom CTCA might be used.

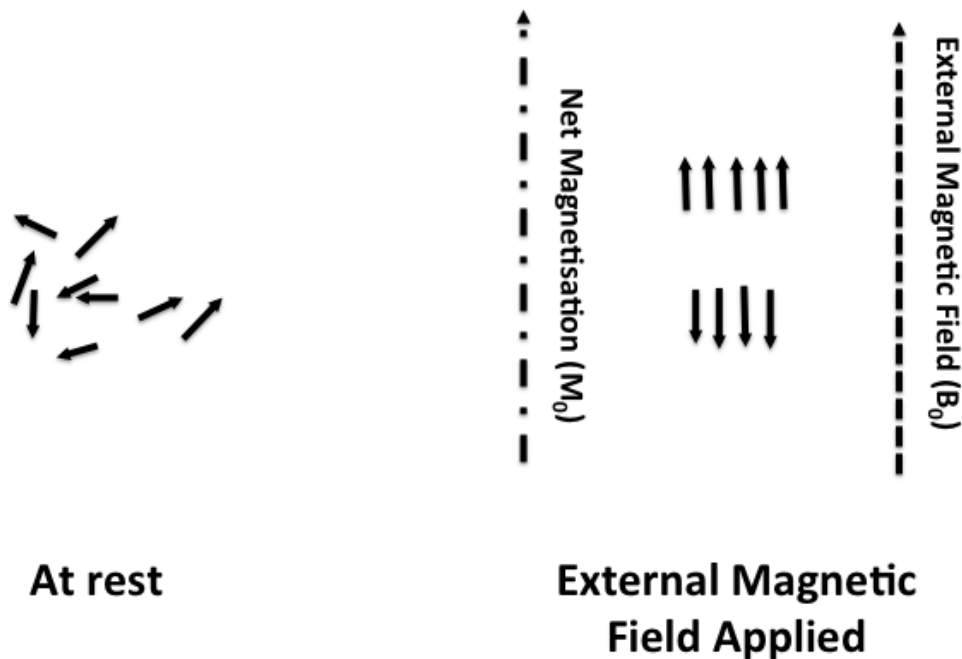
1.4. Cardiovascular Magnetic Resonance (CMR)

1.4.1. Background

CMR refers to the specific use of magnetic resonance imaging (MRI) in the heart. MRI uses the phenomenon of nuclear magnetic resonance (NMR), which was first described in 1938 by Isidor Rabi who was awarded the Nobel Prize for Physics for his work in 1944 and further developed by Felix Block and Edward Purcell, who were awarded the Nobel Prize for Physics in 1952. NMR is refers to the process by which atomic nuclei (the core of the atom composed of protons +/- neutrons) absorb and radiate electromagnetic radiation when placed within a magnetic field. The first use of MRI was reported by Raymond Damadian in 1971 who used NMR in vivo to distinguish between cancerous and healthy tissues (Damadian, 1971), while John Mallard developed the first full body MRI scanner in Aberdeen during the 1970s.

Any atomic nucleus with an odd number of protons and neutrons (such as hydrogen - ^1H , carbon - ^{13}C , sodium - ^{23}Na and phosphorus - ^{31}P) has an intrinsic property known as “spin”. This causes each nucleus to generate a small magnetic field. In isolation this field is negligible, however when put together these can be measured and used in MRI. Due to the large amount of hydrogen contained within water and fat in the body, ^1H is extremely useful for MRI. While these nuclei all spin in different directions normally, when a strong external magnetic field is applied, the nuclei align to precess either towards or against the magnetic field (given the symbol B_0 ; figure 1.5). A slight majority of the nuclei precess towards the direction of the field (known as the net magnetisation, referred to as M_0).

Figure 1-5. Development of the Net Magnetisation



The size of M_0 is determined by the strength of the magnetic field, measured in Tesla (T). The commonest magnetic field strength used in clinical CMR is 1.5T, around 20,000 times the strength of the Earth's magnetic field. The stronger the magnetic field, the greater net magnetisation and subsequent image contrast.

1.4.2. Generation of the MR Image

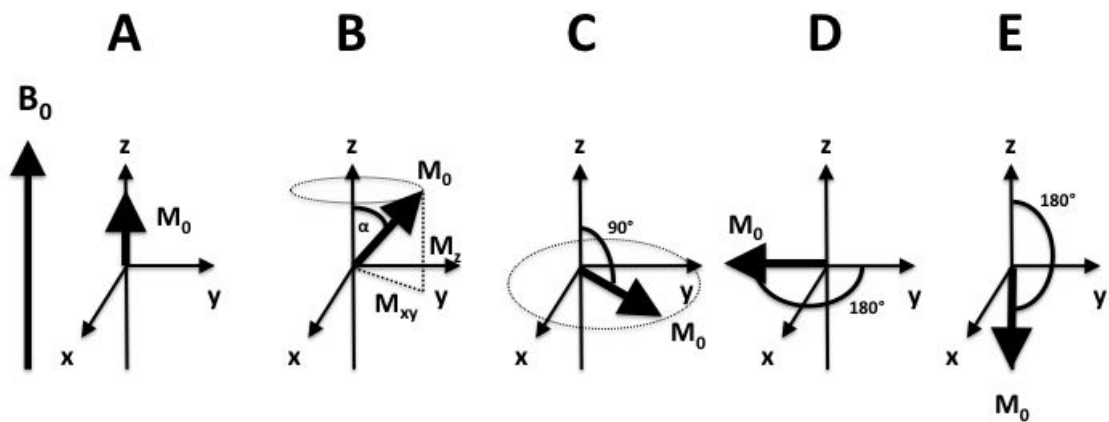
The typical MRI scanner consists of 3 main components – the main magnet which generates a constant magnetic field, usually using a superconductor cooled with liquid helium; 3 gradient coils which generate a signal along the direction of B_0 but can change its strength along one of three directions known as the x, y and z axes; and a radiofrequency (rf) coil which is closest to the patient and generates a smaller magnetic field (B_1) that combines with the main magnetic field to create the signal used to form an image. A receiver coil is also used in CMR to pick up the signal generated during the process.

The generation of an MRI image can be summarised in 5 steps:

1. The patient enters the MRI scanner – all nuclei are exposed to the external magnetic field and align along B_0 creating a net magnetisation.
2. This magnetisation is changed away from the direction of the main magnet by applying an rf pulse (radiofrequency excitation). The angle of change is known as the flip angle.
3. The magnetisation then returns to its resting (equilibrium) state, known as relaxation. The receiver coil collects the signals emitted during relaxation. This process is repeated numerous times.
4. The gradient coils are used to apply various magnetic field gradients to localise the signal from the body.
5. All the signals generated are collected as data called the “k-space” and changed into an image using a mathematical process called Fourier transformation.

Steps 2 and 3 are summarised in figure 1-6.

Figure 1-6. Generation of the MRI signal using various magnetisations (adapted from Ridgway et al. (Ridgway, 2010))



The resting (equilibrium) state is shown in figure 1.6A. This is when the net magnetisation, M_0 (caused by the main magnet) is directly aligned along the plane of the magnet (B_0). If an rf pulse of any number of degrees is applied, the net magnetisation vectors aligns along that angle. This is known as the flip angle (α ; figure 1.6B). If the flip angle is 90° , the net magnetisation tips completely into the xy plane (figure 1.6C). The protons continue to precess around the z axis at a specific frequency known as the Larmor frequency. This is approximately 64MHz at 1.5T. At this point the sequence is said to be fully saturated. This pulse is used for spin-echo sequences. A further 180° pulse can be applied

in a spin-echo sequence, known as a refocusing pulse (figure 1.6D). The specific advantage of this extra pulse is that it removes any dephasing caused by inhomogeneities in the magnetic field, allowing enhanced T2-weighted imaging. A 180° pulse can also be applied when the net magnetisation is at equilibrium (figure 1.6E). This sequence is used in black-blood imaging. This extra pulse (an inversion pulse) nulls the signal from all tissue and blood outwith the slice to be imaged. There is then a time delay until the spin-echo pulse sequence is applied (the inversion time; TI). This allows the blood with inverted magnetisation to pass into the slice to be imaged, appearing dark. This gives the improved contrast seen in black blood imaging.

A slice to be imaged is selected by applying a gradient magnetic field at the same time as applying the rf pulse. A phase encoding gradient is applied in which the protons at higher magnetic field strength have a higher frequency of precession and those where the gradient decreases the field strength have their precession frequency decreased. The gradient is then switched off. The protons will then have changed their relative phase by an amount related to their position along the gradient. A frequency-encoding gradient is then applied at 90° to the phase-encoding gradient, causing the protons to precess at different frequencies dependent on their location along the gradient. After the initial rf pulse (figure 1.6C), the protons begin to dephase and lose coherence. If a further gradient magnetic field is applied in the opposite direction but in the same plane as the original rf pulse, this causes an echo to be applied by rephasing the echo. This causes a reduction in signal decay and increases the amplitude of the signal and is known as gradient echo imaging. The time from the initial rf pulse to the maximal amplitude of the gradient echo signal is known as the echo time (TE).

The signal generated by frequency encoding is analysed using Fourier transformation. Fourier transformation can only be used if data is available for several time points, hence to analyse the phase-encoding sequence, all 3 sequences (slice selection, phase-encoding and frequency-encoding) are repeated at various intervals with the same parameters except different phase-encoding gradients. The time interval is known as the repetition time (TR). Then Fourier transformation can be applied to phase-encoding as well, allowing image generation.

During CMR, all images are synchronised with the ECG. To take a real-time image, the TR can be reduced in order to take as many images as possible, however this limits the

spatial resolution. Therefore, images are taken either at a particular point in the cardiac cycle, or over a number of heartbeats at various points within the cardiac cycle and combined into one to make in “cine” image.

1.4.3. T1, T2 and T2* Imaging

After the rf pulse, M_0 returns to the equilibrium state (B_0). This involves 2 processes:

1. Loss of (transverse) phase coherence (T2 relaxation) – movement out of the xy plane.
2. Recovery of longitudinal magnetisation (T1 relaxation) – reversion to the z axis.

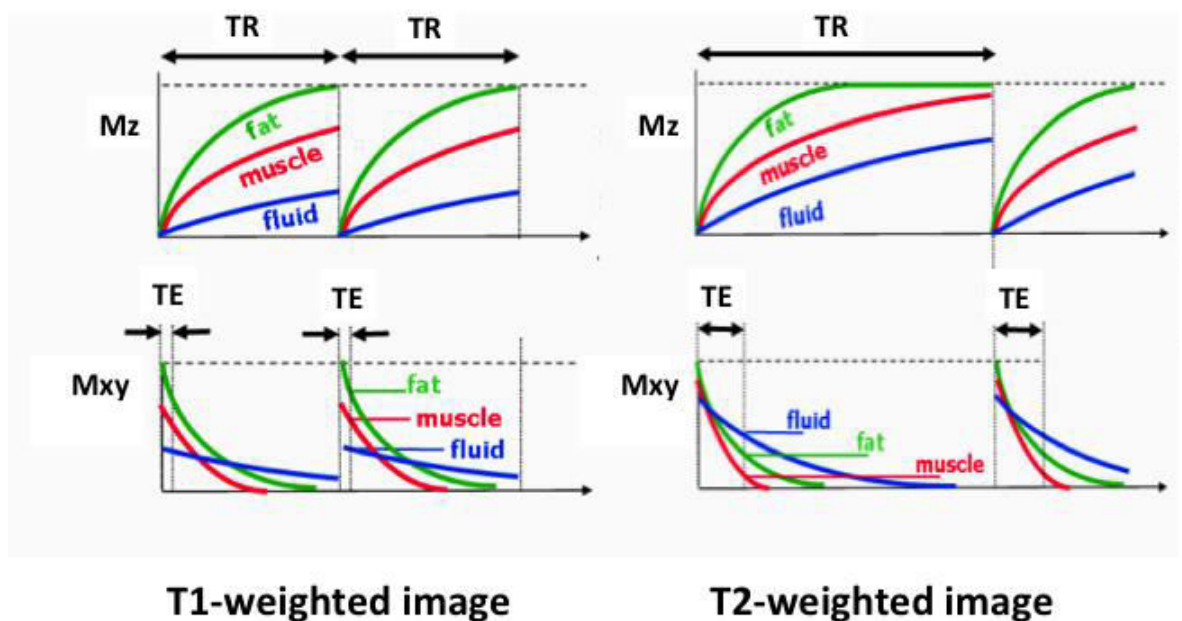
T1 (longitudinal) relaxation is a (relatively) slow exponential process. T1 times are typically 500-1500ms. T2 (transverse) relaxation is typically faster, occurring after less than 100ms. T2 relaxation has two components. Firstly, the interactions between the protons cause them to lose phase coherence so they do not precess around the xy plane together. This is known as T2 relaxation due to spin-spin interaction. Secondly, inhomogeneities within the magnetic field, causing differences in the Larmor frequency, hence the protons precess at different frequencies and also lose phase coherence. In combination with T2 relaxation, this is known as T2* relaxation and is particularly useful in situation where there might be a lot of ferromagnetic signal, for example in iron overload cardiomyopathy, as these field inhomogeneities are more pronounced.

T1 relaxation is affected by the tissue surrounding the protons. Energy is released from the protons as they return to equilibrium, and this is more favourable when the surrounding molecules are moving at a rate similar to the Larmor frequency (64MHz). Fat molecules move near to this frequency and so has a short T1, while water molecules, being smaller, move faster and have a longer T1. Muscle also has a long T1. Intravenous extracellular contrast agents such as gadolinium act to shorten the T1 time.

T2 relaxation is mainly due to the size and position of the molecules. As water has small molecules that move quickly and are far apart, the opportunities for interaction between the molecules are less and so the T2 values are higher than in fat, which has larger molecules.

Both T1 and T2-weighted imaging can be performed using spin-echo or gradient-echo. T1-weighted imaging is produced by using a short TR and short TE. The short TE reduces the differences caused by T2 relaxation, ensuring that the difference in contrast is caused by T1 relaxation. Fat typically appears bright and fluid dark. T2-weighted imaging parameters include a long TR and long TE, reducing T1 signal and emphasizing T2 signal differences. Muscle appears dark due to its short T2, while fluid appears bright (figure 1-7).

Figure 1-7. Parameters for T1 and T2-weighted Imaging (adapted from Ridgway et al. (Ridgway, 2010))



1.5. The Clinical Utility of CMR - Current Knowledge

CMR has two major advantages over other non-invasive imaging modalities. Firstly, it has excellent spatial resolution, due to the various sequences used, and has excellent anatomical definition. This, combined with the lack of interference by body habitus that echocardiography is subject to, make it the current gold-standard for assessment of cardiac structure, size and function. Secondly, with the assessment of T1 and T2 signal, CMR is able to characterize the myocardium beyond any other non-invasive imaging modality. I shall now proceed to review the current clinical use of these advantages in CMR.

1.5.1. Acute Myocardial Infarction

The main limitation with the use of CMR in acute myocardial infarction (AMI) is that it is a time-consuming test that requires the patient to remain still, breath-hold and also leave the monitored environment of the ward or coronary care unit. Even so, there are some data to suggest that CMR is safe in the situation of acute MI. In an early study by Plein et al, 72 patients with a clinical diagnosis of acute non-ST elevation MI (NSTEMI) underwent CMR within 72 hours of presentation. 68 patients underwent the test without any adverse events occurring while 1 was intolerant of adenosine given during the procedure and 2 were claustrophobic. One patient was found not to have had an MI and was excluded (Plein et al., 2004). The safety of CMR in the acute situation was also demonstrated in patients with acute ST elevation MI (STEMI) by Greenwood et al. who evaluated 35 patients with 2-8 days post-admission without any clinically significant adverse events occurring (Greenwood et al., 2007).

These studies also provided evidence of the diagnostic accuracy of CMR in patients with AMI. Plein et al found that a comprehensive CMR protocol had a 94% diagnostic accuracy for prediction of significant coronary stenoses (i.e. identification of the culprit artery) in NSTEMI, while Greenwood et al. reported an 89% diagnostic accuracy in their cohort of STEMI patients. The excellent spatial resolution and signal to noise ratio of CMR allows confident identification of regional wall motion abnormalities. The use of intravenous gadolinium contrast, an extracellular contrast agent, allows identification of myocardial damage when T1-weighted imaging is performed 10 minutes after the injection. When the images are taken from this sequence, known as late gadolinium enhancement (LGE) imaging, normal myocardium appears dark due to the absence of contrast as there is minimal extracellular volume (ECV). In areas of myocardial fibrosis there is more ECV and so gadolinium is retained, causing shortening of the T1 signal, hence the areas of fibrosis appear brighter than the normal myocardium. The presence of LGE has been shown to correlate excellently with histological fibrosis in various cardiac conditions (Mewton et al., 2011). In a study of 161 patients, a comprehensive CMR examination including LGE imaging was found to be a better diagnostic tool than ECG, troponin and a clinical risk score (the Thrombosis In Myocardial Infarction score) for identification of patients with AMI, with wall motion being the best diagnostic tool (Kwong et al., 2003, Eitel et al., 2010).

With use of LGE imaging, CMR is able to accurately quantify the extent of myocardial damaged caused by the infarct. Both scar size and transmural extent of infarction have both been shown to provide prognostic information for prediction of adverse events. CMR is also able to specifically characterise the structure of the infarct zone. Hypointense areas within the bright area of LGE reflect areas of microvascular obstruction (MVO), thought to represent thrombus and haemorrhage into the infarct zone which is often associated with percutaneous coronary intervention, and also portend an adverse prognosis (Wu et al., 1998, Klug et al., 2012). MVO can also be seen during first pass perfusion imaging, where images are acquired immediately after the intravenous injection of gadolinium (Wu, 2012, Yan et al., 2006a). MVO again appears as a hypointense area using this sequence, where the contrast does not immediately penetrate into the infarcted and obstructed area of the myocardium due to the impaired blood flow.

One advantage of CMR in the acute setting is in diagnosis of patients with chest pain and evidence of myocardial damage (for example elevations of cardiac biomarkers such as troponin) but with normal invasive coronary angiograms. CMR is able to provide a definitive diagnosis in this group of patients, allowing appropriate management and/or reassurance to be offered to the patient. Patients with other conditions such as myocarditis or Takotsubo cardiomyopathy can be given a more definitive diagnosis non-invasively, while CMR also has the ability to pick up small infarcts caused by embolus or plaque rupture, despite normal invasive angiography (Assomull et al., 2007).

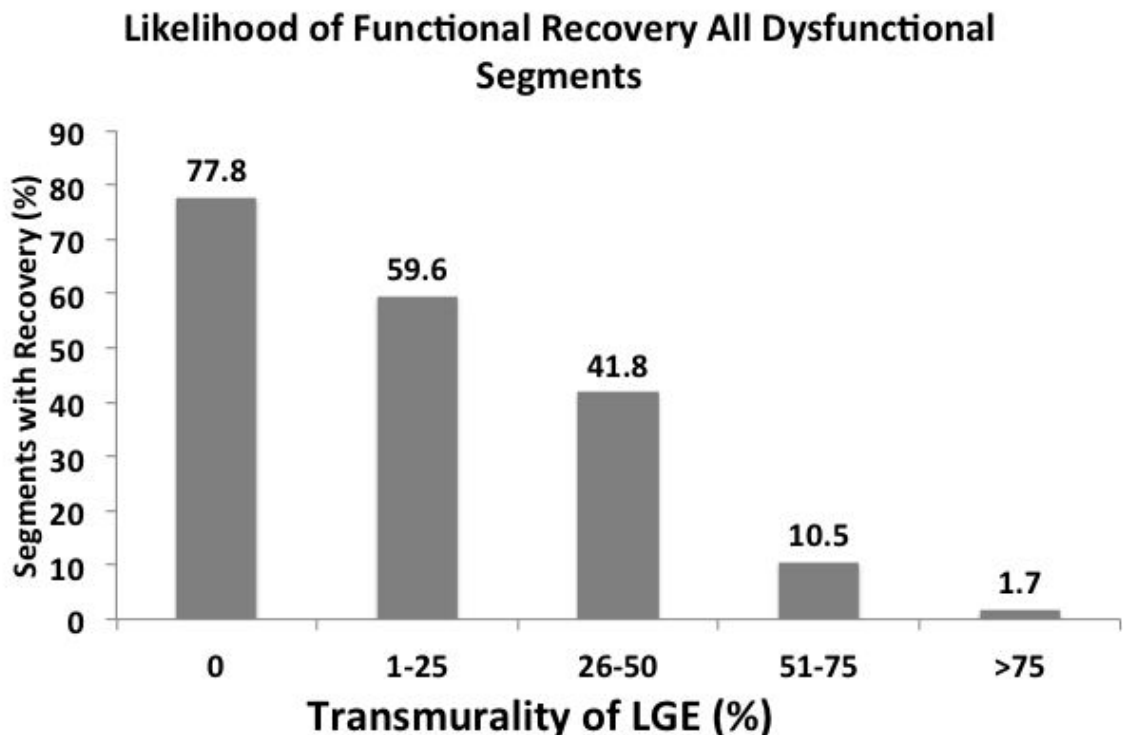
The use of T2-weighted imaging allows assessment of areas of increased water content (oedema, reflected by high T2 signal), caused by the occluded artery. In the context of AMI, this reflects the area-at-risk (AAR) of myocardial infarction. This is useful in both a clinical and research context. Myocardial oedema tends to persist for approximately 4 weeks after the initial injury, hence this can be used to differentiate between acute and chronic MI. Abdel-Aty et al. evaluated 73 patients and found that use of T2-weighted imaging was able to differentiate between acute and chronic infarcts with 96% sensitivity (Abdel-Aty et al., 2004). Areas with high T2 signal but without LGE reflect myocardium with reversible damage that would hopefully recover function with appropriate therapy. Measurement of the AAR compared to the infarct size (myocardial salvage index = (AAR-infarct size)/AAR) has been shown to be a good predictor of the likelihood of functional recovery and major adverse cardiovascular events (Eitel et al., 2010). Infarct size and

myocardial salvage index is now commonly used as an end-point in clinical trials in AMI patients (Carrick et al., 2014).

1.5.2. Chronic Ischaemic Cardiomyopathy

CMR has an increasingly invaluable role in the assessment of patients with chronic IHD. LVEF is a powerful prognostic indicator in patients with heart failure of any cause including those with prior MI (Wong et al., 2004). As the gold-standard non-invasive method of measuring LVEF, CMR can be used as a reliable and reproducible means of assessment (Grothues et al., 2004). This is especially important in treatment decisions, for example the decision to implant lifesaving but expensive defibrillator therapies (implantable cardioverter-defibrillators; ICDs), which is in a large part based on the LVEF (McMurray et al., 2012). CMR also allows clear assessment of regional function of the myocardium due to the excellent contrast definition of the myocardium-blood signal. End-diastolic wall thickness $<6\text{mm}$ has been shown to be diagnostic of infarcted tissue that is non-viable (unlikely to recover function even if revascularised) (Schinkel et al., 2005). The transmural extent of LGE has been shown to be an even better predictor of viable myocardium, as shown in a seminal paper by Kim et al. (figure 1-8) (Kim et al., 2000). A meta-analysis by Romero et al. showed that having minimal LGE ($<50\%$) has $>90\%$ sensitivity for prediction of viable myocardium (Romero et al., 2012).

Figure 1-8. Likelihood of Functional Recovery of Infarcted Myocardium Based on LGE (adapted from Kim et al (Kim et al., 2000))



In this meta-analysis the authors also found that low-dose dobutamine stress CMR (DSCMR) was also useful – segments that showed improvement in function at low-dose dobutamine (typically 10 mcg/kg/min) were likely to be viable with 91% specificity. Viability assessment by nuclear imaging and stress echocardiography has been shown to not improve outcomes in a large multi-centre trial, the Surgical Treatment for Ischemic Heart Failure (STICH) trial, however the use of a comprehensive CMR protocol has yet to be tested in in such a study (Bonow et al., 2011)

Similar to AMI, the presence of LGE has proven to be a predictor of mortality and ventricular arrhythmias in patients with chronic IHD, in both patients with a documented history of MI (Yokota et al., 2008) and those without (Kwong et al., 2006, Cheong et al., 2009). The presence of hibernating, viable myocardium assessed by low-dose DSCMR has also been shown to be an independent indicator of good prognosis (Kelle et al., 2009).

CMR also provides further infarct tissue characterisation. As well as identifying areas of MVO, assessment of the heterogeneity of the infarct has also been shown to be an independent prognostic indicator. Commonly, the presence of LGE has been measured in

areas that have signal intensity 2-5 standard deviations above remote, non-injured myocardium. This area is commonly described as the infarct core. The size of areas of myocardium with signal intensity between the core and the remote myocardium, known as the grey zone, has been shown to predict ventricular arrhythmias (Roes et al., 2009, Wu et al., 2012, Yang et al., 2013). This is thought to be due to aberrant conduction in this area of infarcted tissue mixed with healthy myocardium. The use of CMR has also identified areas of fatty change within infarct scar, known as lipomatous metaplasia and previously only seen in pathological specimens, which might also be associated with arrhythmias (Lucke et al., 2010, Pouliopoulos et al., 2013)

1.5.3. Stable Angina

Stress CMR is now recommended in most guidelines as one of the non-invasive imaging tools that can be used to investigate patients with suspected angina. Stress CMR is most commonly performed using adenosine (for assessment of perfusion) or dobutamine (for assessment of wall motion).

During dobutamine stress CMR (DSCMR), wall motion is assessed at incrementally increases of dobutamine (typically 10, 20, 30 and 40 mcg/kg/min). Typically, one would see an increase in contractility of an ischaemic segment at low dose and then a decrease in contractility at high dose due to decreased coronary flow reserve. In a meta-analysis of 754 patients, DSCMR had a sensitivity of 83% and a specificity of 86% for identifying patients with significant CAD with ICA as the reference standard (Nandalur et al., 2007). The addition of assessment of perfusion during stress has also been shown to incrementally improve diagnostic performance (Lubbers et al., 2008, Gebker et al., 2008), as has the quantitative assessment of wall motion using tagging to analyse myocardial strain and deformation (Kuijpers et al., 2003, Korosoglou et al., 2010).

Adenosine perfusion stress CMR has also shown similar diagnostic accuracy. In the same meta-analysis by Nandalur et al., the authors found the technique had a sensitivity of 91% and a specificity of 81% in 1,516 patients (Nandalur et al., 2007). Clinicians may be more comfortable using adenosine rather than dobutamine, as it generally has a lower risk profile. Adenosine stress CMR has been evaluated in two large trials. MR-IMPACT compared adenosine stress CMR and SPECT against ICA in 241 patients and found that CMR performed as well as SPECT, although this was a sub-analysis of a larger trial

(Schwitter et al., 2008). This led to a larger, prospectively designed study, CE-MARC (Greenwood et al., 2012). In this study 752 patients underwent adenosine stress CMR and SPECT, again with ICA as the diagnostic standard. The results demonstrated the superiority of CMR over SPECT in this scenario, with CMR having a sensitivity of 86.5% and specificity of 83.4% compared to SPECT which had a sensitivity of 66.5% and a specificity of 82.6%.

Both dobutamine and adenosine stress CMR also provide prognostic information. A negative stress CMR appears to herald a good prognosis. In a meta-analysis of 11,636 patients who underwent stress CMR (of either modality), patients with ischaemia had a significantly higher risk of cardiovascular death or MI with an annualised event rate of 4.9% compared to 0.8% in patients with a negative study (Lipinski et al., 2013).

1.5.4. Dilated Non-Ischaemic Cardiomyopathy

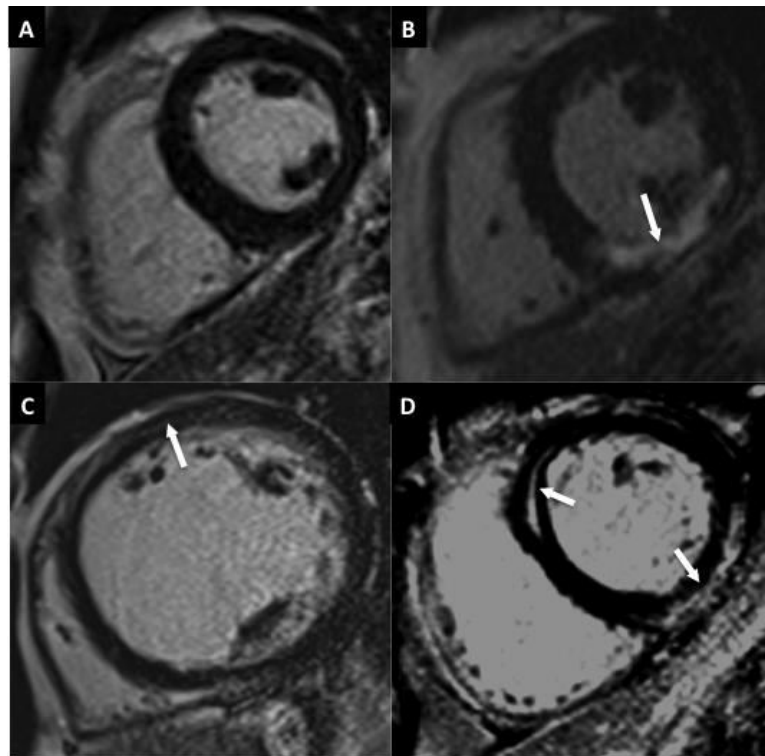
Dilated non-ischaemic cardiomyopathy (DCM) is the final common pathway of a number of conditions, but its phenotype is characterised by a dilated left ventricle with reduced ejection fraction. As with ischaemic cardiomyopathy (ICM), accurate assessment of LVEF has an important role in risk stratification (Rayatzadeh et al., 2013, Taylor et al., 2013). In up to 50% of cases of DCM the aetiology remains unknown, while patients with ICM may also have dilated left ventricles. This often leads to ICA being undertaken which may be unnecessary as there is no significant CAD. The use of CMR to identify the presence of the typical ischaemic pattern of LGE (subendocardial or transmural) appears to be a good tool to act as a gatekeeper to ICA and potentially prevent unnecessary ICA (Assomull et al., 2011).

Typically, patients with DCM will have either no LGE at all, or a midwall line of LGE (McCrohon et al., 2003). The presence of LGE in patients with DCM has been shown to be a strong indicator of adverse prognosis in a large cohort (Gulati et al., 2013, Wu et al., 2008). Novel T1 mapping techniques have recently been developed which are able to identify diffuse myocardial fibrosis not picked up by LGE. Patients with DCM appear to have higher levels of fibrosis than controls using these techniques, which might have additional diagnostic and prognostic value (Dass et al., 2012, Puntmann et al., 2013).

1.5.5. Myocarditis

Myocarditis can often be a difficult diagnosis to make clinically. Typically, the patient may have a resting ECG with non-specific abnormalities, a mild elevation in troponin, and potentially an essentially normal echocardiogram. Often the only way to provide a definitive diagnosis would be endomyocardial biopsy (EMB), although of course this is an invasive procedure with potential risks (Caforio et al., 2013). It also has inherent limitations due to sampling error. CMR has revolutionised the diagnosis of suspected myocarditis, using the Lake Louise Criteria (Friedrich et al., 2009). These criteria are: 1. Increased signal intensity on T2-weighted imaging suggestive of the presence of myocardial oedema; 2. Increased signal intensity on early gadolinium enhancement imaging (taken less than 5 minutes after gadolinium injection); and 3. At least one area of LGE in a non-ischaemic pattern (this is typically epicardial or midwall). The use of these criteria has been shown to have excellent prediction of both suspected (Abdel-Aty et al., 2005) and biopsy proven myocarditis (Lurz et al., 2012, Francone et al., 2014). The different patterns of fibrosis seen using LGE imaging allow differentiation between MI, myocarditis and DCM, where traditional non-invasive methods such as echocardiography might not provide a definitive diagnosis (figure 1-9).

Figure 1-9. Typical Patterns of LGE.



LGE imaging from 4 patients: A – a healthy control patient with no LGE; B – a patient with a prior inferior MI showing the subendocardial pattern of LGE representing myocardial fibrosis (arrow); C – a patient with DCM showing a dilated left ventricle and a faint midwall line of LGE (arrow); D – a patient with myocarditis showing both inferior epicardial LGE and septal midwall LGE in a non-coronary distribution (arrows).

More recently, T1 mapping has also been used to evaluate acute myocarditis and might perhaps be more accurate than T2-weighted imaging (Ferreira et al., 2013) and may even be used to diagnose the myocarditis in patients who are unable to be given contrast (Ferreira et al., 2014). The use of CMR may have some ability to predict functional recovery in patients with myocarditis (Vermes et al., 2014).

1.5.6. Hypertrophic Cardiomyopathy

While hypertrophic cardiomyopathy (HCM) is still diagnosed by echocardiography, CMR has become increasingly important in its evaluation, especially due to its ability to image the heart in various planes. Apical HCM can be difficult to diagnose using echocardiography, however CMR has proved to be more accurate in its identification (Moon et al., 2004a). CMR can also be used to accurately measure myocardial wall

thickness and assess for the presence of left ventricular outflow tract obstruction and systolic motion of the mitral valve (Maron et al., 2009). CMR can potentially differentiate between HCM and other pathologies such as hypertensive heart disease (Puntmann et al., 2010). Abnormalities of the papillary muscles and mitral valve have also been noted using CMR, which may cause symptoms and influence management (Harrigan et al., 2008, Kwon et al., 2008).

There has been much interest in the use of LGE in HCM. This has been shown to correlate with myocardial fibrosis and scarring and is linked to adverse outcome, leading to calls for its use in association with traditional risk factors (Moon et al., 2004b, O'Hanlon et al., 2010). At present, current clinical risk factors still do not identify all patients at high risk of sudden death, and so there has been much research to identify any CMR parameters that may add prognostic value. LGE has been shown to predict heart failure hospitalisations in HCM patients (Green et al., 2012) and also the presence of ventricular arrhythmia on Holter monitoring (Adabag et al., 2008). Despite its link with ventricular arrhythmias on monitoring, LGE has shown mixed results for the prediction of sudden death (Green et al., 2012, Bruder et al., 2010, O'Hanlon et al., 2010, Rubinshtein et al., 2010, Maron et al., 2008). The presence of oedema and reduced perfusion suggestive of myocardial injury and ischaemia has also been seen in HCM, although their prognostic significance has yet to be elucidated (Hueper et al., 2012).

1.5.7. Miscellaneous Conditions

CMR is becoming an increasing part of the clinical assessment of numerous other cardiac conditions, for example in infiltrative cardiomyopathies. Confident non-invasive diagnosis of cardiac amyloidosis is now possible for the first time using LGE (Maceira et al., 2005). The typical pattern of LGE is of a global circumferential ring of LGE. This pattern has also potentially useful as a prognostic marker for prediction of mortality (White et al., 2014). Anderson-Fabry disease is an X-linked recessive condition that causes left ventricular hypertrophy and can lead to heart failure. A characteristic pattern of LGE in the midwall of the basal inferolateral wall of the left ventricle is typical and helps differentiation of the condition from HCM and other infiltrative cardiomyopathies (De Cobelli et al., 2009). CMR can also be used to assess response to treatment by providing reproducible assessment of the level of left ventricular hypertrophy (Imbriaco et al., 2009).

One condition in which CMR has particularly proven to be revolutionary is in the management of iron overload cardiomyopathy, either in haemochromatosis or transfusion-related cardiomyopathy (Wood, 2009). Transfusion-related cardiomyopathy is the leading cause of death in patients with transfusion-dependent anaemia. The use of T2*-weighted imaging, which is affected by iron within the body, has for the first time allowed non-invasive assessment of myocardial iron content. Anderson et al. showed that the T2* signal is inversely correlated to the level of myocardial iron, and directly correlated with LVEF (Anderson et al., 2004). In this study, the authors also showed that treatment with iron chelation therapy increases T2* time, corresponding to an improvement in LVEF. This group then went on to publish data showing that T2* imaging is also provides prognostic information on prediction of heart failure and mortality (Kirk et al., 2009). CMR is now an integral part of the management of iron overload cardiomyopathy. The level of evidence for the use of CMR in this condition (level 6) perhaps provides a model for increasing the clinical use of CMR in other conditions.

1.6. Summary and Thesis Aims

The clinical value of CMR is becoming increasingly recognised. Nevertheless, CMR is a relatively new imaging modality, and perhaps does not yet have the same level of evidence for its clinical utility as more established modalities such as echocardiography and SPECT, particularly in prognostic studies. CMR is limited by its cost, the level of expertise required and reduced availability in comparison to other methods. These factors mean that it is still not widely used in routine clinical practice. In order for CMR to become more utilised, there needs to be more evidence to show that it can change the management of patients.

In this thesis, I aim to show the clinical utility of CMR by using it to answer important clinical questions that are difficult to answer using other modalities. I will specifically look at five questions:

1. Can the use of a comprehensive, multi-parametric CMR protocol using LGE and myocardial deformation imaging (strain measured by tagged magnetic resonance) in addition to assessment of LVEF provide increased prognostic value for prediction of adverse events compared to clinical and LVEF assessment alone?

2. In patients with prior MI, infarct characteristics have been shown to be stronger predictors of adverse prognosis than the infarct size alone. Does the presence of myocardial fat within the infarct territory (lipomatous metaplasia), predict adverse events?
3. Not all heart failure patients requiring ICD therapy require to use their device. Can the structural information provided by pre-implantation CMR be combined with a functional assessment (n-terminal pro B-type natriuretic peptide – nt-proBNP) to provide more powerful prognostic information that could be used to help selection of patients, allowing avoidance of unnecessary device implantation and potentially cost-savings?
4. The differentiation between with early DCM and myocardial adaptation to exercise is not always clear-cut when based on LVEF assessment alone, leading to a potential diagnostic dilemma. Could a multi-parametric assessment using CMR potentially be used to help diagnose patients with DCM?
5. In patients with suspected angina, the presence of left bundle branch block (LBBB) causes difficulties in the interpretation of commonly used non-invasive techniques for evaluation of this presentation. Does the use of multi-parametric stress CMR, combining perfusion and wall motion assessment potentially improve diagnosis compared to dobutamine stress echocardiography?

By aiming to answer these 5 clinically relevant questions, I hope to add to the evidence demonstrating the clinical utility of CMR.

2. General Methods

2.1. Preamble

In this section I will describe the CMR and statistical methods used that were common to studies in this thesis. Detailed study specific methods are described within the relevant chapters.

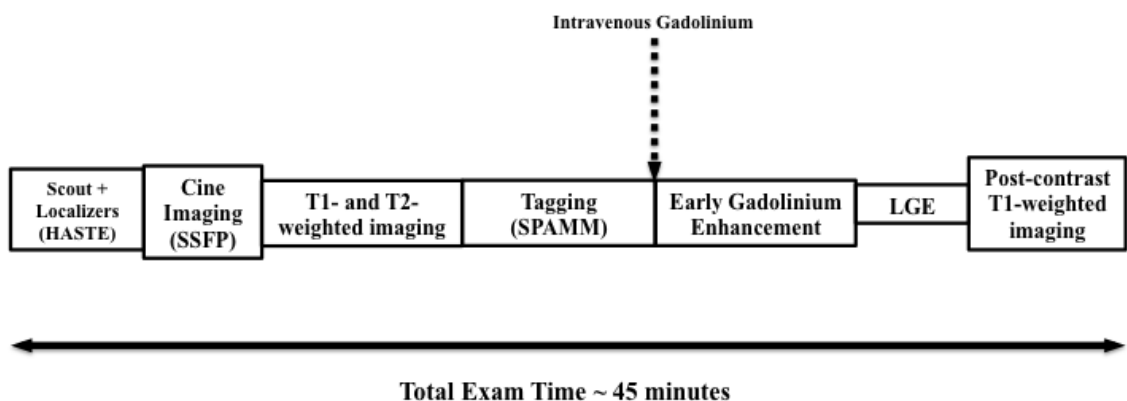
2.2. General Information

All patients underwent CMR examination at the Golden Jubilee National Hospital, Clydebank between January 2009 and March 2014 and were scanned using a 1.5 Tesla scanner with a 12-element phased array cardiac surface coil (Siemens Magnetom Avanto, Erlangen, Germany). All patients had been referred for a clinically indicated scan from hospitals throughout the West of Scotland. Patients were selected for various studies dependent on the referral indication. All patients who had contraindications to CMR examination (severe renal impairment with eGFR <30, metallic implants, pacemakers/implantable defibrillators) were excluded from the studies.

2.3. Standard CMR Protocol

All patients underwent a standard protocol, parts of which were adapted dependent on the specific clinical question to be answered by the CMR examination. All patients had ECG monitoring during the CMR examination. The standard CMR protocol is outlined in figure 2-1.

Figure 2-1. Standard CMR Protocol



The CMR examination began with initial Half-Fourier Acquisition Single-Shot Turbo Spin-Echo (HASTE) images, which allow for localisation of various structures within the body and accurate anatomical detailing, allowing for planning of the rest of the study. Following this, left ventricular mass, volumes and function were assessed with the acquisition of cine images using a steady-state free precession (SSFP) technique. Next, tissue characterisation sequences were acquired. These included T1- and T2-weighted imaging sequences. Tagged magnetic resonance images were obtained using a spatial modulation of magnetisation (SPAMM) sequence for assessment of regional myocardial function, strain and left ventricular torsion (Axel and Dougherty, 1989). Once native tissue characterisation sequences were acquired, gadolinium contrast (0.15 mmol/kg of gadoterate meglumine; Dotarem, Guebert S.A., Villepinte, France) was given intravenously through a peripheral cannula. Early gadolinium enhancement imaging (EGE) was performed 2 minutes post-injection; 10 minutes post-injection, late gadolinium enhancement imaging (LGE) was performed using segmented phase-sensitive inversion recovery turbo fast low-angle shot sequence (PSIR). Following this, a further (post-contrast) T1-weighted sequence was carried out.

I shall now proceed to describe each sequence in more detail.

2.3.1. Half-Fourier Acquisition Single-Shot Turbo Spin-Echo (HASTE)

HASTE imaging is used in the initial planning sequences of the CMR examination. These out of focus images (figure 2-2) are used to localise the anatomical structures of the body and plan the remainder of the examination. HASTE is also known as “black-blood imaging”, due to the low blood signal. HASTE is an ultrafast sequence, which is often used in CMR as it is less sensitive to movement artifacts, primarily as it is a single-shot sequence. This sequence was performed with ECG-triggering and without breath-holding. Typical imaging parameters were as follows: TR 800ms, TE 80ms, 2 R-R intervals/23; flip angle 160°; effective slice thickness, 5 mm without interslice gaps; matrix size, 158 × 256; and spatial resolution, 2.4 × 1.5 mm². HASTE imaging is also useful for assessment of the extracardiac anatomy, including the aorta (Davis et al., 2014), lungs (Vogt et al., 2004), liver (Yu et al., 1998) and kidneys (Irwin et al., 2013) (figure 2-2).

Figure 2-2. An example of HASTE imaging



HASTE imaging in axial (A), sagittal (B) and coronal (C) views. An incidental finding of a right lung lesion is noted (arrows). A – aorta, LA – left atrium, LL – left lung, LV – left ventricle, RA – right atrium, RL – right lung, RV – right ventricle.

2.3.2. Steady-State Free Precession “Cine” Imaging (SSFP)

Sequences for assessment of left ventricular volumes, global function (e.g. ejection fraction) and mass were acquired using an SSFP technique (multi-slice single-shot breath-hold true fast imaging - trueFISP). Cines of the left ventricle were acquired in 3 long axis views (4-chamber, 3-chamber and 2-chamber) and a stack of short axis views (typically 8-10), allowing for complete visualization of left ventricular myocardial structure and motion. Typical sequence parameters were TE 1.2 ms, TR 3.5 ms, flip angle 50°, slice thickness 8mm, gap 2mm, FOV 281 x 340.

2.3.3. T1-Weighted Imaging (“T1 mapping”)

T1-weighted imaging was carried out using a Modified Look Locker Inversion-recovery sequence (MOLLI), initially described by Messroghli et al (Messroghli et al., 2004). Essentially, after the initial inversion pulse, the recovery of longitudinal magnetisation is measured. Several TrueFISP sequences are acquired at different inversion times over a single breath-hold, allowing generation of a “map” showing the individual T1 time of each voxel. 3 short-axis views were obtained to represent the base, mid-ventricular and apical segments of the heart. Motion correction is then applied to account for cardiac movement. Typical parameters were: TE 1.1 ms, initial TI 100 ms; TI increment 80 ms, flip angle 35°, matrix 192 x 124 pixels, spatial resolution 2.1 x 1.1 x 8.0 mm, slice thickness 8 mm, scan time 17 heartbeats.

T1 mapping sequences were obtained both prior to and (on average 7 -10 minutes) after injection of gadolinium contrast, allowing for assessment of “native” T1 and post-contrast T1 signals.

2.3.4. T2-Weighted Imaging

T2-weighted imaging was carried out using two methods. Firstly, a short-tau inversion-recovery sequence (STIR) was used (Simonetti et al., 1996). Again, 3 short-axis slices were obtained to represent 3 levels of the left ventricle. In this sequence, a pair of 180° inversion pulses are applied, followed by a long inversion time. This nulls blood pool signal, hence this is also a “black-blood” sequence. Following this, a further 180° inversion pulse is applied, which has the effect of nulling the signal from fat (which has a short T1) and enhancing the signal from tissues with a longer T1 time (for example those containing water). Typical parameters of this sequence were: TE 63 ms, TR 800 ms, flip angle 180°, acquisition time 8 to 13 seconds, matrix 166×256, bandwidth 235 Hz/pixel. The time interval between the 180° inversion pulses for STIR was 6.74 ms, voxel size was 2.2×1.4×8 mm³. Average breath hold for this sequence was 15 seconds.

After this, a second T2-weighted technique was used, allowing for direct quantification of T2 time analogous to the T1 mapping technique previously described (Giri et al., 2009). Three T2-weighted images were obtained during one breath hold at 0 ms, 24 ms and 55ms, allowing generation of the T2 time for each individual voxel. Again, a motion correction algorithm was applied to allow for movement artefact. Typical imaging parameters were: TE 1.1 ms, TR 260 ms, flip angle 70°, band width ~ 947 Hz/pixel, matrix 160 x 105 pixels, spatial resolution 2.6 x 2.1 x 8.0 mm, slice thickness 8 mm.

2.3.5. Tagging - Spatial Modulation of Magnetisation (SPAMM)

Assessment of regional myocardial function (strain), left ventricular rotation and torsion was carried out using a CMR tagging – spatial modulation of magnetisation (SPAMM) (Axel and Dougherty, 1989). Essentially, magnetic resonance tags are applied to the heart, allowing tracking of myocardial motion through the cardiac cycle. By doing this, assessment of circumferential, radial and longitudinal deformation can be obtained, as well as rotation of heart. Tagged images of the left ventricle were acquired in 3 short axis slices

and in the 4-chamber long-axis view. Grid tags were applied at the start of the ECG R wave and gradient echo cine images acquired to follow myocardial motion using the tags. Imaging parameters were as follows: TR 40.1 ms, TE 3.9 ms, flip angle = 14°, slice thickness = 6 mm, field of view = 380 mm, grid distance 5 mm, 20 cardiac phases/R-R interval on ECG.

2.3.6. Early and Late Gadolinium Enhancement

Following administration of intravenous gadolinium contrast as described above, early gadolinium enhancement imaging was carried out 2 minutes post-injection using a single-shot SSFP sequence with a non-selective inversion pulse. A full short-axis stack was obtained, copied from the cine SSFP sequences. Typical parameters: TE 1.2, TR 2.7, TI 200-350 ms, slice thickness 8 mm, gap 2 mm.

10 minutes post-injection, late gadolinium enhancement imaging was performed. A full short-axis stack and 3 long-axis views (as per SSFP cine imaging) were obtained using a PSIR sequence. Typical imaging parameters were: TE 4.4, TR 630, flip angle = 25°, matrix 192 x 256, bandwidth 130 Hz/pixel, echo spacing 8.7ms, trigger pulse 2, voxel size was 1.7 x 1.2 x 8 mm³. Typical inversion times were 200 to 340 ms, selected to optimally null myocardial signal.

2.4. CMR Image Analysis

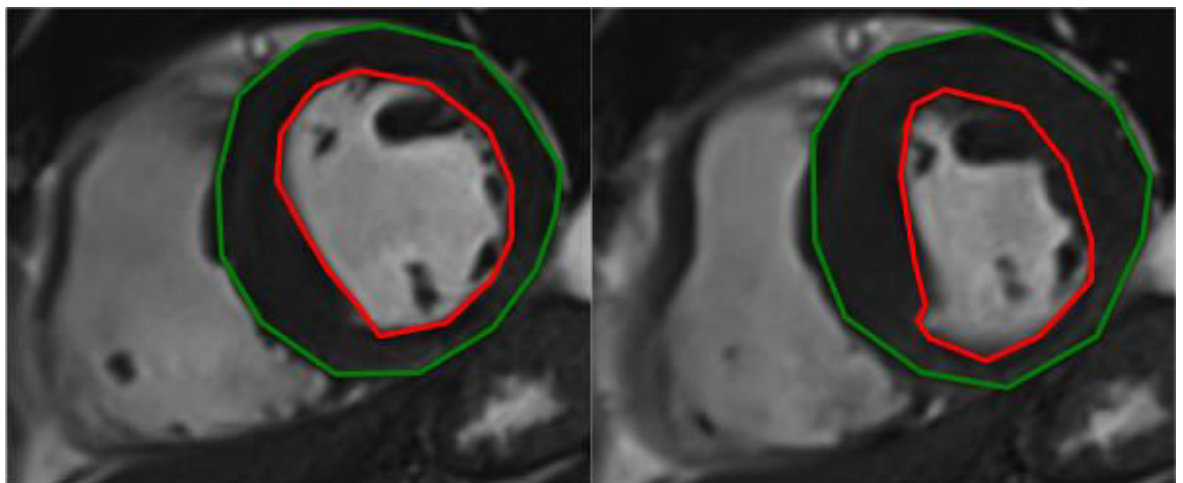
Post-processing of all images were analysed using commercially available proprietary Siemens software (Argus) based on CMR workstations, except for analysis of CMR tagging which was performed using specific tagging analysis software (HARP, Diagnosoft, Durham, North Carolina). All image analysis was performed by I.M., unless otherwise specified.

2.4.1. Assessment of Left Ventricular Mass and Function

Qualitative analysis of left ventricular function was carried by visual assessment of the cine SSFP images for global and regional myocardial motion and wall thickening. Resting (diastolic) wall thickness was measured in the most basal left ventricular slice, as were end-diastolic and end-systolic diameters.

To obtain quantitative measurements of left ventricular mass, volumes and ejection fraction, all cine images were loaded into Argus. The computer software automatically selected end-diastole, while end-systole was manually selected as the image in each slice with the smallest area of blood pool. Once selected, the endocardial and epicardial borders were manually outlined. Papillary muscles were included as part of the myocardial blood pool. Following tracing of the myocardial borders for each slice (typically 8-10 slices depending on the size of the heart), an automated calculation was carried out by the Argus software to obtain left ventricular mass, end-systolic volume, end-diastolic volume and left ventricular ejection fraction using a sum of discs method (figure 2-3).

Figure 2-3. Manual planimetry to obtain left ventricular mass and function using SSFP cine imaging.



End-Diastole

End-Systole

Endocardial (red) and epicardial (green) contours are measured at end-diastole and end-systole. This process is repeated in every slice, allowing for calculation of left ventricular volumes, ejection fraction and mass.

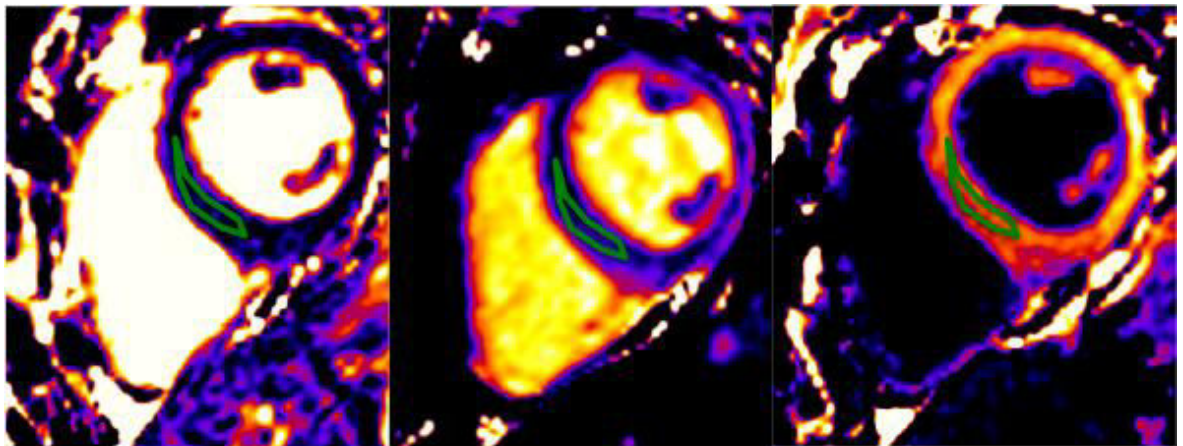
2.4.2. Assessment of T1- and T2-weighted Imaging

Both T1 (native and post-contrast) and T2 maps were qualitatively assessed for image quality and artefacts. It quickly became apparent that apical slices were often subject to poor image quality, often due to signal drop-out from the thinner myocardium, causing

interference from the myocardial blood pool, and so apical slices were not included in quantitative assessment, similarly to other studies (Wong et al., 2012, Moon et al., 2013).

The major advantage of mapping techniques is the ability to perform a fully quantitative measurement of T1 and T2 times of any structure. To do this, a region of interest was drawn within the interventricular septum, taking care to exclude signal from the myocardial blood pool, but ensuring to take as large an area as possible to be truly representative. Again, as the lateral wall is often subject to partial volume effects similarly to the apex, the septum was chosen as the most robust measure. The T1 and T2 times were respectively recorded (figure 2-4).

Figure 2-4. T2, native T1 and post-contrast T1 maps in a normal patient.



T2 Map

**Native T1
Map**

**Post-contrast
T1 Map**

Typical appearances using T1 and T2 mapping in a healthy control. A region of interest can be drawn within the septum to measure T1 and T2 relaxation times (green area).

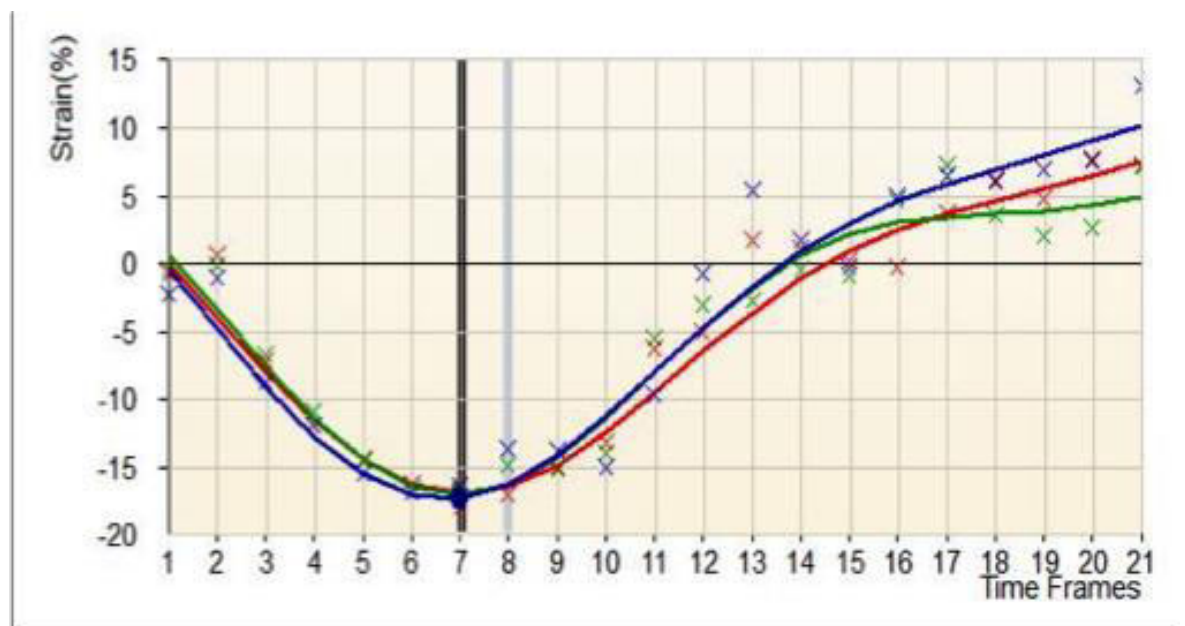
T2-STIR images were also analysed qualitatively, again primarily for the presence of artefacts, often caused by the lengthy breath holds required for this sequence (15-20 seconds). Relative myocardial signal intensity was assessed by comparison of the signal intensity of an area of interest with either a remote area of myocardium or skeletal muscle signal intensity (Abdel-Aty et al., 2005).

2.4.3. Assessment of CMR Tagging

Tagged images were analysed in a specialist software package (HARP, Diagnosoft, North Carolina, USA). 3 short-axis slices were analysed for measurement of circumferential and radial strain and rotation. The 4-chamber view was used to measure longitudinal strain.

Endocardial and epicardial contours were drawn on one image (similarly to those drawn in Argus on cine images for assessment of LV mass and function); these were automatically copied to all other images in the cine sequence by the software and then manually adjusted to ensure adequate tracing of myocardial motion. Following this, an automatic calculation of circumferential and longitudinal strain were obtained. (figure 2-5).

Figure 2-5. CMR tagging for assessment of circumferential strain in a healthy control.



Global circumferential strain measured using tagged CMR at the basal (green), mid (red) and apical (blue) levels of the left ventricle.

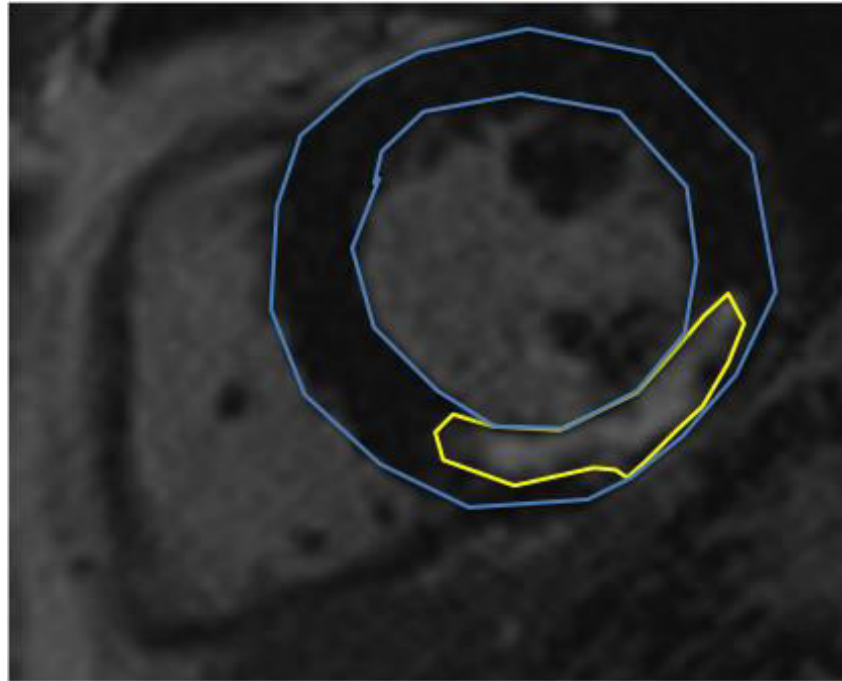
2.4.4. Assessment of Early and Late Gadolinium Enhancement

Early gadolinium enhancement images were analysed qualitatively for the presence of hypointense myocardial regions, typically indicative of microvascular obstruction caused by myocardial infarct (causing reduced penetration of gadolinium contrast within that area).

Late gadolinium enhancement images were first analysed qualitatively for the presence of contrast-enhanced myocardium. If present, quantitative analysis could be carried. Several techniques are available for quantification of LGE volumes using the relative signal intensity of the contrast-enhanced region compared to normal myocardium (Flett et al., 2011). For all studies in this thesis, the presence of LGE was defined as any area with a signal intensity 5 standard deviations (SD) above that of remote myocardium. This technique is commonly used throughout the literature, is robust and has been used in prognostic studies (Flett et al., 2011, Beek et al., 2009).

To do this, firstly a region of interest was drawn within an area that objectively did not have any LGE to act as an area of remote myocardium. The mean signal intensity and standard deviation in this area was displayed on the workstation. After adjusting the “width” setting of the monitor to the mean signal intensity and the “contrast” setting to 5 SD above this, any areas that remained enhanced were contoured and measured. The total left ventricular area was also traced, and the percentage of enhanced myocardium calculated. This was done in each short-axis slice of the left ventricle (using the same slices as for calculation of left ventricular function) in order to calculate the percentage of enhancement in the left ventricle. Intra- and inter-observer variability is as previously described in our group (Payne et al., 2011b). Figure 2-6 illustrates an example of the analysis of LGE imaging.

Figure 2-6. Quantification of late gadolinium enhancement imaging.



Manual planimetry of an area of LGE (yellow) with signal intensity 5SD above remote myocardium. This was repeated in every left ventricular slice and the percentage of myocardium affected by LGE calculated $((\text{area of LGE}/\text{total myocardial area}) \times 100)$.

2.5. Statistical Analysis

All statistical analysis was performed using SPSS (version 21.0, IBM, Armonk, NY, USA). Continuous variables are presented as mean \pm SD while non-continuous variables are presented as number with percentage in brackets. Differences between continuous variables were compared using a two-tailed t-test, while categorical variables were compared using a chi-square test. Correlations were assessed using Pearson's correlation co-efficient. Outcome analysis was performed using Cox logistic regression and time-to-event curves constructed using the Kaplan-Meier method. Receiver-operator characteristic (ROC) curves were formed for assessment of diagnostic accuracy and in order to find best cut-off values for prediction of outcomes of various parameters. For all analysis a p value <0.05 was deemed to be significant, unless otherwise mentioned.

2.6. Ethical Approval

Full ethical approval was obtained for these studies from West of Scotland Research Ethics Committee 3, reference 14/WS/1052 (appendix 1). This allowed inclusion of patients into the studies within this thesis on the basis that all information was anonymised and therefore patients could not be traced, as well as computerised record linkage for follow-up. Prior analysis that had been performed for clinical reasons (such as left ventricular function measurements) could also be used. The protocol for this study allowed for inclusion of analysed data (appendix 2).

2.7. Limitations

While the CMR methods are robust, there are some limitations in the methodology used within this thesis.

Firstly, measurement of the left ventricular volumes can also be performed by including the papillaries as part of the myocardium, which is more accurate. In our unit, volumes are calculated excluding the papillaries, so in order to maintain consistency this was kept the same.

Secondly, our T1 mapping sequence does not include an error map, which can act as a quality control check for the presence of artifacts (Kellman et al., 2013). I was present for as many scans as possible in order to try to pick up artifacts in real time and if necessary repeat the sequence.

3. The Combined Incremental Prognostic Value of Left Ventricular Ejection Fraction, Late Gadolinium Enhancement and Global Circumferential Strain Assessed by Cardiovascular Magnetic Resonance

3.1. Introduction

As discussed in Chapter 1, the primary unique advantages of CMR lie in two main factors – its ability to provide accurate and reproducible assessment of ventricular dimensions and function, such that it is considered the non-invasive gold standard for measurement of LVEF; and secondly, its ability to non-invasively characterise the myocardium using LGE imaging to assess the presence of myocardial fibrosis.

The assessment of LVEF has a vital role in the evaluation and management of patients in cardiology, providing significant prognostic information and guiding treatment decisions (Solomon et al., 2005, Yancy et al., 2013, McMurray et al., 2012). While LVEF is commonly evaluated using echocardiography, CMR is becoming increasingly utilised. CMR is currently recognised as the non-invasive gold standard for assessment of LVEF due to its ability to provide unobstructed views of the heart in any plane and increased reproducibility (Hoffmann et al., 2005).

Tissue characterisation using LGE allows the non-invasive visualisation of myocardial fibrosis. The presence of fibrosis is seen in numerous conditions and has also been shown to have significant prognostic value, independent of LVEF (Kuruvilla et al., 2014, Mavrogeni et al., 2013, Gulati et al., 2013).

Despite LVEF assessment by CMR being well validated, LVEF remains an insensitive tool for assessment of regional myocardial contractility. LVEF is dependent on other factors such as LV loading conditions and dimensions, thus it does not always provide a true index of LV systolic function (Buckberg et al., 2008). It is also increasingly understood that early changes in myocardial contractility occur which might have a sub-clinical, but important impact. The assessment of myocardial contractility, most commonly reported using strain as a measure of deformation, can be carried out using tagging sequences during CMR (Ibrahim el, 2011). This technique is regarded as the non-invasive gold-standard for deformation imaging. The assessment of global circumferential strain (GCS) using tagging has been shown to identify myocardial dysfunction in numerous conditions independent of LVEF. Recently, GCS has been shown to be an independent prognostic indicator in both asymptomatic patients and those with heart failure (Choi et al., 2013, Cho et al., 2009). Assessment of GCS may provide extra information to LVEF.

As yet, no study has assessed the prognostic value of LVEF, LGE and GCS in a combined CMR protocol. The aim of this study was to explore the prognostic value of these parameters in addition to baseline clinical risk factors for prediction of major adverse cardiovascular events in an unselected cohort of patients with suspected cardiac disease referred for clinical assessment.

3.2. Methods

3.2.1. Patient Selection

570 patients referred for clinically indicated CMR were prospectively screened. All patients able to undergo the complete CMR protocol without any contra-indications to the use of gadolinium were eligible. Clinical management of the patients was left to the discretion of the referring physician. Baseline characteristics were obtained at the time of referral using the patients' case notes.

3.2.2. CMR Protocol

All patients underwent a systematic CMR protocol including cine imaging, tagging and LGE as described in Chapter 2. Briefly, cine images were obtained using an SSFP sequence in three long axis planes (2-chamber, 3-chamber, 4-chamber) and in short axis slices through the left ventricle. Then 3 matched short-axis slices were taken to represent the basal, mid and apical levels of the left ventricle using tagged CMR for assessment of GCS. Intravenous gadolinium was then given and LGE imaging was performed after 10 minutes.

All analysis was performed using Argus, other than analysis of tagged CMR images which was performed using Diagnosoft HARP as described in Chapter 2.

3.2.3. Follow-up

The combined primary endpoint for this study was incidence of cardiovascular mortality or major adverse cardiovascular events (MACE). MACE included heart failure hospitalisation, sustained ventricular arrhythmia requiring hospitalisation or defibrillator therapy and survived cardiac arrest.

All patients were followed up using our computerised record linkage system which allows access to patient records, allowing us to identify survival status and hospital admissions (“Clinical Portal”). In case of patients’ in whom the computerised records were not up to date, the patient’s general practitioner was contacted to ensure adequate follow-up status. Events were adjudicated by an independent observer unaware of the results (N.T).

3.2.4. Statistical Methods

As described in Chapter 2, continuous variables are expressed as mean \pm SD and categorical variables are expressed as a number and percentage. Comparison between continuous variables was carried out using a two-tailed t-test, while categorical variables were compared using the chi-square test. Correlation between continuously distributed CMR parameters were assessed using Pearson’s correlation coefficient while non-parametric correlations were assessed using Spearman’s correlation. Outcome analysis was conducted using Cox proportional hazards, and time-to-event curves were drawn using the Kaplan-Meier method. All variables were evaluated using univariate Cox regression analysis to ascertain their prognostic power for prediction of the primary outcome. Hazard ratio and chi-square were obtained. To evaluate the incremental prognostic value of CMR, significant univariable CMR predictors ($p < 0.05$) were then added to the significant multivariable clinical predictors, and further multivariable models using each CMR parameter created. CMR variables were individually added to the clinical model in a forward stepwise selection, to assess their independent prognostic power over and above the previous model. Optimal cut-off points for LVEF, GCS and LGE were calculated using ROC curves. The chi-square of each model was subsequently calculated. This process was then repeated in patients without severe left ventricular systolic dysfunction ($\geq 35\%$). Reproducibility was assessed using Pearson’s correlation coefficient and the intraclass coefficient.

For all analyses a p value < 0.05 was considered statistically significant and all p values are two-tailed.

3.3. Results

3.3.1. Baseline Characteristics

In total 539 patients were included in the final analysis. Of the 31 patients excluded, 8 were unable to undergo LGE imaging due to renal impairment, 11 patients had inadequate image quality due to poor breath-holding ability and 12 had arrhythmias that impaired scan quality such as uncontrolled atrial fibrillation. Baseline clinical characteristics of the 539 patients are shown in table 3-1.

Table 3-1. Baseline Clinical Characteristics.

Variable	
Age (years)	48.1 ± 15.4
Male (%)	343 (63.6)
Ischaemic Heart Disease (%)	61 (11.3)
Diabetes Mellitus (%)	53 (9.8)
Hypertension (%)	77 (14.3)
Smoker (%)	58 (10.8)
ACE inhibitor use (%)	225 (41.7)
Beta-blocker use (%)	223 (41.4)
Mineralocorticoid Antagonist Use (%)	136 (25.2)
Statin use (%)	140 (26.0)
Aspirin use (%)	159 (29.5)

ACE – angiotensin-converting enzyme

Data are presented as mean ± SD if continuous or number (%) if categorical.

The mean age of the cohort was 48.1 ± 15.4 years. 63.6% were male. The majority of patients did not have any clinical risk factors. Reasons for referral for CMR are shown in table 3-2. The majority of patients (56.8%) were referred for assessment of left ventricular function.

Table 3-2. Reasons for Referral for CMR Assessment.

Reason	Number (%)
Presumed dilated non-ischemic cardiomyopathy – assessment of LV function	199 (36.9)
Presumed ischemic cardiomyopathy – assessment of LV function	107 (19.9)
Left ventricular hypertrophy - characterisation	59 (10.9)
Presumed myocarditis	64 (11.9)
Ventricular arrhythmia (specify)	75 (13.9)
Aortic disease	35 (6.5)

Baseline CMR characteristics are shown in table 3-3.

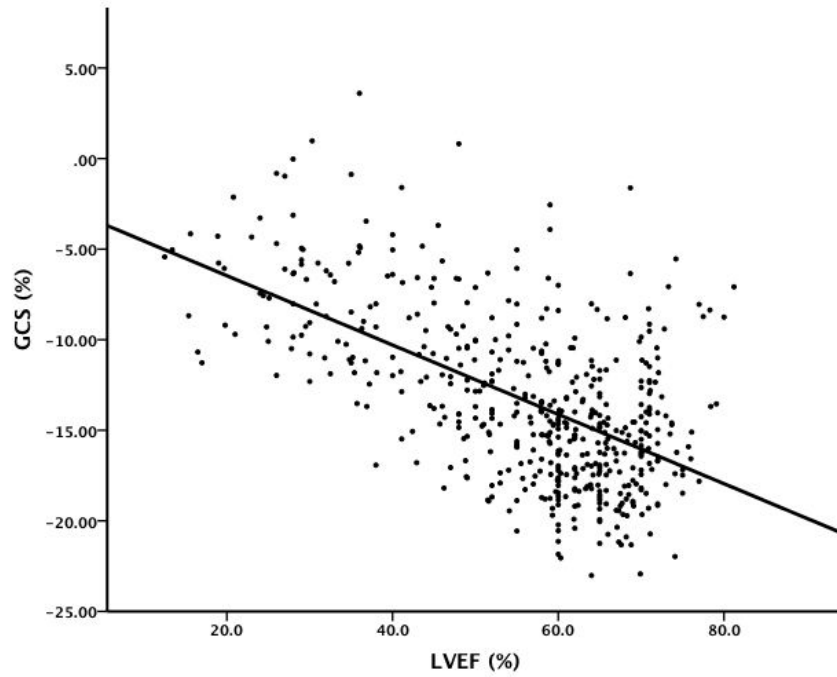
Table 3-3. Baseline CMR Characteristics.

Variable	
Left ventricular ejection fraction (%)	55.9 ± 14.1
Global circumferential strain (%)	-13.4 ± 4.6
Late gadolinium enhancement present	164 (30.4)
Late gadolinium enhancement (%)	0 (0-1.22)

Data are presented as mean ± SD if continuous, median (interquartile range) if non-parametric or number (%) if categorical.

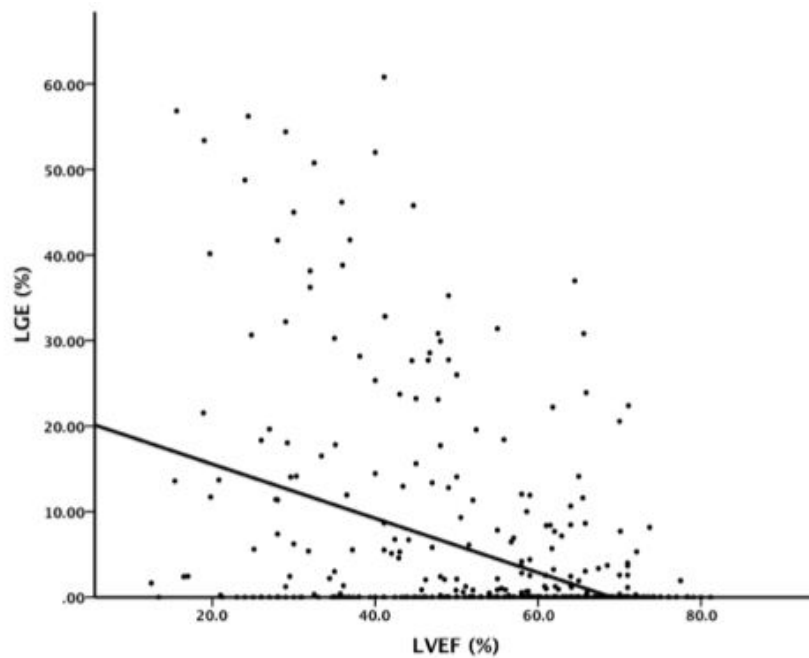
Mean LVEF measured by CMR was 55.9 ± 14.1% and mean GCS was -13.4 ± 4.6%. 164 patients had LGE present (30.4%). The mean volume of LGE was 4.1 ± 10.4%. There was a strong correlation between all three parameters (correlation between LVEF and LGE percentage $r = -0.43$; between LVEF and GCS $r = -0.58$; between GCS and LGE percentage $r = 0.33$, $p < 0.001$ for all; figures 3-1 – 3-3).

Figure 3-1. Correlation between LVEF and GCS.



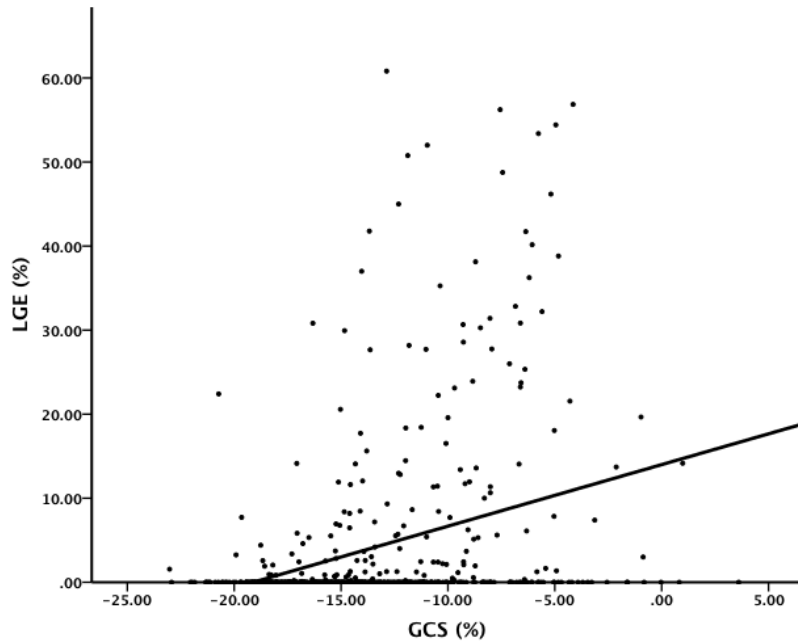
$r=-0.58, p<0.001.$

Figure 3-2. Correlation between LVEF and LGE Percentage.



$r=-0.38, p<0.001$

Figure 3-3. Correlation between GCS and LGE Percentage.



$$r=0.31, p<0.001$$

Mean acquisition time for tagged CMR was 104 ± 22 seconds (1.7 ± 0.37 minutes) while mean time for post-processing analysis of tagged CMR was 3.6 ± 0.7 minutes.

3.3.2. Primary Outcome Analysis

The mean follow-up duration was 2.2 ± 1.2 years. The combined primary outcome occurred in 58 patients, giving an event rate of 10.8%. There were 16 cardiovascular deaths (10 due to heart failure, 4 sudden deaths and 2 due to myocardial infarction), 30 admissions for heart failure, and 12 ventricular arrhythmias requiring treatment. Age, a prior history of ischemic heart disease (IHD), smoking and use of angiotensin converting enzyme inhibitors, beta-blockers, aspirin or statins were all significant univariate clinical predictors of the primary outcome. In multivariable analysis of the significant clinical predictors of the primary outcome only a history of IHD remained a significant predictor of the primary outcome (HR 3.76; 95% CI 1.83-7.72, $p<0.001$), while use of beta-blockers showed a trend towards significance (HR 2.21; 95% CI 0.95-5.17, $p=0.07$) (table 3-4).

Table 3-4. Clinical Predictors of the Primary Outcome.

Variable	Univariable HR (95% CI)	p value	Multivariable HR (95% CI)	p value
Age (years)	1.04 (1.02-1.06)	<0.001	1.02 (1.00-1.05)	0.10
Male	1.64 (0.91-2.96)	0.10		
Ischemic Heart Disease	6.77 (3.80-12.04)	<0.001	3.76 (1.83-7.72)	<0.001
Diabetes Mellitus	1.67 (0.78-3.58)	0.19		
Hypertension	1.36 (0.66-2.80)	0.41		
Smoker	2.09 (1.04-4.19)	0.039	1.50 (0.74-3.05)	0.27
ACE inhibitor use	5.57 (2.74-10.49)	<0.001	1.75 (0.76-4.04)	0.19
Beta-blocker use	5.38 (2.75-10.51)	<0.001	2.21 (0.95-5.17)	0.07
Statin use	2.54 (1.45-4.44)	0.001	0.62 (0.28-1.34)	0.22
Aspirin use	3.16 (1.81-5.54)	<0.001	1.22 (0.52-2.85)	0.64

HR – hazard ratio; CI – confidence interval

3.3.3. Incremental Prognostic Value of CMR Parameters

All 3 CMR parameters were significant univariate predictors of the primary outcome (LVEF: HR 0.92; 95% CI 0.91-0.94, $p < 0.001$; presence of LGE: HR 5.47; 95% CI 3.16-9.48, $p < 0.001$; GCS: HR 1.21; 95% CI 1.16-1.27, $p < 0.001$). When individually added to significant clinical predictors in multivariable analysis, all 3 CMR parameters remained significant (table 3-5).

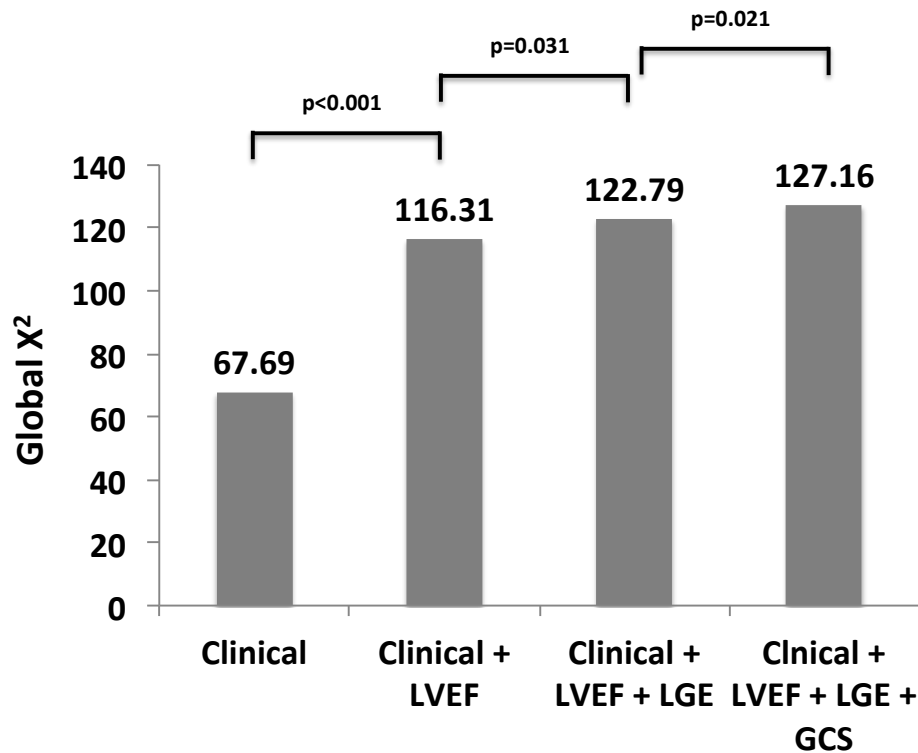
Table 3-5. Multivariable analysis Including CMR Parameters.

Model 1 (Clinical + LVEF)			Model 2 (Clinical + LGE)			Model 3 (Clinical + GCS)			Model 4 (Clinical + LVEF + LGE)			Model 5 (Clinical + LVEF + LGE + GCS)		
	HR (95% CI)	p value		HR (95% CI)	p value		HR (95% CI)	p value		HR (95% CI)	p value		HR (95% CI)	p value
IHD	3.61 (1.96-6.65)	<0.001	IHD	2.73 (1.44-5.17)	0.002	IHD	3.75 (2.03-6.91)	<0.001	IHD	2.58 (1.22-5.01)	0.005	IHD	2.60 (1.34-5.07)	0.005
BB	1.54 (0.70-3.39)	0.28	BB	2.88 (1.40-5.91)	0.004	BB	1.91 (0.90-4.06)	0.09	BB	1.58 (0.72-3.44)	0.25	BB	1.40 (0.64-3.08)	0.40
LVEF	0.94 (0.92-0.96)	<0.001	LGE	3.71 (1.90-7.25)	<0.001	GCS	1.20 (1.12-1.27)	<0.001	LVEF	0.95 (0.93-0.97)	<0.001	LVEF	0.97 (0.94-0.99)	0.01
									LGE	2.29 (1.10-4.77)	0.027	LGE	2.12 (1.03-4.37)	0.041
												GCS	1.10 (1.02-1.20)	0.019

BB – beta blocker; IHD – ischaemic heart disease; LVEF – left ventricular ejection fraction; LGE – late gadolinium enhancement; GCS – global circumferential strain

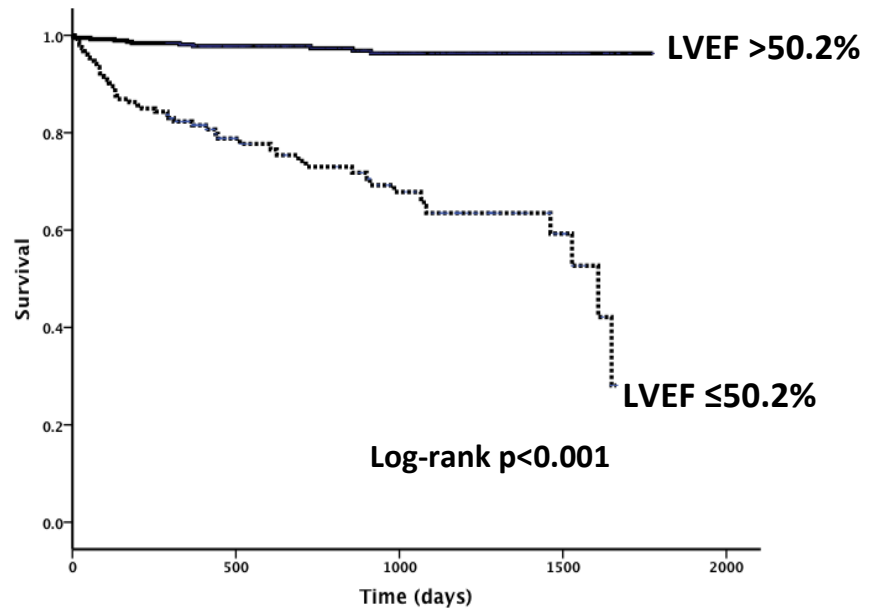
In the final multivariable model, all 3 CMR parameters remained significant predictors of the primary outcome (LVEF: HR 0.97; 95% CI 0.94-0.99, $p=0.01$; presence of LGE: HR 2.12; 95% CI 1.03-4.37, $p=0.041$; GCS: HR 1.10; 95% CI 1.02-1.20, $p=0.019$). The addition of both LGE and GCS had incremental prognostic value when added to clinical predictors and LVEF (figure 3-4).

Figure 3-4. Incremental Value of CMR Parameters for Prediction of the Primary Outcome Shown by Improvement in Chi-Square.



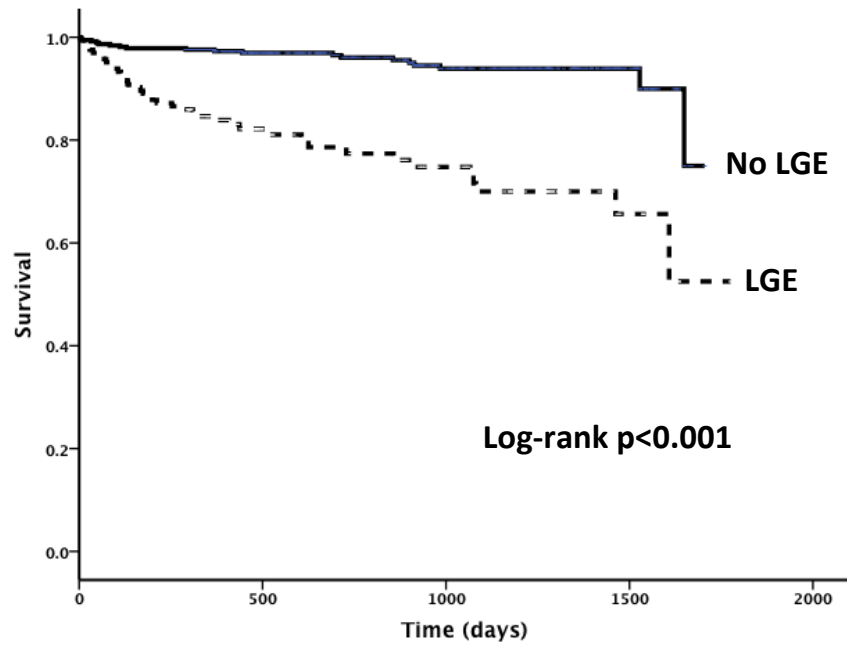
All 3 CMR parameters had reasonable power for prediction of adverse events. The area under the ROC curve for LVEF was 0.834, for LGE 0.699 and for GCS 0.820 (all $p < 0.001$). Using ROC analysis, optimal cut-offs for LVEF and GCS were 50.2% and -12.1% respectively, which provided excellent stratification of risk (figures 3-5 – 3-7).

Figure 3-5. Kaplan-Meier Curve For Survival Based on the Optimal LVEF Cut-Off.



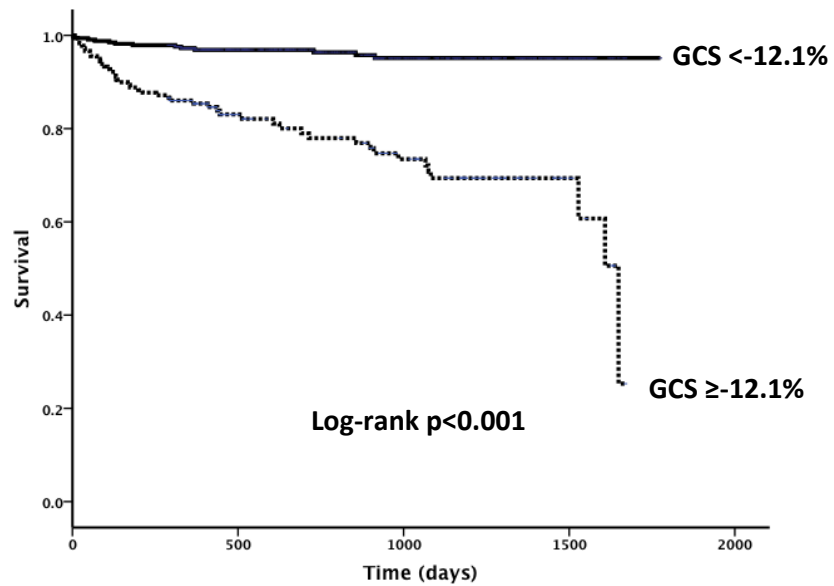
LVEF >50.2%	376	254	152	33
LVEF ≤50.2%	163	73	48	12

Figure 3-6. Kaplan-Meier Curve For Survival Based on the Presence of LGE.



No LGE	375	261	151	32
LGE	164	74	51	13

Figure 3-7. Kaplan-Meier Curve For Survival Based on the Optimal GCS Cut-Off.

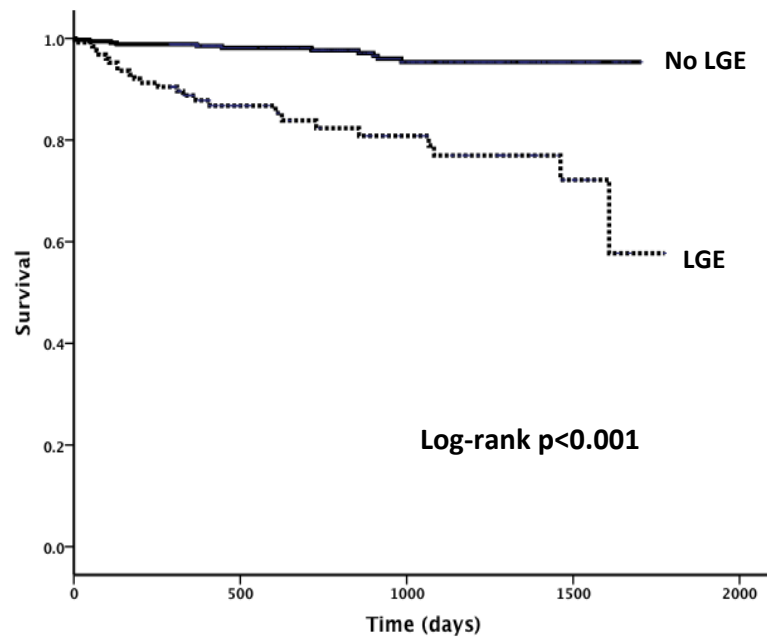


GCS	360	225	128	33
<-12.1%				
GCS	179	88	59	10
≥-12.1%				

3.3.4. Sub-Analysis: Patients Without Severely Impaired LV function

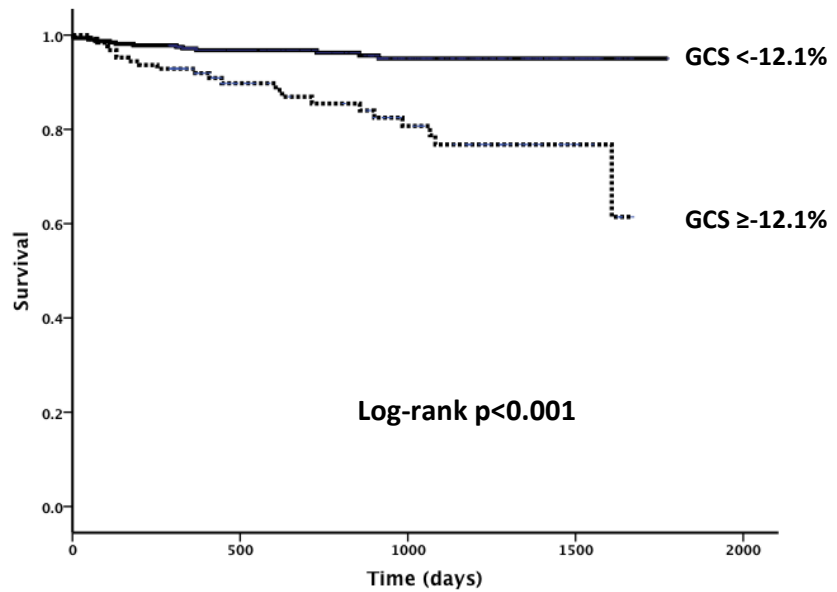
In total there were 474 patients with LVEF $\geq 35\%$, of whom 35 experienced the primary outcome (7.4%) – there were 11 deaths, 14 admissions for heart failure and 10 ventricular arrhythmias. In this group, both the presence of LGE (HR 3.88; 95% CI 1.86-8.09, $p < 0.001$) and GCS (HR 1.09; 95% CI 1.00-1.19, $p = 0.046$) remained significant multivariable predictors of the primary outcome when added to LVEF (HR 0.93; 95% CI 0.90-0.97, $p = 0.001$) (figures 3-8 and 3-9).

Figure 3-8. Kaplan-Meier Curve For Survival Based on the Presence of LGE in Patients with LVEF $\geq 35\%$.



No LGE	348	242	143	30
LGE	126	66	46	13

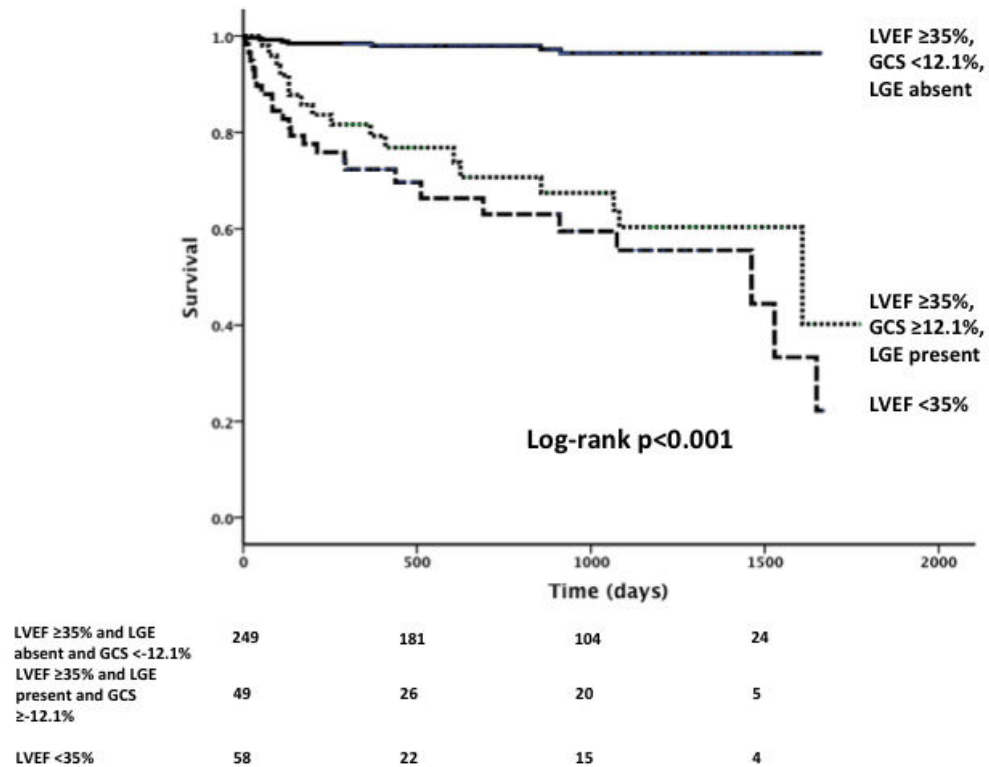
Figure 3-9. Kaplan-Meier Curve For Survival Based on the Optimal GCS Cut-Off in Patients with LVEF $\geq 35\%$.



GCS <-12.1%	335	219	128	33
GCS \geq -12.1%	139	69	46	8

Patients with LVEF $\geq 35\%$ but GCS <-12.1% and LGE present had similarly poor outcomes to patients with LVEF <35% (figure 3.10).

Figure 3-10. Kaplan-Meier Curve For Survival Based on LVEF, GCS and LGE.



3.3.5. Reproducibility of GCS Measurements Using Tagging

30 CMR studies were jointly analysed by I.M. and N.T. to assess reproducibility of GCS measurements. There was excellent intra-observer variability ($r=0.96$, $p<0.01$) and interobserver agreement ($r=0.94$, $p<0.01$). The intraclass correlation coefficient for interobserver agreement was 0.95 (95% CI 0.88-0.98, $p<0.001$).

3.4. Discussion

3.4.1. Study Findings

This study identified two important findings:

- For the first time in a large, prospectively evaluated cohort of unselected patients, I have shown that the assessment of GCS using CMR tagging has independent and incremental value in the prediction of MACE when added to clinical predictors, LVEF and LGE as part of a routine CMR protocol.

- Importantly, this incremental predictive value of GCS held true in the absence of significant left ventricular systolic dysfunction extending its applicability. Indeed, in patients with LVEF $\geq 35\%$, a reduced GCS in association with the presence of LGE had a similarly poor prognosis as those with LVEF $< 35\%$.

3.4.2. Clinical Context

LVEF has been shown to be a strong predictor of adverse outcome (Solomon et al., 2005, Dagues and Hindricks, 2013). The presence of severe left ventricular systolic dysfunction (LVSD), defined by an LVEF $< 35\%$, is a marker of extremely poor prognosis, and is commonly used to guide treatment decisions regarding use of mortality and morbidity improving therapies such as defibrillators and cardiac resynchronization therapy (McMurray et al., 2012, Yancy et al., 2013). Despite these factors, the use of LVEF alone is subject to some limitations. Firstly, it is known that a strict cut-off based on ejection fraction may still miss patients at higher risk as patients with an LVEF $> 35\%$ can still have admissions for heart failure and cardiac death (Gorgels et al., 2003, Makikallio et al., 2005, Stecker et al., 2006). Secondly, LVEF is not purely a measure of contractility as it is affected by volumes, loading conditions, heart rate, and valvular function among other factors. This means that patients with a preserved or mildly reduced LVEF may still have an adverse prognosis (Gustafsson et al., 2003), whereas some healthy patients may actually have reduced LVEF (Abergel et al., 2004). This has led to the search for other parameters that may improve risk stratification.

LGE has emerged as a powerful predictor of adverse outcome in patients with both reduced and preserved LVEF (Kwong et al., 2006, Wu et al., 2008, Krittayaphong et al., 2011, Gulati et al., 2013). Its absence may provide extra reassurance to clinicians in patients who might already be at high risk of MACE. The presence of LGE signifies myocardial fibrosis, which as well as reducing overall myocardial contractility, might also represent a substrate for ventricular arrhythmias which might lead to sudden death (Iles et al., 2011, Scott et al., 2011a, Dawson et al., 2013). This study adds to the increasing evidence suggesting that the presence of LGE is an adverse prognostic indicator, not only in traditionally high-risk patients (LVEF $< 35\%$), but also in those who might be thought to have a reduced risk (LVEF $\geq 35\%$).

3.4.3. The Additional Value of Global Circumferential Strain

The measurement of circumferential strain perhaps aims to resolve some of the problems associated with LVEF related to loading conditions. GCS is a less load-dependent measure than LVEF, and is thought to better reflect myocardial contractile function (Ibrahim et al., 2011). Strain measured using echocardiography has been shown to be an independent marker of adverse prognosis that is potentially stronger than LVEF in a number of studies (Cho et al., 2009, Stanton et al., 2009). However, although CMR tagging is accepted as the gold standard for non-invasive assessment of strain, only one study has evaluated the prognostic value of tagging. A recent study by Choi et al. in the Multi-Ethnic Study of Atherosclerosis cohort evaluated 1,768 asymptomatic patients using CMR tagging (Choi et al., 2013). The authors found that GCS provided incremental prognostic value when added to baseline clinical variables and LVEF. This incremental benefit also persisted in patients with preserved LVEF.

This study, on one hand, parallels the results of Choi et al., and on the other extends its observations to patients with suspected cardiac disease, underscoring the additional clinical value of CMR tagging. Similar to Choi et al., I also found that GCS was an independent predictor of adverse events in a large unselected cohort of patients undergoing CMR examination. In addition, I found that the incremental benefit of GCS was also present when the presence of LGE was included. This is important as most CMR protocols include the use of gadolinium contrast agents and so to have clinical utility it is important that the use of tagging has incremental benefit to both LVEF and LGE.

The incremental benefit of GCS may be due to two reasons. Firstly, changes in strain might reflect a composite of myocardial fibrosis and contractile dysfunction, which LVEF and LGE only measure individually (Buckberg et al., 2008, Rosen et al., 2005). This combined assessment using GCS might provide more powerful prognostic information. Indeed, GCS is the major contributor to left ventricular stroke volume (Buckberg et al., 2008). Secondly, LGE is often not able to identify diffuse myocardial fibrosis due to the need to identify areas of “nulled” healthy myocardium (Mewton et al., 2011). Assessment of GCS may identify areas of reduced contractility caused by diffuse fibrosis not picked up by LGE (Dass et al., 2012). This may also explain the incremental prognostic value of GCS in patients with moderate and preserved LV function. Interestingly, the presence of LGE was a stronger predictor of outcome in this group. This might have implications for

Chapter 3: The Combined Prognostic Value of LVEF, LGE and GCS in a Large Unselected Cohort

the use of defibrillator therapies in this group, as it might suggest that the more common cause of adverse outcome in this group is ventricular arrhythmia rather than pump failure. The results of this study perhaps point to this being the case.

3.4.4. Feasibility of CMR Tagging

The addition of CMR tagging did not add too much time to the standard CMR protocol of cine and LGE imaging. Ultimately, with current the availability of fast acquisition imaging hardware as well as user friendly tagging software, assessment of GCS could potentially be incorporated into routine CMR examinations and provide incremental prognostic value in addition to LVEF and LGE. The identification of patients with LVEF $\geq 35\%$ but reduced GCS and LGE may identify a group that could benefit from more advanced therapies, whereas those impaired LV systolic function but preserved GCS and the absence of LGE might have a better prognosis.

3.4.5. Limitations

This study has two inherent limitations, firstly its single-centre nature, and secondly that it suffers from an element of referral bias as patients were only included if referred for CMR. CMR is not yet a routine part of clinical care (for most conditions), and so this study most likely only included patients in whom the clinician wished to have further information and may have been more concerned about. Nevertheless, by having very few exclusion criteria, and including consecutive patients, the study cohort is still very broad and generalisable to routine clinical care.

Only GCS was assessed in this study. The protocol did not include long-axis views for assessment of global longitudinal strain (GLS) in this cohort in order to keep scan times to a minimum. However, GLS has been shown to be a strong echocardiographic predictor of outcome (Stanton et al., 2009). Additionally, strain rate and diastolic deformation parameters were not assessed in this study, which may also have prognostic value.

3.5. Conclusions

The assessment of GCS by CMR tagging provides incremental prognostic value for prediction of adverse cardiovascular events when added to baseline clinical variables, LVEF and LGE in a routine CMR protocol in patients with and without severe LV systolic dysfunction. Assessment of myocardial strain may be a useful parameter to include in CMR scanning protocols and help identify a group of patients with increased risk despite not initially meeting the current guidelines for being high-risk.

4. Prevalence and Prognostic Significance of Lipomatous Metaplasia in Patients with Prior Myocardial Infarction

4.1. Introduction

In the last chapter I showed the incremental prognostic significance of CMR using techniques that utilise its 2 main advantages, namely its superior ability (compared to other non-invasive techniques) to assess left ventricular function, and its ability to provide information on tissue characterisation.

During scanning the cohort of patients for the study in the previous chapter, it became apparent that in patients with prior myocardial infarction (MI), the pattern of LGE (representing myocardial infarct scar) was not always a confluent area, but in fact contained various components that could be characterised further using other CMR techniques.

Following MI, numerous changes, known as remodeling occur. Among these, the presence and extent of LGE in the injured area is recognised as a strong predictor of adverse outcomes by means of providing a substrate for ventricular arrhythmias and sudden cardiac death (SCD) (Bello et al., 2005, Klem et al., 2012, Kwon et al., 2009, Scott et al., 2011a). It has been recently noted, initially in pathological specimens, that infarcted myocardium can be infiltrated by adipose cells, known as lipomatous metaplasia (LM). Pathological studies have found a prevalence of LM of between 68% and 84% in patients with a history of prior myocardial infarction (Baroldi et al., 1997, Su et al., 2004). It has also been suggested that the presence of myocardial fat may interfere with the conduction system of the heart, perhaps providing a substrate for SCD (Pantanowitz, 2001).

Recognition of LM in early studies was limited as it is not detected by echocardiography or SPECT imaging (Nucifora et al., 2011). Recently, the use of computed tomography (CT) and CMR has allowed in-vivo identification of LM (Winer-Muram et al., 2004, Schmitt et al., 2007, Wu et al., 2007). Recent studies have aimed to characterise the incidence of LM using both CT and CMR, but they have been limited by their small size and/or retrospective nature (Ahn et al., 2009, Goldfarb et al., 2009, Ichikawa et al., 2009, Lucke et al., 2010). Recently there has been evidence that the development of LM in an ovine model of myocardial infarction is associated with an increased of ventricular arrhythmia (Pouliopoulos et al., 2013). To date no study has prospectively characterised the prevalence, functional characteristics and prognostic relevance of LM post-MI.

As well as LGE imaging, acquisition of images 1-2 minutes post-injection of gadolinium (known as early gadolinium enhancement imaging – EGE) allows identification of microvascular obstruction within infarcted myocardium, a known marker of adverse prognosis post-MI (Wu et al., 1998). Meanwhile, T2-weighted sequences such as black-blood short-tau inversion recovery (T2-STIR) allow identification of myocardial oedema, visualized by areas of increased signal (Simonetti et al., 1996). Oedema develops acutely after MI due to the myocyte necrosis, causing release of cellular contents and increased myocardial water content.

These sequences also offer an opportunity to identify fat within the myocardium. T2-STIR sequences give low intensity in areas occupied by fat, and the removal of the STIR pulse will result in signal increase in the corresponding region. In order to identify the present of fat within the infarct territory, a pair of T2-weighted spatially matched images with and without a fat suppressing STIR pulse (henceforth described as T2-STIR+ and T2–STIR-) were added to the CMR protocol.

The aim of this study was to prospectively evaluate the incidence and prognostic significance of LM in an unselected cohort of patients with prior MI using the aforementioned CMR techniques.

4.2. Methods

4.2.1. Patient Selection

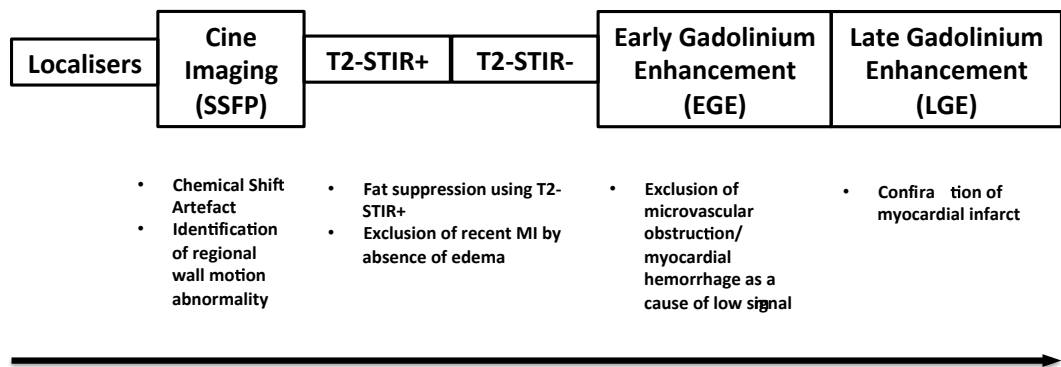
This study included consecutive patients who had a remote history of MI (>6 months), referred by for CMR for evaluation of cardiac symptoms such as chest pain or dyspnoea. Diagnosis of prior MI was confirmed by review of the clinical notes of the index presentation for a combination of typical symptoms (such as typical chest pain, dyspnea, autonomic symptoms), a diagnostic rise in cardiac biomarkers (troponin I >0.04ng/ml) and electrocardiographic changes consistent with type 1 MI (ST elevation/depression, new T wave abnormalities or pathological Q waves) (Thygesen et al., 2012). To corroborate the evidence of type 1 MI secondary to obstructive coronary artery disease, all patients had undergone either invasive or CT coronary angiography (14+/- 10 days post event). Patients with angiographically normal epicardial coronary arteries, stress-related cardiomyopathy

or myocarditis were excluded. Baseline characteristics were obtained from the patients' hospital records.

4.2.2. CMR Protocol

As described in Chapter 2, cine images were obtained for assessment of mass and function using an SSFP sequence in long-axis planes and short-axis slices from the mitral valve to the apex of the left ventricle. Following this, T2-weighted imaging was conducted in 3 matched short-axis slices (representing the basal, mid and apical segments) using a STIR sequence (T2-STIR+) (Simonetti et al., 1996). The identical underlying black-blood sequence was then performed without a third inversion pulse (T2-STIR-). After injection of gadolinium, EGE imaging was obtained at 2 and 5 minutes post-injection as described previously in our unit (Payne et al., 2011a). 10 minutes after the injection LGE imaging was performed using an inversion recovery fast gradient-echo sequence. The CMR protocol is summarised in figure 4-1.

Figure 4-1. Summary of the CMR Examination Sequence.



Left ventricular diameter, mass volumes and function were derived from the short-axis slices using manual tracing of the endocardial and epicardial contours. The presence of LGE was assessed by identification of areas of myocardium with a signal intensity of >5SD above remote myocardium. This area was expressed as percentage of the total left ventricular area measured in short-axis as described in Chapter 2.

The imaging protocol was specifically designed to identify myocardial fat in a comprehensive manner and to try to exclude potential confounders that might be mistaken for fat. To achieve this, the presence of LM was based on several features:

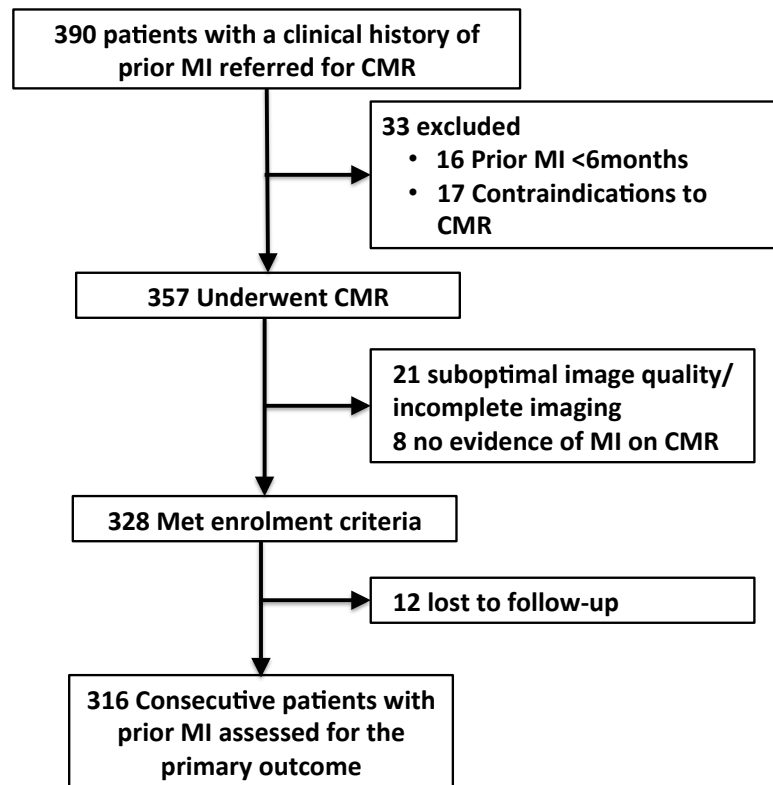
- Firstly, the presence of a “chemical shift artefact” on SSFP imaging in an area with a regional wall motion abnormality (RWMA). This artifact is caused by the difference in signal intensity between fat and myocardium, and has previously been recognised as an indicator of the presence myocardial fat (Lucke et al., 2010).
- Secondly, the presence of an area of hypointense signal on T2-STIR+ images within the areas of myocardial infarct i.e. within the area with the RWMA. Thirdly, the same area should appear isointense on T2-STIR- images (any areas that remained hypointense on T2-STIR- images could be due to intra-infarct hemorrhage which can occur after MI) (Ganame et al., 2009). Also, the absence of hyperintense areas using T2-weighted imaging was designed to confirm the absence of recent myocardial injury (Wright et al., 2009).
- Prior myocardial infarction was confirmed by the presence of LGE in a subendocardial or transmural pattern in the area with a RWMA.
- Finally, to further exclude intramyocardial hemorrhage and microvascular obstruction, the segment(s) with RWMA had to have no hypointense areas on either EGE or LGE imaging, thus excluding the presence of microvascular obstruction (Wu, 2012).

To provide further corroboration of the identification of LM using CMR, CMR findings were compared with cardiac CT in those patients who underwent both, specifically measuring the signal intensity (in Hounsfield units) of those areas where fat was suspected. This also allowed exclusion of a final confounder in our CMR diagnosis of LM, namely the myocardial infarct calcification which may also cause a low signal that could be mistaken for fat using our CMR technique, but causes high signal on CT (Su et al., 2004).

4.2.3. Clinical Follow-up

All patients were followed-up using the computerised record linkage system allowing identification of all deaths and hospital admissions. In total 12 patients were lost to follow-up and were not included in the final analysis (figure 4-2).

Figure 4-2. Derivation of the Study Cohort.



The combined primary outcome was all-cause mortality, sustained ventricular arrhythmia and heart failure hospitalisation. Cause of death was determined from the case notes, records from the patient’s general practitioner and post-mortem or death certificate where available. Sustained ventricular arrhythmia was documented as survived cardiac arrest, any ventricular arrhythmia requiring hospital admission or emergency DC cardioversion for haemodynamic instability or any appropriate implantable cardioverter-defibrillator activation.

4.2.4. Statistical Methods

As described in Chapter 2, continuous variables are reported as mean \pm standard deviation while categorical variables are reported as numbers with percentage in brackets. Comparisons between groups were evaluated using t-tests or χ -squared tests as appropriate. Logistic regression was used to identify independent predictors of the presence of LM. Kaplan-Meier and Cox-proportional hazards methods were used to evaluate the univariable prognostic significance of various factors for the prediction of cardiovascular mortality, ventricular arrhythmias and HF hospitalizations from the time of CMR examination. To determine the independent prognostic significance of the presence of LM, multivariable

models were created including statistically significant univariable predictors in a forward stepwise selection (including variables with significance $p < 0.10$). Only the most significant variables were included to allow one variable for every 10 occurrences of the primary endpoint. Multivariable models were created to separately assess the impact of clinical factors (model 1), LV remodeling (model 2) and infarct characteristics (model 3) before assessing the impact of LM with the strongest overall predictors (model 4). In patients in whom 2 different events occurred the time to first event was used. The c-statistic was calculated for the multivariable model based on the Cox proportional hazards model. For all analyses a p value < 0.05 was considered statistically significant and all p values are two-tailed.

4.3. Results

4.3.1. Baseline Characteristics

390 consecutive patients referred for CMR were screened for inclusion into the study. Of these, 316 patients were eligible and had complete follow-up. Derivation of the cohort is summarised above in figure 4-2.

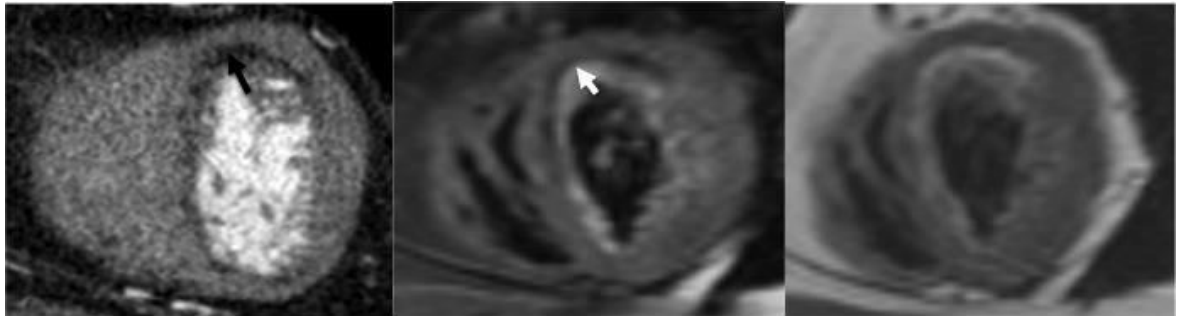
The average age of the cohort was 58.6 ± 10.9 years and the majority were male (75.3%). Median time from MI to CMR examination was 4.0 years (IQR 0.75-9.5 years). 217 patients had undergone invasive coronary angiography (68.7%) and 99 (31.3%) had undergone CT coronary angiography to confirm coronary artery disease. The mean LVEF was $40.2\% \pm 15.1\%$ (median 21%, IQR 10-33%) and mean NYHA class 1.97 ± 0.87 . There was a high prevalence of cardiovascular risk factors (diabetes 26.7%, hypercholesterolemia 20.4% and hypertension 34.3%). Median follow-up was 2.9 years (IQR 1.7-3.5 years). The majority of patients had LAD territory infarcts (35.0%) while 25.4% had multi-vessel infarcts. Mean infarct size was $23.33\% \pm 15.02\%$ (median 21%, IQR 10-33%) of the left ventricle and just over half had transmural infarcts (51.8%).

4.3.2. Comparison with CT

42 patients with LM and 57 without LM underwent coronary CT as well as CMR examination. Using this CMR protocol, the diagnosis of LM corresponded very well to

hypointense areas seen on CT typical of myocardial fat, rather than peri-infarct calcification (figure 4-3).

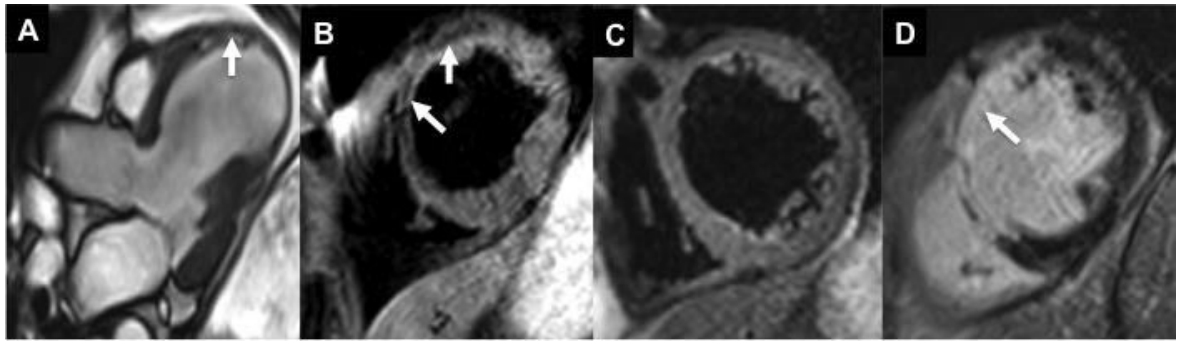
Figure 4-3. Correlation Between CMR and CT for Identification of LM.



A patient with a prior LAD territory myocardial infarct imaged using CT and CMR. Coronary CT shows the presence of subendocardial hypointense signal in the 3-chamber view (-36 Hounsfield units) in the anterior wall (left; arrow). CMR T2-STIR+ imaging also shows the presence of hypointense signal in the same territory as the CT (middle; arrow) which appears isointense using T2-STIR- (right).

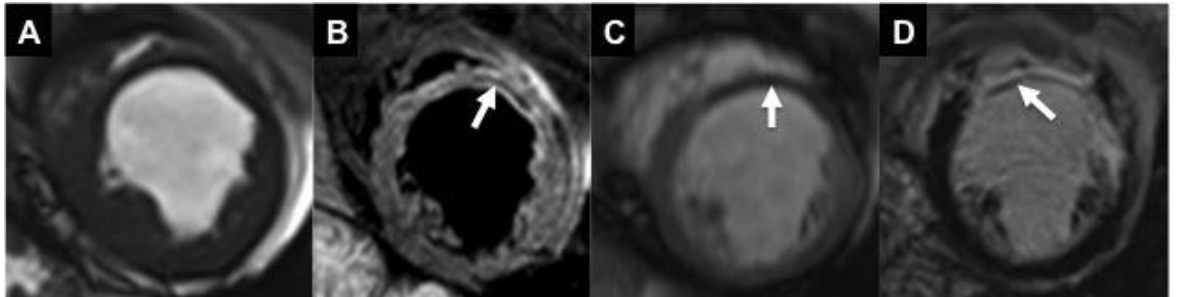
Overall, the mean signal intensity of the areas of LM in the 42 patients with LM was -32 ± 27 Hounsfield units in comparison to normal myocardium which measured 98 ± 38 Hounsfield units. The addition of EGE imaging also allowed us to exclude the presence of myocardial hemorrhage as a cause of hypointense signal on T2-weighted imaging (figures 4-4 and 4-5).

Figure 4-4. CMR Imaging of LM Using The Study Protocol.



The presence of LM in the infarcted area (anteroseptal wall) was seen non-invasively through the presence of chemical shift artefact using steady state free precession imaging (A; arrow). Using T2W+STIR imaging this area appeared hypointense (B; arrows) but isointense using T2W-STIR (C). Late gadolinium enhancement imaging confirmed an LAD territory infarct with fibrosis in the anterior wall and septum and no central area of microvascular obstruction (D; arrow).

Figure 4-5. CMR Imaging of Microvascular Obstruction Using The Study Protocol.



An example of the utility of early and late gadolinium enhancement in differentiating between LM and microvascular obstruction caused by myocardial haemorrhage.

SSFP cine imaging reveals the presence of an anterior wall motion abnormality suspicious of prior MI (A). There is a hypointense area on T2-STIR+ imaging that was suspicious for LM (B; arrow) however this area also appeared hypointense on early gadolinium enhancement imaging (C; arrow), suggesting that it was caused by intra-infarct myocardial haemorrhage rather than fat. This was corroborated by a similar hypointense area within the infarcted myocardium on late gadolinium enhancement imaging corresponding to an area of microvascular obstruction caused by haemorrhage (D; arrow).

4.3.3. Incidence and Functional Impact of LM

Using the CMR diagnostic criteria for LM, 77 patients from the total 316 (24.4%) had evidence of LM (LM+). Clinical and CMR associations with the presence of LM are summarized in tables 4-1 and 4-2.

Table 4-1. Baseline Clinical Characteristics.

Variable	All Patients (n=316)	LM + (n=77)	LM – (n=239)	p value
Age (yrs)	58.6 ± 10.9	59.4 ± 9.7	58.4 ± 11.3	0.46
Male (%)	229 (75.3)	55 (71.4)	174 (76.7)	0.36
Height (m)	1.69 ± 0.10	1.68 ± 0.09	1.69 ± 0.10	0.26
Weight (kg)	82.4 ± 17.7	81.5 ± 15.7	82.7 ± 18.4	0.61
BMI (kg/m ²)	28.9 ± 5.2	29.0 ± 4.8	28.8 ± 5.4	0.81
Diabetes (%)	56 (26.7)	17 (32.7)	39 (24.7)	0.40
AF (%)	26 (12.3)	9 (17)	17 (10.8)	0.23
Hypercholesterolemia (%)	43 (20.4)	11 (20.8)	32 (20.3)	0.94
Chronic Kidney Disease (%)	22 (10.4)	7 (13.2)	15 (9.5)	0.44
Hypertension (%)	69 (34.3)	18 (34.6)	51 (34.2)	0.96
Beta-blocker (%)	278 (88.0)	64 (83.1)	214 (89.5)	0.11
ACEI /ARB (%)	256 (81.0)	63 (81.8)	193 (80.8)	0.91
MRA (%)	112 (35.4)	30 (39)	82 (34.3)	0.56
Statin (%)	48 (76.2)	10 (66.7)	38 (79.2)	0.32
Prior Revascularisation (%)	166 (52.5)	35 (45.5)	132 (55.2)	0.15
Years since MI	6.45 ± 6.62	10.38 ± 7.11	5.19 ± 5.96	<0.001
Mean NYHA Class	1.97 ± 0.87	2.30 ± 0.82	1.86 ± 0.87	0.001

ACEI – angiotensin converting enzyme inhibitor; ARB – angiotensin II receptor antagonist; BMI – body mass index; AF – atrial fibrillation; LVEDD – left ventricular end-diastolic diameter; MRA – mineralocorticoid receptor antagonist

Data are presented as mean ± SD if continuous or number (%) if categorical.

Table 4-2. Baseline CMR Characteristics.

Variable	All Patients (n=316)	LM + (n=77)	LM – (n=239)	p value
LVEF (%)	40.2 ± 15.1	33.1 ± 13.1	42.6 ± 15.0	<0.001
LVEDVi (ml/m ²)	115.3 ± 43.6	136.0 ± 50.2	108.1 ± 38.7	<0.001
LVESVi (ml/m ²)	75.2 ± 49.8	100.9 ± 66.6	66.5 ± 39.0	<0.001
LV Mass (g/m ²)	87.2 ± 26.3	94.1 ± 29.4	84.8 ± 24.8	0.007
LVEDD (cm)	6.67 ± 1.03	7.17 ± 1.18	6.49 ± 0.91	<0.001
LVESD (cm)	5.26 ± 1.34	5.94 ± 1.41	5.02 ± 1.24	<0.001
Infarct Size (%)	23.33 ± 15.02	31.56 ± 12.08	20.45 ± 14.91	<0.001
Transmural Infarct	156 (51.8)	66 (85.7)	90 (40.2)	<0.001
Coronary Artery Territory				0.004
LAD	106 (35.0)	28 (36.4)	78 (34.5)	
LCx	48 (15.8)	7 (9.1)	41 (18.1)	
RCA	72 (23.8)	12 (15.6)	60 (26.5)	
Multi-vessel	77 (25.4)	30 (39.0)	47 (20.8)	
LV Aneurysm	14 (6.6)	10 (17.5)	4 (2.6)	<0.001
LV Thrombus	10 (4.7)	4 (7)	6 (3.9)	0.46

LVEF – left ventricular ejection fraction; LVEDi – left ventricular end-diastolic volume index; LVESVi – left ventricular end-systolic volume index; LVEDD – left ventricular end-diastolic diameter; LVESD – left ventricular end-systolic diameter; WMSI – wall motion score index; LAD – left anterior descending artery; LCx – circumflex artery; RCA – right coronary artery

Data are presented as mean ± SD if continuous or number (%) if categorical.

LM+ patients had older infarcts (mean infarct age 10.38 ± 7.11 years vs. 5.19 ± 5.96; p<0.001), had more extensive infarcts (infarct size 31.56% ± 12.08% vs. 20.45% ± 14.91%; p<0.001; and more often had transmural infarction (85.7% vs. 40.2%; p<0.001). There was no significant difference in the use of beta-blockers, ACE inhibitors or mineralocorticoid receptor antagonists between the two groups. LM was not associated with any clinical factors such as age, gender, weight, body mass index, diabetes, chronic

kidney disease, hypertension, hypercholesterolemia or atrial fibrillation. It was also not associated with prior revascularization (by PCI or CABG).

However, LM was associated with greater degrees of adverse remodeling. LM+ patients had lower LVEF ($33.1\% \pm 13.1\%$ vs. $42.6\% \pm 15.0\%$; $p < 0.001$) and higher left ventricular end-diastolic volume index ($136.0 \pm 50.2 \text{ ml/m}^2$ vs. $108.1 \pm 38.7 \text{ ml/m}^2$; $p < 0.001$) and end-systolic volume index ($100.9 \pm 66.6 \text{ ml/m}^2$ vs. $66.5 \pm 39.0 \text{ ml/m}^2$; $p < 0.001$). LM was also more likely to be present in patients with aneurysmal left ventricular segments (17.5% vs. 2.6% ; $p < 0.001$). There was no association with the presence of LV thrombus (7% vs. 3.9% ; $p = 0.46$). Using logistic regression, both infarct size measured by LGE (OR 1.03; 95% CI 1.01-1.06, $p = 0.003$) and LVEF (OR 0.97; 95% CI 0.95-1.00, $p = 0.022$) were predictors of the presence of LM.

4.3.4. Prediction of Adverse Cardiovascular Outcome

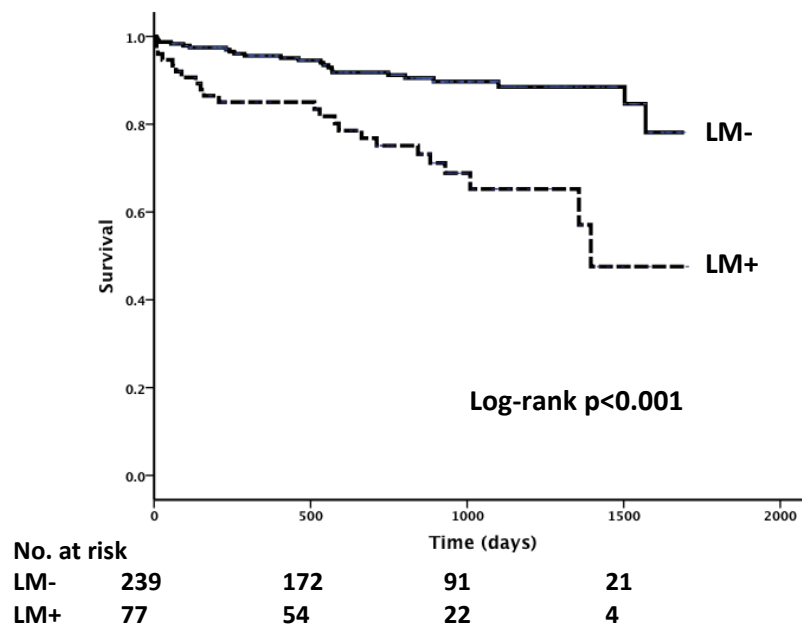
The primary outcome of all-cause mortality, ventricular arrhythmia and HF hospitalisation occurred in 46 patients, 23 LM+ (29.9%) and 23 LM- (9.6%). There were 29 deaths, of which 25 were cardiovascular. 2 were related to malignancy and 2 due to end-stage respiratory failure. There were 12 arrhythmic events, and 5 heart failure hospitalisations. In univariable analysis, LM was a significant predictor of the primary outcome (HR 3.65; 95% CI 2.04-6.52, $p < 0.001$) (table 4-3 and figure 4-6).

Table 4-3. Univariable Predictors of the Primary Outcome.

Variable	HR (95% CI)	p value	χ^2
Age (yrs)	1.01 (0.99-1.04)	0.30	1.09
Male (%)	0.65 (0.35-1.20)	0.16	1.96
Weight (kg)	0.99 (0.98-1.01)	0.37	0.82
Body Mass Index (kg/m ²)	0.99 (0.93-1.05)	0.62	0.24
Diabetes	1.93 (1.06-3.49)	0.03	4.85
Atrial Fibrillation	3.31 (1.68-6.50)	0.001	13.48
Hypercholesterolemia	1.16 (0.52-2.60)	0.72	0.13
Chronic Kidney Disease	1.95 (0.87-4.36)	0.10	2.76
Hypertension	0.94 (0.48-1.86)	0.87	0.03
Statin	1.02 (0.57-1.81)	0.96	0.003
Beta-blocker	0.40 (0.20-0.81)	0.011	6.91
ACE Inhibitors/Angiotensin II Receptor Blocker	0.65 (0.32-1.34)	0.24	1.38
Mineralocorticoid receptor antagonist	0.97 (0.50-1.87)	0.92	0.01
NYHA Class	1.57 (1.19-2.25)	0.012	6.39
LVEF (%)	0.97 (0.95-0.99)	0.003	8.92
LV Mass (g/m ²)	1.00 (0.99-1.01)	0.43	0.61
LVEDD (cm)	1.36 (1.04-1.79)	0.026	4.93
LVESD (cm)	1.31 (1.06-1.63)	0.014	6.14
LVEDVi (ml/m ²)	1.01 (1.00-1.01)	0.026	4.92
LVESVi (ml/m ²)	1.00 (1.00-1.01)	0.11	2.59
LM +	3.65 (2.04-6.52)	<0.001	21.79
Infarct Size (%)	1.02 (1.00-1.04)	0.08	3.17
Infarct Size (per 10% increase)	1.30 (1.02-1.65)	0.035	4.55
Multivessel Infarct	2.29 (1.27-4.12)	0.006	8.03
Transmural Infarct	1.68 (0.92-3.09)	0.09	2.86
LV Aneurysm	2.61 (1.02-6.65)	0.044	4.36

HR – hazard ratio; LVEF – left ventricular ejection fraction; LVEDD – left ventricular end-diastolic diameter; LVESD – left ventricular end-systolic diameter; LVEDVi – left ventricular end-diastolic volume index; LVESVi – left ventricular systolic volume index; LM – lipomatous metaplasia

Figure 4-6. Kaplan-Meier Survival Curves by LM status for Prediction of the Primary Outcome.



Other univariable predictors of the primary outcome were atrial fibrillation (HR 3.31; 95% CI 1.68-6.50, $p=0.001$), diabetes (HR 1.93; 95% CI 1.06-3.49, $p=0.03$), LVEF (HR 0.97 per 1% increase; 95% CI 0.95-0.99, $p=0.003$), infarct size (HR 1.30 per 10% increase; 95% CI 1.02-1.65, $p=0.035$), beta-blocker use (HR 0.40; 95% CI 0.20-0.81, $p=0.011$) and NYHA class (HR 1.57; 95% CI 1.10-2.25, $p=0.012$). Left ventricular dimensions, aneurysms and the presence of multi-vessel infarcts were also significant predictors of the primary outcome. The presence of LM remained significant predictor of the primary outcome in all multivariable models (table 4-4). The addition of LM to multivariable model 4 increased the c-statistic for the prediction of the composite primary outcome from 0.70 (95% CI 0.62-0.79) to 0.76 (95% CI 0.70-0.82; $p=0.15$).

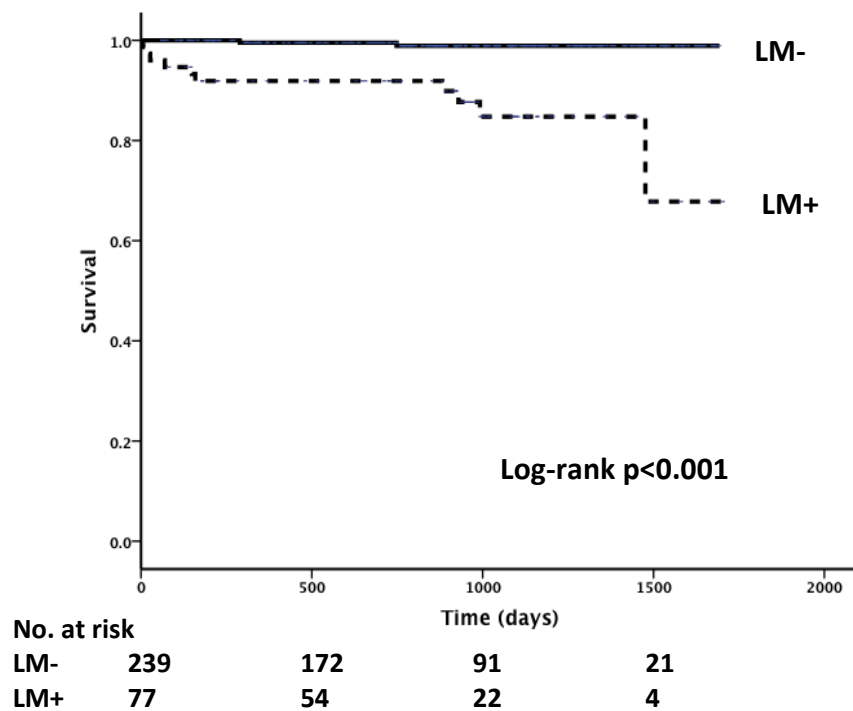
Table 4-4. Multivariable Predictors of the Primary Outcome.

	Variable	HR (95% CI)	p value
Model 1 (clinical)	NYHA Class	1.37 (0.92-2.02)	0.12
	Diabetes	1.88 (0.96-3.68)	0.07
	AF	3.51 (1.69-7.32)	0.001
	Beta-blocker use	0.55 (0.25-1.22)	0.55
	LM +	3.84 (1.75-8.43)	0.001
Model 2 (remodeling)	LVEDV (ml/m ²)	1.00 (0.99-1.01)	0.65
	LVESD (cm)	0.94 (0.47-1.90)	0.87
	LVEDD (cm)	1.07 (0.47-2.42)	0.87
	LVEF (%)	0.97 (0.94-1.01)	0.09
	LM +	3.07 (1.64-5.74)	<0.001
Model 3 (infarct characteristics)	Infarct size (per 10%)	0.97 (0.71-1.34)	0.87
	Multi-vessel infarct	1.89 (0.98-3.65)	0.06
	Aneurysm	1.63 (0.60-4.39)	0.34
	Transmural infarct	1.00 (0.49-2.03)	0.99
	LM +	2.89 (1.48-5.65)	0.002
Model 4 (strongest combined)	AF	2.85 (1.42-5.72)	0.003
	LVEF	0.98 (0.96-1.00)	0.09
	Diabetes	1.93 (1.05-3.56)	0.036
	Multi-vessel infarct	1.38 (0.74-2.58)	0.31
	LM +	2.67 (1.44-4.96)	0.002

AF – atrial fibrillation; LVEF – left ventricular function; LM – lipomatous metaplasia; HR – hazard ratio; LVEF – left ventricular ejection fraction; LVEDD – left ventricular end-diastolic diameter; LVESD – left ventricular end-systolic diameter

There were 12 patients who had recorded ventricular arrhythmias over the follow-up period, 10 in the LM+ group (12.9%) and 2 in the LM- group (0.8%). The presence of LM was the only significant predictor of ventricular arrhythmia (HR 17.65; 95% CI 3.86-80.76, $p < 0.001$) (figure 4-7).

Figure 4-7. Kaplan-Meier Survival Curves by LM status for Prediction of Ventricular Arrhythmia.



4.4. Discussion

4.4.1. Study Findings

This study was the first study to examine the prognostic significance of LM in patients with a history of prior MI. The two main findings were that:

- This study confirmed findings from prior studies suggesting that the presence of LM is associated with older infarcts, lower LVEF, adverse LV remodeling and larger infarct size as measured by LGE in a large cohort.

- In addition, this study has shown for the first time that the presence of LM is an independent predictor of adverse outcome post-MI.

4.4.2. Clinical Context

Following MI, the heart undergoes a process of remodeling involving numerous biochemical pathways which cause inflammation, myocyte hypertrophy and collagen scar formation, leading to morphological changes such as left ventricular dilatation and infarct expansion (Sutton and Sharpe, 2000, Konstam, 2008). The increased use of CMR and CT has provided clinicians with increased ability to characterise tissue, and provide further understanding of the changes in the myocardium that occur post-MI beyond left ventricular dimensions.

The presence of LM has, until recently, only been able to be identified pathologically, inevitably post-mortem. In these pathological studies, it was noted that LM was associated with greater degrees of adverse remodeling, suggesting that its presence might be an adverse prognostic indicator (Baroldi et al., 1997, Su et al., 2004). Of course the very nature of these studies meant that this association could only be postulated. The use of CMR has allowed, for the first time, this hypothesis to be tested.

While ACE inhibitors and beta-blockers are a cornerstone of post-MI therapy due to their beneficial effects on adverse remodeling of the left ventricle, they have less of an effect on infarct scar. Characterisation of infarct scar, including the presence of LM, might provide a new therapeutic target to improve outcomes in this group of patients.

4.4.3. Lipomatous Metaplasia - A Novel Target for Therapeutic Intervention?

In pathological studies, LM appears to be fairly common in patients with a history of prior MI. Baroldi et al were the first to report the presence of LM in MI scar using histopathology, with an incidence of 68% (Baroldi et al., 1997). A further study of explanted hearts by Su et al reported an incidence of 84% (Su et al., 2004). These figures are significantly higher than the incidence reported in this study (24.4%). This might be explained by the lower spatial resolution of CMR compared to histological examination, which means that CMR may miss very small areas of adipose tissue. Su et al found that only 17% of infarcts had adipose >25% of the infarct size – potentially, this may be the

level of adipose tissue which can be identified as LM by CMR. Baroldi et al also reported that only 28% of the patients that they identified with LM had adipose tissue greater than 20%.

The prevalence of LM in this cohort is similar to two large retrospective studies investigating the prevalence of LM. Ahn et al reported a prevalence of 22.4% in 161 patients evaluated by CT, a similar figure to this study (Ahn et al., 2009). The identification of intramyocardial fat by its low attenuation (around -30 Hounsfield units) on CT has been well described (Ichikawa et al., 2009). Another large study of 315 patients using CMR by Lucke et al reported a prevalence of only 11% (Lucke et al., 2010). This may have been because the authors included patients 3-6 months post-MI, when perhaps they had undergone less remodeling. Based on the knowledge that LM tends to reflect adverse remodeling over a duration of time and thus is likely to be linked with older infarcts, patients with an MI less than 6 months prior to CMR were excluded from this study. By using this cut-off the CMR exam would also be a truer reflection of the impact of LM on left ventricular function by allowing more time for any post-infarct myocardial stunning to resolve (Bax et al., 2001).

4.4.4. CMR in Lipomatous Metaplasia

In this study, the presence of LM was associated with more adverse remodeling i.e. ischaemic cardiomyopathy. LM+ patients had lower LVEF and larger left ventricular volumes and diameters. Furthermore, LM was also associated with larger infarcts which were more likely to be transmural and aneurysmal. These findings are in keeping with the original landmark studies of Baroldi and colleagues who reported that LM+ patients had more LV dilatation and more severe left ventricular systolic dysfunction (Baroldi et al., 1997). Pathophysiologically, adipocytes secrete numerous substances within the body, one of which, fatty acid-binding protein is known to depress cardiomyocyte inotropy, perhaps contributing to a reduction in LVEF (Lamounier-Zepter et al., 2009).

Infarct age was the only clinical feature I found to be associated with LM suggesting that its development is progressive (Ahn et al., 2009, Goldfarb et al., 2009, Ichikawa et al., 2009, Lucke et al., 2010). Similar to previously published studies investigating the clinical significance of LM, we did not find any other clinical associations with LM (Ahn et al., 2009, Ichikawa et al., 2009, Lucke et al., 2010). The pathogenesis of adipose deposition

within myocardial infarcts is not clearly understood as yet, however it is known that areas of MI scar display abnormal metabolism with reduced uptake of fatty acids leading to the replacement of collagen with adipocytes (Hansen et al., 1995, Baroldi et al., 1997). It is postulated that newer medical and reperfusion therapies might reduce the development of LM (Su et al., 2004). The prevalence of LM in this study is similar to the earlier histopathological studies (allowing for differences in spatial resolution), despite these therapeutic advances.

This study is the first to demonstrate the independent prognostic significance of LM for prediction of adverse events in a real-world clinical population.

The presence of LM was a stronger predictor than infarct size alone and remained significant when added to left ventricular volumes or ejection fraction. There is an increasing recognition of the prognostic importance of not just infarct scar size, but also its structure (Yan et al., 2006b, Roes et al., 2009, Schmidt et al., 2007). A recent study in a ovine model by Pouliopoulos et al found that the presence of LM in sheep with experimentally induced myocardial infarcts was associated with more inducible ventricular tachycardia (Pouliopoulos et al., 2013). The presence of myocardial fat has also been associated with inducible ventricular tachycardia in humans in the right ventricle (Vignaux et al., 2002). It may be that adipose tissue predisposes to re-entrant tachycardias and impairs myocardial conduction, leading to increased risk of ventricular arrhythmias and death (Pouliopoulos et al., 2013). Strategies to reduce LM may translate to a prognostic benefit in future.

4.4.5. Limitations

This study has some limitations. The lack of histological examination meant that there was no way to pathologically corroborate and validate the CMR findings. This is similar to the other studies and case reports in this area, and is probably a reflection of the reduction in the amount of post-mortems and endomyocardial biopsies conducted in the modern era. The use of CT did however provide some element of confirmation of the CMR techniques. There may also be other reasons for the differences in outcome that we did not explore in this study, for example the presence of any underlying ischemia. This effect was hopefully reduced by selecting consecutive patients. Finally, due to the nature of this study, we are

unable to attribute causation between LM and any of our functional findings. Further studies are required to investigate this.

4.5. Conclusions

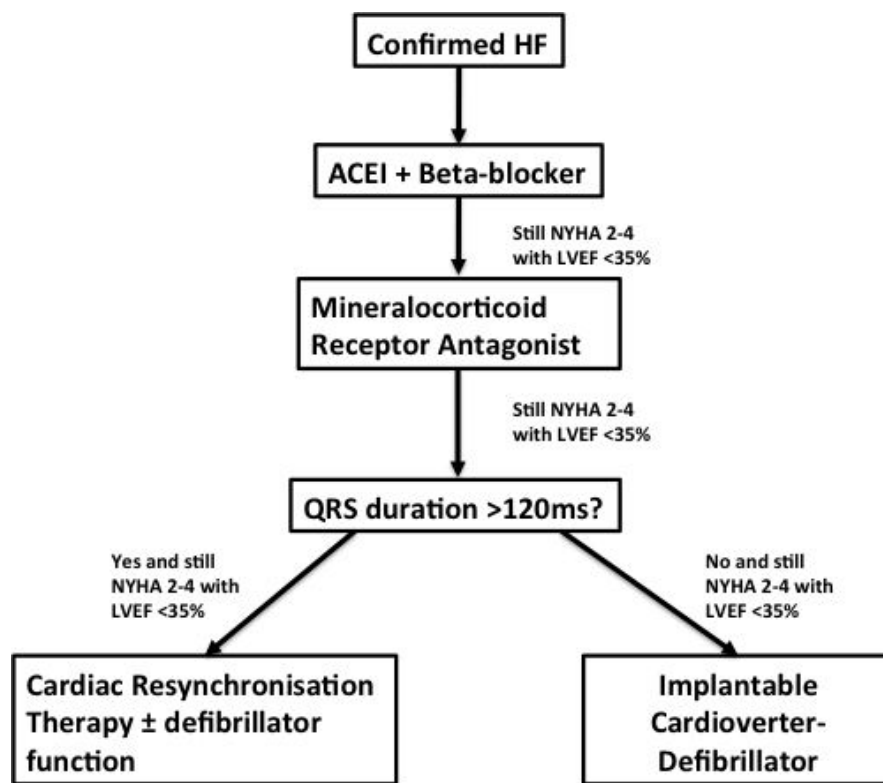
LM is a common finding in patients with prior MI assessed by CMR. It is associated with older and larger infarcts with greater degrees of adverse LV remodeling and more symptomatic heart failure. The presence of LM was an independent predictor of adverse cardiovascular outcome. Additionally, LM appears to act as a substrate for malignant ventricular arrhythmia that may predispose to sudden cardiac death.

5. Late Gadolinium Enhancement and NT-proBNP Identify a Population at Low Risk of Death or Arrhythmic Events in Patients With Primary Prevention Implantable Cardioverter Defibrillators.

5.1. Introduction

In the last chapter I explored the prognostic utility of infarct characteristics in prediction of death and arrhythmias in a cohort of patients with previous MI. The presence of LGE was a significant predictor of adverse outcome. LGE is also present in patients with out infarcts, for example in those with DCM. Both ICM and DCM are common causes of severe heart failure (HF), typically defined as LVEF <35%. Current HF guidelines recommend the use of implantable cardioverter defibrillators (ICDs) in symptomatic patients with severe HF despite optimal medical therapy as these patients are at increased risk of lethal ventricular arrhythmias and sudden death (figure 5-1).

Figure 5-1. Summary of the Current ESC Heart Failure Guidelines (2012).



Adapted from (McMurray et al., 2012). HF – heart failure; ACEI – angiotensin-converting enzyme inhibitor; NYHA – New York Heart Association classification for heart failure symptoms; LVEF – left ventricular ejection fraction.

ICDs and cardiac resynchronization therapy devices with a defibrillator function (CRT-Ds) reduce mortality in symptomatic patients with HF who have not had a prior cardiac arrest, i.e. as primary prevention (Moss et al., 2002, Bardy et al., 2005). Current criteria as

outlined in the ESC HF guidelines rely on the use of LVEF (which is subject to wide variation when measured using standard two-dimensional echocardiography) and NYHA class, which is subjective (based on both the patient's and doctor's interpretation of the patient's symptoms (McMurray et al., 2012). These can be somewhat blunt tools when making the decision to implant these costly devices. The average annual rate of appropriate shocks in clinical trials is only 5.1% and as many as two thirds of patients may never use their ICD after implantation. (Moss et al., 2004, Stecker et al., 2006, Bardy et al., 2005). Therefore, it would be useful to find newer, more accurate methods to improve the identification of individuals who may not be likely to benefit from ICD implantation despite meeting conventional criteria such as NYHA class 2-4 and reduced ejection fraction are needed.

The presence of LGE is associated with a higher risk of all-cause mortality, sudden cardiac death, appropriate ICD activation and admissions for heart failure in HF patients with both ischemic cardiomyopathy (ICM) and dilated cardiomyopathy (DCM) (Bernhardt et al., 2011, Gao et al., 2012, Iles et al., 2011, Kwong et al., 2006, Scott et al., 2011a, Wu et al., 2008, Assomull et al., 2006). I have also demonstrated this relationship in Chapters 3 and 4.

B-type natriuretic peptide (BNP) and N-terminal pro-B type natriuretic peptide (NT-proBNP) are easily measured biomarkers which are presently primarily used in diagnosis of HF. These biomarkers have also been explored as a potential marker of risk in those receiving a primary prevention ICD and predictors of sudden death in HF patients. (Scott et al., 2011b, Biasucci et al., 2012, Berger et al., 2002).

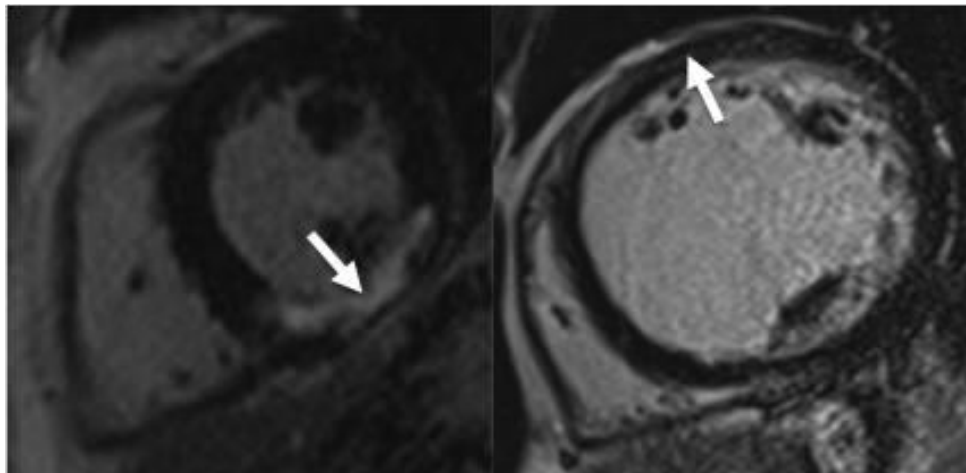
As both LGE and NT-proBNP have been shown to be markers of risk in patients receiving ICDs, it is possible that they may be useful in stratifying high and low-risk patients. The aim of this study was to assess the prognostic utility of LGE and NT-proBNP for prediction of death or appropriate ICD activation in individuals undergoing implantation of a primary prevention ICD. More specifically, I hypothesized that the two markers may be combined in order to predict a group of patients who may be at low risk of ventricular arrhythmia and ICD activation.

5.2. Methods

5.2.1. Patient Selection

157 consecutive patients referred to our tertiary centre for implantation of primary prevention ICD or CRT-D and were referred for a pre-implantation CMR were evaluated. Patients with both ICM and DCM were included. The diagnosis of ICM was made confirmed on the basis of either computed tomography coronary angiography or invasive coronary angiography in conjunction with CMR results. If patients were found to have a small area of late gadolinium enhancement in an ischemic distribution that was felt not to be significant enough to cause the degree of left ventricular systolic impairment seen they were classified as DCM; conversely, in some patients there was a definite regional wall motion abnormality in conjunction with a history of significant stenosis on invasive or CT coronary angiography (>70%) – these patients were classified as having ICM (figure 5-2). All patients referred for a secondary prevention ICD and those with renal impairment unable to be given gadolinium contrast (eGFR<30) were excluded.

Figure 5-2. Typical LGE Patterns.



Typically in ICM enhancement is subendocardial or transmural (left), while in DCM enhancement is midwall or absent (right).

5.2.2. CMR Protocol

All patients underwent a simplified standardised CMR protocol including cine imaging and LGE. Sequences were performed as described in Chapter 2. Briefly, cine images were

obtained using an SSFP sequence in three long axis planes (2-chamber, 3-chamber, 4-chamber) and in short axis slices through the left ventricle. LGE imaging for myocardial infarction was acquired 10 minutes after intravenous gadolinium injection. CMR was performed within a mean of 3 ± 1 day of defibrillator insertion.

All analysis was performed using Argus as described in Chapter 2. Left ventricular diameter, volumes and function were derived from the short-axis slices using manual tracing of the endocardial contours including papillary muscles as part of the ventricular volume. The presence of LGE was assessed by identification of areas of myocardium with a signal intensity of $>5SD$ above normal myocardium. Quantification of LGE was measured using manual planimetry in short-axis and taking this area as percentage of the total left ventricular area measured in short-axis.

5.2.3. NT-proBNP Sampling

Serum NT-proBNP was obtained within 2 ± 1 weeks of defibrillator implantation and analysed in our local laboratory, the methods and reproducibility of which have been previously described (Gardner et al., 2007). Blood samples were collected in ethylenediamine-tetraacetic acid-containing tubes before being centrifuged at 3000rpm for 10 minutes at $0^{\circ}C$ before measurement of NT-proBNP using a chemiluminescent immunoassay kit (Roche Diagnostics, Basel, Switzerland) on a Elecsys 2010 analyzer. Normal values are $<125pg/mL$ in patients aged less than 75 years and $<450pg/mL$ in patients over 75. All participants were stable outpatients ensuring that haemodynamic status at the time of sampling was similar to status at the time of CMR.

5.2.4. Defibrillator Implantation

All patients had an ICD or CRT-D device implanted using standard techniques. Choice of device was at the discretion of the operator.

5.2.5. Clinical Follow-up

The pre-defined primary outcome was death or appropriate ICD therapy, which was either shock for ventricular fibrillation/tachycardia or anti-tachycardia pacing for ventricular

tachycardia. All patients were followed up at 3-6 month intervals using computerized record linkage for death and admissions for ventricular arrhythmias causing appropriate ICD activation. Information about appropriate ICD activation not leading to hospital admission was obtained by searching the records of routine local hospital ICD interrogations. These as performed as a routine out-patient appointment on a 6 monthly basis. Additionally, if the patient experiences an ICD activation for which they are not admitted to hospital, they can also attend hospital for ICD interrogation on an ad-hoc out-patient basis. An independent observer blinded to the CMR analysis and NT-proBNP results adjudicated events (N.T.). No patients were lost to follow-up.

5.2.6. Statistical Methods

As described in Chapter 2, continuous variables are expressed as mean \pm SD and categorical variables are expressed as a number and percentage. Differences between groups were tested using t-tests or the chi-squared tests as appropriate. As the distribution of NT-proBNP was skewed it was log-transformed and geometric means calculated.

Kaplan-Meier and Cox proportional hazards survival analysis was used to examine the association between baseline variables, CMR variables and NT-proBNP and the primary outcome. Percentage LGE and NT-proBNP were most strongly associated with the outcome as assessed by the Chi-squared statistic and were explored further. As NT-proBNP was not normally distributed (log) NT-proBNP was initially evaluated, however to provide clinical relevance the inverse log was then calculated to provide an optimal NT-proBNP value. Multivariable analysis was performed using significant univariable predictors of the primary outcome ($p < 0.05$). The type of device (ICD versus CRT with ICD) was also included to adjust for the potential mortality and morbidity benefits of CRT (Bristow et al., 2004). Correlation between percentage LGE and NT-proBNP was assessed using Pearson's correlation coefficient.

To evaluate optimal discriminatory level of percentage LGE and NT-proBNP for identification of a population at low-risk of death or ventricular arrhythmia, both DCM and ICM cohorts were divided into groups based on percentage of LGE and NT-proBNP. Best cut-off values were identified using ROC curves to obtain the optimal sensitivity and specificity. This allowed stratification of patients by LGE percentage and NT-proBNP into

low and high-risk groups. For all analyses a p value <0.05 was considered statistically significant and all p values are two-tailed.

5.3. Results

5.3.1. Baseline Characteristics

157 patients were included in this study, 60 patients with ICM and 97 patients with DCM. Baseline characteristics of each group are summarized in Table 5-1.

Table 5-1. Baseline clinical and CMR characteristics of the cohort stratified by aetiology.

	Dilated cardiomyopathy (n=96)	Ischemic cardiomyopathy (n=61)	p value
Age (years)	46.0 ± 13.4	57.7 ± 11.2	<0.001
Male	75 (78.1%)	48 (78.6%)	0.69
AF	18 (18.8%)	17 (27.9%)	0.15
Hypertension	14 (14.6%)	13 (21.3%)	0.24
Smoker	19 (19.8%)	23 (37.7%)	0.010
Diabetes	6 (6.3%)	8 (13.1%)	0.13
Prior Revascularisation	6 (6.3%)	32 (52.5%)	<0.001
LBBB	32 (33.3%)	19 (31.1%)	0.86
NYHA Class			0.006
1	15 (15.6)	0 (0.0)	
2	38 (39.6)	24 (39.3)	
3	38 (39.6)	36 (59.0)	
4	5 (5.2)	1 (1.6)	
ACEI/ARB	75 (78.1%)	54 (88.5%)	0.044
Beta-blocker	79 (86.8%)	50 (82.0%)	0.76
Spironolactone	46 (47.9%)	46 (75.4%)	<0.001
Furosemide	52 (54.2%)	45 (73.8%)	0.007
(Ln) NT-proBNP	7.06± 1.24	7.46± 1.05	0.018
LGE present	24 (25)	61 (100)	<0.001
Mean LGE (%)	2.1 ± 6.0	24.8 ± 16.2	<0.001
LVEF (%)	27.2 ± 16.3	28.5 ± 12.9	0.71

AF – atrial fibrillation; LBBB – left bundle branch block; ACEI – angiotensin-converting enzyme inhibitor; ARB – angiotensin II receptor blocker; LVEDD – left ventricular end-diastolic diameter; Ln – natural logarithm; LGE – late gadolinium enhancement; LVEF – left ventricular ejection fraction

Data are presented as mean ± SD if continuous or number (%) if categorical.

Differences between the groups reflected typical risk factors - the ICM cohort was older with more smokers and was more likely to have undergone prior revascularisation. The ICM group was more likely to have LGE on CMR and with a higher mean volume of fibrosis (24.8% vs. 2.1% respectively for ICM vs. DCM patients, $p < 0.001$). The use of evidence-based therapy for heart failure was high in both groups (total on beta-blockers 82.2%; ACE-inhibitors 82.2%; spironolactone 58.9%). The majority of patients had mild to moderately symptomatic heart failure (86.6% NYHA class 2-3 heart failure) and low ejection fraction by CMR, thus meeting the ESC criteria for ICD or CRTD therapy.

5.3.2. Primary Outcome

The median follow-up time of the cohort was 915 days (2.5 years). During the follow-up period 32 patients (20.4%) died or had appropriate defibrillator therapy. There were 12 cardiac deaths (10 due to end-stage heart failure and 2 due to myocardial infarction), 14 appropriate defibrillator shocks and 6 episodes of appropriate anti-tachycardia pacing. The differences between the groups stratified by outcome are summarised in Table 5-2.

Table 5-2. Clinical and CMR characteristics stratified according to occurrence of the primary outcome.

	Primary Outcome (n=32)	Without Primary Outcome (n=125)	p value
Age (years)	51.6 ± 16.8	50.2 ± 13.2	0.64
Male	27 (84.4%)	96 (76.8%)	0.35
ICM	18 (56.2%)	43 (34.4%)	0.024
Diabetes	5 (16.7%)	9 (7.1%)	0.058
LBBB	8 (26.7%)	43 (33.9%)	0.84
NYHA Class			0.11
1	1 (3.1)	14 (11.2)	
2	19 (59.4)	43 (34.4)	
3	11 (34.4)	63 (50.4)	
4	1 (3.1)	5 (4.0)	
ACEI/ARB	18 (60.0%)	111 (87.4%)	0.059
Beta-blocker	18 (60.0%)	111 (87.4%)	0.001
Spirolactone	13 (43.3%)	79 (62.2%)	0.33
Ln NT-proBNP	7.79 ± 1.09	7.02 ± 1.19	0.005
Presence of LGE	19 (59.3)	53 (42.4)	0.015
Mean LGE (%)	18.8 ± 17.7	7.4 ± 13.4	0.01
LVEF (%)	26.2 ± 12.8	27.9 ± 12.8	0.67

Data are presented as mean ± SD if continuous or number (%) if categorical.

ICM – ischaemic cardiomyopathy; LBBB – left bundle branch block; ACEI - angiotensin-converting enzyme inhibitor; ARB – angiotensin II receptor blocker; Ln – natural logarithm; LGE - late gadolinium enhancement; LVEF – left ventricular ejection fraction

ICM patients were more likely to suffer the primary outcome, and overall had a higher mean percentage of LGE (18.8% vs. 7.4%, p=0.01). The patients who suffered the primary outcome were also had a higher NT-proBNP (p=0.005).

Patient characteristics associated with the primary outcome in a univariable analysis are shown in Table 5-3.

Table 5-3. Hazard ratio and 95% confidence interval for the association between clinical and CMR characteristics and death or ICD activation.

Variable	Death/Appropriate ICD Activation (n=32)		Appropriate ICD Activation (n=20)	
	Univariable HR (95% CI)	p value	Univariable HR (95% CI)	p value
Age	1.02 (0.99-1.04)	0.26	1.02 (0.99-1.05)	0.21
Male	1.27 (0.48-3.37)	0.64	0.79 (0.25-2.52)	0.70
ICM	2.42 (1.19-4.90)	0.015	2.63 (1.07-6.50)	0.035
Diabetes	2.14 (0.82-5.58)	0.12	2.75 (0.91-8.29)	0.07
LBBB	1.46 (0.64-3.31)	0.37	1.98 (0.72-5.45)	0.19
NYHA Class 3-4	2.33 (0.92-5.93)	0.08	3.03 (0.82-11.17)	0.10
ACEI/ARB	0.82 (0.36-1.87)	0.64	1.58 (0.47-5.28)	0.46
Beta-blocker	0.53 (0.25-1.13)	0.10	0.66 (0.24-1.82)	0.42
Spirolactone	1.06 (0.51-2.20)	0.87	2.97 (1.01-8.72)	0.047
Ln NT-proBNP	1.71 (1.22-2.39)	0.002	1.84 (1.17-2.88)	0.008
Presence of LGE	3.77 (1.48-9.58)	0.005	3.30 (1.05-10.42)	0.042
LGE (per 1% increase)	1.05 (1.02-1.07)	<0.001	1.05 (1.02-1.08)	0.002
LVEF (%)	1.00 (0.97-1.03)	0.73	1.01 (0.98-1.05)	0.50

All hazard ratios (HR) adjusted for device type (ICD/CRTD).

ICM – ischaemic cardiomyopathy; ICD – implantable cardioverter-defibrillator; Hr – hazard ratio; LBBB – left bundle branch block; ACEI - angiotensin-converting enzyme inhibitor; ARB – angiotensin II receptor blocker; Ln – natural logarithm; LGE - late gadolinium enhancement; LVEF – left ventricular ejection fraction

ICM (HR 2.42; 95% CI 1.19-4.9, p=0.015), the presence of LGE (HR 3.77; 95% CI 1.48-9.58 p=0.005) and the percentage of LGE (HR per 1% increase 1.05; 95% CI 1.02-1.07, p<0.001) were all associated with the primary outcome. Ln NT-proBNP was also a

significant predictor of the primary outcome (HR 1.71; 95% CI 1.22-2.39, p=0.002). Percentage of LGE, (ln) NT-proBNP and aetiology of cardiomyopathy (ICM or DCM) were entered into the multivariable model, again with adjustment for device type (ICD or CRTD). Both LGE percentage (HR 1.04; 95% CI 1.02-1.07 p=0.001) and ln NT-proBNP (HR 1.69; 95% CI 1.15-2.47 p=0.007) remained significant predictors of the primary outcome (table 5-4).

Table 5-4. Multivariable analysis for the prediction of death or appropriate ICD activation.

Variable	Death/Appropriate ICD Activation (n=32)		Appropriate ICD Activation (n=20)	
	HR (95% CI)	P value	HR (95% CI)	P value
LGE (per 1% increase)	1.04 (1.01-1.07)	0.001	1.04 (1.01-1.07)	0.004
Log NT-proBNP	1.69 (1.15-2.47)	0.007	1.81 (1.09-3.03)	0.023
Ischemic Cardiomyopathy	1.01 (0.32-3.16)	0.99	1.39 (0.33-5.89)	0.66

All hazard ratios (HR) adjusted for device type (ICD/CRTD).

LGE – late gadolinium enhancement; HR – hazard ratio; ICD – implantable cardioverter-defibrillator

There was no significant correlation between LGE and ln NT-proBNP (Pearson correlation co-efficient = 0.14, p=0.22).

Based on the combination of LGE percentage and NT-proBNP the cohort could be stratified into 2 groups as follows: low-risk (DCM: 20 patients, LGE=0%, NT-proBNP <545pg/mL; ICM: 11 patients, LGE <23%, NT-proBNP <898 pg/mL) and high-risk (DCM: 76 patients, LGE >0%, NT-proBNP ≥545pg/mL; ICM: 50 patients, LGE ≥23%, NT-proBNP ≥898pg/mL) (Table 5-5).

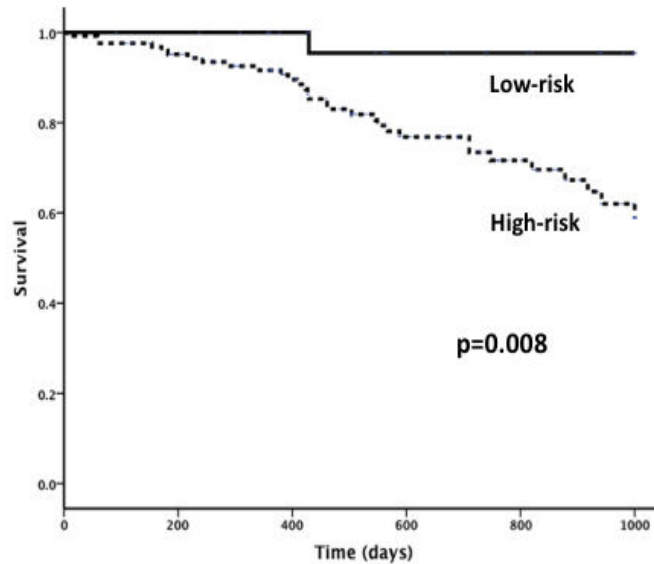
Table 5-5. Hazard ratio and 95% confidence interval for the association between optimal discriminatory level of late gadolinium enhancement and NT-proBNP and death or ICD activation.

Group	Aetiology	LGE (%)	NT-proBNP (pg/mL)	Number of Patients	Death/Appropriate ICD Activation (%)	Appropriate ICD Activation
Low-Risk	DCM	0	<545	20 (20.8)	1 (3.1)	0 (0)
	ICM	<23	<898	11 (18.0)		
High-Risk	DCM	>0	≥545	76 (79.2)	31 (24.6)	20 (15.9)
	ICM	≥23	≥898	50 (82.0)		

DCM – dilated cardiomyopathy; ICM – ischaemic cardiomyopathy; LGE – late gadolinium enhancement; ICD – implantable cardioverter-defibrillator

Both groups had similar numbers of patients from each aetiology ($p=0.67$). In the low-risk group, the primary outcome only occurred in 1 (3%) of the patients (event rate of 1.5% per year). The occurrence of the primary outcome in the high-risk group was 24.6% (occurrence in 31 patients), giving an event rate of 12.3% per year. With the low-risk group as the reference, patients in the high-risk group had a higher risk of the primary outcome and appropriate ICD activation alone (high-risk group HR 9.12; 95% CI 1.24-66.82, $p=0.03$) (figure 5-3).

Figure 5-3. Kaplan-Meier curves of the association between the combination of LGE and NT-proBNP for prediction of the primary outcome.

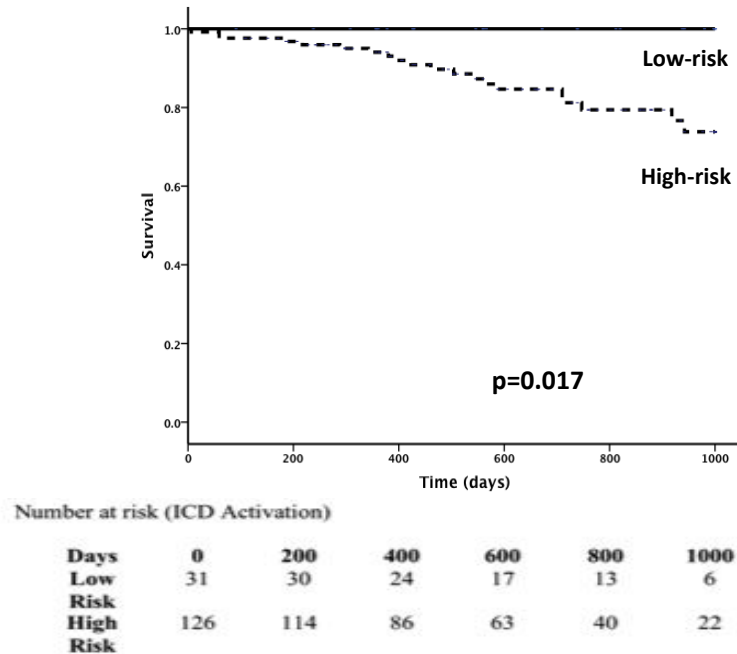


Number at risk (Death/ICD Activation)

Days	0	200	400	600	800	1000
Low Risk	31	30	24	17	13	6
High Risk	126	113	86	59	36	20

When analyzing ventricular arrhythmias only, appropriate activation occurred in 20 patients. Both LGE percentage (HR 1.04; 95% CI 1.01-1.07, $p=0.004$) and ln NT-proBNP (HR 1.81 95% CI 1.09-3.03, $p=0.023$) remained multivariable predictors of outcome (table 5-4). Patients in the high-risk group had a higher risk of the appropriate ICD activation (figure 5-4). Only one patient in the low-risk group had an appropriate ICD activation over the follow-up period, an event rate of 1%/year, in comparison to the high-risk group where the event-rate was 10.1%/year.

Figure 5-4. Kaplan-Meier curves of the association between the combination of LGE and NT-proBNP for prediction of appropriate ICD activation alone.



5.4. Discussion

5.4.1. Study Findings

This study was one of the largest studies to date examining patients undergoing implantation of an ICD or CRTD. A number of important associations were identified:

- LGE and NT-proBNP predict adverse cardiac outcomes in patients with ICDs.
- The increasing burden of myocardial fibrosis (scar) as measured by percentage of LGE was associated with death or appropriate ICD activation independent of HF aetiology (ICM or DCM).
- Finally, this study is the first to show that in primary prevention patients, the LGE percentage and NT-proBNP can be combined to identify a population at significantly increased risk of adverse cardiovascular outcome, and also a population at lower risk in whom (potentially) ICD implantation may not be mandatory, providing extra information on risk stratification.

5.4.2. Clinical Context

While current guidelines for implantation of ICDs and CRTDs are relatively clear, the clinical decision to implant these devices may not be as straightforward as it appears on paper. As described, many patients who currently meet criteria for implantation will never use their device, with the subsequent financial and personal implications (such as potential for device lead infection and the risk of inappropriate shocks). Additionally, there will be some patients who do not meet the criteria for device implantation who could potentially have their lives saved by an implantable defibrillator who may presently be denied this (Stecker et al., 2006).

There is a recognition that both echocardiographic assessment of LVEF and the NYHA classification (table 5-6) can be subject to observational bias, and so there is still a drive to identify further markers that might improve risk stratification and help the clinician make a more informed decision for their patient.

Table 5-6. The New York Heart Association (NYHA) Classification for HF Symptoms.

NYHA Class	Symptoms
I	Cardiac disease, but no symptoms and no limitation in ordinary physical activity, e.g. shortness of breath when walking, climbing stairs etc.
II	Mild symptoms (mild shortness of breath and/or angina) and slight limitation during ordinary activity.
III	Marked limitation in activity due to symptoms, even during less-than-ordinary activity, e.g. walking short distances (20–100 m).
IV	Severe limitations with symptoms at rest.

5.4.3. LGE as a Marker of Adverse Outcome

LGE during CMR identifies areas of myocardial fibrosis. The link between the pathological presence of fibrosis and ventricular arrhythmias leading to sudden death is well established, as the areas of fibrosis form an arrhythmogenic substrate (Bernhardt et

al., 2011, Bolick et al., 1986). Several recent studies have identified the utility of LGE to predict adverse outcomes including ICD activation in both ICM (Kwon et al., 2009, Roes et al., 2009, Scott et al., 2011a, de Haan et al., 2011) and DCM (Wu et al., 2008). This study not only added this evidence, but also further adds that risk increases in proportion with the volume of LGE and that this may provide additional prognostic information than the presence of LGE alone. Two small studies have reported that scar size is associated with adverse outcome in patients with ICM (de Haan et al., 2011, Scott et al., 2011a). Gao *et al* (Gao et al., 2012), studied 124 patients with ICM and DCM and reported that LGE mass was the most significant univariable predictor of their primary outcome (ICD activation, sudden death or survived cardiac arrest), though it was not included in multivariable analysis. This study shows (in a larger cohort) that this association persists regardless of the HF aetiology and additional to NT-proBNP, which is a consistently strong marker of prognosis in heart failure (Pocock et al., 2006). A small retrospective study by Scott *et al* (Scott et al., 2011a) also described a similar relationship in 64 patients with ICM.

5.4.4. NT-proBNP as a Marker of Adverse Outcome

NT-proBNP is secreted by the ventricles in response to increased cardiomyocyte stretch caused by pressure and volume overload (Pocock et al., 2006). It has been shown to be useful as both a diagnostic and a prognostic biomarker in HF (Maisel et al., 2008, Wedel et al., 2009, Masson et al., 2008). Several studies have also examined its utility in predicting adverse outcomes in patients with ICDs. A meta-analysis of 8 studies by Scott *et al* (enrolling a total of 1047 patients) (Scott et al., 2009) found that NT-proBNP (or BNP) levels above the study median increased risk of occurrence of death or ventricular arrhythmia in patients with or without an ICD. Another large study by Verma *et al* evaluated 345 consecutive patients undergoing primary or secondary prevention ICD implantation and found that BNP was the only significant multivariable predictor of death or appropriate ICD activation (Verma et al., 2006). Finally, in a large multi-centre study, Biasucci *et al* evaluated 300 patients with ICM undergoing primary prevention ICD implantation (Biasucci et al., 2012). The main aim of this study was to examine the potential of C-reactive protein as a marker of risk, however the authors also found that NT-proBNP was also a significant predictor of adverse outcome. Nevertheless, the combined

use of NT-proBNP and percentage of LGE have not been prospectively evaluated in one cohort before.

5.4.5. The Combined Prognostic Value of LGE and NT-proBNP

I hypothesised that because LGE and NT-proBNP are markers of different pathological processes, they may be associated with death or ICD activation via different pathways, and that their use in combination would lead to a powerful evaluation of risk. I found that they are both strong predictors of risk in HF patients and that their combination provided additional prognostic information. This is the first study to demonstrate that both markers are able to identify a group of patients at higher risk of adverse outcomes and that the association is present in a cohort of patients with ICM and DCM. Perhaps of more clinical relevance, these two markers can also be combined to identify a group of patients at low risk of events who might not benefit from ICD implantation. This may be important given the social and psychological implications of a defibrillator, and an estimated complication rate of around 4% (Lee et al., 2010).

Wu et al demonstrated the incremental prognostic utility of a combination of imaging and a biomarker in patients with chronic heart failure for prediction of death and arrhythmic events (Wu et al., 2012). The authors found that the combination of LGE and C-reactive protein was able to identify a cohort at very low risk of adverse cardiovascular outcome. Interestingly, the authors also noted that patients with the primary outcome had a higher NT-proBNP, although they did not explore this further.

Another important finding from this study is that even after adjusting for the presence of each other, percentage of LGE and NT-proBNP levels were still associated with adverse outcomes. This is particularly important given the wider availability of serum NT-proBNP testing and its ease of use and interpretation compared to CMR which is perhaps not as widely available. Importantly, the primary outcome occurred in a number of without LGE. Although LGE appears to be an important predictor of adverse outcome, this finding highlights the value of a multi-marker model of risk. Furthermore, NT-proBNP may be of benefit in patients unable to undergo CMR, for example in those with contrast allergy or renal impairment. However, in centres with the access to CMR, the combination of these LGE and NT-proBNP may provide the clinician with further confidence. There may also

be advantages to identifying a group of lower risk patients in which the clinician is unsure as to whether to proceed to ICD insertion, perhaps for example in those with LVEF around 35% and in NYHA class 1/2. LVEF can fluctuate over time while NYHA class can be fairly subjective and these limitations may account for some of the current reduced cost-effectiveness of ICDs. There is an increasing recognition however that risk stratification for ICD implantation may be further refined by using other markers such as LGE and NT-proBNP, hence more studies of this type are required to optimize patient selection and improve outcomes.

5.4.6. Limitations

Although this is the largest study to date to examine this area with a cohort of 157 patients, this is still a single-centre study with a relatively small cohort. Nevertheless, a larger multi-centre study is needed to validate our findings. The overall death rate in this study cohort (8.3%) was lower than reported in MADIT-II (14.2% in 20 months) while the rate of appropriate ICD therapies is also lower than larger multi-centre trials (Moss et al., 2002, Germano et al., 2006). Larger studies might be able to identify the optimal cut-off points for these markers, allowing them added to clinical guidelines to be used as risk stratifiers in order to avoid ICD implantation.

I used a threshold of $>5SD$ between remote myocardium and fibrosed myocardium, rather than other methods such as $>2SD$ or the “full width-half-max” (FWHM) method. A level of $>5SD$ has been shown to be more accurate than $2SD$ and as accurate as FWHM for quantification of fibrosis by LGE (Flett et al., 2011). Additionally, LGE, unlike T1 mapping, does not identify diffuse fibrosis, which may also be of prognostic importance.

5.5. Conclusions

In a population of patients with ICM and DCM both percentage of LGE and NT-proBNP were both associated with poorer outcome. Used in combination, both markers are able to discriminate of risk of death or ICD activation in patients undergoing implantation of a primary prevention ICD. The use of both markers allows identification of a group at low risk for future adverse events in whom ICD implantation may potentially be deferred.

Chapter 5: The Combined Prognostic Utility of LGE and NT-ProBNP in Patients with Defibrillators

Larger studies should be conducted in order to identify the optimal levels of LGE and NT-proBNP in order for these markers to be incorporated into clinical guidelines.

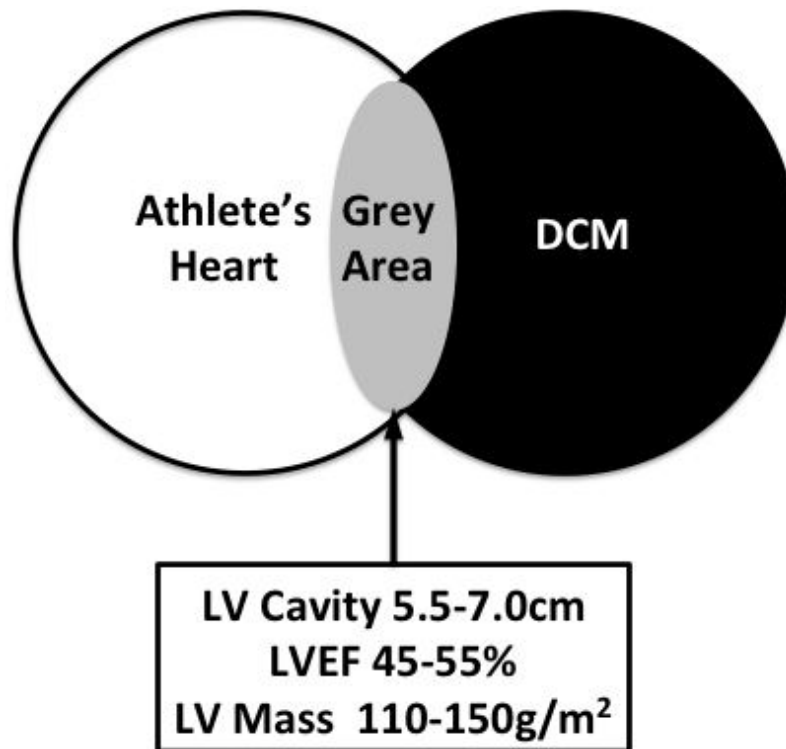
6. Can Advanced CMR Parameters Help To Differentiate Between Early Dilated Non-Ischaemic Cardiomyopathy and Physiological Myocardial Adaptation To Exercise?

6.1. Introduction

In the last chapter I explored the potential role of CMR in solving a diagnostic dilemma in patients with severe DCM. Another diagnostic dilemma is in making the correct diagnosis in patients with a mildly reduced LVEF, which could potentially represent an early manifestation of cardiomyopathy. Many healthy people can demonstrate changes that might be consistent with early DCM such as left ventricular cavity dilatation and consequently mildly reduced LVEF. These changes occur particularly in people who undergo strenuous physical training, including in middle-aged marathon runners (Zilinski et al., 2015). These myocardial adaptations are commonly known as “athlete's heart” (La Gerche et al., 2009, Maron and Pelliccia, 2006). There could potentially be diagnostic problems in the differentiation of early DCM and athlete's heart. Correct diagnosis is of vital importance for future prognosis and management.

In many patients, history, examination and basic imaging can provide a clear answer. For example, in patients with a family history of cardiomyopathy, a significantly dilated left ventricle and moderate to severely reduced LVEF, it is most likely that this phenotype represents DCM. There is however a grey zone, in which these more simple parameters are not able to give a clear diagnosis (Figure 6-1). This is particularly so in middle-aged and older patients, in whom the pre-test probability of cardiomyopathy is probably higher. This is compounded by the fact that an increasing number of older adults are taking up more intense exercise.

Figure 6-1. The Grey Area Between Athlete's Heart and DCM.



Adapted from (Maron et al., 1995).

LGE (particularly the typical midwall pattern of fibrosis) has the potential to add diagnostic confidence and provide prognostic information, allowing the identification of specific etiologies of DCM (Mahrholdt et al., 2005a), (McCrohon et al., 2003) (Assomull et al., 2006, Gulati et al., 2013) Nevertheless, healthy patients with athlete's heart can also have midwall LGE present, which might again cause some diagnostic uncertainty (Mohlenkamp et al., 2008) .

More advanced CMR techniques for assessment of myocardial function and tissue characterization include tagging (for assessment of global and regional strain) (Ibrahim el, 2011) and T1 and T2-weighted imaging (for tissue characterization) (Puntmann et al., 2013, Dass et al., 2012). A reduction in circumferential (GCS) and longitudinal strain (GLS) has been noted in heart failure patients (Kraigher-Krainer et al., 2014). Echocardiographic assessment of GCS and GLS has been shown to be indicator of adverse prognosis in DCM patients (Cho et al., 2009, Stanton et al., 2009). T1 and T2-mapping techniques have been shown to identify diffuse myocardial disease in patients with DCM which may occur prior to the development of more focal changes (Puntmann et al., 2013, Dass et al., 2012).

The purpose of this study was to evaluate the utility of CMR tagging, T1 and T2 mapping in differentiation of athletes and patients with mild DCM, potentially allowing for improvement in diagnostic confidence where assessment of LVEF and LGE may still leave some diagnostic uncertainty.

6.2. Methods

6.2.1. Patient Selection

Three separate cohorts of male patients were included in this study. The first cohort, who acted as the control group, consisted of 21 healthy control patients without any history of cardiovascular disease and normal electrocardiograms. The second group consisted of 21 males with a history of regular aerobic exercise and mildly impaired or borderline LVEF using echocardiography (LVEF using Simpson's biplane 45-50%). All patients in this group undertook over 6 hours of intensive aerobic exercise per week. These patients also had no history of cardiac disease and were on no medications. The final group consisted of 16 patients with confirmed DCM (LVEF 40-50% by echocardiography) and without a history of engagement in significant aerobic exercise. All of these patients had also undergone comprehensive evaluation to exclude ischemic cardiomyopathy with invasive or CT coronary angiography or SPECT imaging (modality chosen at the discretion of their clinician).

6.2.2. CMR Protocol

All patients underwent a systematic CMR protocol including cine imaging, T1 and T2 mapping, tagging and LGE as described in Chapter 2. Briefly, cine images were obtained using an SSFP sequence in three long axis planes (2-chamber, 3-chamber, 4-chamber) and in short axis slices through the left ventricle. Then 3 matched short-axis slices were taken to represent the basal, mid and apical levels of the left ventricle using T1 and T2 mapping. These 3 slices were also repeated using tagged CMR, and an additional 4-chamber image acquired for assessment of GLS. Intravenous gadolinium was then given. T1 mapping was repeated after 10 minutes, and LGE imaging was performed immediately after.

All analysis was performed using Argus, other than analysis of tagged CMR images which was performed using Diagnosoft HARP as described in Chapter 2. To assess myocardial T1 and T2 times, as wide a region of interest as possible was drawn within the septum of the basal and mid-ventricular slices, taking care to avoid blood pool signal. The average of the two values was taken in order to have as representative value of the myocardium as possible. The apical slice and the lateral walls were excluded as these areas were more likely to be affected by artefact. Once the region of interest was drawn, T1 and T2 times were automatically displayed on the workstation. On T1-weighted images a large representative region of interest was also drawn within the blood pool.

Post-contrast T1 mapping allows calculation of the extracellular volume (ECV) of the myocardium within the region of interest chosen. This is known to represent a marker of diffuse fibrosis and corresponds well with histological measurements of fibrosis (Miller et al., 2013). Calculation of ECV relies on knowledge of the patient's haematocrit, therefore a blood sample was taken immediately prior to CMR scanning to analyse the full blood count. The haematocrit was obtained, allowing for calculation of ECV using the equation: $ECV = (1 - \text{haematocrit}) \times (\Delta R1_{\text{myocardium}} / \Delta R1_{\text{blood}})$ (Arheden et al., 1999).

Tagged images were analysed offline. End-diastole was automatically selected while end-systole was manually selected. Endocardial and epicardial contours were drawn for 3 short-axis slices to allow automatic tracking of the myocardial tags. Each frame was then adjusted individually to ensure correct tracking and GCS was derived. The same process was followed for the long-axis image in order to obtain GLS.

6.2.3. Statistical Methods

As described in Chapter 2, continuous variables are expressed as mean \pm SD and categorical variables are expressed as a number and percentage. Comparisons between multiple groups were carried out using a one-way ANOVA with Bonferroni correction applied for multiple group testing. Binary logistic regression was used to identify significant predictors of the diagnosis of cardiomyopathy. Sensitivity and specificity using receiver-operator characteristic (ROC) curves, in order to obtain the area under the curve (AUC). For all analyses a p value <0.05 was considered statistically significant and all p values are two-tailed.

6.3. Results

6.3.1. Correlations Between Tissue Characteristics and Left Ventricular Function

Myocardial T2 times were significantly correlated with both native T1 times ($r=0.43$, $p<0.001$) and ECV ($r=0.44$, $p<0.001$). There was a strong correlation between native T1 and ECV ($r=0.63$, $p<0.001$) and a strong correlation between LVEF and GCS ($r=-0.73$, $p<0.001$). There were modest but significant correlations between GCS and native T1 ($r=0.30$, $p=0.003$) and ECV ($r=0.29$, $p=0.005$).

LVEF was also strongly correlated with both native T1 ($r=-0.40$, $p<0.001$) and ECV ($r=-0.43$, $p<0.001$). T2 signal was not significantly correlated with either LVEF or GCS.

Strain was significantly reduced in patients with LGE present compared to those without (GCS: -10.76% vs. -13.90 , $p=0.01$; GLS: -11.00% vs. -14.83% , $p<0.001$ respectively).

6.3.2. Comparison between Exercisers, DCM Patients and Controls

In total 58 males were evaluated – 21 with a history of aerobic exercise, 16 with mild DCM and 21 age-matched healthy controls. The average age of the cohort was 47.9 ± 14.5 years. Comparisons between the three groups are shown in table 6-1.

Table 6-1. Baseline clinical and CMR characteristics.

	Controls (n=21)	Exercisers (n=21)	DCM Patients (n=16)	p value
Age (years)	47.9 ± 16.0	45.9 ± 10.7	46.1 ± 13.6	0.79
LV Mass (g/m²)	60.7 ± 12.7	84.3 ± 28.2*	68.8 ± 15.5	0.001
LVEF (%)	64.5 ± 4.1	51.2 ± 5.9* ⁺	48.1 ± 4.8* ⁺	<0.001
LVEDV (ml/m²)	78.6 ± 12.4	102.2 ± 36.0 ⁺	101.2 ± 21.2 ⁺	<0.001
LVESV (ml/m²)	28.0 ± 5.9	49.5 ± 16.2 ⁺	52.6 ± 12.2* ⁺	<0.001
GCS (%)	-17.33 ± 2.30	-12.87 ± 3.61* ⁺	-13.05 ± 4.37* ⁺	<0.001
GLS (%)	-16.53 ± 2.44	-14.91 ± 2.18 ⁺	-13.90 ± 3.00 ⁺	<0.001
LGE Present (%)	0 (0)	7 (33.3) ⁺	5 (31.3) ⁺	<0.001
Native T1 (ms)	952 ± 31	958 ± 30 ⁺	1017 ± 42* [§]	<0.001
ECV (%)	26.2 ± 2.8	26.4 ± 6.8 ⁺	31.2 ± 4.1* [§]	0.002
T2 (ms)	52.9 ± 3.3	52.8 ± 3.2	55.9 ± 4.4* ⁺	0.024

**p*<0.01 vs. healthy controls; ⁺*p*<0.01 vs. severe DCM patients; [§]*p*<0.01 vs. athletes.

DCM – dilated cardiomyopathy; LVEF – left ventricular ejection fraction; GCS – global circumferential strain; GLS – global longitudinal strain; LGE – late gadolinium enhancement; ECV – extracellular volume

Data are presented as mean ± SD if continuous or number (%) if categorical.

Both exercisers and DCM patients had significantly increased left ventricular volumes and reduced LVEF compared to controls. Exercisers also had an increased LV mass compared to both controls and to DCM patients.

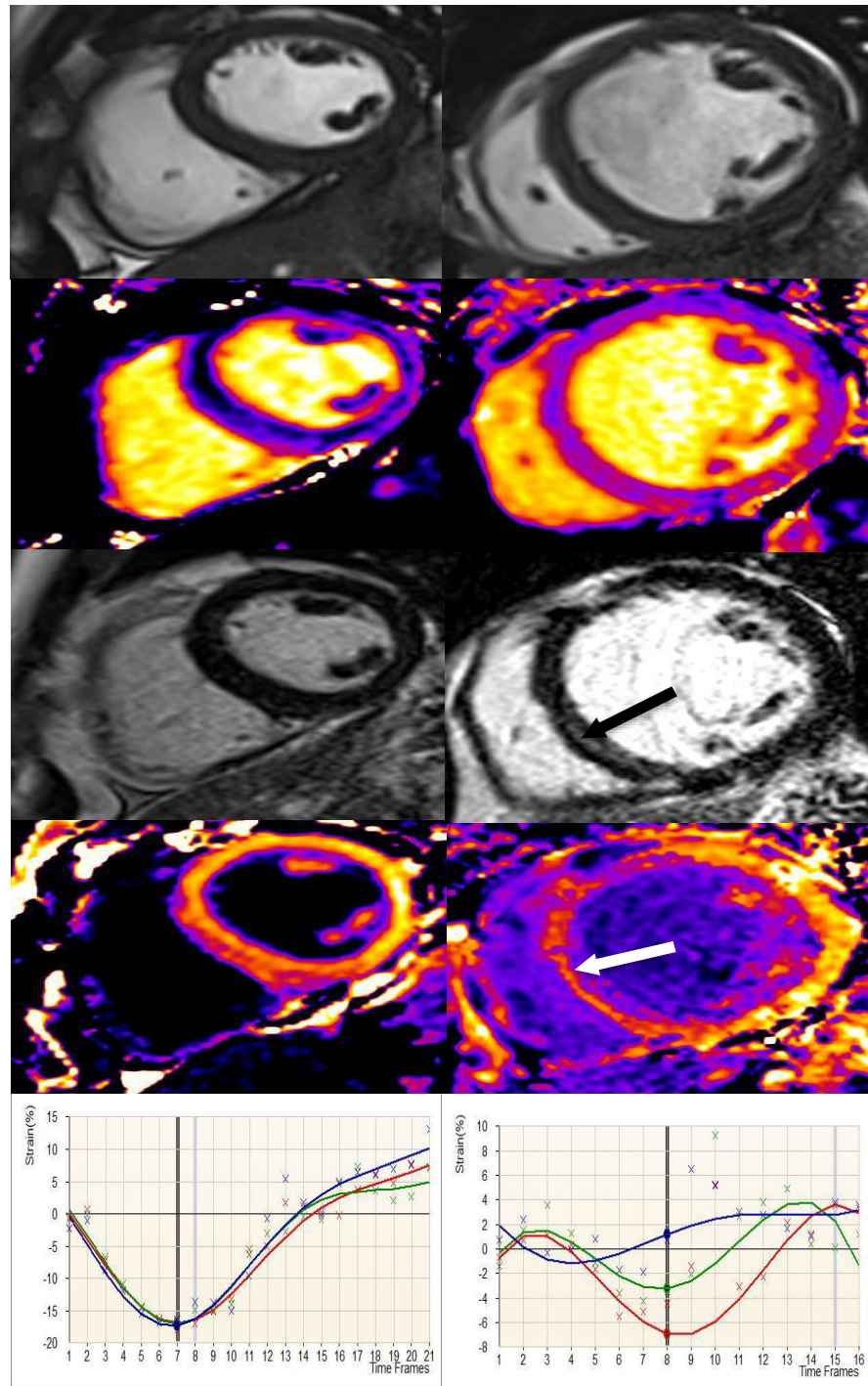
DCM patients were more likely to have LGE than both controls and exercisers (*p*=0.027). There was no subendocardial LGE in any group to suggest prior myocardial infarction.

Both native T1 and ECV were significantly different between athletes and DCM patients (native T1: 957 ± 32 ms vs. 1017 ± 42 ms, *p*<0.001; ECV: 26.3 ± 3.6% vs. 31.2 ± 4.1%, *p*<0.001 respectively). Athletes had a similar native T1 and ECV to controls. T2 relaxation time was also similar between controls and athletes (52.9 ± 3.3 ms vs. 52.8 ± 3.2 ms

Chapter 6: The Potential of CMR to Differentiate Between Athlete's Heart and Dilated Cardiomyopathy

respectively) and significantly lower than in DCM patients (55.9 ± 4.4 ms, $p=0.024$ between all three groups). Figure 6-2 shows examples of the CMR finding while figures 6-3 and 6-4 show the differences between the three groups in T1 mapping parameters.

Figure 6-2. Typical Patterns using T1 Mapping and Tagging in a Healthy Control (left) and a Patient with DCM (right).



Row 1: Cine imaging; Row 2: Native T1 mapping; Row 3: LGE; Row 4: Post-contrast T1 mapping; Row 5: Global circumferential strain using tagging.

Left: A 52 year-old healthy male control with a normal sized left ventricle (end-diastolic diameter 5.6 cm) and preserved left ventricular ejection fraction (57.8%) (Row 1). Septal

Chapter 6: The Potential of CMR to Differentiate Between Athlete's Heart and Dilated Cardiomyopathy

native T1 was 924.9 ms (Row 2) and there was no LGE (Row 3) or significant diffuse fibrosis (post-contrast T1 467.1 ms, ECV 27%, Row 4). GCS was -15.68% (Row 5).

Right: A 58 year-old DCM patient with a dilated left ventricle (end-diastolic diameter 6.7 cm) and mildly impaired left ventricular ejection fraction (45.4%) (Row 1). Septal native T1 1017.8 ms (Row 2). There was midwall LGE row 3; arrow) also reflected by the reduced post-contrast T1 and ECV (post-contrast T1 429.8 ms, ECV 35%, Row 4; arrow). GCS was -5.15% (Row 5).

Figure 6-3. Comparison of Native T1 Times.

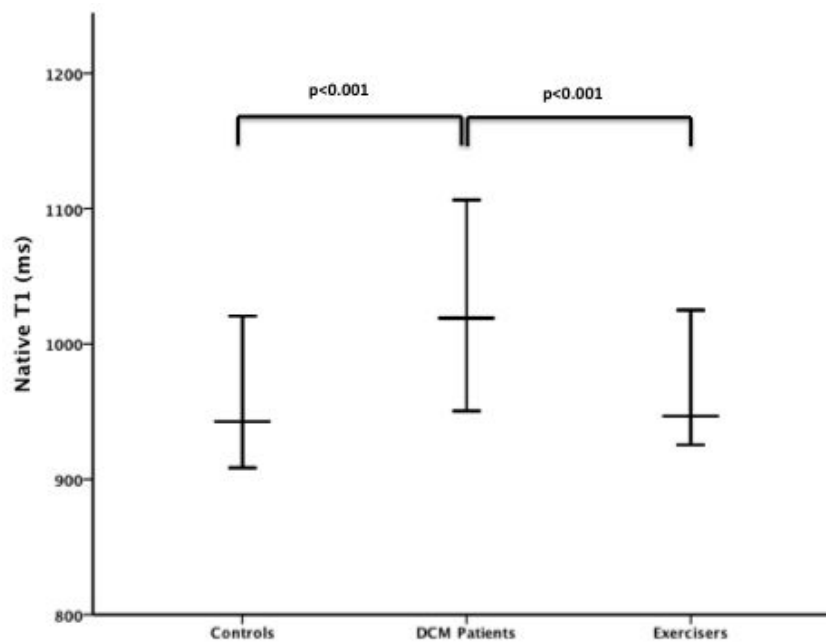
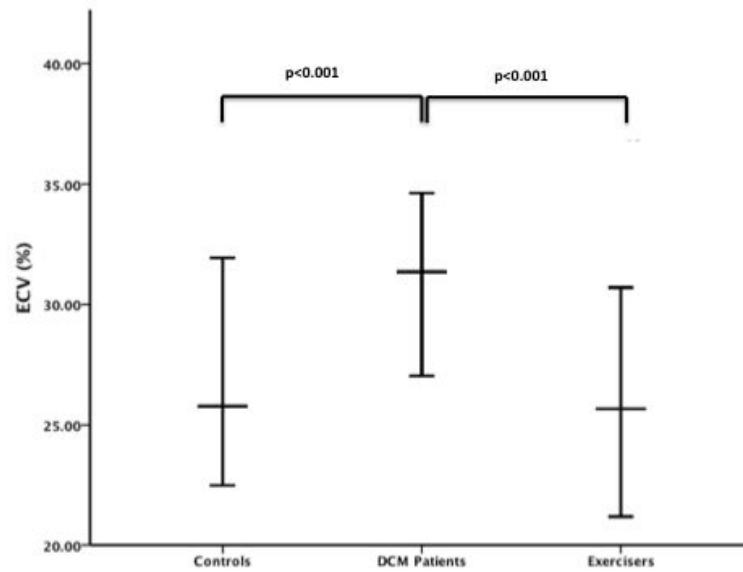
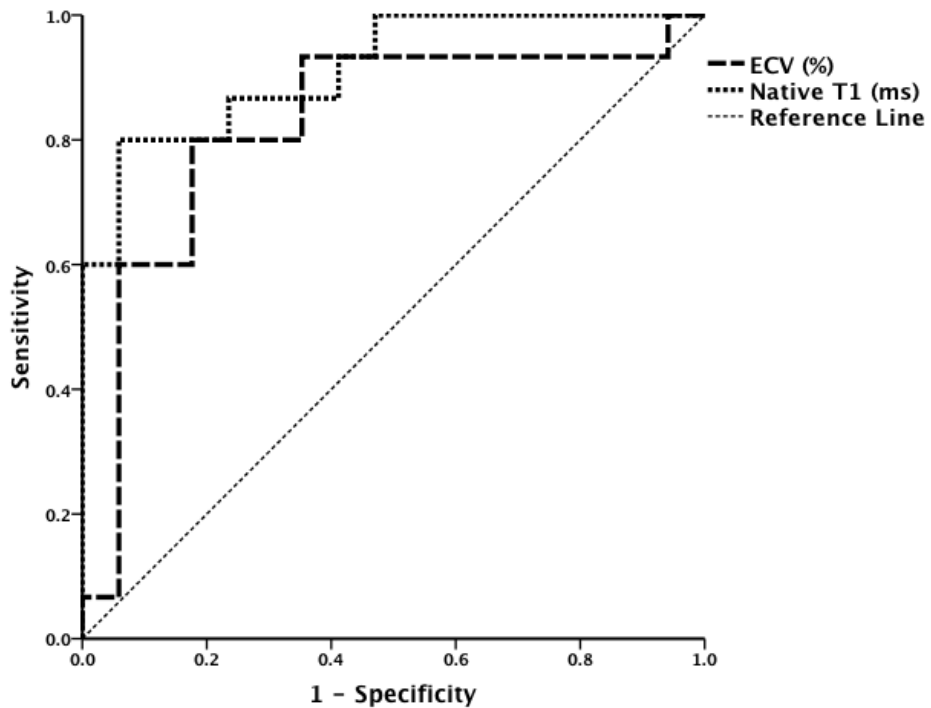


Figure 6-4. Comparison of ECV.



Using multivariable logistic regression analysis, native T1 was the only independent discriminator between exercisers and DCM patients (OR 1.05; 95% CI 1.01-1.10, $p=0.015$). Using ROC analysis, the AUC for differentiation between exercisers and patients with DCM was 0.91 (95% CI 0.82-1.00, $p<0.001$), which was significantly better than ECV (AUC: 0.82; 95% CI 0.67-0.98, $p=0.002$) (figure 6-5).

Figure 6-5. Receiver-operator Characteristic for Differentiation of Exercisers and DCM Patients.



6.4. Discussion

6.4.1. Study Findings

This study identified two important findings:

- Both CMR tagging and T1 mapping identify changes in the myocardium in patients with DCM.
- Native T1 might be a novel parameter that could be used to differentiate between patients with healthy myocardial adaptation to exercise and patients with early DCM, potentially providing a new tool to help in a diagnostic dilemma.

6.4.2. Clinical Context

The screening of athletes and the identification of early cardiomyopathy remains a difficult diagnostic and therapeutic challenge. When exposed to aerobic exercise the myocardium

undergoes changes which are similar to early DCM, particularly in those who predominantly partake in endurance training. This can pose problems for these patients, as they may potentially be excluded from sport, incorrectly, in order to reduce risk (Pelliccia et al., 2005). Conversely, in athletes in whom potential cardiomyopathy is not recognised, the first manifestation of this may be sudden death (Maron et al., 1995). Currently, simple echocardiographic measurements of left ventricular dimensions and ejection fraction may not be enough to differentiate between normal athletic adaptation and cardiomyopathy, while a period of observation without exercise may not be palatable to people who regularly undertake exercise, therefore more parameters are still required to allow confident discrimination between the two phenotypes (La Gerche et al., 2009).

6.4.3. T1 and T2 Mapping in DCM

Both T1 and T2 mapping have emerged as valuable tools in the CMR assessment of non-ischemic cardiomyopathies (Kramer et al., 2013, Parsai et al., 2012). T2 mapping identifies myocardial edema secondary to acute myocardial injury (Nishii et al., 2014). Native T1 times reflect both interstitial and myocyte signals, hence the high correlation between native T1 and T2 times. Finally, the assessment of T1 values after the administration of intravenous gadolinium (which shortens tissue T1 time) allows the measurement of diffuse fibrosis and the ECV. Similarly to other studies, this study shows that these parameters are associated with the presence of DCM and are correlated with adverse remodeling in this condition (Dass et al., 2012, Puntmann et al., 2013). This study also shows, for the first time, that these parameters can provide diagnostic confidence at the 1.5T field strength which is more commonly used in routine clinical practice (Antony et al., 2011).

Puntmann et al studied 27 patients with DCM (included in a cohort with 25 HCM patients) and found that native T1 times were longer in DCM patients compared to controls, while post-contrast T1 values were lower and ECV was higher (Puntmann et al., 2013). The authors found that native T1 was the best predictor of cardiomyopathy. In another study by Dass et al, the authors evaluated 18 DCM patients (along with 28 HCM patients) and again found that native T1 values were increased in DCM patients compared to controls and were significantly correlated with GCS (Dass et al., 2012). In this study I also found that native T1 was significantly higher in patients with DCM.

Numerous myocardial adaptations occur in endurance-trained athletes (La Gerche et al., 2009, Utomi et al., 2014). These include an increase in end-diastolic diameter, volume and mass, leading to a reduction in LVEF (Abergel et al., 2004). These findings were also reflected in this study. LV mass tends to increase in both endurance and strength trained athletes, but also increases in DCM due to the increase in left ventricular size, potentially causing diagnostic difficulty (Pluim et al., 2000). This has important clinical implications, particularly in the differentiation between the normal cardiac adaptations to exercise and athletes in whom the changes in myocardial structure and function are actually the early signs of DCM. The finding that native T1 mapping seems to be able to differentiate between athletes and patients with early DCM might provide an extra parameter to support the diagnosis in these difficult cases.

6.4.4. Global Circumferential and Longitudinal Strain

In this study, both GCS and GLS were significantly correlated with LVEF, but were not able to differentiate between athletes and sedentary patients. Circumferential shortening is mostly mediated by midwall fibers while longitudinal shortening is mediated by subendocardial and subepicardial fibres (Buckberg et al., 2008). Using echocardiography, strain has been shown to correlate well with areas of fibrosis seen using LGE (Saito et al., 2012). The finding that GCS but not GLS was significantly lower in both athletes and sedentary patients compared to controls might be related to the fact that any fibrosis may often be midwall in these patients, thus affecting circumferential shortening more. I found, similarly to echocardiographic studies, that both GLS and GCS were reduced in patients with LGE present. It may be however that T1 mapping identifies different changes in the myocardium to tagging. The finding of lower GCS and GLS compared to controls in this study could also simply be a reflection of the fact that it specifically only included athletes with a mildly reduced LVEF, whereas the majority of previous studies examining myocardial deformation in athletes include athletes with normal ejection fractions.

Studies measuring strain using speckle tracking echocardiography have reported conflicting results (Utomi et al., 2014, Nottin et al., 2009, Simsek et al., 2013, Richand et al., 2007). Richand et al. evaluated 29 professional soccer players using speckle-tracking echocardiography and found that GLS was significantly reduced in these athletes compared to controls (Richand et al., 2007). Exercise has also been shown to reduce GLS

and GCS in athletes compared to pre-exercise deformation measurements (Nottin et al., 2009). A more recent study by Utomi et al. however found that there was no difference in GLS and GCS between endurance-trained athletes and controls (Utomi et al., 2014). On the other hand, a further study by Simsek et al. including 22 marathon runners found increased GLS compared to controls (Simsek et al., 2013). All of these studies are limited by small numbers, but it is possible that strain in athletes is not significantly different compared to sedentary patients with similar ejection fractions, hence these conflicting results. Larger studies are needed to explore this, but the finding in this study that there was no significant difference between strains measured using CMR tagging (the current non-invasive gold standard) in exercisers and DCM patients with similarly reduced ejection fractions might support this.

6.4.5. What Is The Clinical Importance of These Findings?

The importance of these findings is perhaps their potential use in identification of athletes at risk of sudden death, in whom the first presentation of any cardiac abnormality is that of SCD. Vigorous exertion can act as a substrate for ventricular arrhythmias in people with an underlying abnormal myocardium (Maron and Pelliccia, 2006). One theory for this is that repeated myocardial injury (reflected by troponin release) leads to fibrosis and scarring, which may be identified using LGE (Whyte et al., 2007, Waterhouse et al., 2012). These areas of fibrosis lead to an increased susceptibility to ventricular arrhythmias. ECV evaluation using T1 mapping may also identifies these areas, however whether T1 mapping is valid also in athletic hearts remain to be established pathologically. Nevertheless, many athletes (and patients with DCM) do not have fibrosis that can be seen using LGE or ECV imaging. Native T1 mapping appears to identify other processes that are not purely related to fibrosis, for example myocardial inflammation represented by edema (also seen using T2 mapping, for which there is a strong correlation in our study) (Ugander et al., 2012). Speculatively, native T1 mapping may also identify early changes in myocardial function and metabolism, although large studies are awaited to understand the mechanisms and their clinical impact (Dass et al., 2012).

6.4.6. Limitations

This study does have some limitations. First, it is a single-centre study with a relatively small cohort, although to the best of my knowledge, this is the largest cohort studied in this area. Nevertheless, larger studies are required to confirm its findings and identify any potential prognostic benefit.

Secondly, the lack of histological correlation in this study is a limitation as this could have provided further information. This does however reflect the decreasing use of endomyocardial biopsy in routine clinical practice. Also, biopsy itself is limited by sampling error.

Thirdly, although measurement of T1 and T2 times in the septum is accepted in the current literature as being an adequate surrogate for the whole myocardium, both sequences still need to be optimized to allow accurate quantification in the lateral wall and apex without artifact. Only males were included in this study as T1 parameters show gender specific variation (Liu et al., 2013, Piechnik et al., 2013). This study would need to be repeated in order to validate the findings in females. Additionally, T1 mapping values can also be affected by LGE. Measurement of T1 times in different areas of the myocardium may have been changed by the presence or absence of LGE and so could have yielded different results.

Finally, post-contrast T1 imaging was carried out at one time point only, 10 minutes after gadolinium administration. The optimal time for post-contrast T1 mapping has yet to be validated, although 10 minutes is potentially the most accurate for determination of ECV (Puntmann et al., 2013). In order to maintain consistency, I adhered to imaging at 10 minutes for all patients in our protocol.

6.5. Conclusions

Both CMR tagging and T1 mapping parameters can independently predict the presence of DCM. Native T1 mapping could potentially have the ability to both differentiate between patients with early cardiomyopathy and healthy athletes.

7. Comprehensive Dobutamine Stress MRI versus Dobutamine Stress Echocardiography in the Assessment of Patients with Left Bundle Branch Block and Suspected Coronary Artery Disease

7.1. Preamble

So far, I have looked at the prognostic value of CMR in patients with cardiomyopathies, and the diagnostic value of CMR in patients with suspected or potential cardiomyopathy. In scanning patients with cardiomyopathies, the presence of ECG abnormalities is relatively common (Baig et al., 1998, Grunig et al., 1998). One of the commonest I came across was the presence of left bundle branch block (LBBB). Its presence can alert the clinician to the potential presence of a cardiomyopathy. Significant coronary artery disease (CAD) can be a cause of LBBB, and the presence of LBBB can pose a challenge in the non-invasive diagnosis of CAD.

In this chapter, in an extended introduction, I shall describe the clinical problem, and outline why current diagnostic methods are unsatisfactory, and how CMR could potentially provide a solution. This will lead on to the clinical study, in which I shall compare dobutamine stress CMR (DSCMR) against dobutamine stress echocardiography (DSE).

7.2. Introduction

While conventional invasive coronary angiography (ICA) remains the gold-standard for identification and treatment of CAD, most pathways for diagnosis and management of chronic stable angina caused by obstructive CAD include a non-invasive test to risk stratify patients and identify those in whom invasive management would be beneficial, particularly in those patients at low to intermediate risk of CAD (Montalescot et al., 2013). Either anatomical or functional imaging can be used. Common non-invasive tests include exercise stress testing (treadmill or bicycle), nuclear perfusion imaging, stress echocardiography, multislice CT coronary angiography and stress CMR.

The presence of LBBB on the resting ECG in patients with suspected angina presents a diagnostic challenge. Common causes of LBBB are aortic stenosis, dilated cardiomyopathy, acute myocardial infarction, pre-existent coronary artery disease, older age and hypertension. Of course, the cause cannot often be identified from the ECG. Prevalence in the general population is estimated to be 0.43% in men and 0.28% in women while incidence is 3.2 per 10,000 per year in men and 3.7 per 10,000 per year in women (Hardarson et al., 1987). Despite the numerous causes of LBBB, CAD accounts for the

majority of cases. Indeed, the estimated prevalence of CAD in patients with LBBB has been between the range of 30-52% (Hardarson et al., 1987, Mulcahy et al., 1968).

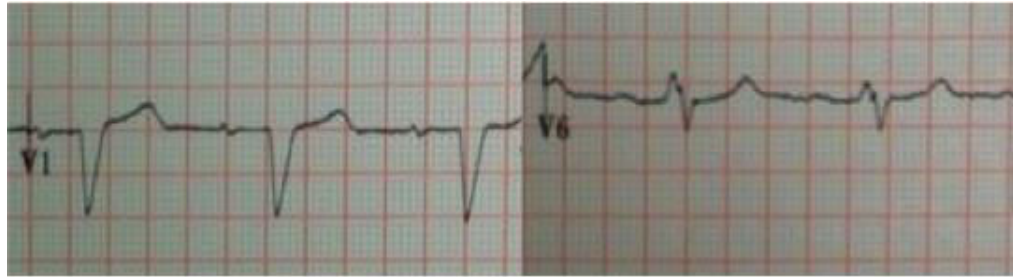
While acute LBBB accompanied by chest pain remains an indication for immediate primary percutaneous coronary intervention, identifying the presence of CAD in patients with chronic LBBB remains challenging. Each non-invasive cardiac imaging modality has its own pitfalls as well as benefits. The aim of this review is to look at techniques for non-invasive investigation of CAD, specifically in patients with LBBB, and to identify their advantages and disadvantages.

7.2.1. The Clinical and Functional Impact of LBBB

The presence of LBBB has been associated with adverse prognosis, including sudden death (Rabkin et al., 1980). In the Framingham study, 48% of patients with LBBB developed CAD or heart failure, while after 18 years of follow-up only 11% of patients with LBBB were free of any cardiovascular disease (Schneider et al., 1979). Despite this, in patients with LBBB but without any clinically significant manifestation of cardiovascular disease, mortality is only slightly increased compared to the general population (Francia et al., 2007). Given this, the presence of LBBB often prompts referral to the cardiologist for further evaluation. With the most common cause being CAD, investigations will often be directed towards the exclusion of significant CAD.

The presence of LBBB causes a number of changes in myocardial function which have an important impact on non-invasive testing for angina. The most obvious is the delay in electrical activation of the left ventricle, recognised as the wide QRS complex on the ECG (>120ms) (figure 7-1) (Mehdirad et al., 1998). This manifests itself as abnormal contraction of the interventricular septum, leading to dyssynchrony in comparison to the posterior wall during systole. These features impact on both assessment of ST segment changes on the ECG during exercise and on assessment of regional wall motion abnormalities (RWMA). The delay in activation of the septum can make it appear as though there is a RWMA, particularly in inexperienced hands.

Figure 7-1. The typical electrocardiographic pattern of left bundle branch block.



Note the wide QRS complex, the QS complex in V₁ and the rSR in V₆.

In an experimental model of LBBB, the induction of LBBB caused impaired septal systolic thickening and an increase in intramyocardial pressure, leading to a relative reduction in myocardial perfusion and glucose uptake within the septum compared to the lateral wall (Ono et al., 1992). This phenomenon was actually found to be related to hyperperfusion of the lateral wall, which was also found in patients with permanent pacemakers (who were paced from the right ventricle, causing an LBBB equivalent), and was also exacerbated by exercise (Koepfli et al., 2009). In this study, the authors explained the presence of lateral hyperperfusion by the delay in lateral wall contraction, causing a reduction in workload in the septum and reduced oxygen demand compared to the lateral wall. During exercise, this phenomenon would be further increased as the lateral wall does more work, causing a more pronounced hyperemic response. This could potentially cause the misrepresentation of septal perfusion defects as indicative of significant coronary stenoses.

The early septal contraction also means that the septum appears thinner at end-systole. As described above, this may cause difficulty with the interpretation of wall motion abnormalities. It may also cause difficulties in the interpretation of perfusion at systole if the spatial resolution of the technique is not high, known as a partial volume effect. In a cohort of LBBB patients without significant CAD examined using positron emission tomography and CMR, the thinned septum had reduced deformation and reduced glucose metabolism in comparison to the lateral wall (Mahrholdt et al., 2005b).

The combination of these myocardial features specific to LBBB may cause difficulties in the use of non-invasive imaging to assess for the presence of CAD, as I shall now describe.

7.2.2. Exercise ECG Stress Testing

This refers to the recording of the electrocardiogram with the patient exercising to achieve a predefined target heart rate (adjusted by age). This is achieved either by exercise on a treadmill or on a bicycle. The level is gradually increased in stages, with ECG monitoring carried out continuously. The test can be considered diagnostic if the patient reaches 85% of their maximum predicted heart rate or if typical symptoms are brought on. Commonly, if either of these points is reached at “low workload” (e.g. less than 6 minutes on exercise treadmill test using full Bruce protocol), patients can then commonly go on to have ICA.

The principal diagnostic endpoint on the ECG is of horizontal or downsloping ST-segment depression. In LBBB however, due to the resting ECG abnormality, it is very difficult to interpret any changes in the ECG during exercise.

Although the exercise ECG may provide some additional diagnostic and prognostic information regarding exercise tolerance, heart rate and blood pressure response and symptoms, the exercise ECG is not presently recommended as a routine investigation in patients with LBBB (Fihn et al., 2012, Montalescot et al., 2013). Given this, imaging modalities must be used in the evaluation of patients with LBBB.

7.2.3. Nuclear Imaging

Nuclear imaging, most commonly performed using single positron emission tomography (SPECT) is one of the most validated techniques for assessment of stable angina.

Intravenous technetium-99 is most commonly used, with thallium-201 less favored due to its increased radiation dose (Baggish and Boucher, 2008). The myocardium is stressed either using exercise (bicycle or treadmill) or pharmacologically (vasodilator – adenosine, dipyridamole; or inotropic – dobutamine +/- atropine). Current recommendations are that exercise should be used whenever possible in order to provide a physiological response, with pharmacological stress only being used in patients unable to exercise. Vasodilator stress works on the principle of coronary artery “steal”. At rest, the stenosed coronary artery is vasodilated in order to maximize blood flow to its supplied territory (i.e. its coronary vasodilator reserve has been utilised). When a vasodilator such as adenosine or dipyridamole is given, the non-diseased arteries dilate, increasing coronary blood flow to 4

to 5 times above normal. The diseased artery however is unable to dilate further, resulting in relative hypoperfusion distal to the coronary stenosis. Conversely, when dobutamine is used as stressor the aims are to mimic exercise by increasing the myocardial contractility and heart rate. The contractility of areas of ischaemic myocardium initially improves with low dose dobutamine, however at higher doses the blood supply is unable to match demand and wall motion abnormalities become more obvious.

Whatever means of stress is used, there is relative hypoperfusion – known as the “steal phenomenon” - of myocardial areas subtended by stenosed coronary arteries and therefore there is a relative decrease in radioactive tracer uptake, suggesting significant CAD. The presence of transient left ventricular dilatation and reduced ejection fraction at stress are also suggestive of the presence of significant CAD.

Nuclear medicine has been the most studied imaging modality. In general nuclear medicine has been shown to be relatively robust in the assessment of CAD in the general population. In the general population with suspected obstructive SPECT has a sensitivity of 87% and specificity of 73% (Salerno and Beller, 2009). It is recognised that in LBBB however SPECT does suffer some limitations, predominantly explained by the impact of LBBB on the myocardium described earlier in this chapter; because of these several early studies found a high rate of positive test results in the LAD territory with inducible perfusion defects being seen in patients without CAD on angiography (Inanir et al., 2001, Higgins et al., 2006).

There are technical reasons that cause an apparent decrease in perfusion in the septum. It has been observed that resting septal radionuclide counts are lower compared to the lateral wall – this is accepted as the lateral wall is closer to the gamma camera, while the partial volume effect also causes an apparent decrease in perfusion due to the limitations of spatial resolution (Prinzen et al., 1995). Despite this, there is also evidence that there is a definite reduction in septal perfusion in patients with LBBB that is picked up during SPECT imaging not caused by significant CAD on invasive coronary angiography. As described earlier, it has been noted that there is a relative hyper-perfusion of the lateral wall, which may cause perfusion in the septum to appear abnormal, due to its decreased workload compared to the lateral wall (Koepfli et al., 2009).

Other mechanisms for a true decrease in perfusion include impairment of diastolic coronary blood flow caused by the abnormal septal post-systolic motion leading to compression of the septal perforators, the phenomenon known as phasic flow (Skalidis et al., 1999) and reduced septal endothelial function and reduced coronary flow reserve leading to microvascular dysfunction, reduction in the length of diastole in LBBB (worsening during exercise, leading to reduced perfusion) (Masoli et al., 2000).

Several methods have been used to overcome these problems. The widespread adoption of ECG-gated SPECT has improved the accuracy of technique. Specifically, viewing gated SPECT images at end-diastole has been found to be the most accurate method of identifying CAD. Demir et al studied 25 patients with LBBB, none of whom had angiographically proven CAD. Non-gated SPECT revealed a 20 septal perfusion defects, gated SPECT with images at end-systole ten and gated-SPECT at end-diastole five, the lowest number of false positives (Demir et al., 2003). These results have been replicated in other studies, suggesting that ECG gating with acquisition in diastole might provide some extra diagnostic confidence in this group of patients (Sugihara et al., 1997, Inanir et al., 2001). Gated SPECT also allows assessment of left ventricular volumes and function which have been shown to have prognostic value in patients with LBBB (America et al., 2007, Jeevanantham et al., 2009, Evangelista et al., 2012).

Algorithms for assessment of septal perfusion defects have also been suggested to improve the diagnostic accuracy of SPECT. By only counting patients with apical defects in addition to septal defects as being positive there seems to increase diagnostic accuracy (Higgins et al., 2006). This appears to be logical, given that the LAD supplies the apex and so patients without significant LAD disease should have normal apical perfusion on SPECT as the apex will not be thinned or dysynchronous. Doing this appears to increase the diagnostic accuracy of SPECT to a similar level to that of dobutamine stress echocardiography (Tandogan et al., 2001). Correlating the perfusion defect with any wall motion abnormality may also prove useful; indeed if there is normal septal wall motion and thickness but abnormal septal perfusion this lends more weight to the result being a true positive. With these caveats, the performance of gated SPECT is more than satisfactory.

Several of the effects mentioned that may lead to false positives are caused by the increase in cardiac inotropy and chronotropy and so vasodilator stress is preferred to exercise or

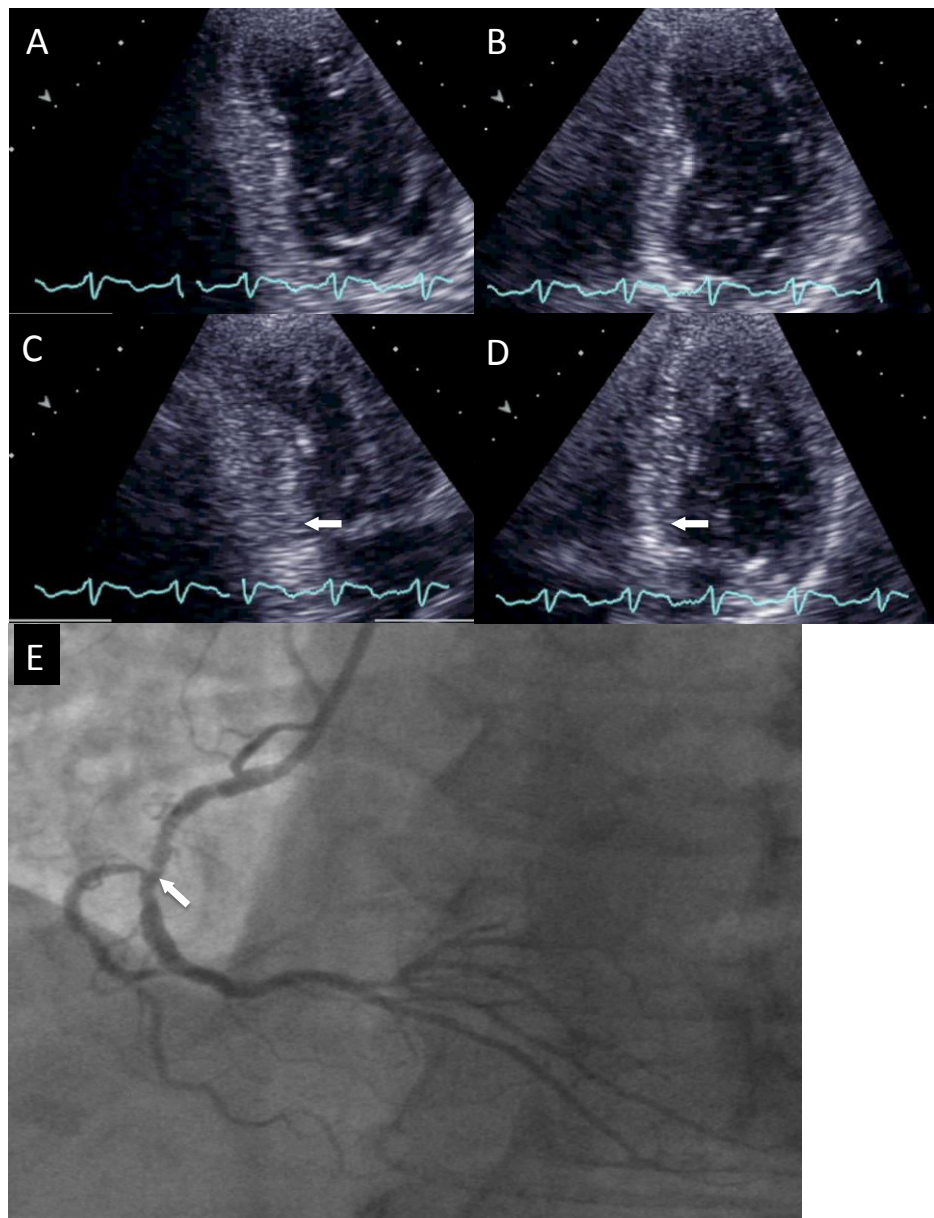
pharmacological in patients with LBBB (Burns et al., 1991, O'Keefe et al., 1993, Vaduganathan et al., 1996). O'Keefe et al reported a specificity of diagnosing septal CAD of 82% using adenosine compared to 42% with exercise stress (O'Keefe et al., 1993). A large retrospective analysis focusing on this was conducted by Vaduganathan et al (Vaduganathan et al., 1996). The authors looked at 383 patients recruited over a 5-year period who had been referred to their unit for myocardial perfusion scintigraphy. Of those, 206 patients were stressed with exercise, 127 had adenosine and in 50 dobutamine was used. They found that all 3 stress modalities performed fairly equally in diagnosis of circumflex (sensitivity and specificity 74% and 96% for exercise; 50% and 100% using dobutamine; 63% and 91% with adenosine) and right coronary artery disease (96% and 86%; 82% and 91%; 79% and 100% respectively). Sensitivity in LAD disease was also acceptable (88%, 79% and 100%, respectively) however, specificity and positive predictive value in diagnosing LAD disease was rather disappointing with exercise compared to pharmacological methods (36% and 51% for exercise, 81% and 85% for adenosine and 80% and 90% for dobutamine respectively). Therefore, in patients with LBBB it may be recommended to perform a gated-SPECT study with adenosine or dipyridamole. Two drawbacks with this large study are that only 40% of patients underwent invasive coronary angiography (ICA) and the retrospective nature of the study calling therefore for caution in interpreting the results.

Positron emission tomography (PET) scanning is another nuclear imaging technique that can be used for assessment of ischaemia. Generally speaking, it is slightly more accurate than SPECT (Bateman et al., 2006). It is however not widely available and is more expensive than SPECT. It does however provide the ability to quantify absolute blood flow, however, PET does seem to be afflicted with the same problems as SPECT (Zanco et al., 2000). Indeed, PET scanning has shown the lateral wall hyperperfusion during stress (Koepfli et al., 2009, Lindner et al., 2005).

7.2.4. Stress Echocardiography

Stress echocardiography is also well validated for identification of CAD. Again, all forms of stress (exercise, vasodilators and inotropes) can be used. Unlike SPECT, rather than perfusion, stress echocardiography (most commonly) looks for the presence of inducible regional wall motion abnormalities during stress (figure 7-2).

Figure 7-2. Dobutamine Stress Echocardiography in LBBB.



DSE revealing an inducible wall motion abnormality at peak stress in the RCA territory (basal inferoseptal; B, D - arrows) confirmed on ICA (E - arrow).

Sensitivity in the general population is around 74-97% for exercise echocardiography, 61-95% for dobutamine and 61-81% for dipyridamole/adenosine while specificity is 64-86%, 51-95% and 90-94% respectively (Marwick, 2003). Again, exercise echocardiography is preferred to pharmacological stress if feasible.

There have been mixed results with use of stress echocardiography in patients with LBBB. The main problem lies with the abnormal septal motion seen in LBBB which is aggravated by tachycardia. Nevertheless, several studies have found that stress echocardiography had

a better diagnostic accuracy than SPECT for detection of CAD (Schartl et al., 1997, Mairesse et al., 1995, Tandogan et al., 2001). Some more recent studies have improved this slightly, perhaps suggesting that more familiarity with the techniques has improved diagnostic accuracy, however, the fact that echocardiography mainly relies on wall motion analysis means that its accuracy, especially in diagnosis of LAD disease is reduced. In a retrospective review of 60 patients who underwent stress echocardiography, Lewis et al found that the technique had a poor specificity (64%) despite a sensitivity of 100% (Lewis et al., 2007). Positive predictive value was poor at around 40% for patients with or without prior MI.

Dobutamine stress echocardiography has shown some good results in other studies however. Yanik et al studied 30 patients with LBBB and left ventricular dysfunction and found that dobutamine stress echocardiography had a sensitivity of 82%, specificity 95% and an overall diagnostic accuracy of 90% (Yanik et al., 2000). One of the largest studies employing stress echocardiography was a prospective evaluation of 64 patients in a multi-center study by Geleijnse et al. (Geleijnse et al., 2000). All patients had been referred for ICA for suspected CAD. They all underwent dobutamine/atropine stress echocardiography. Significant CAD was confirmed angiographically in 19 patients. Sensitivity for the detection of CAD was 68% while specificity was better than what had been previously measured by SPECT at 91%. Diagnostic accuracy overall was 84%. Similar to SPECT, the authors found that the lowest level of diagnostic accuracy was in patients with abnormal septal wall thickening at rest, which made it difficult to diagnose LAD disease correctly. Given that septal abnormalities are the highest cause of false positives, it is of concern that this area provided so much diagnostic uncertainty.

Prognostically, stress echocardiography has been shown to be helpful. A large study by Bouzas-Mosquera et al. identified 618 patients with LBBB who underwent exercise (treadmill) echocardiography. They found that patients who developed ischemia had almost double the 5-year mortality rate and major adverse cardiac event rate to patients who did not (24.6% vs. 12.6% and 18.1% vs. 9.7% respectively) (Bouzas-Mosquera et al., 2009). Similar prognostic information has been shown using dobutamine stress echocardiography (Supariwala et al., 2014) and in patients over the age of 80 (Innocenti et al., 2011).

The use of advanced echocardiographic techniques can also be used to further improve the diagnostic accuracy of stress echocardiography. The quantification of long-axis shortening using tissue Doppler appears to be more accurate than simple wall motion scoring for differentiation of patients with and those without CAD undergoing dobutamine stress echocardiography (Duncan et al., 2003). Badran et al evaluated the addition of tissue Doppler analysis in 62 patients undergoing dobutamine stress echocardiography 6 weeks prior to ICA. As well as standard wall motion analysis, post-systolic shortening velocity, post-systolic peak velocity and peak early and late diastolic velocities were measured. Using these techniques they were able to obtain a sensitivity of 90% and specificity of 87% (Badran et al., 2007). The use of vector velocity imaging to assess strain and strain rate has also been shown to add additional prognostic information in prediction adverse cardiovascular events in patients with LBBB (Shan et al., 2009).

The use of myocardial contrast echocardiography (MCE) may also improve diagnostic accuracy of stress echocardiography. The use of contrast not only allows clearer endocardial border definition, but also allows assessment of myocardial perfusion. Given that the development of perfusion defects are earlier than wall motion abnormalities in the ischaemic cascade, in theory the assessment of perfusion might increase the diagnostic accuracy of stress echocardiography. Karavidas et al. compared adenosine stress echocardiography against SPECT and ICA (Karavidas et al., 2006). This study was prospective, with 47 patients suspected of having CAD undergoing SPECT, then MCE 1-3 days later before having ICA within 1 week. In the study MCE outperformed SPECT significantly. Sensitivity was 73% vs. 91%, specificity 72% vs. 92%, positive predictive value 44% vs. 77% and negative predictive value 90% vs. 97% respectively. Overall, diagnostic accuracy was 72% for SPECT and 97% for MCE. The authors also found that MCE maintained its high performance in the diagnosis of LAD disease. Similar figures were found by Hayat et al, who took 83 patients, reporting a sensitivity of 92% and specificity of 95% using MCE, which significantly outperformed SPECT (Hayat et al., 2008).

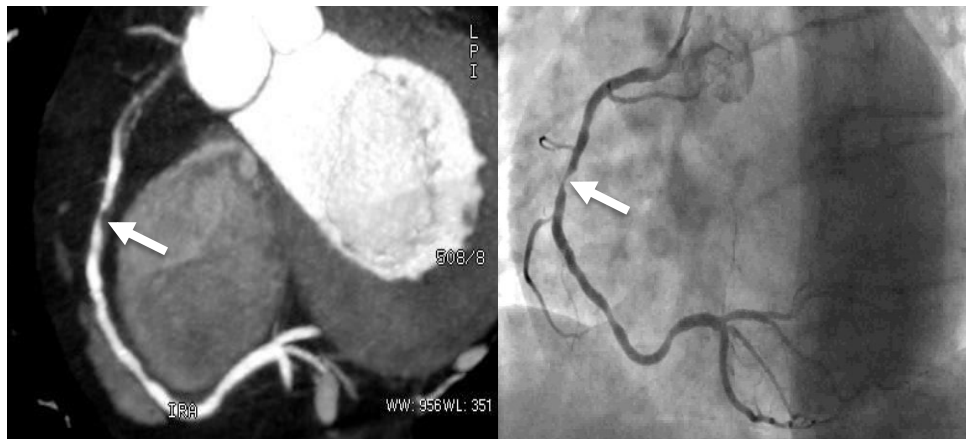
Dobutamine stress echocardiography, in experienced hands, appears to perform at least as well as SPECT in diagnosis of CAD in patients with LBBB. The use of more advanced techniques such as tissue Doppler imaging, speckle tracking and myocardial contrast echocardiography could potentially increase diagnostic accuracy.

7.2.5. Cardiac Computed Tomography

Given the limitations with techniques reliant on wall motion and that the gold standard they are compared with is ICA, it would perhaps be hoped that an anatomical non-invasive imaging technique – multislice cardiac computed tomography angiography (MSCT) – might overcome some of these problems.

In current guidelines, MSCT is usually recommended in patients with a low pre-test probability of CAD (typically less than 15%) to exclude the presence of CAD (Montalescot et al., 2013). The diagnostic accuracy for CTCA in detecting CAD in this group is very good (sensitivity >95%, specificity ~80%) (figure 7-3) (Budoff et al., 2008, Meijboom et al., 2008). But for the majority of patients who fall within an intermediate pre-test probability of CAD, functional imaging is usually recommended to assess whether the coronary artery lesions are functionally significant.

Figure 7-3. Computed Tomography in LBBB.



CT coronary angiography correctly identifies an RCA lesion (left, arrow), with confirmation on invasive coronary angiography (right, arrow).

While the presence of LBBB in itself does not cause technical problems with CTCA, given the prevalence of co-morbidities in patients with LBBB, most of these patients will have at least an intermediate pre-test probability of CAD. Despite this fact, one large study comparing MSCT against ICA reported extremely favourable results. Ghostine et al. looked at 66 patients with LBBB but no prior history of CAD using 64-slice CT and found that on a per-patient basis MSCT had a sensitivity of 97%, specificity of 95% and positive predictive value of 93% compared with ICA (Ghostine et al., 2006). Sensitivity did drop to

72% however when analyzing CAD per AHA segment. The performance of MSCT was also reduced in patients with more than one coronary artery stenosis (multivessel disease). MSCT does certainly appear to be a viable option in patients with low pre-test probability and LBBB (Perrier et al., 2006).

Newer techniques such as CT stress myocardial perfusion imaging and non-invasive measurement of fractional flow reserve have shown some improvement in diagnostic accuracy in the general population, with the ability to provide some functional information, however these have not yet been studied in patients with LBBB (Ko et al., 2012b, Koo et al., 2011).

7.2.6. Cardiovascular Magnetic Resonance

CMR can use a combination of sequences to evaluate both inducible wall motion abnormalities and perfusion defects and can be performed using either dobutamine or adenosine stress. Typical CMR sequences for the assessment of CAD are cine imaging for measurements of chamber size and function and assessment of wall motion, T2 weighted imaging for edema, first pass perfusion imaging at rest and stress using dobutamine, dipyridamole or adenosine and LGE for assessment of myocardial fibrosis (for example in prior infarcts) (Schmid et al., 2010, Karamitsos et al., 2011).

Both DSCMR and adenosine stress CMR appear to have good diagnostic accuracy, especially when combination techniques are used, such as LGE. In the general population DSCMR seems to be at least equal to SPECT and stress echocardiography – it has been shown to have a sensitivity of 83-89% and a specificity of 84-86%. Prognostically it has also been shown to be useful, with a 96.2% 2-year survival rate in patients with suspected ischemia but a negative DSCMR (Nandalur et al., 2007). Perfusion imaging with adenosine is perhaps more commonly carried out clinically, and two large trials have also confirmed its diagnostic accuracy, and suggest it may be better than SPECT, with additional prognostic value. It has also been shown to have reasonable accuracy in diagnosis of patients with CAD (Schwitter et al., 2012, Pilz et al., 2008, Greenwood et al., 2012).

CMR seems to have some potential to overcome the limitations of other non-invasive functional techniques for investigation of suspected CAD in patients with LBBB, but as of yet there have been no studies evaluating its diagnostic accuracy in this group of patients.

7.3. Review Summary

Obstructive CAD is common in patients with LBBB, however all common non-invasive imaging techniques do appear to suffer some limitations, which are summarised in table 7-1.

Table 7-1. Summary of Advantages and Disadvantages of Non-Invasive Techniques For Investigation of CAD in LBBB.

Investigation	Advantages	Disadvantages
Exercise ECG	<ul style="list-style-type: none"> • Cheap • Easily available 	<ul style="list-style-type: none"> • Too unreliable for regular use
Nuclear Imaging	<ul style="list-style-type: none"> • Most studied • Widely available in many areas • Large number of centres and expertise • Prognostic data available 	<ul style="list-style-type: none"> • High rate of false positives in the septum • Radiation exposure
Stress Echocardiography	<ul style="list-style-type: none"> • Readily available in many centres • Prognostic data available • No radiation exposure • Safe • Cheap • Can make non-coronary diagnoses 	<ul style="list-style-type: none"> • Perhaps a lower rate of false positives than nuclear testing, but high variability between operators • Can be limited by poor windows
Cardiac CT	<ul style="list-style-type: none"> • Excellent anatomical definition • Can deliver extra-cardiac diagnosis • Addition of perfusion allows functional analysis 	<ul style="list-style-type: none"> • Not as useful in patients with high probability of coronary artery disease • High radiation dose (especially if perfusion added) • High calcium may not correlate to significant stenosis
Stress CMR	<ul style="list-style-type: none"> • Not limited by “windows” 	<ul style="list-style-type: none"> • Not widely available

	<p>unlike echocardiography</p> <ul style="list-style-type: none"> • Allows functional testing • Able to make non-coronary diagnoses • Improvement in angiographic techniques may allow anatomical diagnosis • No ionising radiation 	<ul style="list-style-type: none"> • More technically challenging • Claustrophobia • Expensive • Not as validated as SPECT or stress echocardiography
--	---	---

Both SPECT and stress echocardiography have reduced diagnostic accuracy in this group of patients, while although MSCT and stress CMR may hold some promise, large studies and prognostic data are still lacking for these techniques in LBBB. Important note must be made of the difficulties in diagnosis of significant LAD territory disease.

It is important to mention some caveats with studies of imaging techniques. Firstly, many of these studies do suffer from post-test referral bias, as with many studies in diagnostic testing. That is, in most studies, patients with positive results are preferentially referred on for angiography. This means that the number of false positives is much higher than the number of true negatives, thus giving potentially (artificially) lower test specificity (Hachamovitch and Di Carli, 2008). Also, physicians may preferentially refer high-risk patients for angiography without imaging. This may mean that the patients included in studies might be lower risk and not wholly representative of the general population, especially relevant in patients with LBBB where there is a high prevalence of CAD.

The other important point to note is that most studies have defined the presence of CAD on the basis of angiographic stenosis of greater than or equal to 50%, often based on visual assessment, or at best quantitative coronary angiography. It is now accepted that lesions of this size (or larger) are not always functionally significant, and that lesions that appear smaller might actually be so. Again, this (at least theoretically) may artificially lower the sensitivity and specificity noted in non-invasive imaging. No studies have been done specifically in patients with LBBB to compare non-invasive imaging modalities with invasive function assessments such as fractional flow reserve.

At present, it would be preferable that non-invasive imaging of patients with LBBB should be performed wherever possible to avoid unnecessary angiography. Selection of the technique used probably should come down to physician preference, confidence and perhaps more importantly, an awareness of the limitations of each technique and methods to overcome these. Gated SPECT and vasodilator stress echocardiography are probably the most widely available techniques, however, stress CMR might be able to provide a solution to this difficult clinical problem. I shall now go on to test this hypothesis in a study comparing dobutamine stress CMR against dobutamine stress echocardiography in a group of patients with stable angina and LBBB.

7.4. Study Introduction

So far in this chapter I have described the difficulties posed to the clinician in the non-invasive assessment of LBBB. Because of the prevalence of CAD in patients with LBBB (Eriksson et al., 1998, Hardarson et al., 1987), initial investigation of patients with this ECG abnormality is often directed to the exclusion of significant CAD, particularly when the history is suggestive.

It appears that non-invasive techniques that use a combination of parameters to assess ischaemia appear to hold the best promise in accounting for the limitations of individual techniques, for example the difficulty in assessing wall motion, or the presence of perfusion defects unrelated to the presence of significant obstructive CAD (Badran et al., 2007, Karavidas et al., 2006).

Dobutamine stress CMR (DSCMR) can assess both wall motion and perfusion, and this perhaps has the ability to overcome some of the disadvantages of other non-invasive investigations (Charoenpanichkit and Hundley, 2010). DSCMR allows confident diagnosis of stress-induced wall motion abnormalities with excellent differentiation of the myocardial border, while the use of gadolinium contrast allows visualisation of myocardial fibrosis caused by the presence of CAD. Additionally, the visualisation of myocardial perfusion during the first pass of gadolinium at rest and stress also provides another potential tool for diagnosis of CAD. Nevertheless, the utility and potential superiority of DSCMR in this setting has not yet been established.

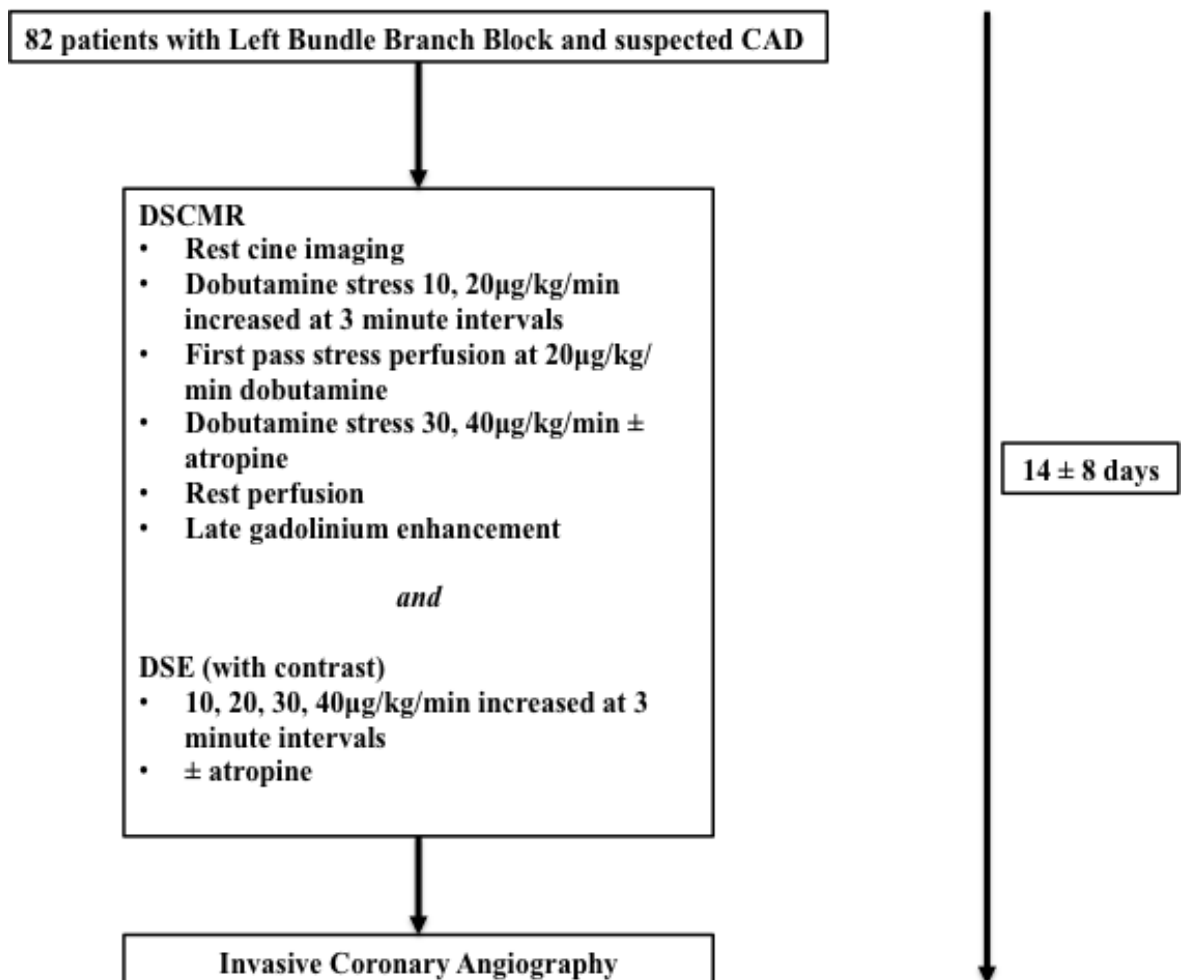
The aim of this study was to compare a comprehensive DSCMR examination including wall motion analysis, perfusion and LGE imaging with dobutamine stress echocardiography (DSE) compared to the gold-standard of invasive coronary angiography (ICA). Two aspects of DSCMR were evaluated – firstly, the diagnostic accuracy of CMR wall motion analysis alone (analogous to DSE), and then the additional diagnostic value of the addition of perfusion and LGE imaging.

7.5. Methods

7.5.1. Patient Selection

82 consecutive patients with LBBB who were referred for assessment of suspected CAD were recruited. All patients underwent DSE, DSCMR and ICA. All tests were performed within 14 ± 8 days by observers blinded to results of the other tests. The study is summarized in figure 7-4.

Figure 7-4. Study Summary



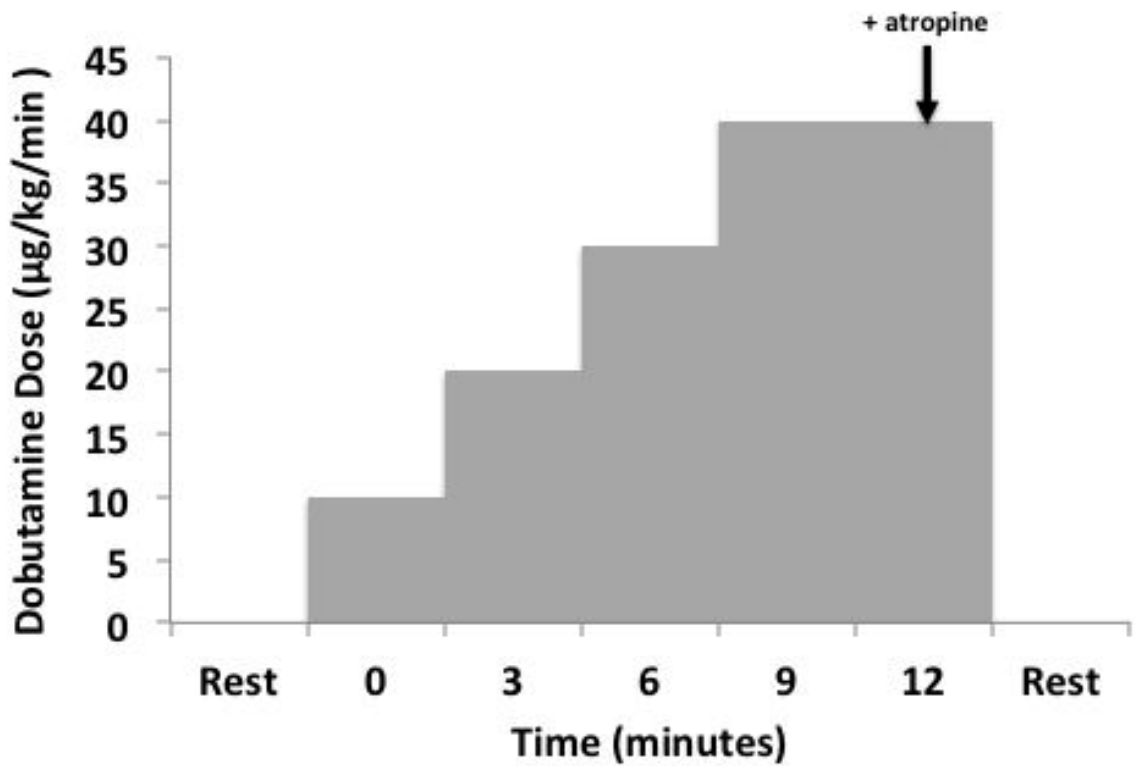
Currently, it is recommended that non-invasive functional imaging for investigation of stable angina should be used in patients with intermediate probability of CAD (Montalescot et al., 2013, Skinner et al., 2010) and therefore no patients of low or high risk were chosen (<10% or >80% pre-test probability). To ensure this, all patients were age ≥ 40

years and had typical features of angina (exertional chest pain or dyspnoea) with one or more risk factors. In addition to the standard CMR exclusion criteria (described in Chapter 2), patients with uncontrolled hypertension (baseline systolic BP of >190 mmHg or diastolic BP of >100 mmHg), those with atrial fibrillation with fast ventricular response were also excluded. Patients were allowed to continue their anti-anginal medications, including oral beta-blockers, calcium channel blockers and nitrates, before DSCMR. For DSCMR, DSE and ICA analysis was performed by two observers blinded to the results of the other investigations. All patients provided written informed consent to undergo DSCMR, DSE, ICA.

7.5.2. Dobutamine Stress Echocardiography

Two-dimensional transthoracic DSE was carried out in all patients using an IE33 scanner (Philips, Amsterdam, Netherlands). All patients were scanned in the left lateral position and with continuous ECG monitoring employed. All patients were pharmacologically stressed using dobutamine starting at a rate of 10 µg/kg/min and increased at 3-minute intervals by increments of 10 µg/kg/min to a maximum of 40 µg/kg/min. If target heart rate (85% of 220 - age) was not reached at 40 µg/kg/min of dobutamine intravenous boluses of atropine sulphate were also given (0.25-0.5 mg aliquots up to a maximum total dose of 2 mg) to increase the heart rate response. Standard echocardiographic views were taken (parasternal long and short axes, apical 2, 3, 4 and 5 chamber and subcostal views). Images were acquired at rest and peak stress. The dobutamine infusion was stopped were: the patient reaching target heart rate (i.e. 85% of predicted for age), occurrence of a new wall motion abnormality, development of significant symptoms (e.g. chest pain, dyspnoea) or significant ECG changes such as arrhythmias. In order to improve endocardial border definition intravenous contrast was used for all patients during at both rest and stress. The DSE protocol is summarised in figure 7-5.

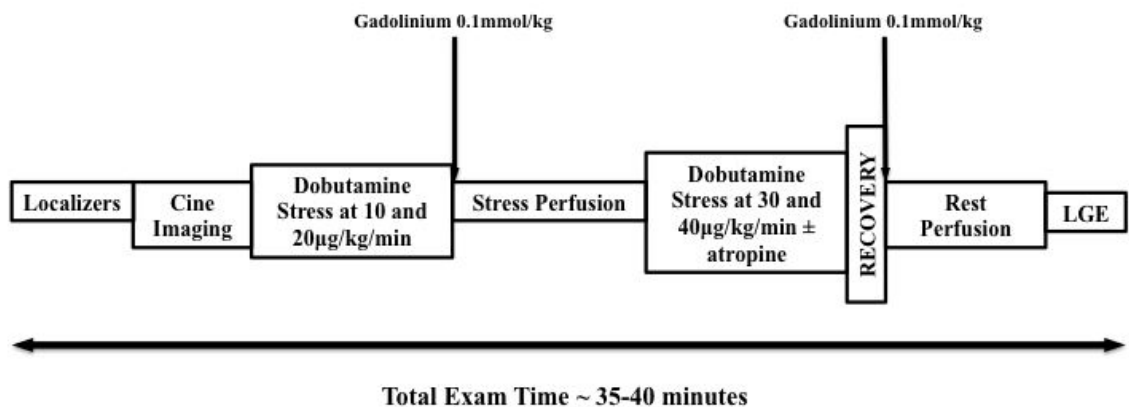
Figure 7-5. DSE Protocol



7.5.3. Dobutamine Stress CMR

DSCMR was performed using the same scanner as before. The order of sequences is summarized in Figure 7-6.

Figure 7-6. DSCMR Protocol



All patients underwent HASTE and cine imaging as previously described. Following this, dobutamine was infused at progressive 3-minute stages of 10, 20, 30, and 40 mcg/kg/min, analogous to DSE. Again, intravenous boluses of atropine sulphate were used at 30 or 40 mcg/kg/min stages in the case of an inadequate heart rate response. At 20µg/kg/min dobutamine stress (intermediate dose), intravenous gadolinium-DOTA (0.1mmol/kg) was injected and first-pass myocardial perfusion images were acquired at 3 short-axis slices (representing the basal, mid and apical levels of the left ventricle) and the 4-chamber long-axis view. This dose was selected as there was concern that at higher doses of dobutamine the increase in myocardial contractility and heart rate might cause difficulty interpretation of first-pass perfusion images. There is evidence to suggest that this dose can cause adequate vasodilatation and augmentation of blood flow to allow assessment of myocardial perfusion equivalent to perfusion imaging using adenosine (al-Saadi et al., 2002, Bartunek et al., 1999, Severi et al., 1995). Following stress perfusion imaging and stress wall motion analysis and return to resting heart rate, a further dose of intravenous gadolinium was given and rest perfusion images acquired using the same views as at peak stress. 10 minutes after this second dose of gadolinium LGE imaging was performed.

Two experienced readers blinded to patients' clinical history and outcome interpreted the dobutamine-CMR images. The presence of regional wall motion abnormalities (RWMAs) each stage was analyzed according to the standardized American Heart Association 17-segment model (Cerqueira et al., 2002). At each dobutamine stage segments were graded as 1 = normal, 2 = hypokinesia, 3 = akinesia, and 4 = dyskinesia. An inducible RWMA was defined as the presence of wall motion grade >1 and absence of wall thickening during progressive dobutamine stress, apart from the progression of segmental akinesia to dyskinesia which was considered non-specific. Segmental RWMAs had to be present in both short and long axis views to be considered true ischaemic defects.

For perfusion imaging, the 3 slices were qualitatively analysed for the presence of perfusion defects. The left ventricular myocardium was segmented into 6 sectors at the basal and mid ventricular slices and 4 sectors at the apical slice, again following the American Heart Association model. Each myocardial segment was qualitatively interpreted as having normal perfusion or abnormal hypoperfusion (reduction in signal). Ischemia by myocardial perfusion imaging was defined by any persistent segmental reduction in signal in absence of delayed hyper-enhancement by delayed imaging or, in patients who had evidence of prior MI on LGE imaging, the presence of peri-infarct

ischemia was also counted as a positive perfusion defect. In detecting coronary stenosis, myocardial ischemia by WMI or MPI was only considered true positive if the myocardial segment was in the same territory of a significant stenosis. Using CMR cine imaging alone, CMR was judged to be positive if an inducible regional wall motion abnormality (RMWA) was seen. In the comprehensive DSCMR examination, the test was adjudged to be positive if either there was LGE present in a distribution typical of infarction (subendocardial or transmural) with evidence of peri-infarct ischemia; or if there was no LGE, if there was an inducible perfusion defect which corresponded to an inducible RMWA.

Infarcted myocardium was quantitated by semiautomatic detection of any region with signal intensity 5 standard deviations above the mean signal intensity of the remote myocardium as previously validated. The presence of LGE was only counted as positive if it was present in a sub-endocardial or transmural distribution typical of CAD (other patterns such as midwall LGE were excluded).

Using CMR cine imaging alone, the test judged to be positive if an inducible RMWA was present. In the comprehensive DSCMR examination, the test was ruled positive if either there was LGE present in a distribution typical of CAD, with or without evidence of peri-infarct ischemia. If no LGE was present, only the presence of an inducible perfusion defect corresponding to an inducible RMWA was ruled as a positive test.

7.5.4. Invasive Coronary Angiography

ICA was performed in all 82 patients. All angiograms were performed by experienced operators at the Golden Jubilee National Hospital. The operators were blinded to both DSE and DSCMR findings. To improve the accuracy of the assessment of the significance of coronary stenoses quantitative coronary angiography analysis (QCA) was performed using GE automated edge detection software, which calibrates using the coronary guide catheter as its reference diameter (Centricity Cardiology CA1000, GE Healthcare, Dornstadt, Germany). In order to ensure that significant, ischaemia causing stenoses were identified, significant stenoses were defined as $\geq 70\%$ luminal narrowing in the most severe view ($\geq 50\%$ for left main stenosis). Patients were classified as having 1, 2 and 3-vessel disease.

7.5.5. Statistical Methods

In addition to the statistical methods described in Chapter 2, several other analyses were conducted. Sensitivities, specificities, positive predictive and negative predictive values, chi-square statistic and the area under the curve (AUC) of DSE, CMR cine imaging and the complete DSCMR examination for detection of significant CAD (> 70% coronary artery stenoses) were calculated. Comparisons between diagnostic techniques were made with the McNemar test. The AUC between the tests was calculated using the method of DeLong et al (DeLong et al., 1988).

7.6. Results

7.6.1. Baseline Characteristics

All 82 patients underwent all 3 investigations without any complication. Image quality was satisfactory in all patients. The mean peak dose of dobutamine given was 35.4 ± 5.7 $\mu\text{g}/\text{kg}/\text{min}$ and mean peak heart rate attained was 143.3 ± 10.0 beats/minute. Patient characteristics are summarized in table 7-2 while hemodynamic parameters are summarized in table 7-3.

Table 7-2. Baseline characteristics of the cohort.

	All Patients (n=82)	CAD (n=34)	No CAD (n=48)	p value
Age (years)	56.5 ± 7.8	57.2 ± 9.2	56.0 ± 6.6	0.50
Male	53 (64.6)	23 (67.6)	30 (62.5)	0.63
QRS duration (ms)	133.0 ± 8.1	134.5 ± 7.0	132.2 ± 8.7	0.19
Hypertension	38 (46.3)	21 (61.8)	17 (35.4)	0.018
Diabetes Mellitus	19 (23.2)	11 (32.4)	8 (16.7)	0.10
Peripheral Arterial Disease	17 (20.7)	7 (20.6)	10 (20.8)	0.98
Chronic Obstructive Pulmonary Disease	12 (14.6)	6 (17.6)	6 (12.5)	0.54
Hyperlipidaemia	39 (47.6)	14 (41.2)	25 (52.1)	0.33
Smoker	33 (40.2)	12 (35.3)	21 (43.8)	0.44
Alcohol excess	9 (11.0)	3 (8.8)	6 (12.5)	0.73
Family History	37 (45.1)	13 (38.2)	24 (50.0)	0.29
Aspirin use	22 (26.8)	9 (26.5)	13 (37.1)	0.34
Beta-blocker use	13 (15.9)	6 (17.6)	7 (14.6)	0.71
Oral Nitrate use	4 (4.9)	0 (0.0)	4 (8.3)	0.14
Statin use	32 (39.0)	13 (38.2)	19 (39.6)	0.90
Calcium Channel Antagonist use	25 (30.5)	14 (41.2)	11 (22.9)	0.08
Angiotensin-Converting Enzyme Inhibitor use	31 (37.8)	16 (47.1)	15 (31.3)	0.15

Data are presented as mean ± SD if continuous or number (%) if categorical.

CAD – coronary artery disease

Table 7-3. Haemodynamic data for DSCMR.

Resting HR (bpm)	71 ± 9
Maximal HR (bpm)	143.3 ± 10.0
Resting Systolic BP (mmHg)	132 ± 20
Peak Systolic BP (mmHg)	162 ± 10
Resting Diastolic BP (mmHg)	72 ± 9
Peak Diastolic BP	71 ± 11
Peak Dose of Dobutamine (mg)	35.4 ± 5.71
Number reaching target HR (85% of predicted) (%)	82 (100)
Atropine Given (%)	79 (96.3)

Data are presented as mean ± SD if continuous or number (%) if categorical. HR – heart rate; bpm – beats/minute; BP – blood pressure

There was no significant difference in mean age between patients with CAD compared to those without significant CAD (57.1 ± 8.9 years vs. 55.9 ± 6.6 years, $p=0.50$). As would be expected in a cohort of patients with an intermediate pre-test probability for CAD, a significant proportion had CAD risk factors. The commonest risk factors within this patient population were hypercholesterolaemia, hypertension, smoking and a family history of CAD. The presence of hypertension was the only significant difference between the two groups (61.8% in patients with CAD vs. 35.4% in patients without CAD; $p=0.018$).

7.6.2. DSE and DSCMR Compared to ICA

Based on the results of quantitative analysis of ICA, 34 patients were deemed to have significant CAD. For assessment of inducible wall motion abnormalities DSCMR cine imaging and DSE had the same sensitivity (70.6%), however cine imaging had improved specificity (87.5% vs 72.9%), and consequently higher diagnostic accuracy (80.4% vs. 72.0%). Positive and negative predictive values for wall motion interpretation by DSCMR cine imaging were 80.0% and 80.8% respectively while for echocardiography values were 64.9% and 77.8% (Table 7-7).

Table 7-4. Per-patient diagnostic performance of DSE and DSCMR.

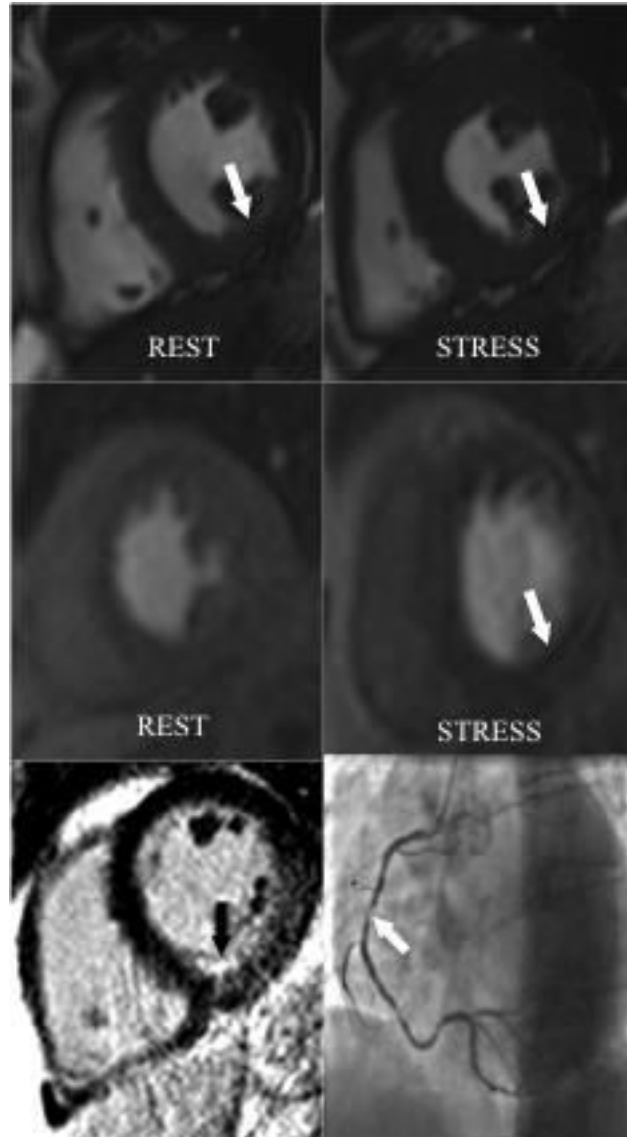
	Sensitivity (%)	Specificity (%)	Accuracy (%)	PPV (%)	NPV (%)	AUC
DSE	70.6	72.9	72.0	64.9	77.8	0.72
DSCMR Cine Imaging	70.6	87.5	80.4	80.0	80.8	0.79
First Pass Perfusion	70.6	93.8	84.1	88.9	81.8	0.82
LGE	41.5	100	72.0	100	67.6	0.66
Comprehensive DSCMR	82.4	95.8	90.2	93.3	88.5	0.89*

PPV - positive predictive value; NPV - negative predictive value; AUC - area under the curve; DSE - dobutamine stress echocardiography; DSCMR - dobutamine stress cardiovascular magnetic resonance imaging

** $p < 0.05$ between comprehensive DSCMR and DSE*

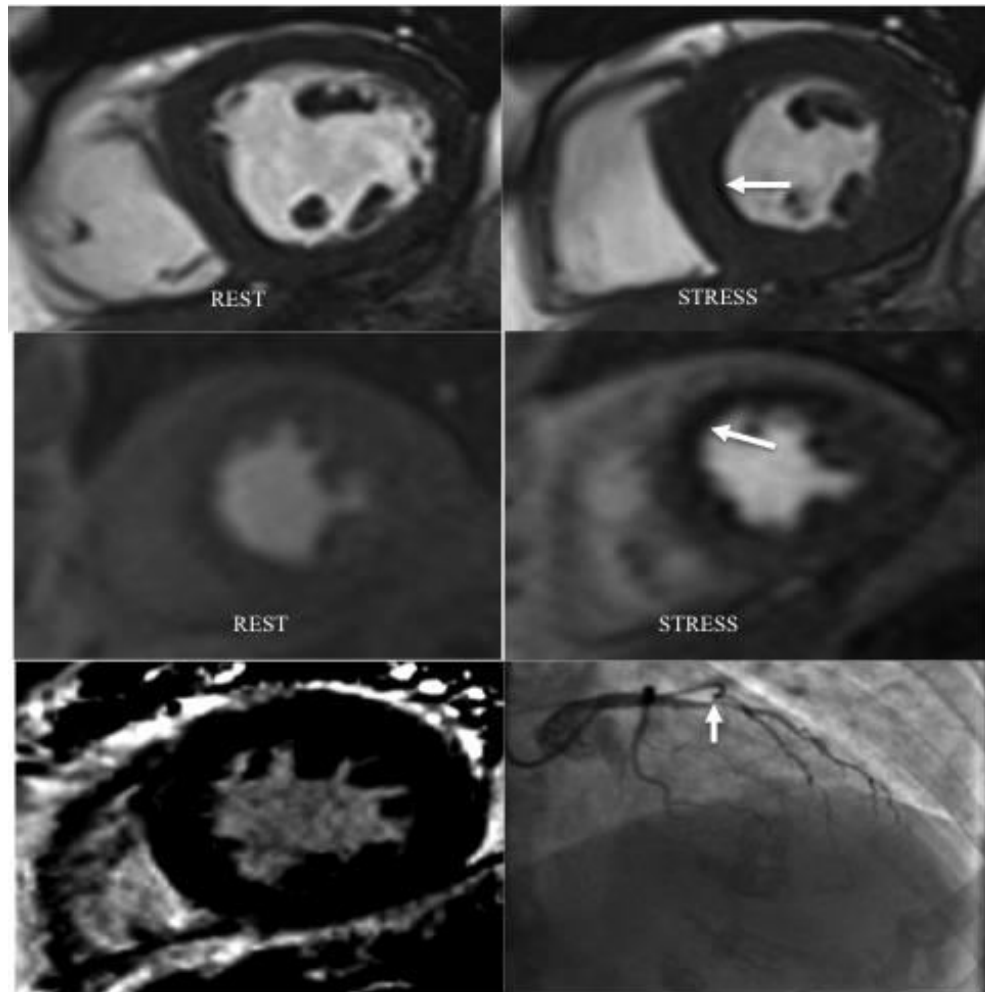
There was an incremental improvement in diagnostic accuracy following the addition of stress perfusion imaging and LGE results, outlined in table 8-3. 11 patients had an ischaemic pattern of LGE. Sensitivity of the comprehensive DSCMR exam was 82.4% while specificity increased to 95.8%, leading to an improved overall diagnostic accuracy of 90.2%. Using the receiver-operator characteristic, the area under the curve was greatest for a comprehensive DSCMR examination and was significantly better than DSE (AUC 0.89 vs. 0.72 respectively, $p < 0.05$). Examples of typical findings using DSCMR are shown in figures 7-7 to 7-9.

Figure 7-7. An example of a patient correctly identified with CAD using DSCMR.



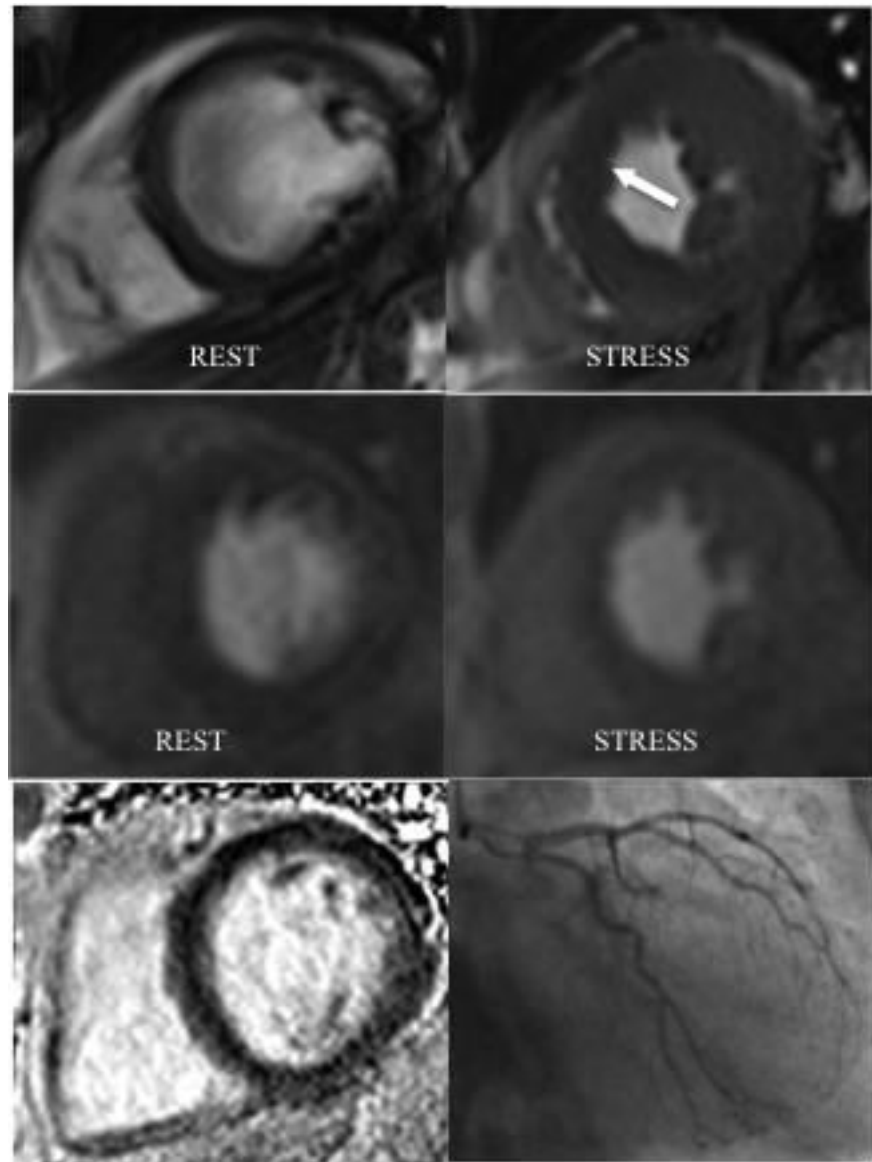
This patient had an inducible inferior RWMA seen using cine imaging (top, arrows). Perfusion imaging showed a stress-induced defect in the inferior wall (middle, arrows), with subendocardial LGE typical of CAD in this area (bottom left, arrow). ICA confirmed the presence of a right coronary artery stenosis.

Figure 7-8. An example of a patient with a septal wall motion abnormality typical of LBBB correctly identified with CAD using DSCMR.



This patient had an inducible septal RWMA seen using cine imaging (top, arrow). Perfusion imaging showed a stress-induced defect in the septum and anterior wall (middle, arrow). There was no LGE present (bottom left). ICA confirmed the presence of a left anterior descending artery stenosis.

Figure 7-9. An example of a false positive septal wall motion abnormality for CAD using DSCMR cine imaging only but correctly identified as not having significant CAD using the comprehensive DSCMR examination.



This patient had an inducible septal RWMA seen using cine imaging (top, arrow). There was no perfusion defect seen (middle) and no LGE present (bottom left). ICA confirmed the absence of any significant CAD.

Of the 34 patients with diagnosed with CAD by invasive angiography, 14 had left anterior descending (LAD) stenoses, 14 had circumflex (Cx) disease, 5 had right coronary artery disease (RCA) disease and one had two-vessel disease. Table 7-8 summarises the respective performance of DSE and DSCMR for in correctly identifying the affected coronary artery.

Table 7-5. Percentage of patients correctly identified per vessel by echocardiography and CMR.

	DSE	DSCMR Cine Imaging	Comprehensive DSCMR
No CAD	72.9 (35/48)	87.5 (42/48)	95.8 (46/48)
LAD	64.3 (9/14)	57.1 (8/14)	71.4 (10/14)
LCx	64.3 (9/14)	78.6 (11/14)	92.9 (13/14)
RCA	100 (5/5)	80.0 (4/5)	80.0 (4/5)
2-Vessel Disease	100 (1/1)	100 (1/1)	100 (1/1)

CAD – Coronary Artery Disease; ICA - invasive coronary angiography; DSE - dobutamine stress echocardiography; DSCMR - dobutamine stress cardiovascular magnetic resonance imaging

In two coronary artery territories, comprehensive DSCMR had improved sensitivity in comparison to DSE and DSCMR cine imaging (LAD: 71.4% vs. 64.3% vs. 57.1%; LCx: 92.9% vs. 64.3% vs. 78.6% respectively). Sensitivity for the left-sided circulation was DSE: 64.2%, CMR cine imaging: 67.9% and comprehensive DSCMR: 82.1%. Both CMR techniques failed to identify one RCA lesion that was correctly identified by DSE. All three techniques correctly identified the presence of 2-vessel disease in one patient.

7.7. Discussion

7.7.1. Study Findings

This study was the first prospective evaluation using a comprehensive DSCMR examination of patients with LBBB for the diagnosis of CAD.

- Regarding the primary hypothesis, DSCMR cine imaging proved to have higher diagnostic accuracy than DSE.
- Additionally, there was an incremental benefit in diagnostic accuracy in using a comprehensive exam including cine imaging, first pass stress perfusion and LGE over wall motion analysis using DSCMR cine imaging alone.

7.7.2. Clinical Context

LBBB becomes more prevalent with age (around 17% of people at age of 80 in a Northern European population) and it is known to confer an adverse prognosis, at least in part due to the risk of cardiac death (Hardarson et al., 1987, Eriksson et al., 2005, Eriksson et al., 1998). The prevalence of CAD in patients with LBBB is thought to be between 30-50% therefore, given the poor prognosis of LBBB it would be beneficial to identify those who may benefit from revascularization to alleviate some of the risk of cardiovascular mortality and morbidity (Schneider et al., 1981).

Despite improvements in non-invasive imaging, diagnosis of CAD in patients with LBBB remains difficult. Functional non-invasive tests (exercise ECG, SPECT and stress echocardiography) are all affected adversely by LBBB as described in chapter 7 (Gibbons et al., 1997, DePuey et al., 1988), (Geleijnse et al., 2000). MSCT has been shown to have good diagnostic accuracy in LBBB, however in patients with intermediate pre-test probability of CAD, such as the population in our study, current guidelines suggest the use of a functional rather than anatomical imaging as first-line (Ghoshine et al., 2006, Meijboom et al., 2007, Skinner et al., 2010). Due to these limitations and the consequent diagnostic uncertainty, many patients may end up undergoing ICA, which may indeed be unnecessary and exposes them to the risks of this invasive procedure.

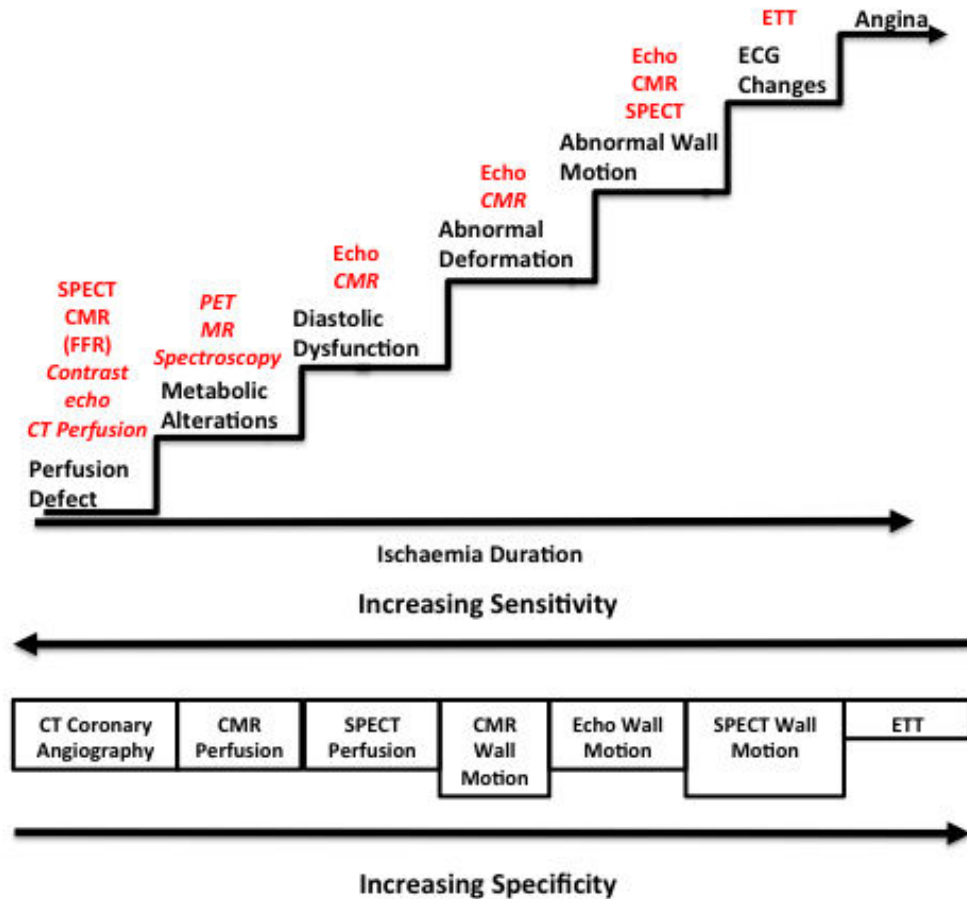
The limitations of current non-invasive imaging techniques for the diagnosis of CAD mean that the ideal non-invasive imaging technique has not yet been found for patients with LBBB. The improved diagnostic accuracy of DSCMR in this study is therefore encouraging and perhaps offers a potential solution to this clinical problem.

7.7.3. DSCMR Cine Imaging vs. DSE

DSCMR has been shown to have good diagnostic accuracy in patients with suspected CAD, with several studies reporting good sensitivity and specificity (Charoenpanichkit and Hundley, 2010). In one of the largest studies using DSCMR for detection of significant CAD, using cine imaging alone, Gebker et al. evaluated 455 patients and reported a sensitivity of 85% and a specificity of 82%, with an increase in sensitivity to 91% with the addition of first pass perfusion, at the cost of a decrease in specificity to 70% (Gebker et

al., 2008). The authors suggested that this was due to the fact that perfusion defects tend to occur before RWMA and therefore may be caused by less significant CAD (figure 7-10).

Figure 7-10. The ischaemic cascade and the consequences for diagnostic accuracy of non-invasive imaging techniques.



The ischaemic cascade (top). Perfusion defects are the earliest sign of ischaemia caused by CAD, which eventually causes the clinical symptoms of angina. Wall motion abnormalities occur later on in the ischaemic process. This leads to consequences in the accuracy of diagnostic techniques, where techniques that identify perfusion defects have increased sensitivity at the cost of specificity, with the converse true for techniques reliant on wall motion (bottom).

The difficulty in assessing RWMA in patients with LBBB would explain the lower sensitivity seen in this study compared to others using DSCMR (in patients without LBBB). The reduced sensitivity of DSCMR cine imaging alone was also shown in a study by Paetsch et al, who reported a sensitivity of 78.2% and specificity of 87% (Paetsch et al., 2006). The sensitivity and specificity for DSE in this study corresponds well to a study of

64 patients by Geleijnse et al., who reported sensitivity of 68% and specificity of 91% (Geleijnse et al., 2000). The number of false negatives may be due to the difficulties in knowing whether any abnormal septal motion seen is due simply to the presence of LBBB or rather is truly representative of significant CAD. The higher specificity of DSCMR cine imaging (reduced false positives) compared to DSE may be due to the increased spatial resolution and clearer endocardial blood pool definition, allowing easier and more accurate wall motion analysis. In this respect our results correspond fairly well to those of Nagel et al in patients without LBBB, who also proposed that the improved diagnostic accuracy using CMR cine imaging alone was due to the increased spatial resolution of CMR (Nagel et al., 1999).

7.7.4. The Incremental Value of Perfusion and LGE

Given the reduced sensitivity of DSCMR due to the resting myocardial abnormalities in LBBB, I hypothesized that the addition of first-pass stress perfusion and LGE imaging would enhance the diagnostic accuracy of the CMR exam, which was proven to be correct. The incremental value of perfusion imaging in addition to wall motion analysis was shown in a study by Lubbers et al. in which the authors found that the addition of first pass perfusion imaging during dobutamine stress reduced the number of false positives. Indeed, in their study, all four patients that had an inducible wall motion abnormality with no perfusion defect had LBBB, giving some early evidence that this might be technique that could be used in this group of patients (Lubbers et al., 2008).

The addition of first pass stress perfusion and LGE increased diagnostic accuracy markedly. Cine, perfusion and LGE imaging are 3 techniques that can each independently diagnose CAD, hence an examination combining the 3 gives greater diagnostic confidence. Of clinical importance is the improved performance of the comprehensive DSCMR exam in left-sided coronary disease, which poses particular difficulties in patients with LBBB. Sensitivity increased from 64.2% with DSE to 82.1% with comprehensive DSCMR. Speculatively, this may lead to some prognostic benefit in improved identification of patients who need invasive management. This has been shown in a general population of patients with suspected CAD (Bingham and Hachamovitch, 2011). Similarly to other studies, we have shown that a comprehensive CMR exam can be performed relatively safely in routine clinical practice (Bingham and Hachamovitch, 2011).

The additional value of LGE appears to be in its increased specificity/positive predictive value, although this may only apply to a cohort with typical anginal symptoms and an intermediate pre-test probability of CAD. An associated inducible perfusion defect along with the presence of LGE may indicate peri-infarct ischemia. In other groups of patients, such as those without anginal symptoms, this may not apply as the presence of LGE may be more indicative of a cardiomyopathy, especially if not in a typical coronary distribution, obviating the need for invasive angiography (Mahmod et al., 2012). The increase in sensitivity found by using the comprehensive examination is probably due to the strict criteria for a positive result, which mean that a patient must have either LGE (with or without a perfusion defect) or an inducible RWMA and a perfusion defect, meaning that the criteria are more strict. This combination lead to the overall improved diagnostic performance of the comprehensive DSCMR exam.

Performing first pass perfusion at an intermediate dose of dobutamine appears to provide adequate diagnostic confidence for the assessment of inducible perfusion defects by direct comparison against ICA. Prior studies suggest that the majority of the increase in myocardial blood flow and vasodilatation caused by dobutamine occurs at 20 µg/kg/min; beyond this there is simply an increase in heart rate and contractility, which may make it more difficult to identify the presence of perfusion defects (al-Saadi et al., 2002, Bartunek et al., 1999, Severi et al., 1995). Furthermore, the false positive perfusion defects seen in SPECT are most often due to the fast heart rate at peak stress – the rate of false positives reduces significantly in patients with LBBB when vasodilator stress is used rather than dobutamine (Iskandrian, 2006).

7.7.5. Limitations

Although this study is the first prospective evaluation of DSCMR in patients with LBBB using CMR, there are some limitations. Firstly, although all patients in our study were referred for ICA and this reduced post-test referral bias, the use of quantitative analysis of coronary stenoses as the gold standard was not ideal. The importance of the functional impact of coronary stenoses has been well established and it is known that visual assessment of angiographic stenoses is not optimal (Tonino et al., 2009). Results may have been different if DSCMR had been compared to a functional invasive test such as fractional flow reserve. In order to combat this limitation, stricter criteria than usually used

were used to define the presence of significant CAD (stenosis severity over 70% by QCA rather than 50%, which is most often used).

Secondly, this study was also conducted in a single centre with high volumes of both CMR and angiography hence may be difficult to reproduce these results in lower volume centres. Thirdly, the number of patients in this study is relatively small. Further information could be gained by larger, multi-centre trials with the potential for obtaining prognostic information.

Finally, additional echocardiographic techniques, which have been shown to improve diagnostic accuracy of DSE such as strain analysis, were not used (Badran et al., 2007).

7.8. Conclusions

DSCMR is a feasible, safe non-invasive investigation for the exclusion of CAD in patients with LBBB that outperforms DSE. The addition of perfusion and LGE sequences to DSCMR cine imaging improves sensitivity, specificity and overall diagnostic accuracy. Comprehensive DSCMR provides a viable non-invasive functional investigation for with LBBB and suspected CAD and may overcome some of the disadvantages of DSE in this group.

8. Discussion

8.1. Summary of Thesis Findings

The aim of this thesis was to demonstrate the clinical utility of CMR by demonstrating its potential ability to answer clinical dilemmas that have previously not been answered but might have clinical significance to patients. The main findings of this thesis were:

- The two main advantages of CMR, namely its accuracy in measurement of left ventricular function, and its ability to characterise the presence of myocardial fibrosis using gadolinium contrast, provide incremental prognostic significance for prediction of adverse cardiovascular events when added to baseline clinical variables in a general cohort of patients.
- In patients with a history of prior MI, the presence of fat within the infarct scar, known as lipomatous metaplasia, is a predictor of mortality and ventricular arrhythmias.
- In patients being considered for implantable cardioverter-defibrillators, the combined use of a cardiac biomarker (NT-proBNP) and a marker of structural myocardial injury (LGE) prior to device implantation is able to further stratify risk into groups of patients who may or may not benefit from these devices.
- In patients with mild left ventricular systolic impairment, characterisation of the myocardium using T1 mapping may help differentiate between those with early cardiomyopathy and those without.
- In patients with LBBB and suspected CAD, dobutamine stress CMR has improved diagnostic accuracy compared to dobutamine stress echocardiography for the identification of significant coronary artery stenoses identified by invasive coronary angiography.

8.2. Clinical Implications of the Thesis

As a relatively new technique, CMR has not yet been included as a mainstay in most clinical guidelines. Echocardiography and nuclear imaging remain the predominant non-invasive imaging techniques in use, both in the UK and worldwide, mainly due to increased operator experience with these modalities, cost and the undoubted breadth and depth of evidence validating both techniques in various conditions.

For CMR to become more widely adopted, and perhaps even part of clinical guidelines, more evidence needs to be gathered showing that CMR can change clinical management and make a difference to patient prognosis, as well as potentially providing cost savings to clinical services. Harking back to Chapter 1, there is still a relative paucity of evidence in CMR to suggest that it has patient and societal outcome efficacy, and also diagnostic efficacy in some conditions. The studies in this thesis aim to add to the literature and provide further evidence of the efficacy of CMR.

In Chapter 3 I demonstrated that CMR assessment of LVEF, strain and LGE provide additional prognostic information in addition to baseline clinical variables in a large unselected cohort of patients. While LGE is well-established as a clinical predictor (Parsai et al., 2012), the utility of strain assessment has not been as well-validated, with only one large study in asymptomatic patients (Choi et al., 2013). In this study, I extended the findings to patients with symptoms and those with reduced ejection fractions, and also showed the additional value of strain in combination with LGE and LVEF. These findings might suggest that there is a role for CMR in identifying patients who might have a worse prognosis than at first thought when echocardiography is used alone.

The incremental prognostic utility of CMR was expanded on in Chapters 4 and 5. In Chapter 4, I showed for the first time, the prognostic significance of lipomatous metaplasia in patients with a prior history of MI. The ability to non-invasively identify LM is specific to CMR and CT, and so this may provide a new prognostic marker. CMR has the advantages of being able to be repeated without radiation exposure and the ability to provide functional information, perhaps making it a more favourable technique than CT. The suggestion that LM could provide a substrate for arrhythmias could also provide a new therapeutic target which could improve patient outcomes.

In Chapter 5, I showed that CMR could be used, in combination with biomarkers, to predict death and defibrillator use in patients with ICDs. We know that many patients who meet the current criteria for ICD implantation never use their device, and conversely, many patients who would benefit from an ICD do not meet the current criteria for one. The use of CMR might help in clinical decision-making, potentially identifying a group at higher-risk who might benefit from these devices and identifying a lower-risk group who might not need an ICD. This might lead on to societal benefits in cost savings, as well as avoiding potentially needless device implantation.

In Chapters 6 and 7, I explored the diagnostic utility of CMR in two areas that pose difficulties to clinicians. In Chapter 6, I showed that the use of the novel T1 mapping sequence might help differentiate between normal myocardial adaptation and early cardiomyopathy in patients with mildly reduced LVEF. The clinical implications of this finding are potentially very important. Early diagnosis of cardiomyopathy may allow early introduction of disease-modifying therapies. The ability to reassure patients by diagnosing athlete's heart would provide huge patient benefit. Professional athletes might also be able to be reassured and continue competitive sport.

The final study, in Chapter 7, utilised dobutamine stress CMR to potentially offer another solution to another clinical problem, namely the diagnosis of significant CAD in patients with LBBB. The main benefit of any stress test is the ability to rule out prognostically significant CAD, avoiding the need for invasive coronary angiography. The presence of LBBB tends to mitigate this, exposing patients to the risks of an invasive procedure. The enhanced diagnostic accuracy using DSCMR might allow improved selection of patients for invasive angiography. Furthermore, a patient with negative DSCMR study has an extremely low chance of having an adverse event (<1%/year) (Lipinski et al., 2013). If this finding was extrapolated to patients with LBBB, there would be likely to be significant benefits.

8.3. Limitations of the Thesis

In addition to the limitations relevant to each individual study described in each chapter, there are a number of limitations relevant to the thesis as a whole. The cross-sectional design of each study meant that I was unable to test further hypotheses about progression of conditions, with imaging only being carried out at one time point. This is particularly relevant to the studies in Chapters 3 (overall prognosis using CMR) and 4 (lipomatous metaplasia), where progression over time would have given further information on prognosis.

A second limitation is that a number of the scans in these studies were analysed retrospectively, as they occurred before conception of the thesis. Nevertheless, the majority of patients were prospectively analysed, and events were prospectively recorded, reducing the potential limitations caused by retrospective analysis.

Finally, as CMR is not a routine standard of care in most conditions at present, the studies may have been subject to referral bias. This was hopefully minimised by studying consecutive patients, however the cohorts may not be completely representative of the general population as it may have included those in whom their clinician was more concerned than usual.

8.4. Future Directions

These studies hopefully demonstrate the potential power of CMR and its ability to impact on clinical decision-making. Generally, larger, multi-centre studies are required to demonstrate the prognostic impact of CMR and its cost-effectiveness in order for it to become more widely adopted and be incorporated into clinical guidelines.

Regarding the specific studies in this thesis, there are a number of further studies that could be performed to advance our knowledge:

- A multi-centre study could be performed evaluating the role of multi-parametric CMR in assessing prognosis in patients referred for cardiological opinion compared to the routine standard of care (e.g. using echocardiography).
- Serial CMR examinations could be performed in patients post-MI to clarify if the development of lipomatous metaplasia is indeed a condition that develops with time, and to identify the processes that influence its development. This could lead to identification of therapeutic targets to reduce adverse outcomes.
- A large multi-centre study could be performed to assess the impact of a CMR-guided strategy for ICD implantation in patients on cardiovascular outcome. This could be particularly relevant in patients who do not meet the current guidelines for ICD implantation.
- The prognostic value of T1 mapping has yet to be assessed in a large cohort. This novel parameter could be a new biomarker and lead to new therapeutic directions.
- The diagnostic accuracy of stress CMR has yet to be tested against the invasive gold-standard (fractional flow reserve) for the diagnosis of significant coronary artery disease. A large multi-centre study using adenosine stress CMR is currently recruiting patients with this gold-standard, however dobutamine stress CMR has not been evaluated in this way as yet (Hussain et al., 2012). The use of quantitative

wall motion and perfusion analysis using CMR could also improve its accuracy in LBBB.

8.5. Conclusions

Cardiovascular magnetic resonance holds huge promise as a non-invasive imaging technique for a variety of conditions. The studies in this thesis demonstrate its diagnostic and prognostic utility, and add further evidence of the clinical utility of cardiovascular magnetic resonance.

Appendix 1: Ethical Approval

WoSRES

West of Scotland Research Ethics Service



Dr Ify Mordi
Golden Jubilee National Hospital
Agamemnon Street
Clydebank
G81 4DY

West of Scotland REC 3

Ground Floor - Tennent Building
Western Infirmary
38 Church Street
Glasgow
G11 6NT

Date 07 August 2014

Direct line 0141 211 2482

Fax 0141 211 1847

E-mail WoSREC3@ggc.scot.nhs.uk

Dear Dr Mordi

Study title: **Assessment of the Clinical Utility of Cardiovascular Imaging using Analysis of MRI, CT and Echocardiography.**
REC reference: **14/WS/1052**
IRAS project ID: **146085**

Thank you for your letter of 4 August 2014 responding to the Committee's request for further information on the above research and submitting revised documentation.

The further information has been considered on behalf of the Committee by the Alternate Vice-Chair.

We plan to publish your research summary wording for the above study on the HRA website, together with your contact details. Publication will be no earlier than three months from the date of this opinion letter. Should you wish to provide a substitute contact point, require further information, or wish to make a request to postpone publication, please contact the REC Manager, Mrs Liz Jamieson, wosrec3@ggc.scot.nhs.uk.

Confirmation of ethical opinion

On behalf of the Committee, I am pleased to confirm a favourable ethical opinion for the above research on the basis described in the application form, protocol and supporting documentation as revised, subject to the conditions specified below.

Conditions of the favourable opinion

The favourable opinion is subject to the following conditions being met prior to the start of the study.

Management permission or approval must be obtained from each host organisation prior to the start of the study at the site concerned.

Management permission ("R&D approval") should be sought from all NHS organisations involved in the study in accordance with NHS research governance arrangements.

Guidance on applying for NHS permission for research is available in the Integrated Research Application System or at <http://www.rdforum.nhs.uk>.

Where a NHS organisation's role in the study is limited to identifying and referring potential participants to research sites ("participant identification centre"), guidance should be sought from the R&D office on the information it requires to give permission for this activity.

For non-NHS sites, site management permission should be obtained in accordance with the procedures of the relevant host organisation.

Sponsors are not required to notify the Committee of approvals from host organisations

Registration of Clinical Trials

All clinical trials (defined as the first four categories on the IRAS filter page) must be registered on a publically accessible database within 6 weeks of recruitment of the first participant (for medical device studies, within the timeline determined by the current registration and publication trees).

There is no requirement to separately notify the REC but you should do so at the earliest opportunity e.g when submitting an amendment. We will audit the registration details as part of the annual progress reporting process.

To ensure transparency in research, we strongly recommend that all research is registered but for non clinical trials this is not currently mandatory.

If a sponsor wishes to contest the need for registration they should contact Catherine Blewett (catherineblewett@nhs.net), the HRA does not, however, expect exceptions to be made. Guidance on where to register is provided within IRAS.

It is the responsibility of the sponsor to ensure that all the conditions are complied with before the start of the study or its initiation at a particular site (as applicable).

Ethical review of research sites

NHS sites

The favourable opinion applies to all NHS sites taking part in the study, subject to management permission being obtained from the NHS/HSC R&D office prior to the start of the study (see "Conditions of the favourable opinion" below).

Approved documents

The final list of documents reviewed and approved by the Committee is as follows:

<i>Document</i>	<i>Version</i>	<i>Date</i>
Covering letter on headed paper [Cover Letter]		04 August 2014
IRAS Checklist XML [Checklist_04082014]		04 August 2014
Letter from sponsor [Caldicott]		23 June 2014
REC Application Form [REC_Form_07072014]		07 July 2014
Research protocol or project proposal [Protocol]	1.3	03 August 2014
Summary CV for Chief Investigator (CI) [Mordi Updated CV]		
Summary CV for supervisor (student research)	1	04 July 2014

Statement of compliance

The Committee is constituted in accordance with the Governance Arrangements for Research Ethics Committees and complies fully with the Standard Operating Procedures for Research Ethics Committees in the UK.

After ethical review

Reporting requirements

The attached document “*After ethical review – guidance for researchers*” gives detailed guidance on reporting requirements for studies with a favourable opinion, including:

- Notifying substantial amendments
- Adding new sites and investigators
- Notification of serious breaches of the protocol
- Progress and safety reports
- Notifying the end of the study

The HRA website also provides guidance on these topics, which is updated in the light of changes in reporting requirements or procedures.

User Feedback

The Health Research Authority is continually striving to provide a high quality service to all applicants and sponsors. You are invited to give your view of the service you have received and the application procedure. If you wish to make your views known please use the feedback form available on the HRA website:

<http://www.hra.nhs.uk/about-the-hra/governance/quality-assurance/>

HRA Training

We are pleased to welcome researchers and R&D staff at our training days – see details at

<http://www.hra.nhs.uk/hra-training/>

14/WS/1052

Please quote this number on all correspondence

With the Committee's best wishes for the success of this project.

Yours sincerely

A handwritten signature in black ink that reads "R Galbcher". The letter "R" is large and stylized, followed by the name "Galbcher" in a cursive script.

On behalf of
Mrs Rosie Rutherford
Alternate Vice Chair

Enclosures: "After ethical review – guidance for
researchers" [\[SL-AR2\]](#)

Copy to: *Dr Catherine Sinclair, Golden Jubilee National Hospital*

Appendix 2: Protocol Submitted to Ethics Committee

Full Title: Assessment of the Clinical Utility of Cardiovascular Imaging

Short Title: The Clinical Utility of Cardiovascular MRI

Study protocol: Version 1.3

Date: 03rd August 2014

Authors

Ify Mordi, Niko Tzemos

Golden Jubilee National Hospital and Institute of Cardiovascular and Medical Sciences,
University of Glasgow.

Summary

We plan to undertake analysis of scans carried out for clinical reasons in the Golden Jubilee from 2008 to 2012.

Since 2012 there has been a cardiovascular imaging database, however consent for this does not cover scans acquired prior to this.

During each scan there is a multitude of data acquired which is additional to that required for clinical purposes and therefore not analysed in detail. Over 2000 scans have been done in this period and so there is a lot of data that could provide useful information but has not yet been studied to show its utility such as:

Regional dysfunction in patients using MRI

Prognosis of scarring in patients undergoing ICD implantation combined with other markers

Utility of stress MRI

Arterial stiffness measured by MRI and CT

Fat seen using MRI and CT in patients with prior myocardial infarction

Inflammation and scarring in patients with cardiomyopathies

Microscopic and diffuse fibrosis seen using MRI

We wish to analyse prior scans anonymously for these parameters. We plan to search the radiology system (RIS) to identify patients (via CHI number) who have had a CT or MRI, and then analyse scans in the Golden Jubilee using the in-hospital workstations. If possible we would like to use computerised record linkage (e.g. Clinical Portal, SCI store, Cathi) to check for patient deaths/adverse events.

This analysis will not require any further input from the patient (we will not be calling them or their family up), and will not impact on their care in anyway (all scans have been reported and analysed by members of the clinical team).

1. Background

The Golden Jubilee National Hospital, as the West of Scotland Regional Heart and Lung Centre, is in a unique position. Every year, thousands of scans are undertaken, specifically cardiac MRI scans. These are requested for clinical purposes to provide optimal patient care.

As an academic centre, we are also at the forefront of new imaging techniques. Because of this, many of our imaging protocols and studies have parts that are not yet well validated for clinical purposes. Both these sequences, and more routine ones that we do report for clinical reasons, could provide a wealth of information which could be useful in patient care but we are not yet aware of their significance.

Since 2011 there has been a cardiovascular imaging database in place, which allows for the prospective consent of patients undergoing clinically indicated scans for research analysis purposes. Of course, this does not cover the analysis of scans prior to this date, of which there are several hundred. We believe that not utilising and investigating this data would not only be a missed opportunity, but may also mean missing out on information which could help us (as clinicians) to provide optimal care to our patients.

2. Aim

To examine the potential clinical utility of cardiovascular MRI using the scans undertaken at the Golden Jubilee National Hospital since 2008.

3. Hypothesis

We hypothesise that advanced retrospective analysis of cardiac structure and function on MRI, with linkage to subsequent clinical outcomes will identify potential prognostic features that as yet are undefined.

4. Design and Methods

Personnel

All analysis will be undertaken by Dr Ify Mordi and Dr Niko Tzemos.

Methods

We wish to undertake analysis of MRI scans carried out since 2008. Using the radiology database, we will be able to identify (by name and CHI number) all patients who had undergone MRI scans. We will collate these details onto a database kept on the secure hospital intranet.

We will then recall these scans from the hospital MRI archive and load them onto the hospital MRI workstations, where we will undertake further analysis. This will include:

Measurement of cardiac structure and function using both ejection fraction (from cine imaging) and strain (used tagged MRI)

Measurement of areas of fibrosis (using both late gadolinium enhancement imaging and T1 mapping)

Arterial stiffness assessment (using phase contrast imaging)

Measurement of areas of myocardial injury (using T2 weighted imaging).

The results of this analysis will also be kept on this database.

Furthermore, we wish to correlate the results of our analysis with outcome. Specifically, we will look at mortality (all cause and cardiovascular), hospital admission for cardiovascular reasons (e.g. heart failure, MI), coronary revascularisation, stroke and ventricular arrhythmias. To do this, we would like to use the patient details (CHI number) to search our computer systems (Clinical Portal, SCI Store etc.) to search for these events. The patients themselves will not be contacted and will not be required to partake in any further testing. We will not include any patients who have not consented to take part in the database.

We hope that because we are looking specifically at these parameters, rather than “re-reporting” the studies, this would cause no further inconvenience to patients, and also would reduce the possibility of any new clinically significant findings being discovered.

We have a large cohort of patients. A recent paper by Gulati et al (JAMA 2013) examined the association of fibrosis measured by late gadolinium enhancement and adverse cardiovascular outcome in 472 patients with dilated cardiomyopathy and found that it provided independent prognostic information. The incidence of measured fibrosis was 30%. This is one of the largest studies to date examining this, and provides a good guide for our analysis. Our number of patients is at least as extensive, and we expect should provide us with good results.

Data sharing

Identifiable data will not be shared beyond the aforementioned staff (Drs Mordi and Tzemos) within the Golden Jubilee.

All identifiable data, including the CHI number, are restricted to NHS computers in the Golden Jubilee National Hospital. Data which are moved from this environment will be de-identified. All identifiable data will only be kept for a maximum of 24 months after analysis to allow time for publication and dissemination of studies conducted.

New or incidental findings

A main concern regarding this type of analysis is of course the discovery of incidental findings on scans which may not have been originally noted. Despite this, all of scans will have been reported initially by the imaging experts in the Golden Jubilee at the time of scanning and the reports (and relevant actions, if any) communicated to the physician responsible for the patient.

There is however the possibility that there may be a new discovery. In this case, we will discuss with the result with the clinician who initially requested the scan, and following this, arrange appropriate correspondence with the patient's GP (normally by the requesting clinician). The patient will not be directly contacted.

Protection of Patient Identity

All data will be stored on password-accessible NHS computers. Any data to be moved outside of an NHS network can only be done after anonymisation.

Arrangements for Governance

Governance

The Database Management Group (DMG) is directly responsible to the R&D Steering Group, the Caldicott Guardian of the National Waiting Times Board and the West of Scotland Research Ethics Committee. The DMG will generate a quarterly report to list the Project Requests received and approved, number of patients recruited, and also mention feedback on active projects as appropriate. This report will be submitted to the R&D Steering Group and to the NHS West Cardiovascular and Metabolic Specialty Group. The DMG will provide an annual report to the Research Ethics Committee which will summarise the information in quarterly reports.

Patient representation

The design of this project has been discussed with patients who have been treated in our hospital. In addition, the Lay Member of the R&D Steering Group will have access to the project information through this group.

References

- ABDEL-ATY, H., BOYE, P., ZAGROSEK, A., WASSMUTH, R., KUMAR, A., MESSROGHLI, D., BOCK, P., DIETZ, R., FRIEDRICH, M. G. & SCHULZ-MENGER, J. 2005. Diagnostic performance of cardiovascular magnetic resonance in patients with suspected acute myocarditis: comparison of different approaches. *J Am Coll Cardiol*, 45, 1815-22.
- ABDEL-ATY, H., ZAGROSEK, A., SCHULZ-MENGER, J., TAYLOR, A. J., MESSROGHLI, D., KUMAR, A., GROSS, M., DIETZ, R. & FRIEDRICH, M. G. 2004. Delayed enhancement and T2-weighted cardiovascular magnetic resonance imaging differentiate acute from chronic myocardial infarction. *Circulation*, 109, 2411-6.
- ABERGEL, E., CHATELLIER, G., HAGEGE, A. A., OBLAK, A., LINHART, A., DUCARDONNET, A. & MENARD, J. 2004. Serial left ventricular adaptations in world-class professional cyclists: implications for disease screening and follow-up. *J Am Coll Cardiol*, 44, 144-9.
- ADABAG, A. S., MARON, B. J., APPELBAUM, E., HARRIGAN, C. J., BUROS, J. L., GIBSON, C. M., LESSER, J. R., HANNA, C. A., UDELSON, J. E., MANNING, W. J. & MARON, M. S. 2008. Occurrence and frequency of arrhythmias in hypertrophic cardiomyopathy in relation to delayed enhancement on cardiovascular magnetic resonance. *J Am Coll Cardiol*, 51, 1369-74.
- AHN, S. S., KIM, Y. J., HUR, J., LEE, H. J., KIM, T. H., CHOE, K. O. & CHOI, B. W. 2009. CT detection of subendocardial fat in myocardial infarction. *AJR Am J Roentgenol*, 192, 532-7.
- AL-SAAD, N., GROSS, M., PAETSCH, I., SCHNACKENBURG, B., BORNSTEDT, A., FLECK, E. & NAGEL, E. 2002. Dobutamine induced myocardial perfusion reserve index with cardiovascular MR in patients with coronary artery disease. *J Cardiovasc Magn Reson*, 4, 471-80.
- ALLAM, A. H., THOMPSON, R. C., WANN, L. S., MIYAMOTO, M. I. & THOMAS, G. S. 2009. Computed tomographic assessment of atherosclerosis in ancient Egyptian mummies. *JAMA*, 302, 2091-4.
- AMERICA, Y. G., BAX, J. J., BOERSMA, E., STOKKEL, M. & VAN DER WALL, E. E. 2007. Prognostic value of gated SPECT in patients with left bundle branch block. *J Nucl Cardiol*, 14, 75-81.
- ANDERSON, L. J., WESTWOOD, M. A., HOLDEN, S., DAVIS, B., PRESCOTT, E., WONKE, B., PORTER, J. B., WALKER, J. M. & PENNELL, D. J. 2004. Myocardial iron clearance during reversal of siderotic cardiomyopathy with intravenous desferrioxamine: a prospective study using T2* cardiovascular magnetic resonance. *Br J Haematol*, 127, 348-55.
- ANTONY, R., DAGHEM, M., MCCANN, G. P., DAGHEM, S., MOON, J., PENNELL, D. J., NEUBAUER, S., DARGIE, H. J., BERRY, C., PAYNE, J., PETRIE, M. C. & HAWKINS, N. M. 2011. Cardiovascular magnetic resonance activity in the United Kingdom: a survey on behalf of the British Society of Cardiovascular Magnetic Resonance. *J Cardiovasc Magn Reson*, 13, 57.
- ARHEDEN, H., SAEED, M., HIGGINS, C. B., GAO, D. W., BREMERICH, J., WYTTENBACH, R., DAE, M. W. & WENDLAND, M. F. 1999. Measurement of the distribution volume of gadopentetate dimeglumine at echo-planar MR imaging to quantify myocardial infarction: comparison with ^{99m}Tc-DTPA autoradiography in rats. *Radiology*, 211, 698-708.
- ASHLEY, E. A., MYERS, J. & FROELICHER, V. 2000. Exercise testing in clinical medicine. *Lancet*, 356, 1592-7.
- ASSOMULL, R. G., LYNE, J. C., KEENAN, N., GULATI, A., BUNCE, N. H., DAVIES, S. W., PENNELL, D. J. & PRASAD, S. K. 2007. The role of cardiovascular magnetic resonance in patients presenting with chest pain, raised troponin, and unobstructed coronary arteries. *Eur Heart J*, 28, 1242-9.
- ASSOMULL, R. G., PRASAD, S. K., LYNE, J., SMITH, G., BURMAN, E. D., KHAN, M., SHEPPARD, M. N., POOLE-WILSON, P. A. & PENNELL, D. J. 2006. Cardiovascular magnetic resonance, fibrosis, and prognosis in dilated cardiomyopathy. *J Am Coll Cardiol*, 48, 1977-85.
- ASSOMULL, R. G., SHAKESPEARE, C., KALRA, P. R., LLOYD, G., GULATI, A., STRANGE, J., BRADLOW, W. M., LYNE, J., KEEGAN, J., POOLE-WILSON, P., COWIE, M. R.,

References

- PENNELL, D. J. & PRASAD, S. K. 2011. Role of cardiovascular magnetic resonance as a gatekeeper to invasive coronary angiography in patients presenting with heart failure of unknown etiology. *Circulation*, 124, 1351-60.
- AXEL, L. & DOUGHERTY, L. 1989. MR imaging of motion with spatial modulation of magnetization. *Radiology*, 171, 841-5.
- BADRAN, H. M., ELNOAMANY, M. F. & SETEHA, M. 2007. Tissue velocity imaging with dobutamine stress echocardiography--a quantitative technique for identification of coronary artery disease in patients with left bundle branch block. *J Am Soc Echocardiogr*, 20, 820-31.
- BAGGISH, A. L. & BOUCHER, C. A. 2008. Radiopharmaceutical agents for myocardial perfusion imaging. *Circulation*, 118, 1668-74.
- BAIG, M. K., GOLDMAN, J. H., CAFORIO, A. L., COONAR, A. S., KEELING, P. J. & MCKENNA, W. J. 1998. Familial dilated cardiomyopathy: cardiac abnormalities are common in asymptomatic relatives and may represent early disease. *J Am Coll Cardiol*, 31, 195-201.
- BARDY, G. H., LEE, K. L., MARK, D. B., POOLE, J. E., PACKER, D. L., BOINEAU, R., DOMANSKI, M., TROUTMAN, C., ANDERSON, J., JOHNSON, G., MCNULTY, S. E., CLAPP-CHANNING, N., DAVIDSON-RAY, L. D., FRAULO, E. S., FISHBEIN, D. P., LUCERI, R. M. & IP, J. H. 2005. Amiodarone or an implantable cardioverter-defibrillator for congestive heart failure. *N Engl J Med*, 352, 225-37.
- BAROLDI, G., SILVER, M. D., DE MARIA, R., PARODI, O. & PELLEGRINI, A. 1997. Lipomatous metaplasia in left ventricular scar. *Can J Cardiol*, 13, 65-71.
- BARTUNEK, J., WIJNS, W., HEYNDRICKX, G. R. & DE BRUYNE, B. 1999. Effects of dobutamine on coronary stenosis physiology and morphology: comparison with intracoronary adenosine. *Circulation*, 100, 243-9.
- BATEMAN, T. M., HELLER, G. V., MCGHIE, A. I., FRIEDMAN, J. D., CASE, J. A., BRYNGELSON, J. R., HERTENSTEIN, G. K., MOUTRAY, K. L., REID, K. & CULLOM, S. J. 2006. Diagnostic accuracy of rest/stress ECG-gated Rb-82 myocardial perfusion PET: comparison with ECG-gated Tc-99m sestamibi SPECT. *J Nucl Cardiol*, 13, 24-33.
- BAX, J. J., VISSER, F. C., POLDERMANS, D., ELHENDY, A., CORNEL, J. H., BOERSMA, E., VAN LINGEN, A., FIORETTI, P. M. & VISSER, C. A. 2001. Time course of functional recovery of stunned and hibernating segments after surgical revascularization. *Circulation*, 104, 1314-8.
- BEEK, A. M., BONDARENKO, O., AFSHARZADA, F. & VAN ROSSUM, A. C. 2009. Quantification of late gadolinium enhanced CMR in viability assessment in chronic ischemic heart disease: a comparison to functional outcome. *J Cardiovasc Magn Reson*, 11, 6.
- BELLO, D., FIENO, D. S., KIM, R. J., PERELES, F. S., PASSMAN, R., SONG, G., KADISH, A. H. & GOLDBERGER, J. J. 2005. Infarct morphology identifies patients with substrate for sustained ventricular tachycardia. *J Am Coll Cardiol*, 45, 1104-8.
- BERGER, R., HUELSMAN, M., STRECKER, K., BOJIC, A., MOSER, P., STANEK, B. & PACHER, R. 2002. B-type natriuretic peptide predicts sudden death in patients with chronic heart failure. *Circulation*, 105, 2392-7.
- BERNHARDT, P., STILLER, S., KOTTMAIR, E., BINNER, L., SPIESS, J., GROSSMANN, G., RASCHE, V., WALCHER, D. & HOMBACH, V. 2011. Myocardial scar extent evaluated by cardiac magnetic resonance imaging in ICD patients: relationship to spontaneous VT during long-term follow-up. *Int J Cardiovasc Imaging*, 27, 893-900.
- BEZERRA, H. G., ATTIZZANI, G. F., SIRBU, V., MUSUMECI, G., LORTKIPANIDZE, N., FUJINO, Y., WANG, W., NAKAMURA, S., ERGLIS, A., GUAGLIUMI, G. & COSTA, M. A. 2013. Optical coherence tomography versus intravascular ultrasound to evaluate coronary artery disease and percutaneous coronary intervention. *JACC Cardiovasc Interv*, 6, 228-36.
- BIASUCCI, L. M., BELLOCCI, F., LANDOLINA, M., RORDORF, R., VADO, A., MENARDI, E., GIUBILATO, G., ORAZI, S., SASSARA, M., CASTRO, A., MASSA, R., KHEIR, A., ZACCONE, G., KLERSY, C., ACCARDI, F. & CREA, F. 2012. Risk stratification of

References

- ischaemic patients with implantable cardioverter defibrillators by C-reactive protein and a multi-markers strategy: results of the CAMI-GUIDE study. *Eur Heart J*, 33, 1344-50.
- BINGHAM, S. E. & HACHAMOVITCH, R. 2011. Incremental prognostic significance of combined cardiac magnetic resonance imaging, adenosine stress perfusion, delayed enhancement, and left ventricular function over preimaging information for the prediction of adverse events. *Circulation*, 123, 1509-18.
- BOLICK, D. R., HACKEL, D. B., REIMER, K. A. & IDEKER, R. E. 1986. Quantitative analysis of myocardial infarct structure in patients with ventricular tachycardia. *Circulation*, 74, 1266-79.
- BONOW, R. O., MAURER, G., LEE, K. L., HOLLY, T. A., BINKLEY, P. F., DESVIGNE-NICKENS, P., DROZDZ, J., FARSKY, P. S., FELDMAN, A. M., DOENST, T., MICHLER, R. E., BERMAN, D. S., NICOLAU, J. C., PELLIKKA, P. A., WROBEL, K., ALOTTI, N., ASCH, F. M., FAVALORO, L. E., SHE, L., VELAZQUEZ, E. J., JONES, R. H. & PANZA, J. A. 2011. Myocardial viability and survival in ischemic left ventricular dysfunction. *N Engl J Med*, 364, 1617-25.
- BOUZAS-MOSQUERA, A., PETEIRO, J., ALVAREZ-GARCIA, N., BROULLON, F. J., GARCIA-BUENO, L., FERRO, L., PEREZ, R., BOUZAS, B., FABREGAS, R. & CASTRO-BEIRAS, A. 2009. Prognostic value of exercise echocardiography in patients with left bundle branch block. *JACC Cardiovasc Imaging*, 2, 251-9.
- BRISTOW, M. R., SAXON, L. A., BOEHMER, J., KRUEGER, S., KASS, D. A., DE MARCO, T., CARSON, P., DICARLO, L., DEMETS, D., WHITE, B. G., DEVRIES, D. W. & FELDMAN, A. M. 2004. Cardiac-resynchronization therapy with or without an implantable defibrillator in advanced chronic heart failure. *N Engl J Med*, 350, 2140-50.
- BRUDER, O., WAGNER, A., JENSEN, C. J., SCHNEIDER, S., ONG, P., KISPERS, E. M., NASSENSTEIN, K., SCHLOSSER, T., SABIN, G. V., SECHTEM, U. & MAHRHOLDT, H. 2010. Myocardial scar visualized by cardiovascular magnetic resonance imaging predicts major adverse events in patients with hypertrophic cardiomyopathy. *J Am Coll Cardiol*, 56, 875-87.
- BUCKBERG, G., HOFFMAN, J. I., MAHAJAN, A., SALEH, S. & COGLAN, C. 2008. Cardiac mechanics revisited: the relationship of cardiac architecture to ventricular function. *Circulation*, 118, 2571-87.
- BUDOFF, M. J., DOWE, D., JOLLIS, J. G., GITTER, M., SUTHERLAND, J., HALAMERT, E., SCHERER, M., BELLINGER, R., MARTIN, A., BENTON, R., DELAGO, A. & MIN, J. K. 2008. Diagnostic performance of 64-multidetector row coronary computed tomographic angiography for evaluation of coronary artery stenosis in individuals without known coronary artery disease: results from the prospective multicenter ACCURACY (Assessment by Coronary Computed Tomographic Angiography of Individuals Undergoing Invasive Coronary Angiography) trial. *J Am Coll Cardiol*, 52, 1724-32.
- BURNS, R. J., GALLIGAN, L., WRIGHT, L. M., LAWAND, S., BURKE, R. J. & GLADSTONE, P. J. 1991. Improved specificity of myocardial thallium-201 single-photon emission computed tomography in patients with left bundle branch block by dipyridamole. *Am J Cardiol*, 68, 504-8.
- CAFORIO, A. L., PANKUWEIT, S., ARBUSTINI, E., BASSO, C., GIMENO-BLANES, J., FELIX, S. B., FU, M., HELIO, T., HEYMANS, S., JAHNS, R., KLINGEL, K., LINHART, A., MAISCH, B., MCKENNA, W., MOGENSEN, J., PINTO, Y. M., RISTIC, A., SCHULTHEISS, H. P., SEGGEWISS, H., TAVAZZI, L., THIENE, G., YILMAZ, A., CHARRON, P. & ELLIOTT, P. M. 2013. Current state of knowledge on aetiology, diagnosis, management, and therapy of myocarditis: a position statement of the European Society of Cardiology Working Group on Myocardial and Pericardial Diseases. *Eur Heart J*, 34, 2636-48, 2648a-2648d.
- CARRICK, D., OLDROYD, K. G., MCENTEGART, M., HAIG, C., PETRIE, M. C., ETEIBA, H., HOOD, S., OWENS, C., WATKINS, S., LAYLAND, J., LINDSAY, M., PEAT, E., RAE, A., BEHAN, M., SOOD, A., HILLIS, W. S., MORDI, I., MAHROUS, A., AHMED, N., WILSON, R., LASALLE, L., GENEREUX, P., FORD, I. & BERRY, C. 2014. A randomized trial of deferred stenting versus immediate stenting to prevent no- or slow-reflow in acute ST-segment elevation myocardial infarction (DEFER-STEMI). *J Am Coll Cardiol*, 63, 2088-98.

References

- CERQUEIRA, M. D., WEISSMAN, N. J., DILSIZIAN, V., JACOBS, A. K., KAUL, S., LASKEY, W. K., PENNELL, D. J., RUMBERGER, J. A., RYAN, T. & VERANI, M. S. 2002. Standardized myocardial segmentation and nomenclature for tomographic imaging of the heart. A statement for healthcare professionals from the Cardiac Imaging Committee of the Council on Clinical Cardiology of the American Heart Association. *Circulation*, 105, 539-42.
- CHAROENPANICHKIT, C. & HUNDLEY, W. G. 2010. The 20 year evolution of dobutamine stress cardiovascular magnetic resonance. *J Cardiovasc Magn Reson*, 12, 59.
- CHEONG, B. Y., MUTHUPILLAI, R., WILSON, J. M., SUNG, A., HUBER, S., AMIN, S., ELAYDA, M. A., LEE, V. V. & FLAMM, S. D. 2009. Prognostic significance of delayed-enhancement magnetic resonance imaging: survival of 857 patients with and without left ventricular dysfunction. *Circulation*, 120, 2069-76.
- CHO, G. Y., MARWICK, T. H., KIM, H. S., KIM, M. K., HONG, K. S. & OH, D. J. 2009. Global 2-dimensional strain as a new prognosticator in patients with heart failure. *J Am Coll Cardiol*, 54, 618-24.
- CHOI, E. Y., ROSEN, B. D., FERNANDES, V. R., YAN, R. T., YONEYAMA, K., DONEKAL, S., OPDAHL, A., ALMEIDA, A. L., WU, C. O., GOMES, A. S., BLUEMKE, D. A. & LIMA, J. A. 2013. Prognostic value of myocardial circumferential strain for incident heart failure and cardiovascular events in asymptomatic individuals: the Multi-Ethnic Study of Atherosclerosis. *Eur Heart J*, 34, 2354-61.
- CHOW, B. J., ABRAHAM, A., WELLS, G. A., CHEN, L., RUDDY, T. D., YAM, Y., GOVAS, N., GALBRAITH, P. D., DENNIE, C. & BEANLANDS, R. S. 2009. Diagnostic accuracy and impact of computed tomographic coronary angiography on utilization of invasive coronary angiography. *Circ Cardiovasc Imaging*, 2, 16-23.
- DAGRES, N. & HINDRICKS, G. 2013. Risk stratification after myocardial infarction: is left ventricular ejection fraction enough to prevent sudden cardiac death? *Eur Heart J*, 34, 1964-71.
- DAMADIAN, R. 1971. Tumor detection by nuclear magnetic resonance. *Science*, 171, 1151-3.
- DASS, S., SUTTIE, J. J., PIECHNIK, S. K., FERREIRA, V. M., HOLLOWAY, C. J., BANERJEE, R., MAHMUD, M., COCHLIN, L., KARAMITSOS, T. D., ROBSON, M. D., WATKINS, H. & NEUBAUER, S. 2012. Myocardial tissue characterization using magnetic resonance noncontrast t1 mapping in hypertrophic and dilated cardiomyopathy. *Circ Cardiovasc Imaging*, 5, 726-33.
- DAVIS, A. E., LEWANDOWSKI, A. J., HOLLOWAY, C. J., NTUSI, N. A., BANERJEE, R., NETHONONDA, R., PITCHER, A., FRANCIS, J. M., MYERSON, S. G., LEESON, P., DONOVAN, T., NEUBAUER, S. & RIDER, O. J. 2014. Observational study of regional aortic size referenced to body size: production of a cardiovascular magnetic resonance nomogram. *J Cardiovasc Magn Reson*, 16, 9.
- DAWSON, D. K., HAWLISCH, K., PRESCOTT, G., ROUSSIN, I., DI PIETRO, E., DEAC, M., WONG, J., FRENNEAUX, M. P., PENNELL, D. J. & PRASAD, S. K. 2013. Prognostic role of CMR in patients presenting with ventricular arrhythmias. *JACC Cardiovasc Imaging*, 6, 335-44.
- DE BACQUER, D., DE BACKER, G., KORNTITZER, M. & BLACKBURN, H. 1998a. Prognostic value of ECG findings for total, cardiovascular disease, and coronary heart disease death in men and women. *Heart*, 80, 570-7.
- DE BACQUER, D., DE BACKER, G., KORNTITZER, M., MYNY, K., DOYEN, Z. & BLACKBURN, H. 1998b. Prognostic value of ischemic electrocardiographic findings for cardiovascular mortality in men and women. *J Am Coll Cardiol*, 32, 680-5.
- DE BRUYNE, B., PIJLS, N. H., KALESAN, B., BARBATO, E., TONINO, P. A., PIROTH, Z., JAGIC, N., MOBIUS-WINKLER, S., RIOUFOL, G., WITT, N., KALA, P., MACCARTHY, P., ENGSTROM, T., OLDROYD, K. G., MAVROMATIS, K., MANOHARAN, G., VERLEE, P., FROBERT, O., CURZEN, N., JOHNSON, J. B., JUNI, P. & FEARON, W. F. 2012. Fractional flow reserve-guided PCI versus medical therapy in stable coronary disease. *N Engl J Med*, 367, 991-1001.
- DE COBELLI, F., ESPOSITO, A., BELLONI, E., PIERONI, M., PERSEGHIN, G., CHIMENTI, C., FRUSTACI, A. & DEL MASCHIO, A. 2009. Delayed-enhanced cardiac MRI for

References

- differentiation of Fabry's disease from symmetric hypertrophic cardiomyopathy. *AJR Am J Roentgenol*, 192, W97-102.
- DE HAAN, S., MEIJERS, T. A., KNAAPEN, P., BEEK, A. M., VAN ROSSUM, A. C. & ALLAART, C. P. 2011. Scar size and characteristics assessed by CMR predict ventricular arrhythmias in ischaemic cardiomyopathy: comparison of previously validated models. *Heart*, 97, 1951-6.
- DELONG, E. R., DELONG, D. M. & CLARKE-PEARSON, D. L. 1988. Comparing the areas under two or more correlated receiver operating characteristic curves: a nonparametric approach. *Biometrics*, 44, 837-45.
- DEMIR, H., ERBAY, G., KIR, K. M., OMURLU, K., BERK, F. & AKTOLUN, C. 2003. Clinical validation of technetium-99m MIBI-gated single-photon emission computed tomography (SPECT) for avoiding false positive results in patients with left bundle-branch block: comparison with stress-rest nongated SPECT. *Clin Cardiol*, 26, 182-7.
- DEPUEY, E. G., GUERTLER-KRAWCZYNSKA, E. & ROBBINS, W. L. 1988. Thallium-201 SPECT in coronary artery disease patients with left bundle branch block. *J Nucl Med*, 29, 1479-85.
- DUNCAN, A. M., FRANCIS, D. P., GIBSON, D. G. & HENEIN, M. Y. 2003. Differentiation of ischemic from nonischemic cardiomyopathy during dobutamine stress by left ventricular long-axis function: additional effect of left bundle-branch block. *Circulation*, 108, 1214-20.
- EINSTEIN, A. J., HENZLOVA, M. J. & RAJAGOPALAN, S. 2007. Estimating risk of cancer associated with radiation exposure from 64-slice computed tomography coronary angiography. *JAMA*, 298, 317-23.
- EITEL, I., DESCH, S., FUERNAU, G., HILDEBRAND, L., GUTBERLET, M., SCHULER, G. & THIELE, H. 2010. Prognostic significance and determinants of myocardial salvage assessed by cardiovascular magnetic resonance in acute reperfused myocardial infarction. *J Am Coll Cardiol*, 55, 2470-9.
- ELHENDY, A., VAN DOMBURG, R. T., VANTRIMPONT, P., POLDERMANS, D., BAX, J. J., VAN GELDER, T., BAAN, C. C., SCHINKEL, A., ROELANDT, J. R. & BALK, A. H. 2002. Prediction of mortality in heart transplant recipients by stress technetium-99m tetrofosmin myocardial perfusion imaging. *Am J Cardiol*, 89, 964-8.
- ERIKSSON, P., HANSSON, P. O., ERIKSSON, H. & DELLBORG, M. 1998. Bundle-branch block in a general male population: the study of men born 1913. *Circulation*, 98, 2494-500.
- ERIKSSON, P., WILHELMSSEN, L. & ROSENGREN, A. 2005. Bundle-branch block in middle-aged men: risk of complications and death over 28 years. The Primary Prevention Study in Goteborg, Sweden. *Eur Heart J*, 26, 2300-6.
- EVANGELISTA, L., NAI FOVINO, L., SALADINI, F., SALADINI, G., RAZZOLINI, R., MORMINO, G. P., AL-NAHHAS, A. & RUBELLO, D. 2012. Diagnostic and prognostic value of gated myocardial perfusion single-photon emission computed tomography in low-risk patients with left bundle-branch block. *Nucl Med Commun*, 33, 491-7.
- FERREIRA, V. M., PIECHNIK, S. K., DALL'ARMELLINA, E., KARAMITSOS, T. D., FRANCIS, J. M., NTUSI, N., HOLLOWAY, C., CHOUDHURY, R. P., KARDOS, A., ROBSON, M. D., FRIEDRICH, M. G. & NEUBAUER, S. 2013. T(1) mapping for the diagnosis of acute myocarditis using CMR: comparison to T2-weighted and late gadolinium enhanced imaging. *JACC Cardiovasc Imaging*, 6, 1048-58.
- FERREIRA, V. M., PIECHNIK, S. K., DALL'ARMELLINA, E., KARAMITSOS, T. D., FRANCIS, J. M., NTUSI, N., HOLLOWAY, C., CHOUDHURY, R. P., KARDOS, A., ROBSON, M. D., FRIEDRICH, M. G. & NEUBAUER, S. 2014. Native T1-mapping detects the location, extent and patterns of acute myocarditis without the need for gadolinium contrast agents. *J Cardiovasc Magn Reson*, 16, 36.
- FIHN, S. D., GARDIN, J. M., ABRAMS, J., BERRA, K., BLANKENSHIP, J. C., DALLAS, A. P., DOUGLAS, P. S., FOODY, J. M., GERBER, T. C., HINDERLITER, A. L., KING, S. B., 3RD, KLIGFIELD, P. D., KRUMHOLZ, H. M., KWONG, R. Y., LIM, M. J., LINDERBAUM, J. A., MACK, M. J., MUNGER, M. A., PRAGER, R. L., SABIK, J. F., SHAW, L. J., SIKKEMA, J. D., SMITH, C. R., JR., SMITH, S. C., JR., SPERTUS, J. A., WILLIAMS, S. V. & ANDERSON, J. L. 2012. 2012 ACCF/AHA/ACP/AATS/PCNA/SCAI/STS guideline for the diagnosis and management

References

- of patients with stable ischemic heart disease: a report of the American College of Cardiology Foundation/American Heart Association task force on practice guidelines, and the American College of Physicians, American Association for Thoracic Surgery, Preventive Cardiovascular Nurses Association, Society for Cardiovascular Angiography and Interventions, and Society of Thoracic Surgeons. *Circulation*, 126, e354-471.
- FLETT, A. S., HASLETON, J., COOK, C., HAUSENLOY, D., QUARTA, G., ARITI, C., MUTHURANGU, V. & MOON, J. C. 2011. Evaluation of techniques for the quantification of myocardial scar of differing etiology using cardiac magnetic resonance. *JACC Cardiovasc Imaging*, 4, 150-6.
- FRANCIA, P., BALLA, C., PANENI, F. & VOLPE, M. 2007. Left bundle-branch block--pathophysiology, prognosis, and clinical management. *Clin Cardiol*, 30, 110-5.
- FRANCONE, M., CHIMENTI, C., GALEA, N., SCOPELLITI, F., VERARDO, R., GALEA, R., CARBONE, I., CATALANO, C., FEDELE, F. & FRUSTACI, A. 2014. CMR sensitivity varies with clinical presentation and extent of cell necrosis in biopsy-proven acute myocarditis. *JACC Cardiovasc Imaging*, 7, 254-63.
- FRIEDRICH, M. G., SECHTEM, U., SCHULZ-MENGER, J., HOLMVANG, G., ALAKIJA, P., COOPER, L. T., WHITE, J. A., ABDEL-ATY, H., GUTBERLET, M., PRASAD, S., ALETRAS, A., LAISSY, J. P., PATERSON, I., FILIPCHUK, N. G., KUMAR, A., PAUSCHINGER, M. & LIU, P. 2009. Cardiovascular magnetic resonance in myocarditis: A JACC White Paper. *J Am Coll Cardiol*, 53, 1475-87.
- FRYBACK, D. G. & THORNBURY, J. R. 1991. The efficacy of diagnostic imaging. *Med Decis Making*, 11, 88-94.
- GANAME, J., MESSALLI, G., DYMARKOWSKI, S., RADEMAKERS, F. E., DESMET, W., VAN DE WERF, F. & BOGAERT, J. 2009. Impact of myocardial haemorrhage on left ventricular function and remodelling in patients with reperfused acute myocardial infarction. *Eur Heart J*, 30, 1440-9.
- GAO, P., YEE, R., GULA, L., KRAHN, A. D., SKANES, A., LEONG-SIT, P., KLEIN, G. J., STIRRAT, J., FINE, N., PALLAVESHI, L., WISENBERG, G., THOMPSON, T. R., PRATO, F., DRANGOVA, M. & WHITE, J. A. 2012. Prediction of arrhythmic events in ischemic and dilated cardiomyopathy patients referred for implantable cardiac defibrillator: evaluation of multiple scar quantification measures for late gadolinium enhancement magnetic resonance imaging. *Circ Cardiovasc Imaging*, 5, 448-56.
- GARDNER, R. S., CHONG, K. S., MORTON, J. J. & MCDONAGH, T. A. 2007. A change in N-terminal pro-brain natriuretic peptide is predictive of outcome in patients with advanced heart failure. *Eur J Heart Fail*, 9, 266-71.
- GEBKER, R., JAHNKE, C., MANKA, R., HAMDAN, A., SCHNACKENBURG, B., FLECK, E. & PAETSCH, I. 2008. Additional value of myocardial perfusion imaging during dobutamine stress magnetic resonance for the assessment of coronary artery disease. *Circ Cardiovasc Imaging*, 1, 122-30.
- GELEIJNSE, M. L., VIGNA, C., KASPRZAK, J. D., RAMBALDI, R., SALVATORI, M. P., ELHENDY, A., CORNEL, J. H., FIORETTI, P. M. & ROELANDT, J. R. 2000. Usefulness and limitations of dobutamine-atropine stress echocardiography for the diagnosis of coronary artery disease in patients with left bundle branch block. A multicentre study. *Eur Heart J*, 21, 1666-73.
- GERMANO, J. J., REYNOLDS, M., ESSEBAG, V. & JOSEPHSON, M. E. 2006. Frequency and causes of implantable cardioverter-defibrillator therapies: is device therapy proarrhythmic? *Am J Cardiol*, 97, 1255-61.
- GHOSTINE, S., CAUSSIN, C., DAOUD, B., HABIS, M., PERRIER, E., PESENTI-ROSSI, D., SIGAL-CINQUALBRE, A., ANGEL, C. Y., LANCELIN, B., CAPDEROU, A. & PAUL, J. F. 2006. Non-invasive detection of coronary artery disease in patients with left bundle branch block using 64-slice computed tomography. *J Am Coll Cardiol*, 48, 1929-34.
- GIBBONS, R. J., BALADY, G. J., BEASLEY, J. W., BRICKER, J. T., DUVERNOY, W. F., FROELICHER, V. F., MARK, D. B., MARWICK, T. H., MCCALLISTER, B. D., THOMPSON, P. D., JR., WINTERS, W. L., YANOWITZ, F. G., RITCHIE, J. L., GIBBONS, R. J., CHEITLIN, M. D., EAGLE, K. A., GARDNER, T. J., GARSON, A., JR., LEWIS, R. P., O'ROURKE, R. A. & RYAN, T. J. 1997. ACC/AHA Guidelines for Exercise Testing. A report of the American College of Cardiology/American Heart

References

- Association Task Force on Practice Guidelines (Committee on Exercise Testing). *J Am Coll Cardiol*, 30, 260-311.
- GIRI, S., CHUNG, Y. C., MERCHANT, A., MIHAI, G., RAJAGOPALAN, S., RAMAN, S. V. & SIMONETTI, O. P. 2009. T2 quantification for improved detection of myocardial edema. *J Cardiovasc Magn Reson*, 11, 56.
- GOLDFARB, J. W., ROTH, M. & HAN, J. 2009. Myocardial fat deposition after left ventricular myocardial infarction: assessment by using MR water-fat separation imaging. *Radiology*, 253, 65-73.
- GORGELS, A. P., GIJSBERS, C., DE VREEDE-SWAGEMAKERS, J., LOUSBERG, A. & WELLENS, H. J. 2003. Out-of-hospital cardiac arrest--the relevance of heart failure. The Maastricht Circulatory Arrest Registry. *Eur Heart J*, 24, 1204-9.
- GREEN, J. J., BERGER, J. S., KRAMER, C. M. & SALERNO, M. 2012. Prognostic value of late gadolinium enhancement in clinical outcomes for hypertrophic cardiomyopathy. *JACC Cardiovasc Imaging*, 5, 370-7.
- GREENWOOD, J. P., MAREDA, N., YOUNGER, J. F., BROWN, J. M., NIXON, J., EVERETT, C. C., BIJSTERVELD, P., RIDGWAY, J. P., RADJENOVIC, A., DICKINSON, C. J., BALL, S. G. & PLEIN, S. 2012. Cardiovascular magnetic resonance and single-photon emission computed tomography for diagnosis of coronary heart disease (CE-MARC): a prospective trial. *Lancet*, 379, 453-60.
- GREENWOOD, J. P., YOUNGER, J. F., RIDGWAY, J. P., SIVANANTHAN, M. U., BALL, S. G. & PLEIN, S. 2007. Safety and diagnostic accuracy of stress cardiac magnetic resonance imaging vs exercise tolerance testing early after acute ST elevation myocardial infarction. *Heart*, 93, 1363-8.
- GROTHUES, F., MOON, J. C., BELLENGER, N. G., SMITH, G. S., KLEIN, H. U. & PENNELL, D. J. 2004. Interstudy reproducibility of right ventricular volumes, function, and mass with cardiovascular magnetic resonance. *Am Heart J*, 147, 218-23.
- GRUNIG, E., TASMAN, J. A., KUCHERER, H., FRANZ, W., KUBLER, W. & KATUS, H. A. 1998. Frequency and phenotypes of familial dilated cardiomyopathy. *J Am Coll Cardiol*, 31, 186-94.
- GULATI, A., JABBOUR, A., ISMAIL, T. F., GUHA, K., KHWAJA, J., RAZA, S., MORARJI, K., BROWN, T. D., ISMAIL, N. A., DWECK, M. R., DI PIETRO, E., ROUGHTON, M., WAGE, R., DARYANI, Y., O'HANLON, R., SHEPPARD, M. N., ALPENDURADA, F., LYON, A. R., COOK, S. A., COWIE, M. R., ASSOMULL, R. G., PENNELL, D. J. & PRASAD, S. K. 2013. Association of fibrosis with mortality and sudden cardiac death in patients with nonischemic dilated cardiomyopathy. *JAMA*, 309, 896-908.
- GUSTAFSSON, F., TORP-PEDERSEN, C., BRENDORP, B., SEIBAEK, M., BURCHARDT, H. & KOBER, L. 2003. Long-term survival in patients hospitalized with congestive heart failure: relation to preserved and reduced left ventricular systolic function. *Eur Heart J*, 24, 863-70.
- HACHAMOVITCH, R., BERMAN, D. S., SHAW, L. J., KIAT, H., COHEN, I., CABICO, J. A., FRIEDMAN, J. & DIAMOND, G. A. 1998. Incremental prognostic value of myocardial perfusion single photon emission computed tomography for the prediction of cardiac death: differential stratification for risk of cardiac death and myocardial infarction. *Circulation*, 97, 535-43.
- HACHAMOVITCH, R. & DI CARLI, M. F. 2008. Methods and limitations of assessing new noninvasive tests: Part II: Outcomes-based validation and reliability assessment of noninvasive testing. *Circulation*, 117, 2793-801.
- HAMM, C. W., BASSAND, J. P., AGEWALL, S., BAX, J., BOERSMA, E., BUENO, H., CASO, P., DUDEK, D., GIELEN, S., HUBER, K., OHMAN, M., PETRIE, M. C., SONNTAG, F., UVA, M. S., STOREY, R. F., WIJNS, W. & ZAHGER, D. 2011. ESC Guidelines for the management of acute coronary syndromes in patients presenting without persistent ST-segment elevation: The Task Force for the management of acute coronary syndromes (ACS) in patients presenting without persistent ST-segment elevation of the European Society of Cardiology (ESC). *Eur Heart J*, 32, 2999-3054.
- HANSEN, C. L., KULKARNI, P. V., UGOLINI, V. & CORBETT, J. R. 1995. Detection of alterations in left ventricular fatty acid metabolism in patients with acute myocardial

References

- infarction by 15-(p-123I-phenyl)-pentadecanoic acid and tomographic imaging. *Am Heart J*, 129, 476-81.
- HARDARSON, T., ARNASON, A., ELIASSON, G. J., PALSSON, K., EYJOLFSSON, K. & SIGFUSSON, N. 1987. Left bundle branch block: prevalence, incidence, follow-up and outcome. *Eur Heart J*, 8, 1075-9.
- HARRIGAN, C. J., APPELBAUM, E., MARON, B. J., BUROS, J. L., GIBSON, C. M., LESSER, J. R., UDELSON, J. E., MANNING, W. J. & MARON, M. S. 2008. Significance of papillary muscle abnormalities identified by cardiovascular magnetic resonance in hypertrophic cardiomyopathy. *Am J Cardiol*, 101, 668-73.
- HAYAT, S. A., DWIVEDI, G., JACOBSEN, A., LIM, T. K., KINSEY, C. & SENIOR, R. 2008. Effects of left bundle-branch block on cardiac structure, function, perfusion, and perfusion reserve: implications for myocardial contrast echocardiography versus radionuclide perfusion imaging for the detection of coronary artery disease. *Circulation*, 117, 1832-41.
- HEISS, H. W. 1992. Werner Forssmann: a German problem with the Nobel Prize. *Clin Cardiol*, 15, 547-9.
- HIGGINS, J. P., WILLIAMS, G., NAGEL, J. S. & HIGGINS, J. A. 2006. Left bundle-branch block artifact on single photon emission computed tomography with technetium Tc 99m (Tc-99m) agents: mechanisms and a method to decrease false-positive interpretations. *Am Heart J*, 152, 619-26.
- HOFFMANN, R., VON BARDELEBEN, S., TEN CATE, F., BORGES, A. C., KASPRZAK, J., FIRSCHKE, C., LAFITTE, S., AL-SAAD, N., KUNTZ-HEHNER, S., ENGELHARDT, M., BECHER, H. & VANOVERSHELDE, J. L. 2005. Assessment of systolic left ventricular function: a multi-centre comparison of cineventriculography, cardiac magnetic resonance imaging, unenhanced and contrast-enhanced echocardiography. *Eur Heart J*, 26, 607-16.
- HOU, Z. H., LU, B., GAO, Y., JIANG, S. L., WANG, Y., LI, W. & BUDOFF, M. J. 2012. Prognostic value of coronary CT angiography and calcium score for major adverse cardiac events in outpatients. *JACC Cardiovasc Imaging*, 5, 990-9.
- HUEPER, K., ZAPF, A., SKROK, J., PINHEIRO, A., GOLDSTEIN, T. A., ZHENG, J., ZIMMERMAN, S. L., KAMEL, I. R., ABRAHAM, R., WACKER, F., BLUEMKE, D. A., ABRAHAM, T. & VOGEL-CLAUSSEN, J. 2012. In hypertrophic cardiomyopathy reduction of relative resting myocardial blood flow is related to late enhancement, T2-signal and LV wall thickness. *PLoS One*, 7, e41974.
- HURST, J. W. 1998. Naming of the waves in the ECG, with a brief account of their genesis. *Circulation*, 98, 1937-42.
- HUSSAIN, S. T., PAUL, M., PLEIN, S., MCCANN, G. P., SHAH, A. M., MARBER, M. S., CHIRIBIRI, A., MORTON, G., REDWOOD, S., MACCARTHY, P., SCHUSTER, A., ISHIDA, M., WESTWOOD, M. A., PERERA, D. & NAGEL, E. 2012. Design and rationale of the MR-INFORM study: stress perfusion cardiovascular magnetic resonance imaging to guide the management of patients with stable coronary artery disease. *J Cardiovasc Magn Reson*, 14, 65.
- IBRAHIM EL, S. H. 2011. Myocardial tagging by cardiovascular magnetic resonance: evolution of techniques--pulse sequences, analysis algorithms, and applications. *J Cardiovasc Magn Reson*, 13, 36.
- ICHIKAWA, Y., KITAGAWA, K., CHINO, S., ISHIDA, M., MATSUOKA, K., TANIGAWA, T., NAKAMURA, T., HIRANO, T., TAKEDA, K. & SAKUMA, H. 2009. Adipose tissue detected by multislice computed tomography in patients after myocardial infarction. *JACC Cardiovasc Imaging*, 2, 548-55.
- ILES, L., PFLUGER, H., LEFKOVITS, L., BUTLER, M. J., KISTLER, P. M., KAYE, D. M. & TAYLOR, A. J. 2011. Myocardial fibrosis predicts appropriate device therapy in patients with implantable cardioverter-defibrillators for primary prevention of sudden cardiac death. *J Am Coll Cardiol*, 57, 821-8.
- IMBRIACO, M., PISANI, A., SPINELLI, L., CUOCOLO, A., MESSALLI, G., CAPUANO, E., MARMO, M., LIUZZI, R., VISCIANO, B., CIANCIARUSO, B. & SALVATORE, M. 2009. Effects of enzyme-replacement therapy in patients with Anderson-Fabry disease: a prospective long-term cardiac magnetic resonance imaging study. *Heart*, 95, 1103-7.

References

- INANIR, S., CAYMAZ, O., OKAY, T., DEDE, F., OKTAY, A., DEGER, M. & TURGUT TUROGLU, H. 2001. Tc-99m sestamibi gated SPECT in patients with left bundle branch block. *Clin Nucl Med*, 26, 840-6.
- INNOCENTI, F., TOTTI, A., BARONCINI, C., FATTIROLI, F., BURGISSER, C. & PINI, R. 2011. Prognostic value of dobutamine stress echocardiography in octogenarians. *Int J Cardiovasc Imaging*, 27, 65-74.
- IRWIN, R. B., NEWTON, T., PEEBLES, C., BORG, A., CLARK, D., MILLER, C., ABIDIN, N., GREAVES, M. & SCHMITT, M. 2013. Incidental extra-cardiac findings on clinical CMR. *Eur Heart J Cardiovasc Imaging*, 14, 158-66.
- ISKANDRIAN, A. E. 2006. Detecting coronary artery disease in left bundle branch block. *J Am Coll Cardiol*, 48, 1935-7.
- JEEVANANTHAM, V., MANNE, K., SENGODAN, M., HALEY, J. M. & HSI, D. H. 2009. Predictors of coronary artery disease in patients with left bundle branch block who undergo myocardial perfusion imaging. *Cardiol J*, 16, 321-6.
- JENKINS, C., BRICKNELL, K., HANEKOM, L. & MARWICK, T. H. 2004. Reproducibility and accuracy of echocardiographic measurements of left ventricular parameters using real-time three-dimensional echocardiography. *J Am Coll Cardiol*, 44, 878-86.
- KARAMITSOS, T. D., DALL'ARMELLINA, E., CHOUDHURY, R. P. & NEUBAUER, S. 2011. Ischemic heart disease: comprehensive evaluation by cardiovascular magnetic resonance. *Am Heart J*, 162, 16-30.
- KARAVIDAS, A. I., MATSAKAS, E. P., LAZAROS, G. A., BRESTAS, P. S., AVRAMIDIS, D. A., ZACHAROULIS, A. A., FOTIADIS, I. N., KORRES, D. A. & ZACHAROULIS, A. A. 2006. Comparison of myocardial contrast echocardiography with SPECT in the evaluation of coronary artery disease in asymptomatic patients with LBBB. *Int J Cardiol*, 112, 334-40.
- KELLE, S., ROES, S. D., KLEIN, C., KOKOCINSKI, T., DE ROOS, A., FLECK, E., BAX, J. J. & NAGEL, E. 2009. Prognostic value of myocardial infarct size and contractile reserve using magnetic resonance imaging. *J Am Coll Cardiol*, 54, 1770-7.
- KELLMAN, P., ARAI, A. E. & XUE, H. 2013. T1 and extracellular volume mapping in the heart: estimation of error maps and the influence of noise on precision. *J Cardiovasc Magn Reson*, 15, 56.
- KIM, R. J., WU, E., RAFAEL, A., CHEN, E. L., PARKER, M. A., SIMONETTI, O., KLOCKE, F. J., BONOW, R. O. & JUDD, R. M. 2000. The use of contrast-enhanced magnetic resonance imaging to identify reversible myocardial dysfunction. *N Engl J Med*, 343, 1445-53.
- KIRK, P., ROUGHTON, M., PORTER, J. B., WALKER, J. M., TANNER, M. A., PATEL, J., WU, D., TAYLOR, J., WESTWOOD, M. A., ANDERSON, L. J. & PENNELL, D. J. 2009. Cardiac T2* magnetic resonance for prediction of cardiac complications in thalassemia major. *Circulation*, 120, 1961-8.
- KLEM, I., WEINSAFT, J. W., BAHNSON, T. D., HEGLAND, D., KIM, H. W., HAYES, B., PARKER, M. A., JUDD, R. M. & KIM, R. J. 2012. Assessment of myocardial scarring improves risk stratification in patients evaluated for cardiac defibrillator implantation. *J Am Coll Cardiol*, 60, 408-20.
- KLUG, G., MAYR, A., SCHENK, S., ESTERHAMMER, R., SCHOCKE, M., NOCKER, M., JASCHKE, W., PACHINGER, O. & METZLER, B. 2012. Prognostic value at 5 years of microvascular obstruction after acute myocardial infarction assessed by cardiovascular magnetic resonance. *J Cardiovasc Magn Reson*, 14, 46.
- KO, B. S., CAMERON, J. D., LEUNG, M., MEREDITH, I. T., LEONG, D. P., ANTONIS, P. R., CROSSETT, M., TROUPIS, J., HARPER, R., MALAIAPAN, Y. & SENEVIRATNE, S. K. 2012a. Combined CT coronary angiography and stress myocardial perfusion imaging for hemodynamically significant stenoses in patients with suspected coronary artery disease: a comparison with fractional flow reserve. *JACC Cardiovasc Imaging*, 5, 1097-111.
- KO, B. S., CAMERON, J. D., MEREDITH, I. T., LEUNG, M., ANTONIS, P. R., NASIS, A., CROSSETT, M., HOPE, S. A., LEHMAN, S. J., TROUPIS, J., DEFRANCE, T. & SENEVIRATNE, S. K. 2012b. Computed tomography stress myocardial perfusion

References

- imaging in patients considered for revascularization: a comparison with fractional flow reserve. *Eur Heart J*, 33, 67-77.
- KOEPFLI, P., WYSS, C. A., GAEMPERLI, O., SIEGRIST, P. T., KLAINGUTI, M., SCHEPIS, T., NAMDAR, M., BECHIR, M., HOEFFLINGHAUS, T., DURU, F. & KAUFMANN, P. A. 2009. Left bundle branch block causes relative but not absolute septal underperfusion during exercise. *Eur Heart J*, 30, 2993-9.
- KONSTAM, M. A. 2008. Patterns of ventricular remodeling after myocardial infarction: clues toward linkage between mechanism and morbidity. *JACC Cardiovasc Imaging*, 1, 592-4.
- KOO, B. K., ERGLIS, A., DOH, J. H., DANIELS, D. V., JEGERE, S., KIM, H. S., DUNNING, A., DEFRANCE, T., LANSKY, A., LEIPSIC, J. & MIN, J. K. 2011. Diagnosis of ischemia-causing coronary stenoses by noninvasive fractional flow reserve computed from coronary computed tomographic angiograms. Results from the prospective multicenter DISCOVER-FLOW (Diagnosis of Ischemia-Causing Stenoses Obtained Via Noninvasive Fractional Flow Reserve) study. *J Am Coll Cardiol*, 58, 1989-97.
- KOROSOGLOU, G., LEHRKE, S., WOCHLE, A., HOERIG, B., LOSSNITZER, D., STEEN, H., GIANNITSIS, E., OSMAN, N. F. & KATUS, H. A. 2010. Strain-encoded CMR for the detection of inducible ischemia during intermediate stress. *JACC Cardiovasc Imaging*, 3, 361-71.
- KRAIGHER-KRAINER, E., SHAH, A. M., GUPTA, D. K., SANTOS, A., CLAGGETT, B., PIESKE, B., ZILE, M. R., VOORS, A. A., LEFKOWITZ, M. P., PACKER, M., MCMURRAY, J. J. & SOLOMON, S. D. 2014. Impaired systolic function by strain imaging in heart failure with preserved ejection fraction. *J Am Coll Cardiol*, 63, 447-56.
- KRAMER, C. M., CHANDRASHEKHAR, Y. & NARULA, J. 2013. T1 mapping by CMR in cardiomyopathy: a noninvasive myocardial biopsy? *JACC Cardiovasc Imaging*, 6, 532-4.
- KRITTAYAPHONG, R., SAIVIROONPORN, P., BOONYASIRINANT, T. & UDOMPUNTURAK, S. 2011. Prevalence and prognosis of myocardial scar in patients with known or suspected coronary artery disease and normal wall motion. *J Cardiovasc Magn Reson*, 13, 2.
- KUIJPERS, D., HO, K. Y., VAN DIJKMAN, P. R., VLIEGENTHART, R. & OUDKERK, M. 2003. Dobutamine cardiovascular magnetic resonance for the detection of myocardial ischemia with the use of myocardial tagging. *Circulation*, 107, 1592-7.
- KURUVILLA, S., ADENAW, N., KATWAL, A. B., LIPINSKI, M. J., KRAMER, C. M. & SALERNO, M. 2014. Late gadolinium enhancement on cardiac magnetic resonance predicts adverse cardiovascular outcomes in nonischemic cardiomyopathy: a systematic review and meta-analysis. *Circ Cardiovasc Imaging*, 7, 250-8.
- KWON, D. H., HALLEY, C. M., CARRIGAN, T. P., ZYSEK, V., POPOVIC, Z. B., SETSER, R., SCHOENHAGEN, P., STARLING, R. C., FLAMM, S. D. & DESAI, M. Y. 2009. Extent of left ventricular scar predicts outcomes in ischemic cardiomyopathy patients with significantly reduced systolic function: a delayed hyperenhancement cardiac magnetic resonance study. *JACC Cardiovasc Imaging*, 2, 34-44.
- KWON, D. H., SETSER, R. M., THAMILARASAN, M., POPOVIC, Z. V., SMEDIRA, N. G., SCHOENHAGEN, P., GARCIA, M. J., LEVER, H. M. & DESAI, M. Y. 2008. Abnormal papillary muscle morphology is independently associated with increased left ventricular outflow tract obstruction in hypertrophic cardiomyopathy. *Heart*, 94, 1295-301.
- KWONG, R. Y., CHAN, A. K., BROWN, K. A., CHAN, C. W., REYNOLDS, H. G., TSANG, S. & DAVIS, R. B. 2006. Impact of unrecognized myocardial scar detected by cardiac magnetic resonance imaging on event-free survival in patients presenting with signs or symptoms of coronary artery disease. *Circulation*, 113, 2733-43.
- KWONG, R. Y., SCHUSSHEIM, A. E., REKHRAJ, S., ALETRAS, A. H., GELLER, N., DAVIS, J., CHRISTIAN, T. F., BALABAN, R. S. & ARAI, A. E. 2003. Detecting acute coronary syndrome in the emergency department with cardiac magnetic resonance imaging. *Circulation*, 107, 531-7.
- LA GERCHE, A., TAYLOR, A. J. & PRIOR, D. L. 2009. Athlete's heart: the potential for multimodality imaging to address the critical remaining questions. *JACC Cardiovasc Imaging*, 2, 350-63.
- LAMOUNIER-ZEPTEP, V., LOOK, C., ALVAREZ, J., CHRIST, T., RAVENS, U., SCHUNCK, W. H., EHRHART-BORNSTEIN, M., BORNSTEIN, S. R. & MORANO, I. 2009.

References

- Adipocyte fatty acid-binding protein suppresses cardiomyocyte contraction: a new link between obesity and heart disease. *Circ Res*, 105, 326-34.
- LEE, D. S., KRAHN, A. D., HEALEY, J. S., BIRNIE, D., CRYSTAL, E., DORIAN, P., SIMPSON, C. S., KHAYKIN, Y., CAMERON, D., JANMOHAMED, A., YEE, R., AUSTIN, P. C., CHEN, Z., HARDY, J. & TU, J. V. 2010. Evaluation of early complications related to De Novo cardioverter defibrillator implantation insights from the Ontario ICD database. *J Am Coll Cardiol*, 55, 774-82.
- LEWIS, W. R., GANIM, R. & SABAPATHY, R. 2007. Utility of stress echocardiography in identifying significant coronary artery disease in patients with left bundle-branch block. *Crit Pathw Cardiol*, 6, 127-30.
- LIKOFF, M. J., CHANDLER, S. L. & KAY, H. R. 1987. Clinical determinants of mortality in chronic congestive heart failure secondary to idiopathic dilated or to ischemic cardiomyopathy. *Am J Cardiol*, 59, 634-8.
- LINDNER, O., VOGT, J., BALLER, D., KAMMEIER, A., WIELEPP, P., HOLZINGER, J., LAMP, B., HORSTKOTTE, D. & BURCHERT, W. 2005. Global and regional myocardial oxygen consumption and blood flow in severe cardiomyopathy with left bundle branch block. *Eur J Heart Fail*, 7, 225-30.
- LIPINSKI, M. J., MCVEY, C. M., BERGER, J. S., KRAMER, C. M. & SALERNO, M. 2013. Prognostic value of stress cardiac magnetic resonance imaging in patients with known or suspected coronary artery disease: a systematic review and meta-analysis. *J Am Coll Cardiol*, 62, 826-38.
- LIU, C. Y., LIU, Y. C., WU, C., ARMSTRONG, A., VOLPE, G. J., VAN DER GEEST, R. J., LIU, Y., HUNDLEY, W. G., GOMES, A. S., LIU, S., NACIF, M., BLUEMKE, D. A. & LIMA, J. A. 2013. Evaluation of age-related interstitial myocardial fibrosis with cardiac magnetic resonance contrast-enhanced T1 mapping: MESA (Multi-Ethnic Study of Atherosclerosis). *J Am Coll Cardiol*, 62, 1280-7.
- LUBBERS, D. D., JANSSEN, C. H., KUIJPERS, D., VAN DIJKMAN, P. R., OVERBOSCH, J., WILLEMS, T. P. & OUDKERK, M. 2008. The additional value of first pass myocardial perfusion imaging during peak dose of dobutamine stress cardiac MRI for the detection of myocardial ischemia. *Int J Cardiovasc Imaging*, 24, 69-76.
- LUCKE, C., SCHINDLER, K., LEHMKUHL, L., GROTHOFF, M., EITEL, I., SCHULER, G., THIELE, H., KIVELITZ, D. & GUTBERLET, M. 2010. Prevalence and functional impact of lipomatous metaplasia in scar tissue following myocardial infarction evaluated by MRI. *Eur Radiol*, 20, 2074-83.
- LURZ, P., EITEL, I., ADAM, J., STEINER, J., GROTHOFF, M., DESCH, S., FUERNAU, G., DE WAHA, S., SAREBAN, M., LUECKE, C., KLINGEL, K., KANDOLF, R., SCHULER, G., GUTBERLET, M. & THIELE, H. 2012. Diagnostic performance of CMR imaging compared with EMB in patients with suspected myocarditis. *JACC Cardiovasc Imaging*, 5, 513-24.
- MACEIRA, A. M., JOSHI, J., PRASAD, S. K., MOON, J. C., PERUGINI, E., HARDING, I., SHEPPARD, M. N., POOLE-WILSON, P. A., HAWKINS, P. N. & PENNELL, D. J. 2005. Cardiovascular magnetic resonance in cardiac amyloidosis. *Circulation*, 111, 186-93.
- MAHMUD, M., KARAMITSOS, T. D., SUTTIE, J. J., MYERSON, S. G., NEUBAUER, S. & FRANCIS, J. M. 2012. Prevalence of cardiomyopathy in asymptomatic patients with left bundle branch block referred for cardiovascular magnetic resonance imaging. *Int J Cardiovasc Imaging*, 28, 1133-40.
- MAHRHOLDT, H., WAGNER, A., JUDD, R. M., SECHTEM, U. & KIM, R. J. 2005a. Delayed enhancement cardiovascular magnetic resonance assessment of non-ischaemic cardiomyopathies. *Eur Heart J*, 26, 1461-74.
- MAHRHOLDT, H., ZHYDKOV, A., HAGER, S., MEINHARDT, G., VOGELSBERG, H., WAGNER, A. & SECHTEM, U. 2005b. Left ventricular wall motion abnormalities as well as reduced wall thickness can cause false positive results of routine SPECT perfusion imaging for detection of myocardial infarction. *Eur Heart J*, 26, 2127-35.
- MAIRESSE, G. H., MARWICK, T. H., ARNESE, M., VANOVERSCHELDE, J. L., CORNEL, J. H., DETRY, J. M., MELIN, J. A. & FIORETTI, P. M. 1995. Improved identification of coronary artery disease in patients with left bundle branch block by use of dobutamine

References

- stress echocardiography and comparison with myocardial perfusion tomography. *Am J Cardiol*, 76, 321-5.
- MAISEL, A., MUELLER, C., ADAMS, K., JR., ANKER, S. D., ASPROMONTE, N., CLELAND, J. G., COHEN-SOLAL, A., DAHLSTROM, U., DEMARIA, A., DI SOMMA, S., FILIPPATOS, G. S., FONAROW, G. C., JOURDAIN, P., KOMAJDA, M., LIU, P. P., MCDONAGH, T., MCDONALD, K., MEBAZAA, A., NIEMINEN, M. S., PEACOCK, W. F., TUBARO, M., VALLE, R., VANDERHYDEN, M., YANCY, C. W., ZANNAD, F. & BRAUNWALD, E. 2008. State of the art: using natriuretic peptide levels in clinical practice. *Eur J Heart Fail*, 10, 824-39.
- MAKIKALLIO, T. H., BARTHEL, P., SCHNEIDER, R., BAUER, A., TAPANAINEN, J. M., TULPPO, M. P., SCHMIDT, G. & HUIKURI, H. V. 2005. Prediction of sudden cardiac death after acute myocardial infarction: role of Holter monitoring in the modern treatment era. *Eur Heart J*, 26, 762-9.
- MARON, B. J. & PELLICCIA, A. 2006. The heart of trained athletes: cardiac remodeling and the risks of sports, including sudden death. *Circulation*, 114, 1633-44.
- MARON, B. J., PELLICCIA, A. & SPIRITO, P. 1995. Cardiac disease in young trained athletes. Insights into methods for distinguishing athlete's heart from structural heart disease, with particular emphasis on hypertrophic cardiomyopathy. *Circulation*, 91, 1596-601.
- MARON, M. S., APPELBAUM, E., HARRIGAN, C. J., BUROS, J., GIBSON, C. M., HANNA, C., LESSER, J. R., UDELSON, J. E., MANNING, W. J. & MARON, B. J. 2008. Clinical profile and significance of delayed enhancement in hypertrophic cardiomyopathy. *Circ Heart Fail*, 1, 184-91.
- MARON, M. S., MARON, B. J., HARRIGAN, C., BUROS, J., GIBSON, C. M., OLIVOTTO, I., BILLER, L., LESSER, J. R., UDELSON, J. E., MANNING, W. J. & APPELBAUM, E. 2009. Hypertrophic cardiomyopathy phenotype revisited after 50 years with cardiovascular magnetic resonance. *J Am Coll Cardiol*, 54, 220-8.
- MARWICK, T. H. 2003. Stress echocardiography. *Heart*, 89, 113-8.
- MARWICK, T. H. 2006. Measurement of strain and strain rate by echocardiography: ready for prime time? *J Am Coll Cardiol*, 47, 1313-27.
- MASOLI, O., BALINO, N. P., SABATE, D., JALON, J., MERETTA, A., CRAGNOLINO, D., SARMIENTO, R. & DICARLI, M. F. 2000. Effect of endothelial dysfunction on regional perfusion in myocardial territories supplied by normal and diseased vessels in patients with coronary artery disease. *J Nucl Cardiol*, 7, 199-204.
- MASSON, S., LATINI, R., ANAND, I. S., BARLERA, S., ANGELICI, L., VAGO, T., TOGNONI, G. & COHN, J. N. 2008. Prognostic value of changes in N-terminal pro-brain natriuretic peptide in Val-HeFT (Valsartan Heart Failure Trial). *J Am Coll Cardiol*, 52, 997-1003.
- MAVROGENI, S., PETROU, E., KOLOVOU, G., THEODORAKIS, G. & ILIODROMITIS, E. 2013. Prediction of ventricular arrhythmias using cardiovascular magnetic resonance. *Eur Heart J Cardiovasc Imaging*, 14, 518-25.
- MCCROHON, J. A., MOON, J. C., PRASAD, S. K., MCKENNA, W. J., LORENZ, C. H., COATS, A. J. & PENNELL, D. J. 2003. Differentiation of heart failure related to dilated cardiomyopathy and coronary artery disease using gadolinium-enhanced cardiovascular magnetic resonance. *Circulation*, 108, 54-9.
- MCMURRAY, J. J., ADAMOPOULOS, S., ANKER, S. D., AURICCHIO, A., BOHM, M., DICKSTEIN, K., FALK, V., FILIPPATOS, G., FONSECA, C., GOMEZ-SANCHEZ, M. A., JAARSMA, T., KOBER, L., LIP, G. Y., MAGGIONI, A. P., PARKHOMENKO, A., PIESKE, B. M., POPESCU, B. A., RONNEVIK, P. K., RUTTEN, F. H., SCHWITTER, J., SEFEROVIC, P., STEPINSKA, J., TRINDADE, P. T., VOORS, A. A., ZANNAD, F. & ZEIHNER, A. 2012. ESC Guidelines for the diagnosis and treatment of acute and chronic heart failure 2012: The Task Force for the Diagnosis and Treatment of Acute and Chronic Heart Failure 2012 of the European Society of Cardiology. Developed in collaboration with the Heart Failure Association (HFA) of the ESC. *Eur Heart J*, 33, 1787-847.
- MEHDIRAD, A. A., NELSON, S. D., LOVE, C. J., SCHAAL, S. F. & TCHOU, P. J. 1998. QRS duration widening: reduced synchronization of endocardial activation or transseptal conduction time? *Pacing Clin Electrophysiol*, 21, 1589-94.

References

- MEIJBOOM, W. B., MEIJS, M. F., SCHUIJF, J. D., CRAMER, M. J., MOLLET, N. R., VAN MIEGHEM, C. A., NIEMAN, K., VAN WERKHOVEN, J. M., PUNDZIUTE, G., WEUSTINK, A. C., DE VOS, A. M., PUGLIESE, F., RENSING, B., JUKEMA, J. W., BAX, J. J., PROKOP, M., DOEVENDANS, P. A., HUNINK, M. G., KRESTIN, G. P. & DE FEYTER, P. J. 2008. Diagnostic accuracy of 64-slice computed tomography coronary angiography: a prospective, multicenter, multivendor study. *J Am Coll Cardiol*, 52, 2135-44.
- MEIJBOOM, W. B., VAN MIEGHEM, C. A., MOLLET, N. R., PUGLIESE, F., WEUSTINK, A. C., VAN PELT, N., CADEMARTIRI, F., NIEMAN, K., BOERSMA, E., DE JAEGERE, P., KRESTIN, G. P. & DE FEYTER, P. J. 2007. 64-slice computed tomography coronary angiography in patients with high, intermediate, or low pretest probability of significant coronary artery disease. *J Am Coll Cardiol*, 50, 1469-75.
- MESSROGLI, D. R., RADJENOVIC, A., KOZERKE, S., HIGGINS, D. M., SIVANANTHAN, M. U. & RIDGWAY, J. P. 2004. Modified Look-Locker inversion recovery (MOLLI) for high-resolution T1 mapping of the heart. *Magn Reson Med*, 52, 141-6.
- MEWTON, N., LIU, C. Y., CROISILLE, P., BLUEMKE, D. & LIMA, J. A. 2011. Assessment of myocardial fibrosis with cardiovascular magnetic resonance. *J Am Coll Cardiol*, 57, 891-903.
- MILLER, C. A., NAISH, J. H., BISHOP, P., COUTTS, G., CLARK, D., ZHAO, S., RAY, S. G., YONAN, N., WILLIAMS, S. G., FLETT, A. S., MOON, J. C., GREISER, A., PARKER, G. J. & SCHMITT, M. 2013. Comprehensive validation of cardiovascular magnetic resonance techniques for the assessment of myocardial extracellular volume. *Circ Cardiovasc Imaging*, 6, 373-83.
- MILLER, J. M., ROCHITTE, C. E., DEWEY, M., ARBAB-ZADEH, A., NINUMA, H., GOTTLIEB, I., PAUL, N., CLOUSE, M. E., SHAPIRO, E. P., HOE, J., LARDO, A. C., BUSH, D. E., DE ROOS, A., COX, C., BRINKER, J. & LIMA, J. A. 2008. Diagnostic performance of coronary angiography by 64-row CT. *N Engl J Med*, 359, 2324-36.
- MOHLENKAMP, S., LEHMANN, N., BREUCKMANN, F., BROCKER-PREUSS, M., NASSENSTEIN, K., HALLE, M., BUDDE, T., MANN, K., BARKHAUSEN, J., HEUSCH, G., JOCKEL, K. H. & ERBEL, R. 2008. Running: the risk of coronary events : Prevalence and prognostic relevance of coronary atherosclerosis in marathon runners. *Eur Heart J*, 29, 1903-10.
- MONTALESCOT, G., SECHTEM, U., ACHENBACH, S., ANDREOTTI, F., ARDEN, C., BUDAJ, A., BUGIARDINI, R., CREA, F., CUISSET, T., DI MARIO, C., FERREIRA, J. R., GERSH, B. J., GITT, A. K., HULOT, J. S., MARX, N., OPIE, L. H., PFISTERER, M., PRESCOTT, E., RUSCHITZKA, F., SABATE, M., SENIOR, R., TAGGART, D. P., VAN DER WALL, E. E., VRINTS, C. J., ZAMORANO, J. L., ACHENBACH, S., BAUMGARTNER, H., BAX, J. J., BUENO, H., DEAN, V., DEATON, C., EROL, C., FAGARD, R., FERRARI, R., HASDAI, D., HOES, A. W., KIRCHHOF, P., KNUUTI, J., KOLH, P., LANCELLOTTI, P., LINHART, A., NIHOYANNOPOULOS, P., PIEPOLI, M. F., PONIKOWSKI, P., SIRNES, P. A., TAMARGO, J. L., TENDERA, M., TORBICKI, A., WIJNS, W., WINDECKER, S., KNUUTI, J., VALGIMIGLI, M., BUENO, H., CLAEYS, M. J., DONNER-BANZHOF, N., EROL, C., FRANK, H., FUNCK-BRENTANO, C., GAEMPERLI, O., GONZALEZ-JUANATEY, J. R., HAMILOS, M., HASDAI, D., HUSTED, S., JAMES, S. K., KERVINEN, K., KOLH, P., KRISTENSEN, S. D., LANCELLOTTI, P., MAGGIONI, A. P., PIEPOLI, M. F., PRIES, A. R., ROMEO, F., RYDEN, L., SIMOONS, M. L., SIRNES, P. A., STEG, P. G., TIMMIS, A., WIJNS, W., WINDECKER, S., YILDIRIR, A. & ZAMORANO, J. L. 2013. 2013 ESC guidelines on the management of stable coronary artery disease: the Task Force on the management of stable coronary artery disease of the European Society of Cardiology. *Eur Heart J*, 34, 2949-3003.
- MOON, J. C., FISHER, N. G., MCKENNA, W. J. & PENNELL, D. J. 2004a. Detection of apical hypertrophic cardiomyopathy by cardiovascular magnetic resonance in patients with non-diagnostic echocardiography. *Heart*, 90, 645-9.
- MOON, J. C., MESSROGLI, D. R., KELLMAN, P., PIECHNIK, S. K., ROBSON, M. D., UGANDER, M., GATEHOUSE, P. D., ARAI, A. E., FRIEDRICH, M. G., NEUBAUER, S., SCHULZ-MENGER, J. & SCHELBERT, E. B. 2013. Myocardial T1 mapping and

References

- extracellular volume quantification: a Society for Cardiovascular Magnetic Resonance (SCMR) and CMR Working Group of the European Society of Cardiology consensus statement. *J Cardiovasc Magn Reson*, 15, 92.
- MOON, J. C., REED, E., SHEPPARD, M. N., ELKINGTON, A. G., HO, S. Y., BURKE, M., PETROU, M. & PENNELL, D. J. 2004b. The histologic basis of late gadolinium enhancement cardiovascular magnetic resonance in hypertrophic cardiomyopathy. *J Am Coll Cardiol*, 43, 2260-4.
- MOSS, A. J., GREENBERG, H., CASE, R. B., ZAREBA, W., HALL, W. J., BROWN, M. W., DAUBERT, J. P., MCNITT, S., ANDREWS, M. L. & ELKIN, A. D. 2004. Long-term clinical course of patients after termination of ventricular tachyarrhythmia by an implanted defibrillator. *Circulation*, 110, 3760-5.
- MOSS, A. J., ZAREBA, W., HALL, W. J., KLEIN, H., WILBER, D. J., CANNOM, D. S., DAUBERT, J. P., HIGGINS, S. L., BROWN, M. W. & ANDREWS, M. L. 2002. Prophylactic implantation of a defibrillator in patients with myocardial infarction and reduced ejection fraction. *N Engl J Med*, 346, 877-83.
- MULCAHY, R., HICKEY, N. & MAURER, B. 1968. Aetiology of bundle-branch block. *Br Heart J*, 30, 34-7.
- NAGEL, E., LEHMKUHL, H. B., BOCKSCH, W., KLEIN, C., VOGEL, U., FRANTZ, E., ELLMER, A., DREYSSE, S. & FLECK, E. 1999. Noninvasive diagnosis of ischemia-induced wall motion abnormalities with the use of high-dose dobutamine stress MRI: comparison with dobutamine stress echocardiography. *Circulation*, 99, 763-70.
- NANDALUR, K. R., DWAMENA, B. A., CHOUDHRI, A. F., NANDALUR, M. R. & CARLOS, R. C. 2007. Diagnostic performance of stress cardiac magnetic resonance imaging in the detection of coronary artery disease: a meta-analysis. *J Am Coll Cardiol*, 50, 1343-53.
- NISHII, T., KONO, A. K., SHIGERU, M., TAKAMINE, S., FUJIWARA, S., KYOTANI, K., AOYAMA, N. & SUGIMURA, K. 2014. Cardiovascular magnetic resonance T2 mapping can detect myocardial edema in idiopathic dilated cardiomyopathy. *Int J Cardiovasc Imaging*, 30 Suppl 1, 65-72.
- NORGAARD, B. L., LEIPSIC, J., GAUR, S., SENEVIRATNE, S., KO, B. S., ITO, H., JENSEN, J. M., MAURI, L., DE BRUYNE, B., BEZERRA, H., OSAWA, K., MARWAN, M., NABER, C., ERGLIS, A., PARK, S. J., CHRISTIANSEN, E. H., KALTOFT, A., LASSEN, J. F., BOTKER, H. E. & ACHENBACH, S. 2014. Diagnostic performance of noninvasive fractional flow reserve derived from coronary computed tomography angiography in suspected coronary artery disease: the NXT trial (Analysis of Coronary Blood Flow Using CT Angiography: Next Steps). *J Am Coll Cardiol*, 63, 1145-55.
- NOTTIN, S., DOUCENDE, G., SCHUSTER, I., TANGUY, S., DAUZAT, M. & OBERT, P. 2009. Alteration in left ventricular strains and torsional mechanics after ultralong duration exercise in athletes. *Circ Cardiovasc Imaging*, 2, 323-30.
- NUCIFORA, G., AQUARO, G. D., MASCI, P. G., BARISON, A., TODIERE, G., PINGITORE, A. & LOMBARDI, M. 2011. Lipomatous metaplasia in ischemic cardiomyopathy: current knowledge and clinical perspective. *Int J Cardiol*, 146, 120-2.
- O'HANLON, R., GRASSO, A., ROUGHTON, M., MOON, J. C., CLARK, S., WAGE, R., WEBB, J., KULKARNI, M., DAWSON, D., SULAIBEEKH, L., CHANDRASEKARAN, B., BUCCIARELLI-DUCCI, C., PASQUALE, F., COWIE, M. R., MCKENNA, W. J., SHEPPARD, M. N., ELLIOTT, P. M., PENNELL, D. J. & PRASAD, S. K. 2010. Prognostic significance of myocardial fibrosis in hypertrophic cardiomyopathy. *J Am Coll Cardiol*, 56, 867-74.
- O'KEEFE, J. H., JR., BATEMAN, T. M. & BARNHART, C. S. 1993. Adenosine thallium-201 is superior to exercise thallium-201 for detecting coronary artery disease in patients with left bundle branch block. *J Am Coll Cardiol*, 21, 1332-8.
- OLSZEWSKI, R., TIMPERLEY, J., SZMIGIELSKI, C., MONAGHAN, M., NIHOYANNOPOULOS, P., SENIOR, R. & BECHER, H. 2007. The clinical applications of contrast echocardiography. *Eur J Echocardiogr*, 8, S13-23.
- ONO, S., NOHARA, R., KAMBARA, H., OKUDA, K. & KAWAI, C. 1992. Regional myocardial perfusion and glucose metabolism in experimental left bundle branch block. *Circulation*, 85, 1125-31.

References

- ORGANIZATION, W. H. 2010. *International statistical classification of diseases and related health problems. - 10th revision, edition.*, Switzerland, World Health Organization.
- OTTERSTAD, J. E., FROELAND, G., ST JOHN SUTTON, M. & HOLME, I. 1997. Accuracy and reproducibility of biplane two-dimensional echocardiographic measurements of left ventricular dimensions and function. *Eur Heart J*, 18, 507-13.
- PAETSCH, I., JAHNKE, C., FERRARI, V. A., RADEMAKERS, F. E., PELLIKKA, P. A., HUNDLEY, W. G., POLDERMANS, D., BAX, J. J., WEGSCHEIDER, K., FLECK, E. & NAGEL, E. 2006. Determination of interobserver variability for identifying inducible left ventricular wall motion abnormalities during dobutamine stress magnetic resonance imaging. *Eur Heart J*, 27, 1459-64.
- PANTANOWITZ, L. 2001. Fat infiltration in the heart. *Heart*, 85, 253.
- PARISE, H., MAEHARA, A., STONE, G. W., LEON, M. B. & MINTZ, G. S. 2011. Meta-analysis of randomized studies comparing intravascular ultrasound versus angiographic guidance of percutaneous coronary intervention in pre-drug-eluting stent era. *Am J Cardiol*, 107, 374-82.
- PARSAI, C., O'HANLON, R., PRASAD, S. K. & MOHIADDIN, R. H. 2012. Diagnostic and prognostic value of cardiovascular magnetic resonance in non-ischaemic cardiomyopathies. *J Cardiovasc Magn Reson*, 14, 54.
- PAYNE, A. R., BERRY, C., KELLMAN, P., ANDERSON, R., HSU, L. Y., CHEN, M. Y., MCPHADEN, A. R., WATKINS, S., SCHENKE, W., WRIGHT, V., LEDERMAN, R. J., ALETRAS, A. H. & ARAI, A. E. 2011a. Bright-blood T(2)-weighted MRI has high diagnostic accuracy for myocardial hemorrhage in myocardial infarction: a preclinical validation study in swine. *Circ Cardiovasc Imaging*, 4, 738-45.
- PAYNE, A. R., CASEY, M., MCCLURE, J., MCGEOCH, R., MURPHY, A., WOODWARD, R., SAUL, A., BI, X., ZUEHLSDORFF, S., OLDROYD, K. G., TZEMOS, N. & BERRY, C. 2011b. Bright-blood T2-weighted MRI has higher diagnostic accuracy than dark-blood short tau inversion recovery MRI for detection of acute myocardial infarction and for assessment of the ischemic area at risk and myocardial salvage. *Circ Cardiovasc Imaging*, 4, 210-9.
- PELLICCIA, A., FAGARD, R., BJORNSTAD, H. H., ANASTASSAKIS, A., ARBUSTINI, E., ASSANELLI, D., BIFFI, A., BORJESSON, M., CARRE, F., CORRADO, D., DELISE, P., DORWARTH, U., HIRTH, A., HEIDBUCHEL, H., HOFFMANN, E., MELLWIG, K. P., PANHUYZEN-GOEDKOOP, N., PISANI, A., SOLBERG, E. E., VAN-BUUREN, F., VANHEES, L., BLOMSTROM-LUNDQVIST, C., DELIGIANNIS, A., DUGMORE, D., GLIKSON, M., HOFF, P. I., HOFFMANN, A., HOFFMANN, E., HORSTKOTTE, D., NORDREHAUG, J. E., OUDHOF, J., MCKENNA, W. J., PENCO, M., PRIORI, S., REYBROUCK, T., SENDEN, J., SPATARO, A. & THIENE, G. 2005. Recommendations for competitive sports participation in athletes with cardiovascular disease: a consensus document from the Study Group of Sports Cardiology of the Working Group of Cardiac Rehabilitation and Exercise Physiology and the Working Group of Myocardial and Pericardial Diseases of the European Society of Cardiology. *Eur Heart J*, 26, 1422-45.
- PERRIER, E., MANEN, O., DOIREAU, P., PAUL, J. F., GHOSTINE, S., LERECOUVREUX, M., DEROCHE, J., LEDUC, P. A., GENERO, M., PARIS, J. F., MARTEL, V., CARLIOZ, R., GEFFROY, S., CAUSSIN, C., PLOTTON, C. & GOURBAT, J. P. 2006. LBBB in aircrew with low cardiac risk: diagnostic application of multislice CT. *Aviat Space Environ Med*, 77, 613-8.
- PIECHNIK, S. K., FERREIRA, V. M., LEWANDOWSKI, A. J., NTUSI, N. A., BANERJEE, R., HOLLOWAY, C., HOFMAN, M. B., SADO, D. M., MAESTRINI, V., WHITE, S. K., LAZDAM, M., KARAMITSOS, T., MOON, J. C., NEUBAUER, S., LEESON, P. & ROBSON, M. D. 2013. Normal variation of magnetic resonance T1 relaxation times in the human population at 1.5 T using ShMOLLI. *J Cardiovasc Magn Reson*, 15, 13.
- PIERS, L. H., DIKKERS, R., WILLEMS, T. P., DE SMET, B. J., OUDKERK, M., ZIJLSTRA, F. & TIO, R. A. 2008. Computed tomographic angiography or conventional coronary angiography in therapeutic decision-making. *Eur Heart J*, 29, 2902-7.
- PILZ, G., JESKE, A., KLOS, M., ALI, E., HOEFLING, B., SCHECK, R. & BERNHARDT, P. 2008. Prognostic value of normal adenosine-stress cardiac magnetic resonance imaging. *Am J Cardiol*, 101, 1408-12.

References

- PLEIN, S., GREENWOOD, J. P., RIDGWAY, J. P., CRANNY, G., BALL, S. G. & SIVANANTHAN, M. U. 2004. Assessment of non-ST-segment elevation acute coronary syndromes with cardiac magnetic resonance imaging. *J Am Coll Cardiol*, 44, 2173-81.
- PLUIM, B. M., ZWINDERMAN, A. H., VAN DER LAARSE, A. & VAN DER WALL, E. E. 2000. The athlete's heart. A meta-analysis of cardiac structure and function. *Circulation*, 101, 336-44.
- POCOCK, S. J., WANG, D., PFEFFER, M. A., YUSUF, S., MCMURRAY, J. J., SWEDBERG, K. B., OSTERGREN, J., MICHELSON, E. L., PIEPER, K. S. & GRANGER, C. B. 2006. Predictors of mortality and morbidity in patients with chronic heart failure. *Eur Heart J*, 27, 65-75.
- POULIOPOULOS, J., CHIK, W. W., KANTHAN, A., SIVAGANGABALAN, G., BARRY, M. A., FAHMY, P. N., MIDEKIN, C., LU, J., KIZANA, E., THOMAS, S. P., THIAGALINGAM, A. & KOVOOR, P. 2013. Intramyocardial adiposity after myocardial infarction: new implications of a substrate for ventricular tachycardia. *Circulation*, 128, 2296-308.
- PRINZEN, F. W., CHERIEX, E. C., DELHAAS, T., VAN OOSTERHOUT, M. F., ARTS, T., WELLENS, H. J. & RENEMAN, R. S. 1995. Asymmetric thickness of the left ventricular wall resulting from asynchronous electric activation: a study in dogs with ventricular pacing and in patients with left bundle branch block. *Am Heart J*, 130, 1045-53.
- PUNTMANN, V. O., JAHNKE, C., GEBKER, R., SCHNACKENBURG, B., FOX, K. F., FLECK, E. & PAETSCH, I. 2010. Usefulness of magnetic resonance imaging to distinguish hypertensive and hypertrophic cardiomyopathy. *Am J Cardiol*, 106, 1016-22.
- PUNTMANN, V. O., VOIGT, T., CHEN, Z., MAYR, M., KARIM, R., RHODE, K., PASTOR, A., CARR-WHITE, G., RAZAVI, R., SCHAEFFTER, T. & NAGEL, E. 2013. Native T1 mapping in differentiation of normal myocardium from diffuse disease in hypertrophic and dilated cardiomyopathy. *JACC Cardiovasc Imaging*, 6, 475-84.
- RABKIN, S. W., MATHEWSON, F. A. & TATE, R. B. 1980. Natural history of left bundle-branch block. *Br Heart J*, 43, 164-9.
- RAYATZADEH, H., PATEL, S. J., HAUSER, T. H., NGO, L. L., SHAW, J. L., TAN, A., BUXTON, A. E., ZIMETBAUM, P., JOSEPHSON, M. E., APPELBAUM, E., MANNING, W. J. & NEZAFAT, R. 2013. Volumetric left ventricular ejection fraction is superior to 2-dimensional echocardiography for risk stratification of patients for primary prevention implantable cardioverter-defibrillator implantation. *Am J Cardiol*, 111, 1175-9.
- RICHAND, V., LAFITTE, S., REANT, P., SERRI, K., LAFITTE, M., BRETTE, S., KEROUANI, A., CHALABI, H., DOS SANTOS, P., DOUARD, H. & ROUDAUT, R. 2007. An ultrasound speckle tracking (two-dimensional strain) analysis of myocardial deformation in professional soccer players compared with healthy subjects and hypertrophic cardiomyopathy. *Am J Cardiol*, 100, 128-32.
- RIDGWAY, J. P. 2010. Cardiovascular magnetic resonance physics for clinicians: part I. *J Cardiovasc Magn Reson*, 12, 71.
- ROES, S. D., BORLEFFS, C. J., VAN DER GEEST, R. J., WESTENBERG, J. J., MARSAN, N. A., KAANDORP, T. A., REIBER, J. H., ZEPPENFELD, K., LAMB, H. J., DE ROOS, A., SCHALIJ, M. J. & BAX, J. J. 2009. Infarct tissue heterogeneity assessed with contrast-enhanced MRI predicts spontaneous ventricular arrhythmia in patients with ischemic cardiomyopathy and implantable cardioverter-defibrillator. *Circ Cardiovasc Imaging*, 2, 183-90.
- ROMERO, J., XUE, X., GONZALEZ, W. & GARCIA, M. J. 2012. CMR imaging assessing viability in patients with chronic ventricular dysfunction due to coronary artery disease: a meta-analysis of prospective trials. *JACC Cardiovasc Imaging*, 5, 494-508.
- ROSEN, B. D., EDVARDSEN, T., LAI, S., CASTILLO, E., PAN, L., JEROSCH-HEROLD, M., SINHA, S., KRONMAL, R., ARNETT, D., CROUSE, J. R., 3RD, HECKBERT, S. R., BLUEMKE, D. A. & LIMA, J. A. 2005. Left ventricular concentric remodeling is associated with decreased global and regional systolic function: the Multi-Ethnic Study of Atherosclerosis. *Circulation*, 112, 984-91.
- RUBINSHTAIN, R., GLOCKNER, J. F., OMMEN, S. R., ARAOZ, P. A., ACKERMAN, M. J., SORAJJA, P., BOS, J. M., TAJIK, A. J., VALETI, U. S., NISHIMURA, R. A. & GERSH, B. J. 2010. Characteristics and clinical significance of late gadolinium enhancement by

References

- contrast-enhanced magnetic resonance imaging in patients with hypertrophic cardiomyopathy. *Circ Heart Fail*, 3, 51-8.
- SAITO, M., OKAYAMA, H., YOSHII, T., HIGASHI, H., MORIOKA, H., HIASA, G., SUMIMOTO, T., INABA, S., NISHIMURA, K., INOUE, K., OGIMOTO, A., SHIGEMATSU, Y., HAMADA, M. & HIGAKI, J. 2012. Clinical significance of global two-dimensional strain as a surrogate parameter of myocardial fibrosis and cardiac events in patients with hypertrophic cardiomyopathy. *Eur Heart J Cardiovasc Imaging*, 13, 617-23.
- SALERNO, M. & BELLER, G. A. 2009. Noninvasive assessment of myocardial perfusion. *Circ Cardiovasc Imaging*, 2, 412-24.
- SCHARTL, M., BECKMANN, S., BOCKSCH, W., FATEH-MOGHADAM, S. & FLECK, E. 1997. Stress echocardiography in special groups: in women, in left bundle branch block, in hypertension and after heart transplantation. *Eur Heart J*, 18 Suppl D, D63-7.
- SCHINKEL, A. F., BAX, J. J. & POLDERMANS, D. 2005. Clinical assessment of myocardial hibernation. *Heart*, 91, 111-7.
- SCHMID, M., DANIEL, W. G. & ACHENBACH, S. 2010. Cardiovascular magnetic resonance evaluation of the patient with known or suspected coronary artery disease. *Heart*, 96, 1586-92.
- SCHMIDT, A., AZEVEDO, C. F., CHENG, A., GUPTA, S. N., BLUEMKE, D. A., FOO, T. K., GERSTENBLITH, G., WEISS, R. G., MARBAN, E., TOMASELLI, G. F., LIMA, J. A. & WU, K. C. 2007. Infarct tissue heterogeneity by magnetic resonance imaging identifies enhanced cardiac arrhythmia susceptibility in patients with left ventricular dysfunction. *Circulation*, 115, 2006-14.
- SCHMITT, M., SAMANI, N. & MCCANN, G. 2007. Images in cardiovascular medicine. Lipomatous metaplasia in ischemic cardiomyopathy: a common but unappreciated entity. *Circulation*, 116, e5-6.
- SCHNEIDER, J. F., THOMAS, H. E., JR., KREGER, B. E., MCNAMARA, P. M. & KANNEL, W. B. 1979. Newly acquired left bundle-branch block: the Framingham study. *Ann Intern Med*, 90, 303-10.
- SCHNEIDER, J. F., THOMAS, H. E., JR., SORLIE, P., KREGER, B. E., MCNAMARA, P. M. & KANNEL, W. B. 1981. Comparative features of newly acquired left and right bundle branch block in the general population: the Framingham study. *Am J Cardiol*, 47, 931-40.
- SCHWITTER, J., WACKER, C. M., VAN ROSSUM, A. C., LOMBARDI, M., AL-SAAD, N., AHLSTROM, H., DILL, T., LARSSON, H. B., FLAMM, S. D., MARQUARDT, M. & JOHANSSON, L. 2008. MR-IMPACT: comparison of perfusion-cardiac magnetic resonance with single-photon emission computed tomography for the detection of coronary artery disease in a multicentre, multivendor, randomized trial. *Eur Heart J*, 29, 480-9.
- SCHWITTER, J., WACKER, C. M., WILKE, N., AL-SAAD, N., SAUER, E., HUETTLE, K., SCHONBERG, S. O., DEBL, K., STROHM, O., AHLSTROM, H., DILL, T., HOEBEL, N. & SIMOR, T. 2012. Superior diagnostic performance of perfusion-cardiovascular magnetic resonance versus SPECT to detect coronary artery disease: The secondary endpoints of the multicenter multivendor MR-IMPACT II (Magnetic Resonance Imaging for Myocardial Perfusion Assessment in Coronary Artery Disease Trial). *J Cardiovasc Magn Reson*, 14, 61.
- SCOTLAND, A. 2012. *Cardiology Services*, Edinburgh, Audit Scotland.
- SCOTT, P. A., BARRY, J., ROBERTS, P. R. & MORGAN, J. M. 2009. Brain natriuretic peptide for the prediction of sudden cardiac death and ventricular arrhythmias: a meta-analysis. *Eur J Heart Fail*, 11, 958-66.
- SCOTT, P. A., MORGAN, J. M., CARROLL, N., MURDAY, D. C., ROBERTS, P. R., PEEBLES, C. R., HARDEN, S. P. & CURZEN, N. P. 2011a. The extent of left ventricular scar quantified by late gadolinium enhancement MRI is associated with spontaneous ventricular arrhythmias in patients with coronary artery disease and implantable cardioverter-defibrillators. *Circ Arrhythm Electrophysiol*, 4, 324-30.
- SCOTT, P. A., TOWNSEND, P. A., NG, L. L., ZEB, M., HARRIS, S., RODERICK, P. J., CURZEN, N. P. & MORGAN, J. M. 2011b. Defining potential to benefit from implantable cardioverter defibrillator therapy: the role of biomarkers. *Europace*, 13, 1419-27.

References

- SEVERI, S., UNDERWOOD, R., MOHIADDIN, R. H., BOYD, H., PATERNI, M. & CAMICI, P. G. 1995. Dobutamine stress: effects on regional myocardial blood flow and wall motion. *J Am Coll Cardiol*, 26, 1187-95.
- SHAN, Y., VILLARRAGA, H. R., PISLARU, C., SHAH, A. A., CHA, S. S. & PELLIKKA, P. A. 2009. Quantitative assessment of strain and strain rate by velocity vector imaging during dobutamine stress echocardiography to predict outcome in patients with left bundle branch block. *J Am Soc Echocardiogr*, 22, 1212-9.
- SIMONETTI, O. P., FINN, J. P., WHITE, R. D., LAUB, G. & HENRY, D. A. 1996. "Black blood" T2-weighted inversion-recovery MR imaging of the heart. *Radiology*, 199, 49-57.
- SIMSEK, Z., HAKAN TAS, M., DEGIRMENCI, H., GOKHAN YAZICI, A., IPEK, E., DUMAN, H., GUNDOGDU, F., KARAKELLEOGLU, S. & SENOCAK, H. 2013. Speckle tracking echocardiographic analysis of left ventricular systolic and diastolic functions of young elite athletes with eccentric and concentric type of cardiac remodeling. *Echocardiography*, 30, 1202-8.
- SKALIDIS, E. I., KOCHIADAKIS, G. E., KOUKOURAKI, S. I., PARTHENAKIS, F. I., KARKAVITSAS, N. S. & VARDAS, P. E. 1999. Phasic coronary flow pattern and flow reserve in patients with left bundle branch block and normal coronary arteries. *J Am Coll Cardiol*, 33, 1338-46.
- SKINNER, J. S., SMEETH, L., KENDALL, J. M., ADAMS, P. C. & TIMMIS, A. 2010. NICE guidance. Chest pain of recent onset: assessment and diagnosis of recent onset chest pain or discomfort of suspected cardiac origin. *Heart*, 96, 974-8.
- SOLOMON, S. D., ANAVEKAR, N., SKALI, H., MCMURRAY, J. J., SWEDBERG, K., YUSUF, S., GRANGER, C. B., MICHELSON, E. L., WANG, D., POCOCK, S. & PFEFFER, M. A. 2005. Influence of ejection fraction on cardiovascular outcomes in a broad spectrum of heart failure patients. *Circulation*, 112, 3738-44.
- STANTON, T., LEANO, R. & MARWICK, T. H. 2009. Prediction of all-cause mortality from global longitudinal speckle strain: comparison with ejection fraction and wall motion scoring. *Circ Cardiovasc Imaging*, 2, 356-64.
- STECKER, E. C., VICKERS, C., WALTZ, J., SOCOTEANU, C., JOHN, B. T., MARIANI, R., MCANULTY, J. H., GUNSON, K., JUI, J. & CHUGH, S. S. 2006. Population-based analysis of sudden cardiac death with and without left ventricular systolic dysfunction: two-year findings from the Oregon Sudden Unexpected Death Study. *J Am Coll Cardiol*, 47, 1161-6.
- STEG, P. G., JAMES, S. K., ATAR, D., BADANO, L. P., BLOMSTROM-LUNDQVIST, C., BORGER, M. A., DI MARIO, C., DICKSTEIN, K., DUCROCQ, G., FERNANDEZ-AVILES, F., GERSHLICK, A. H., GIANNUZZI, P., HALVORSEN, S., HUBER, K., JUNI, P., KASTRATI, A., KNUUTI, J., LENZEN, M. J., MAHAFFEY, K. W., VALGIMIGLI, M., VAN 'T HOF, A., WIDIMSKY, P. & ZAHGER, D. 2012. ESC Guidelines for the management of acute myocardial infarction in patients presenting with ST-segment elevation. *Eur Heart J*, 33, 2569-619.
- SU, L., SIEGEL, J. E. & FISHBEIN, M. C. 2004. Adipose tissue in myocardial infarction. *Cardiovasc Pathol*, 13, 98-102.
- SUGIHARA, H., TAMAKI, N., NOZAWA, M., OHMURA, T., INAMOTO, Y., TANIGUCHI, Y., AOKI, E., MITSUNAMI, K. & KINOSHITA, M. 1997. Septal perfusion and wall thickening in patients with left bundle branch block assessed by technetium-99m-sestamibi gated tomography. *J Nucl Med*, 38, 545-7.
- SUPARIWALA, A. A., PO, J. R., MOHAREB, S., ASLAM, F., KADDAHA, F., MIAN, Z. I., CHAUDHRY, F., OTOKITI, A. & CHAUDHRY, F. A. 2014. Prevalence and Long-Term Prognosis of Patients with Complete Bundle Branch Block (Right or Left Bundle Branch) with Normal Left Ventricular Ejection Fraction Referred for Stress Echocardiography. *Echocardiography*.
- SUTTON, M. G. & SHARPE, N. 2000. Left ventricular remodeling after myocardial infarction: pathophysiology and therapy. *Circulation*, 101, 2981-8.
- SUTTON, M. S., GROVES, A., MACNEILL, A., SHARLAND, G. & ALLAN, L. 1994. Assessment of changes in blood flow through the lungs and foramen ovale in the normal human fetus with gestational age: a prospective Doppler echocardiographic study. *Br Heart J*, 71, 232-7.

References

- TADAMURA, E., KUDOH, T., MOTOOKA, M., INUBUSHI, M., SHIRAKAWA, S., HATTORI, N., OKADA, T., MATSUDA, T., KOSHIJI, T., NISHIMURA, K., MATSUDA, K. & KONISHI, J. 1999. Assessment of regional and global left ventricular function by reinjection Tl-201 and rest Tc-99m sestamibi ECG-gated SPECT: comparison with three-dimensional magnetic resonance imaging. *J Am Coll Cardiol*, 33, 991-7.
- TANDOGAN, I., YETKIN, E., YANIK, A., ULUSOY, F. V., TEMIZHAN, A., CEHRELI, S. & SASMAZ, A. 2001. Comparison of thallium-201 exercise SPECT and dobutamine stress echocardiography for diagnosis of coronary artery disease in patients with left bundle branch block. *Int J Cardiovasc Imaging*, 17, 339-45.
- TAYLOR, A. J., ELLIMS, A., LEW, P. J., MURPHY, B., PALLY, S. & YOUNIE, S. 2013. Impact of cardiac magnetic resonance imaging on cardiac device and surgical therapy: a prospective study. *Int J Cardiovasc Imaging*, 29, 855-64.
- THOMAS, D. E., WHEELER, R., YOUSEF, Z. R. & MASANI, N. D. 2009. The role of echocardiography in guiding management in dilated cardiomyopathy. *Eur J Echocardiogr*, 10, iii15-21.
- THYGESEN, K., ALPERT, J. S., JAFFE, A. S., SIMOONS, M. L., CHAITMAN, B. R., WHITE, H. D., THYGESEN, K., ALPERT, J. S., WHITE, H. D., JAFFE, A. S., KATUS, H. A., APPLE, F. S., LINDAHL, B., MORROW, D. A., CHAITMAN, B. A., CLEMMENSEN, P. M., JOHANSON, P., HOD, H., UNDERWOOD, R., BAX, J. J., BONOW, R. O., PINTO, F., GIBBONS, R. J., FOX, K. A., ATAR, D., NEWBY, L. K., GALVANI, M., HAMM, C. W., URETSKY, B. F., STEG, P. G., WIJNS, W., BASSAND, J. P., MENASCHE, P., RAVKILDE, J., OHMAN, E. M., ANTMAN, E. M., WALLENTIN, L. C., ARMSTRONG, P. W., SIMOONS, M. L., JANUZZI, J. L., NIEMINEN, M. S., GHEORGHIADE, M., FILIPPATOS, G., LUEPKER, R. V., FORTMANN, S. P., ROSAMOND, W. D., LEVY, D., WOOD, D., SMITH, S. C., HU, D., LOPEZ-SENDON, J. L., ROBERTSON, R. M., WEAVER, D., TENDERA, M., BOVE, A. A., PARKHOMENKO, A. N., VASILIEVA, E. J. & MENDIS, S. 2012. Third universal definition of myocardial infarction. *Eur Heart J*, 33, 2551-67.
- TONINO, P. A., DE BRUYNE, B., PIJLS, N. H., SIEBERT, U., IKENO, F., VAN' T VEER, M., KLAUSS, V., MANOHARAN, G., ENGSTROM, T., OLDROYD, K. G., VER LEE, P. N., MACCARTHY, P. A. & FEARON, W. F. 2009. Fractional flow reserve versus angiography for guiding percutaneous coronary intervention. *N Engl J Med*, 360, 213-24.
- TOWNSEND N, W. K., BHATNAGAR P, SMOLINA K, NICHOLS M, LEAL J, LUENGO-FERNANDEZ R, RAYNER M 2012. *Coronary heart disease statistics 2012 edition.*, London, British Heart Foundation.
- UGANDER, M., BAGI, P. S., OKI, A. J., CHEN, B., HSU, L. Y., ALETRAS, A. H., SHAH, S., GREISER, A., KELLMAN, P. & ARAI, A. E. 2012. Myocardial edema as detected by pre-contrast T1 and T2 CMR delineates area at risk associated with acute myocardial infarction. *JACC Cardiovasc Imaging*, 5, 596-603.
- UTOMI, V., OXBOROUGH, D., ASHLEY, E., LORD, R., FLETCHER, S., STEMBRIDGE, M., SHAVE, R., HOFFMAN, M. D., WHYTE, G., SOMAUROO, J., SHARMA, S. & GEORGE, K. 2014. Predominance of normal left ventricular geometry in the male 'athlete's heart'. *Heart*, 100, 1264-71.
- VADUGANATHAN, P., HE, Z. X., RAGHAVAN, C., MAHMARIAN, J. J. & VERANI, M. S. 1996. Detection of left anterior descending coronary artery stenosis in patients with left bundle branch block: exercise, adenosine or dobutamine imaging? *J Am Coll Cardiol*, 28, 543-50.
- VAHANIAN, A., ALFIERI, O., ANDREOTTI, F., ANTUNES, M. J., BARON-ESQUIVIAS, G., BAUMGARTNER, H., BORGER, M. A., CARREL, T. P., DE BONIS, M., EVANGELISTA, A., FALK, V., IUNG, B., LANCELLOTTI, P., PIERARD, L., PRICE, S., SCHAFERS, H. J., SCHULER, G., STEPINSKA, J., SWEDBERG, K., TAKKENBERG, J., VON OPPELL, U. O., WINDECKER, S., ZAMORANO, J. L. & ZEMBALA, M. 2012. Guidelines on the management of valvular heart disease (version 2012). *Eur Heart J*, 33, 2451-96.
- VERMA, A., KILICASLAN, F., MARTIN, D. O., MINOR, S., STARLING, R., MARROUCHE, N. F., ALMAHAMMED, S., WAZNI, O. M., DUGGAL, S., ZUZEK, R., YAMAJI, H., CUMMINGS, J., CHUNG, M. K., TCHOU, P. J. & NATALE, A. 2006. Preimplantation

References

- B-type natriuretic peptide concentration is an independent predictor of future appropriate implantable defibrillator therapies. *Heart*, 92, 190-5.
- VERMES, E., CHILDS, H., FARIS, P. & FRIEDRICH, M. G. 2014. Predictive value of CMR criteria for LV functional improvement in patients with acute myocarditis. *Eur Heart J Cardiovasc Imaging*.
- VIGNAUX, O., LAZARUS, A., VARIN, J., COSTE, J., CARLIER, P., ARGAUD, C., LAFORET, P., WEBER, S., LEGMANN, P. & DUBOC, D. 2002. Right ventricular MR abnormalities in myotonic dystrophy and relationship with intracardiac electrophysiologic test findings: initial results. *Radiology*, 224, 231-5.
- VOGT, F. M., HERBORN, C. U., HUNOLD, P., LAUENSTEIN, T. C., SCHRODER, T., DEBATIN, J. F. & BARKHAUSEN, J. 2004. HASTE MRI versus chest radiography in the detection of pulmonary nodules: comparison with MDCT. *AJR Am J Roentgenol*, 183, 71-8.
- WATERHOUSE, D. F., ISMAIL, T. F., PRASAD, S. K., WILSON, M. G. & O'HANLON, R. 2012. Imaging focal and interstitial fibrosis with cardiovascular magnetic resonance in athletes with left ventricular hypertrophy: implications for sporting participation. *Br J Sports Med*, 46 Suppl 1, i69-77.
- WEDEL, H., MCMURRAY, J. J., LINDBERG, M., WIKSTRAND, J., CLELAND, J. G., CORNEL, J. H., DUNSELMAN, P., HJALMARSON, A., KJEKSHUS, J., KOMAJDA, M., KUUSI, T., VANHAECKE, J. & WAAGSTEIN, F. 2009. Predictors of fatal and non-fatal outcomes in the Controlled Rosuvastatin Multinational Trial in Heart Failure (CORONA): incremental value of apolipoprotein A-1, high-sensitivity C-reactive peptide and N-terminal pro B-type natriuretic peptide. *Eur J Heart Fail*, 11, 281-91.
- WHITE, J. A., KIM, H. W., SHAH, D., FINE, N., KIM, K. Y., WENDELL, D. C., AL-JAROUDI, W., PARKER, M., PATEL, M., GWADRY-SRIDHAR, F., JUDD, R. M. & KIM, R. J. 2014. CMR imaging with rapid visual T1 assessment predicts mortality in patients suspected of cardiac amyloidosis. *JACC Cardiovasc Imaging*, 7, 143-56.
- WHYTE, G. P., SHEPPARD, M., GEORGE, K. P., SHAVE, R. E., WILSON, M., STEPHENS, N., SENIOR, R. & SHARMA, S. 2007. Arrhythmias and the athlete: mechanisms and clinical significance. *Eur Heart J*, 28, 1399-401; author reply 1401.
- WINER-MURAM, H. T., TANN, M., AISEN, A. M., FORD, L., JENNINGS, S. G. & BRETZ, R. 2004. Computed tomography demonstration of lipomatous metaplasia of the left ventricle following myocardial infarction. *J Comput Assist Tomogr*, 28, 455-8.
- WONG, M., STASZEWSKY, L., LATINI, R., BARLERA, S., GLAZER, R., AKNAY, N., HESTER, A., ANAND, I. & COHN, J. N. 2004. Severity of left ventricular remodeling defines outcomes and response to therapy in heart failure: Valsartan heart failure trial (Val-HeFT) echocardiographic data. *J Am Coll Cardiol*, 43, 2022-7.
- WONG, T. C., PIEHLER, K., MEIER, C. G., TESTA, S. M., KLOCK, A. M., ANEIZI, A. A., SHAKESPRERE, J., KELLMAN, P., SHROFF, S. G., SCHWARTZMAN, D. S., MULUKUTLA, S. R., SIMON, M. A. & SCHELBERT, E. B. 2012. Association between extracellular matrix expansion quantified by cardiovascular magnetic resonance and short-term mortality. *Circulation*, 126, 1206-16.
- WOOD, J. C. 2009. History and current impact of cardiac magnetic resonance imaging on the management of iron overload. *Circulation*, 120, 1937-9.
- WRIGHT, J., ADRIAENSSENS, T., DYMARKOWSKI, S., DESMET, W. & BOGAERT, J. 2009. Quantification of myocardial area at risk with T2-weighted CMR: comparison with contrast-enhanced CMR and coronary angiography. *JACC Cardiovasc Imaging*, 2, 825-31.
- WU, K. C. 2012. CMR of microvascular obstruction and hemorrhage in myocardial infarction. *J Cardiovasc Magn Reson*, 14, 68.
- WU, K. C., GERSTENBLITH, G., GUALLAR, E., MARINE, J. E., DALAL, D., CHENG, A., MARBAN, E., LIMA, J. A., TOMASELLI, G. F. & WEISS, R. G. 2012. Combined cardiac magnetic resonance imaging and C-reactive protein levels identify a cohort at low risk for defibrillator firings and death. *Circ Cardiovasc Imaging*, 5, 178-86.
- WU, K. C., WEISS, R. G., THIEMANN, D. R., KITAGAWA, K., SCHMIDT, A., DALAL, D., LAI, S., BLUEMKE, D. A., GERSTENBLITH, G., MARBAN, E., TOMASELLI, G. F. & LIMA, J. A. 2008. Late gadolinium enhancement by cardiovascular magnetic resonance

References

- heralds an adverse prognosis in nonischemic cardiomyopathy. *J Am Coll Cardiol*, 51, 2414-21.
- WU, K. C., ZERHOUNI, E. A., JUDD, R. M., LUGO-OLIVIERI, C. H., BAROUCH, L. A., SCHULMAN, S. P., BLUMENTHAL, R. S. & LIMA, J. A. 1998. Prognostic significance of microvascular obstruction by magnetic resonance imaging in patients with acute myocardial infarction. *Circulation*, 97, 765-72.
- WU, Y. W., TADAMURA, E., YAMAMURO, M., KANAO, S., ABE, M., KIMURA, T., KITA, T. & TOGASHI, K. 2007. Identification of lipomatous metaplasia in old infarcted myocardium by cardiovascular magnetic resonance and computed tomography. *Int J Cardiol*, 115, e15-6.
- XIE, X., ZHAO, Y., DE BOCK, G. H., DE JONG, P. A., MALI, W. P., OUDKERK, M. & VLEGENTHART, R. 2013. Validation and prognosis of coronary artery calcium scoring in nontriggered thoracic computed tomography: systematic review and meta-analysis. *Circ Cardiovasc Imaging*, 6, 514-21.
- YAN, A. T., GIBSON, C. M., LAROSE, E., ANAVEKAR, N. S., TSANG, S., SOLOMON, S. D., REYNOLDS, G. & KWONG, R. Y. 2006a. Characterization of microvascular dysfunction after acute myocardial infarction by cardiovascular magnetic resonance first-pass perfusion and late gadolinium enhancement imaging. *J Cardiovasc Magn Reson*, 8, 831-7.
- YAN, A. T., SHAYNE, A. J., BROWN, K. A., GUPTA, S. N., CHAN, C. W., LUU, T. M., DI CARLI, M. F., REYNOLDS, H. G., STEVENSON, W. G. & KWONG, R. Y. 2006b. Characterization of the peri-infarct zone by contrast-enhanced cardiac magnetic resonance imaging is a powerful predictor of post-myocardial infarction mortality. *Circulation*, 114, 32-9.
- YANCY, C. W., JESSUP, M., BOZKURT, B., BUTLER, J., CASEY, D. E., JR., DRAZNER, M. H., FONAROW, G. C., GERACI, S. A., HORWICH, T., JANUZZI, J. L., JOHNSON, M. R., KASPER, E. K., LEVY, W. C., MASOUDI, F. A., MCBRIDE, P. E., MCMURRAY, J. J., MITCHELL, J. E., PETERSON, P. N., RIEGEL, B., SAM, F., STEVENSON, L. W., TANG, W. H., TSAI, E. J. & WILKOFF, B. L. 2013. 2013 ACCF/AHA guideline for the management of heart failure: a report of the American College of Cardiology Foundation/American Heart Association Task Force on Practice Guidelines. *J Am Coll Cardiol*, 62, e147-239.
- YANG, Y., CONNELLY, K. A., ZEIDAN-SHWIRI, T., LU, Y., PAUL, G., ROIFMAN, I., ZIA, M. I., GRAHAM, J. J., DICK, A. J., CRYSTAL, E. & WRIGHT, G. A. 2013. Multi-contrast late enhancement CMR determined gray zone and papillary muscle involvement predict appropriate ICD therapy in patients with ischemic heart disease. *J Cardiovasc Magn Reson*, 15, 57.
- YANIK, A., YETKIN, E., SENEN, K., ATAK, R., ILERI, M., KURAL, T. & GOKSEL, S. 2000. Value of dobutamine stress echocardiography for diagnosis of coronary artery disease in patients with left bundle branch blockage. *Coron Artery Dis*, 11, 545-8.
- YOKOTA, H., HEIDARY, S., KATIKIREDDY, C. K., NGUYEN, P., PAULY, J. M., MCCONNELL, M. V. & YANG, P. C. 2008. Quantitative characterization of myocardial infarction by cardiovascular magnetic resonance predicts future cardiovascular events in patients with ischemic cardiomyopathy. *J Cardiovasc Magn Reson*, 10, 17.
- YU, J. S., KIM, K. W., KIM, Y. H., JEONG, E. K. & CHIEN, D. 1998. Comparison of multishot turbo spin echo and HASTE sequences for T2-weighted MRI of liver lesions. *J Magn Reson Imaging*, 8, 1079-84.
- ZANCO, P., DESIDERI, A., MOBILIA, G., CARGNEL, S., MILAN, E., CELEGON, L., BUCHBERGER, R. & FERLIN, G. 2000. Effects of left bundle branch block on myocardial FDG PET in patients without significant coronary artery stenoses. *J Nucl Med*, 41, 973-7.
- ZILINSKI, J. L., CONTURSI, M. E., ISAACS, S. K., DELUCA, J. R., LEWIS, G. D., WEINER, R. B., HUTTER, A. M., JR., D'HEMERCOURT, P. A., TROYANOS, C., DYER, K. S. & BAGGISH, A. L. 2015. Myocardial adaptations to recreational marathon training among middle-aged men. *Circ Cardiovasc Imaging*, 8.